

Copyright is owned by the Author of the thesis. Permission is given for a copy to be downloaded by an individual for the purpose of research and private study only. The thesis may not be reproduced elsewhere without the permission of the Author.

THE PHYSICAL PROPERTIES OF  
TRIACYLGLYCEROLS  
IN RELATION TO MILKFAT

A thesis presented for the degree of  
Doctor of Philosophy  
in Chemistry  
at Massey University

by  
Robert Norris

1977

ABSTRACT

Enantiomeric and racemic triacylglycerols (TGs) representative of the major structural classes in milkfat were synthesised and their polymorphism was characterised by differential scanning calorimetry (DSC) and infrared (IR) spectroscopy.

With butyric (B), oleic (O), palmitic (P) and stearic (S) acids as starting materials, 22 racemic TGs were prepared. The main TG classes were: 1) palmitoyl-stearoyl TGs (e.g. PSS), 2) 1-butyryl TGs (BPS), 3) 1-oleoyl TGs (OPS), 4) 2-oleoyl TGs (POS), 5) 1-butyryl-2-oleoyl TGs (BOS) and 6) 1,2-dioleoyl TGs (OOS). Three TGs containing elaidic acid (E) were also synthesised (BES, ESS and SES). In addition, enantiomers of three of the racemic TGs belonging to the 1-butyryl and 1-oleoyl classes were prepared (sn-SSB, -SSO and -PPO).

The polymorphic forms of each TG were classified as  $\alpha$ ,  $\beta'$  or  $\beta$  by comparison of their IR spectra with the spectra of the polymorphic forms of monoacid TGs. Solvent crystallised forms were also characterised by X-ray powder diffraction. Melting points of all polymorphs and heats of fusion of the least stable ( $\alpha$ ) and most stable forms were determined by DSC. However, the determination of the polymorphic assignment and heat of fusion of the intermediate forms was often uncertain because of the difficulty in obtaining a pure phase.

The principal findings were:-

- 1) Corresponding enantiomeric and racemic TGs exhibited similar polymorphic behaviour except that the  $\alpha$  forms of the enantiomers transformed more rapidly than those of their racemates.
- 2) For TGs in which one fatty acid was very different from the other two (e.g. BSS, OOS), the position of the unusual acid determined the chain packing of the stable form. If the acid was in a primary position, the TG was  $\beta'$ -stable (e.g. BSS, OSS, OOS), while if it was in the secondary position, the TG was  $\beta$ -stable (e.g. SOS, SBS).
- 3) There were close parallels between the stable forms of corresponding butyryl and oleoyl TGs (e.g. BSS, OSS; SBS, SOS; BOS, OOS), although in other respects their polymorphism had little in common. The stable forms of BSP and OSP showed anomalous thermal, diffraction and spectral data compared with the remaining 1-butyryl and 1-oleoyl TGs.
- 4) The results obtained for the 1-oleoyl, 2-oleoyl and 1,2-dioleoyl TGs were in general agreement with earlier reports, although some differences were noted in the transformation of OSP, OPS, SOS and POP.

Furthermore, previously undetected transitions were observed for all the oleoyl TGs, although these were minor. A new polymorph of OPP was also characterised. With the exception of POS, all monooleoyl TGs showed anomalous crystallisation behaviour.

- 5) The results for the polymorphism of the palmitoyl-stearoyl and elaidoyl-stearoyl TGs were also in accord with previous reports. The presence of a  $\beta'_2$  form was confirmed for all TGs except SPS and PSP. The heats of fusion of the  $\beta$  forms of SPS and PSP were comparable with those of their unsymmetrical counterparts, PSS and PPS, but the heats of fusion of their stable  $\beta'$  forms were much higher than those of  $\beta'$  SSS, PSS, PPS and PPP.

These findings are discussed in relation to the principles of close packing and their relevance to the phase behaviour of milkfat.

### ACKNOWLEDGEMENTS

I would particularly like to thank my two supervisors, Dr J.C. Hawke and Prof. G.N. Malcolm, for the opportunity to work at Massey University. I am also indebted to the New Zealand Dairy Research Institute for financial support during the course of this work.

In the preparation of the thesis, thanks are due to Mrs M.A. Stretton for drawing most of the figures, to Miss V.L. Bethell and Dr D.A.D. Parry for proof-reading and to Mrs J.R. Parry for typing. I am similarly obligated to Messrs P.T. Tuttiett and D.S. Munro, who wrote the computer programs for graphical presentation of the thermal analysis data. Dr M.W. Taylor made helpful suggestions of a general nature.

Finally, I am grateful to my wife and family for their continued interest and encouragement over what must have seemed an interminable period.

TABLE OF CONTENTS

		<u>Page</u>
Chapter 1.	INTRODUCTION	1
1.1	Polymorphism of Triacylglycerols	1
1.1.1	Historical Background	1
1.1.2	Structural Features of Lipids in the Solid State	2
1.1.3	Monoacid Saturated Triacylglycerols	5
1.1.4	Unsaturated Triacylglycerols	13
1.1.5	Diacid Saturated Triacylglycerols	18
1.1.6	Enantiomeric Triacylglycerols	21
1.2	Infrared Spectroscopy of Triacylglycerols in the Solid State	22
1.2.1	Assignments of Characteristic Absorption Bands	22
1.2.2	Spectral Differences between Polymorphic Forms	24
1.3	Melting and Solidification of Fats	27
1.3.1	Technical Importance of the Phase Behaviour of Fats	27
1.3.2	Polymorphism of Fats	27
1.3.3	Solid Miscibility of Fats	28
1.3.4	Melting and Solidification of Milkfat and Milkfat Fractions	29
1.4	Aim of the Present Work	33
1.4.1	Selection of Triacylglycerols for Synthesis	33
Chapter 2.	MATERIALS AND METHODS	36
A	Analytical and Synthetic Methods	36
2.1	Materials	36
2.1.1	Solvents	36
2.1.2	Reagents	36
2.1.3	Fatty Acids	37
2.1.4	Storage of Glycerides and Synthetic Intermediates	37
2.2	Analytical Methods	37
2.2.1	Thin-Layer Chromatography	37
2.2.2	Column Chromatography	39
2.2.3	Gas-Liquid Chromatography	40
2.2.4	Structural Analysis of Triacylglycerols	40

	<u>Page</u>	
2.3	Preparation of Racemic Triacylglycerols	40
2.3.1	Acyl Chlorides	42
2.3.2	1-Acyglycerols	42
2.3.3	1,3-Diacylglycerols	44
2.3.4	1,2-Distearoylglycerol	47
2.3.5	Triacylglycerols	49
2.4	Preparation of Enantiomeric Triacylglycerols	50
2.4.1	1,2-Isopropylidene- <u>sn</u> -glycerol	50
2.4.2	1,2-Diacyl- <u>sn</u> -glycerols	52
2.4.3	Triacylglycerols	53
B	Physical Methods	54
2.5	Melting Point Determination	54
2.6	X-Ray Powder Diffraction	54
2.6.1	Apparatus	54
2.6.2	Preparation of Samples	54
2.6.3	Identification of Polymorphs	54
2.7	Infrared Spectroscopy	55
2.7.1	Apparatus	55
2.7.2	Investigation of Polymorphism	55
2.7.3	Identification of Polymorphs	56
2.8	Thermal Analysis	56
2.8.1	Apparatus	56
2.8.2	Calibration	57
2.8.3	Presentation of Data	57
2.8.4	Investigation of Polymorphism	59
2.8.5	Identification of Polymorphs	61
2.9	Preparation of $\beta$ PSP and $\beta'$ SPS	61
Chapter 3.	RESULTS	62
3.1	Structural Analysis of Triacylglycerols	62
3.2	Polymorphism of Racemic Triacylglycerols	62
3.2.1	Palmitoyl-Stearoyl and Elaidoyl-Stearoyl Triacylglycerols	62
3.2.2	1-Butyryl-2-Oleoyl and 1,2-Dioleoyl Triacylglycerols	64
3.2.3	1,2-Dibutyryl-3-palmitoylglycerol	66

	<u>Page</u>	
3.2.4	2-Oleoyl Triacylglycerols	67
3.2.5	2-Butyryl-1,3-distearoylglycerol	72
3.2.6	1-Butyryl Triacylglycerols	73
3.2.7	1-Butyryl-2-elaidoyl-3-stearoylglycerol	75
3.2.8	1-Oleoyl Triacylglycerols	76
3.3	Polymorphism of Enantiomeric Triacylglycerols	81
3.3.1	Comparison of the Polymorphism of Corresponding Enantiomeric and Racemic Triacylglycerols	81
Chapter 4.	DISCUSSION	120
4.1	Polymorphism of Racemic Triacylglycerols	120
4.1.1	Palmitoyl-Stearoyl and Elaidoyl-Stearoyl Triacylglycerols	120
4.1.2	1-Butyryl-2-Oleoyl and 1,2-Dioleoyl Triacylglycerols	121
4.1.3	1,2-Dibutyryl-3-palmitoylglycerol	123
4.1.4	2-Oleoyl Triacylglycerols	124
4.1.5	2-Butyryl-1,3-distearoylglycerol	127
4.1.6	1-Butyryl Triacylglycerols	128
4.1.7	1-Butyryl-2-elaidoyl-3-stearoylglycerol	132
4.1.8	1-Oleoyl Triacylglycerols	133
4.2	Polymorphism of Enantiomeric Triacylglycerols	136
4.2.1	Comparison of the Polymorphism of Corresponding Enantiomeric and Racemic Triacylglycerols	136
4.3	Conclusion	138
	APPENDIX	140
	Thermal and Spectral Data for the Polymorphic Forms of the Individual Triacylglycerols	
	BIBLIOGRAPHY	193

LIST OF TABLES

<u>Table</u>		<u>Page</u>
1.1	Classification of the Polymorphic Forms of Glycerides	8
1.2	The Polymorphs of 1-Oleoyl and 2-Oleoyl Disaturated Triacylglycerols	15
1.3	Characteristic Bands in the Solid State Spectra of Triacylglycerols	23
1.4	Methylene Wagging Band Distributions for the Alpha Forms of the Monoacid Triacylglycerols of Elaidic, Oleic, Palmitic and Stearic Acids	25
1.5	Comparison of the Spectra of $\alpha$ , $\beta'$ and $\beta$ Polymorphs of Monoacid Saturated Triacylglycerols	26
1.6	Selection of Triacylglycerols for Synthesis	34
3.1	Positional Analysis of Synthetic Triacylglycerols	83
3.2	Stereospecific Analysis of <u>sn</u> -SSO and <u>sn</u> -SSB	83
3.3	X-Ray Short Spacings of the Solvent Crystallised Forms of Palmitoyl-Stearoyl and Elaidoyl-Stearoyl Triacylglycerols	84
3.4	Melting Points and Heats of Fusion of the Polymorphic Forms of Palmitoyl-Stearoyl and Elaidoyl-Stearoyl Triacylglycerols	85
3.5	Melting Points and Heats of Fusion of the Polymorphic Forms of OOS, OOP, BOS, BOP and BBP.	86
3.6	X-Ray Short Spacings of the Solvent Crystallised Forms of SOS, POS, POP and SBS	87
3.7	Melting Points and Heats of Fusion of the Polymorphic Forms of SOS, POS, POP and SBS	88
3.8	X-Ray Short Spacings of the Solvent Crystallised Forms of BSS, BSP, BPS, BPP and BES	89
3.9	Melting Points and Heats of Fusion of the Polymorphic Forms of BSS, BSP, BPS, BPP and BES	89
3.10	X-Ray Short Spacings of the Solvent Crystallised Forms of OSS, OSP, OPS and OPP	90
3.11	Melting Points and Heats of Fusion of the Polymorphic Forms of OSS, OSP, OPS and OPP	91
3.12	X-Ray Short Spacings of the Solvent Crystallised Forms of Corresponding Racemic and Enantiomeric Triacylglycerols	92
3.13	Melting Points and Heats of Fusion of the Polymorphic Forms of Corresponding Racemic and Enantiomeric Triacylglycerols	92

## APPENDIX

1	Melting Points of the Stable Forms of Triacylglycerols	141
2	Some Common Bands in the Infrared Spectra of Related Stable Forms	142
3	Some Common Bands in the Infrared Spectra of Related $\beta$ and $\beta'$ Forms	143

LIST OF FIGURES

<u>Figure</u>		<u>Page</u>
1-1	Triclinic parallel and orthorhombic perpendicular subcells	3
1-2	The main polymorphic forms of monoacid triacylglycerols	6
1-3	Melting points of monoacid triacylglycerols	9
1-4	Molecular arrangement of trilaurin, b-axis projection	10
1-5	Triacylglycerols in the liquid state, proposed lamellar structure	12
1-6	Triple chain structure of the $\beta$ stable form of 2-oleoyl-distearoylglycerol	16
1-7	Layer stacking of methyl end groups in the $\beta$ forms of $C_n/C_{n\pm 2}$ triacylglycerols showing the two terrace structures	20
1-8	Triacylglycerols of milkfat	31
2-1	Scheme for the preparation of oleic acid	38
2-2	General scheme for the synthesis of racemic triacylglycerols	41
2-3	Synthesis of racemic triacylglycerols	43
2-4	Synthesis of racemic 1,2-diacylglycerol	48
2-5	Synthesis of enantiomeric triacylglycerols	51
2-6	Conventions for the presentation of thermal analysis data	58
3-1	X-Ray diffraction patterns of the $\beta$ stable forms of palmitoyl-stearoyl and elaidoyl-stearoyl triacylglycerols	93
3-2	X-Ray diffraction patterns of the $\beta$ and $\beta'$ forms of PSP and SPS	94
3-3	Melting thermograms of $\alpha$ SSS, SPS, PPP and SES	95
3-4	Melting thermograms of $\alpha$ PSP, PSS, PPS and ESS	96
3-5	Melting thermograms of $\beta'$ SSS, PPP and SES	97
3-6	Melting thermograms of $\beta'$ PSS, PPS and ESS	98
3-7	Melting thermograms of the solvent crystallised $\beta'$ and $\beta$ forms of SPS and PSP	99
3-8	IR spectra of the $\beta'$ stable forms of OOS, OOP, BOS and BOP	100
3-9	Melting thermograms of $\alpha$ OOS, OOP, BOS and BOP	101
3-10	X-Ray diffraction patterns of the $\beta$ stable forms of SOS, POS, POP and SBS	102
3-11	IR spectra of the $\beta$ stable forms of SOS, POS, POP, SBS, SES and ESS	103
3-12	IR spectra of comparative $\beta_2$ and $\beta'$ polymorphs of SOS, POS and POP	104
3-13	Melting thermograms of $\alpha$ SOS, POS and POP	105
3-14	Melting thermograms of the intermediate forms of SOS, POS and POP	106
3-15	Polymorphism of SOS, POS and POP	107

<u>Figure</u>		<u>Page</u>
3-16	IR spectra of the $\beta'$ stable forms of OXY and BXY triacylglycerols	108
3-17	X-Ray diffraction patterns of the $\beta'$ stable forms of OXY and BXY triacylglycerols	109
3-18	Melting thermograms of $\alpha$ BSS, BSP, BPS and BPP	110
3-19	Melting thermograms of the intermediate forms of BSS, BSP, BPS and BPP	111
3-20	Melting thermograms of $\alpha$ OSS, OSP, OPS and OPP showing the presence of the $\alpha_2$ form at high heating rates	112
3-21	Melting thermograms of $\alpha$ OSS, OSP, OPS and OPP recorded after tempering at the $\alpha_2$ peak temperature	113
3-22	Melting thermograms of $\alpha$ OSS, OSP, OPS and OPP recorded at low heating rates	114
3-23	Melting thermograms of the intermediate forms of OSS, OSP, OPS and OPP	115
3-24	Polymorphism of OSS, OSP, OPS and OPP	116
3-25	IR spectra of the $\beta'$ stable forms of racemic and enantiomeric triacylglycerols	117
3-26	X-Ray diffraction patterns of the stable forms of corresponding racemic and enantiomeric triacylglycerols	118
3-27	Melting thermograms of the $\alpha$ forms of <u>rac</u> - and <u>sn</u> -SSB and SSO showing the more rapid transformation of the antipodes	119
4-1	Comparison of glycerol conformations in "tuning-fork" and "chair" structures	130

## APPENDIX

1	Thermal behaviour of SSS	144
2	Thermal behaviour of PSS	145
3	Thermal behaviour of PPS	146
4	Thermal behaviour of PPP	147
5	Thermal behaviour of SPS	148
6	Thermal behaviour of PSP	149
7	Thermal behaviour of SES	150
8	IR spectra of SES	151
9	Thermal behaviour of ESS	152
10	IR spectra of ESS	153
11	Thermal behaviour of OOS	154
12	IR spectra of OOS	155
13	Thermal behaviour of OOP	156
14	IR spectra of OOP	157
15	Thermal behaviour of BOS	158
16	IR spectra of BOS	159
17	Thermal behaviour of BOP	160

<u>Figure</u>		<u>Page</u>
18	IR spectra of BOP	161
19	Thermal behaviour of BBP	162
20	IR spectra of BBP	163
21	Thermal behaviour of SOS	164
22	Crystallisation of SOS from the melt	165
23	IR spectra of SOS	166
24	Thermal behaviour of POS	167
25	IR spectra of POS	168
26	Thermal behaviour of POP	169
27	IR spectra of POP	170
28	Thermal behaviour of SBS	171
29	IR spectra of SBS	172
30	Thermal behaviour of <u>sn</u> -SSB	173
31	Thermal behaviour of BSS	174
32	IR spectra of BSS	175
33	Thermal behaviour of BSP	176
34	IR spectra of BSP	177
35	Thermal behaviour of BPS	178
36	Thermal behaviour of BPP	179
37	IR spectra of BPP	180
38	Thermal behaviour of BES	181
39	IR spectra of BES	182
40	Thermal behaviour of <u>sn</u> -SSO	183
41	Thermal behaviour of OSS	184
42	IR spectra of OSS	185
43	Thermal behaviour of OSP	186
44	IR spectra of OSP	187
45	Thermal behaviour of OPS	188
46	IR spectra of OPS	189
47	Thermal behaviour of <u>sn</u> -PPO	190
48	Thermal behaviour of OPP	191
49	IR spectra of OPP	192

## NOMENCLATURE

In general, the recommendations of the IUPAC-IUB Commission on Biochemical Nomenclature (1976; Lipids 12 (1977), 455) are followed for the nomenclature of lipids containing glycerol. However, the abbreviations MG, DG and TG are used for mono-, di- and triacylglycerol respectively. For the sake of brevity, TGs are specified by a three letter code in which the letters indicate the acyl group (B, butyryl; E, elaidoyl; L, lauroyl; O, oleoyl; P, palmitoyl and S, stearoyl) and the order of the symbols represents the position of the acyl group in the TG molecule. Enantiomeric TGs are distinguished by the prefix 'sn-', while TGs without a prefix are understood to be racemic. Thus sn-PPO represents 1,2-dipalmitoyl-3-oleoyl-sn-glycerol and POS (or SOP) represents rac-1-palmitoyl-2-oleoyl-3-stearoylglycerol.

The polymorphic forms of TGs are designated according to Larsson's modification (Larsson, 1966a) on Lutton's system of classification (Lutton, 1950). Where necessary, the chain multiplicity of a particular form is indicated by a suffix. Thus the term ' $\beta$ -2' represents a  $\beta$  form with a chain multiplicity of 2.

## Chapter 1

INTRODUCTION1.1 Polymorphism of Triacylglycerols1.1.1 Historical Background

The multiple melting behaviour of saturated triacylglycerols (TGs) was first observed in 1849. However, the basis for this phenomenon was not understood until 1934 when Clarkson and Malkin demonstrated that it was due to polymorphism, i.e. the occurrence for a given compound of different crystal forms. Clarkson and Malkin recorded the X-ray diffraction patterns of only two crystal forms ( $\alpha$  and  $\beta$  in modern notation) for even monoacid TGs, although three melting points were earlier known to exist. Presuming that the third form was vitreous, they gave an erroneous conjunction between melting points and phases. In 1945, Lutton and other American workers re-examined the polymorphism of the monoacid TGs and discovered the error in Malkin's association of melting points with X-ray diffraction patterns. Lutton obtained the diffraction pattern of the intermediate form ( $\beta'$ ) and was able to give a correct description of the polymorphism. Unfortunately, Malkin did not accept this correction, but regarded the  $\beta'$  form as a fourth modification. The controversy continued for several years until Chapman (1955-1965) introduced infrared (IR) spectroscopy into studies of glyceride polymorphism and confirmed Lutton's results.

Although Chapman's work resolved many of the earlier questions about TG polymorphism, neither IR spectroscopy nor X-ray powder diffraction could give the detailed structural information made available by application of single crystal X-ray techniques. The first single crystal analysis of a TG was performed in 1951, when Vand and Bell determined the chain structure of the stable  $\beta$  form of trilaurin. However, it was not until 1960 that the general molecular arrangement was resolved (Vand, private communication to Chapman, 1962). The complete structure determination was finally reported by Larsson in 1963 and in the same year Jensen and Mabis solved the essentially isomorphous structure of  $\beta$  tricaprin. Larsson subsequently made an incomplete analysis of the  $\beta'$  form of trilaurin in which the main features of the crystal structure were revealed (1964b, 1971). Only one further TG structure has been reported, that of the  $\beta$  form of the diacid TG, rac-2-(11-bromoundecanoyl)-1,3-dicaproylglycerol (Doynes and Gordon, 1968). In spite of the small

number of structures that have been solved, X-ray single crystal analyses have provided a most important contribution to our understanding of TG polymorphism.

### 1.1.2 Structural Features of Lipids in the Solid State

The structural principles involved in the molecular arrangement of lipids are a consequence of the requirements of close packing. Kitaigorodskii (1957) explained these principles in a thorough analysis of the packing of simple lipids and Larsson (1964b, 1972) subsequently extended the concepts to include glyceride structures.

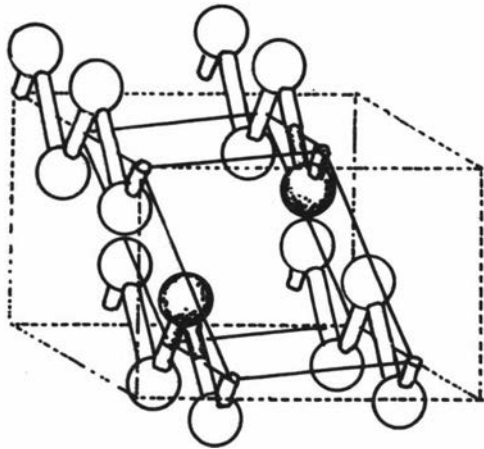
#### (a) Molecular Direction

Except for cases where strong ionic forces are involved, the solid state structure of lipids is dominated by the lateral packing of the hydrocarbon chains. The chains are arranged in an extended planar zig-zag conformation with their axes aligned parallel to one another to form molecular layers. This arrangement gives the closest packing and hence the highest possible van der Waals interaction between chains. The layers are stacked so that the terminal planes of end groups are in contact. Hydrocarbon derivatives with a head group at one end (e.g. fatty acids) are arranged head-to-head in a bimolecular repetition layer to allow maximum interaction between the polar groups.

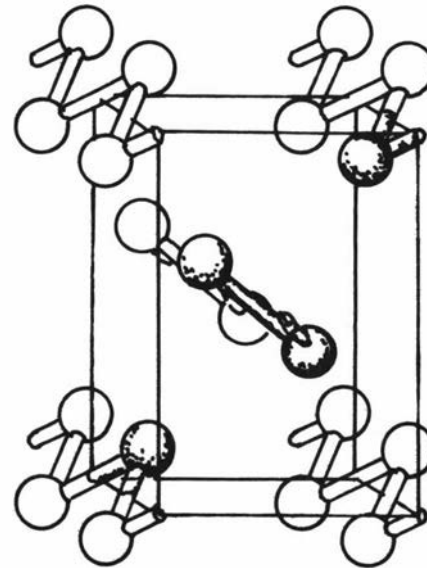
As a consequence of their molecular arrangement, long chain compounds give X-ray powder diffraction patterns which consist of two independent groups of spacings, referred to as long and short spacings. The long spacings give the thickness of the unit layer while the short spacings are related to the lateral packing or cross-sectional arrangement of the chains.

#### (b) Chain Packing

Perhaps the most important structural feature of long chain hydrocarbon compounds is that the chains can pack in a number of different lateral arrangements which are energetically almost equivalent (i.e. have similar van der Waals interaction energies). The alternative packing modes, which form the most common basis for lipid polymorphism, can best be described in terms of their subcell symmetry, where the subcell corresponds to the smallest repetition unit within the chain structure (Muller, 1927; Vand, 1951). Two of the most common chain packings are shown in Fig. 1-1. They are: T//, triclinic parallel, in which all the zig-zag planes of carbon atoms are parallel (Vand and Bell, 1951) and O⊥, orthorhombic perpendicular, in which there are two equal sets of chain planes arranged so that every chain plane is approximately



TRICLINIC SUBCELL,  
T II



ORTHORHOMBIC SUBCELL,  
O ⊥

FIG. 1-1 TRICLINIC PARALLEL AND ORTHORHOMBIC  
PERPENDICULAR SUBCELLS

perpendicular to its four nearest neighbours (Bunn, 1939). In addition to T// and O $\perp$ , several other subcells with parallel or perpendicular chain plane arrangements are known (Larsson, 1972), although they have been observed only rarely.

Many long chain compounds crystallise from the melt in a form, usually called  $\alpha$ , in which the hydrocarbon chains either rotate or undergo torsional oscillation. The chains pack together like a bundle of long cylinders in a hexagonal array (Muller, 1932), although the actual crystallographic symmetry may be lower than that for true hexagonal packing (Larsson, 1967). Because of the rotational freedom of the chains, the hexagonal form (subcell H) has a lower packing density than subcells in which the chains are in the planar zig-zag conformation. Geometrically, the hexagonal form may be considered a variant on the O $\perp$  subcell, derived by an increase in the long axis until the angle between the basal diagonals is 60°. In fact, both rise in temperature and steric distortion cause O $\perp$  to approach the hexagonal form in this manner (Abrahamsson, Stållberg-Stenhagen and Stenhagen, 1963).

(c) Layer Stacking and Angle of Tilt

The subcell regularity of the layers is unchanged by relative chain displacements of an integral multiple of the subcell axis in the chain direction ( $C_s$ ). Different angles of tilt between the chain axes and the end group planes are therefore possible for every chain packing. However, the number of possible angles of tilt for a particular chain packing is severely constrained by the opposing requirements of the polar and methyl end groups (Kitaigorodskii, 1957). A high angle of tilt gives more space for bulky polar end groups, but results in a reduced van der Waals interaction in the methyl end group region because of contacts between methyl and methylene groups. Thus, in simple carbon chain compounds such as the n-alkanes and n-fatty acids, the displacement of adjacent chains does not exceed one subcell period,  $C_s$  (Abrahamsson et al., 1963).

The particular tilt arrangement of a structure is best represented by the Miller indices of the subcell plane containing the methyl end groups or layer boundary (Vand, 1954). This classification is more informative than merely giving the angle of tilt since it illustrates other structural features such as the occurrence of terraces in the  $\beta$  form of simple TGs (Larsson, 1964b).

(d) Summary

The packing of hydrocarbon chain compounds in the solid state can be visualised as:-

- 1) lateral packing of the chains to form unit layers - the packing is represented by the subcell
- 2) stacking of the unit layers into the three-dimensional structure - the stacking is determined by the end group interactions and represented by the subcell indices of the layer boundary.

Generally, polymorphism in lipids arises from differences in either the subcell or the layer stacking, both of which must therefore be specified to define a particular form. The demands of close packing restrict the number of possible polymorphs and thus similar structures are often found for different long chain compounds (Abrahamsson et al., 1963).

The same packing principles are also applicable to TG structures. The three acyl groups may be regarded as separate chain units with the constraint that attachment to the glycerol head group results in a loss of translational freedom (Larsson, 1972).

1.1.3 Monoacid Saturated Triacylglycerols(a) Description of Polymorphism

Monoacid saturated TGs of n-fatty acids exhibit three main crystal forms,  $\alpha$ ,  $\beta'$  and  $\beta$  (Lutton's terminology, 1950). Related polymorphic forms occur in more complex TGs and in many fats and oils. Fig. 1-2 shows the subcell and layer boundary classifications of the three forms and the transformational relationships which occur in simple TGs (Larsson, 1964b). Rapid cooling of the melt gives the vertical  $\alpha$  form in which the chains have cylindrical symmetry, subcell H. In contrast to simple lipids, the chains cannot rotate freely in the  $\alpha$  form of TGs and, instead, undergo a torsional oscillation which increases with temperature (Larsson, 1964b). The  $\alpha$  form has the lowest melting point of the three TG polymorphs and transforms irreversibly on heating to either  $\beta'$  or  $\beta$ . The  $\beta'$  form, which in simple TGs is of intermediate stability, has O1 subcell symmetry. It is normally obtained by transformation of the  $\alpha$  form at its melting point or crystallisation of the melt at the same temperature. The stable  $\beta$  form, which like  $\beta'$  is a tilted form, is prepared by crystallisation from solvents or by transformation of  $\alpha$  or  $\beta'$ . TG polymorphism is monotropic, that is, there is only one form thermodynamically stable under all conditions. Transitions

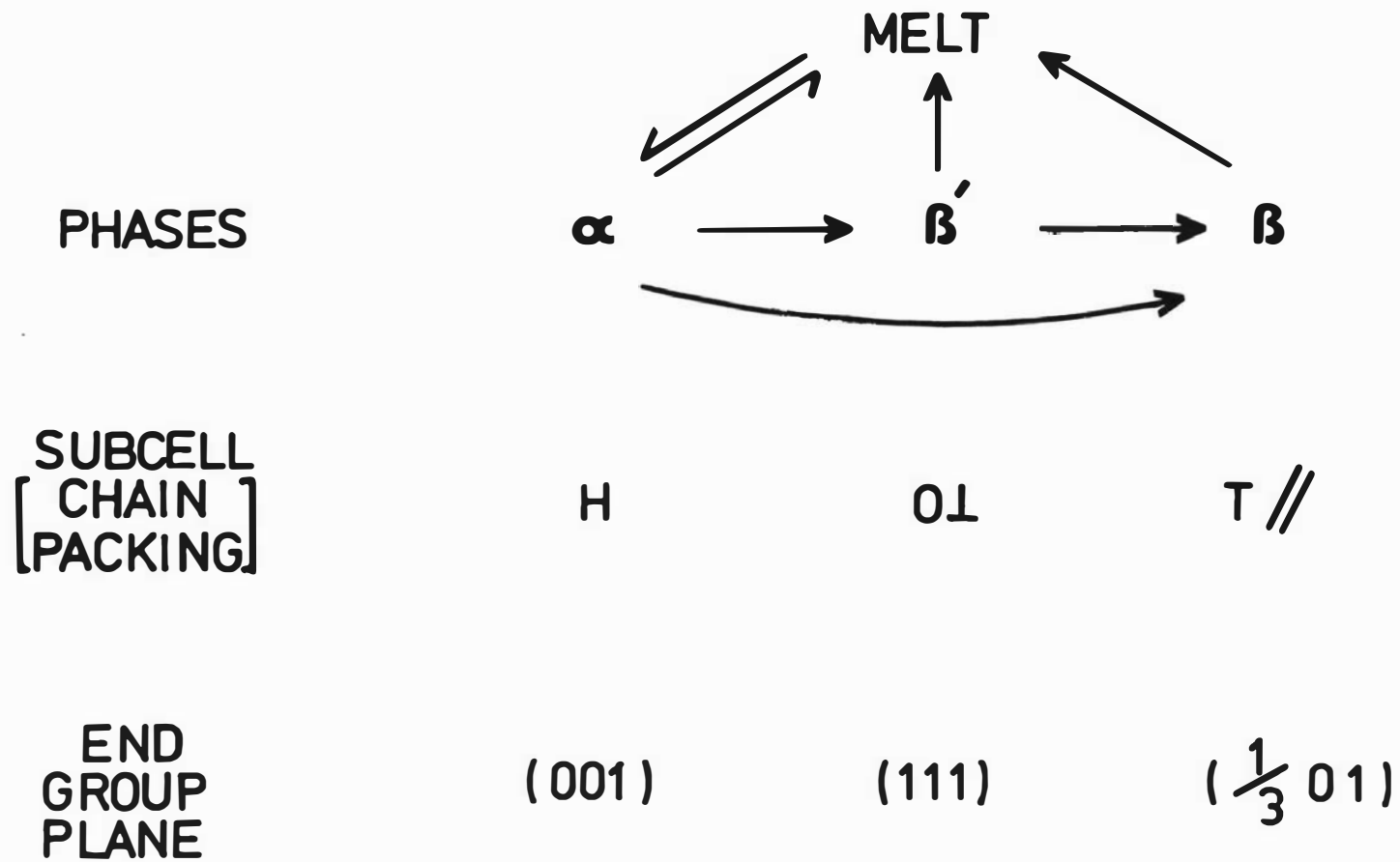


FIG. 1-2 THE MAIN POLYMORPHIC FORMS OF MONOACID TRIACYLGLYCEROLS

between the forms occur in only one direction under all conditions (Fig. 1-2).

Criteria for the classification of TG polymorphs are given in Table 1.1. Lutton's scheme (Lutton, 1950) is based on the characteristic short spacings of the three main subcells, H, O $\perp$  and T//. A weakness of this classification, however, is that short spacing data may be unreliable in cases of subcell distortion or uninterpretable in the presence of an unusual subcell. Accordingly, Larsson (1964b, 1966a) suggested a generalisation of Lutton's scheme in which both IR spectra and X-ray short spacing data are used to classify the forms unequivocally according to the arrangement of the chain planes ( $\alpha$ , rotating;  $\beta'$ , perpendicular;  $\beta$ , parallel).

Fig. 1-3 shows the  $\alpha$ ,  $\beta'$  and  $\beta$  melting points of the monoacid TGs of C<sub>10:0</sub> to C<sub>22:0</sub> n-fatty acids (Lutton and Fehl, 1970). For each TG the order of increasing melting point is  $\alpha < \beta' < \beta$ . The melting points of the three forms increase with chain length, but only the  $\beta$  melting point shows alternation between even and odd members of the series. Such alternation depends on differences in packing densities at the layer interface (Larsson, 1964b; 1966b). If the layer boundary has the same appearance for even and odd members of an homologous series of isomorphous forms, then the series will be non-alternating and vice versa. For the T// subcell, none of the possible layer boundaries has the same structure for even and odd chains, so the  $\beta$  polymorphs of monoacid TGs form an alternating series. However, the  $\alpha$  polymorphs are non-alternating because of the rotational symmetry of the chains, which results in an equivalent end group structure for even and odd regardless of the layer boundary. In the case of the O $\perp$  subcell, there are no end group planes with exactly the same structure for even and odd, but layer boundaries such as (0, n, 1) or (n, n, 1) for n = 1, 3, 5 ... show very close resemblance between even and odd. Since the layer boundary of the  $\beta'$  form of monoacid TGs satisfies the latter condition, the  $\beta'$  polymorphs show no detectable alternation of physical properties.

(b) Molecular Arrangement of  $\beta$  and  $\beta'$  Forms

Fig. 1-4 shows the b-axis projection of the  $\beta$  form of trilaurin (Larsson, 1963; 1964a). The molecular conformation may be described as an unsymmetrical 'tuning-fork' in which chains 1 and 2 are extended in a straight line and chain 3 is close packed alongside chain 1. The molecules are arranged in double chain layers with the glycerol residues at the centre and the methyl groups on the layer boundaries. This arrangement corresponds to the head-to-head bimolecular layer structure common to many long chain compounds.

Table 1.1: Classification of the Polymorphic Forms of Glycerides

			Criteria for Classification	
			Lutton <sup>a</sup>	Larsson <sup>b</sup>
Basis for Classification	Characteristic short spacings of H, O and T// subcells		Arrangement of chain planes (rotating, perpendicular or parallel)	
Polymorphic Forms	Sub- $\alpha$	a low temperature phase transforming reversibly or irreversibly to $\alpha$ ; spacings near 4.2 and 3.8 $\text{\AA}$		1) a phase transforming reversibly to $\alpha$ irrespective of spacings (Larsson 1964b), or 2) this term is eliminated (Larsson, 1966a)
	$\alpha$	single <u>strong spacing</u> near 4.1 $\text{\AA}$		single <u>strong spacing</u> near 4.1 $\text{\AA}$
	$\beta'$	strong spacings near 4.2 and 3.8 $\text{\AA}$		1) spacings near 4.2 and 3.8 $\text{\AA}$ <u>or</u> 4.3, 4.0 and 3.7 $\text{\AA}$ , and 2) doublet near 720 $\text{cm}^{-1}$ in the IR spectrum
	$\beta$	a strong (usually the strongest) line near 4.6 $\text{\AA}$		does not satisfy criteria for $\alpha$ or $\beta'$
Nomenclature for two forms satisfying the same criteria (e.g. $\beta$ )		sub- $\beta$ and $\beta$ in order of increasing melting point		$\beta_2$ and $\beta_1$ in order of increasing melting point

a Lutton (1950); Wille and Lutton (1966); Lutton and Fehl (1970). In Lutton's terminology the chain multiplicity is denoted by a suffix: thus,  $\beta'-2$ ,  $\beta-3$ .

b Larsson (1964b; 1966a). Larsson recommended elimination of the term sub- $\alpha$  because if the transition to  $\alpha$  is second order, then sub- $\alpha$  is not a separate phase, while if the transition to  $\alpha$  is first order, then sub- $\alpha$  is more properly named  $\beta'$ .

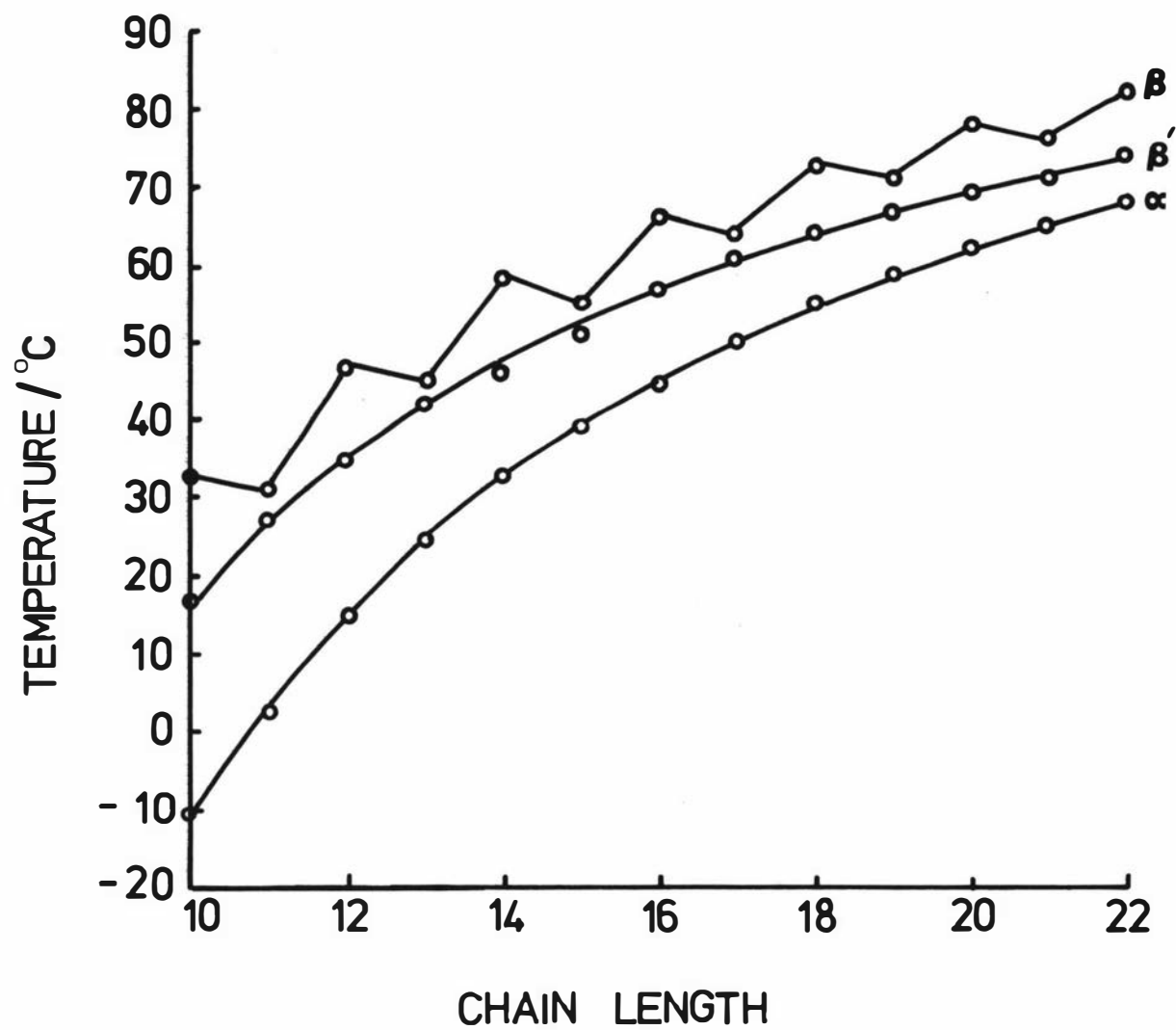


FIG. 1-3 MELTING POINTS OF MONOACID TRIACYLGLYCEROLS  
(LUTTON AND FEHL, 1970)

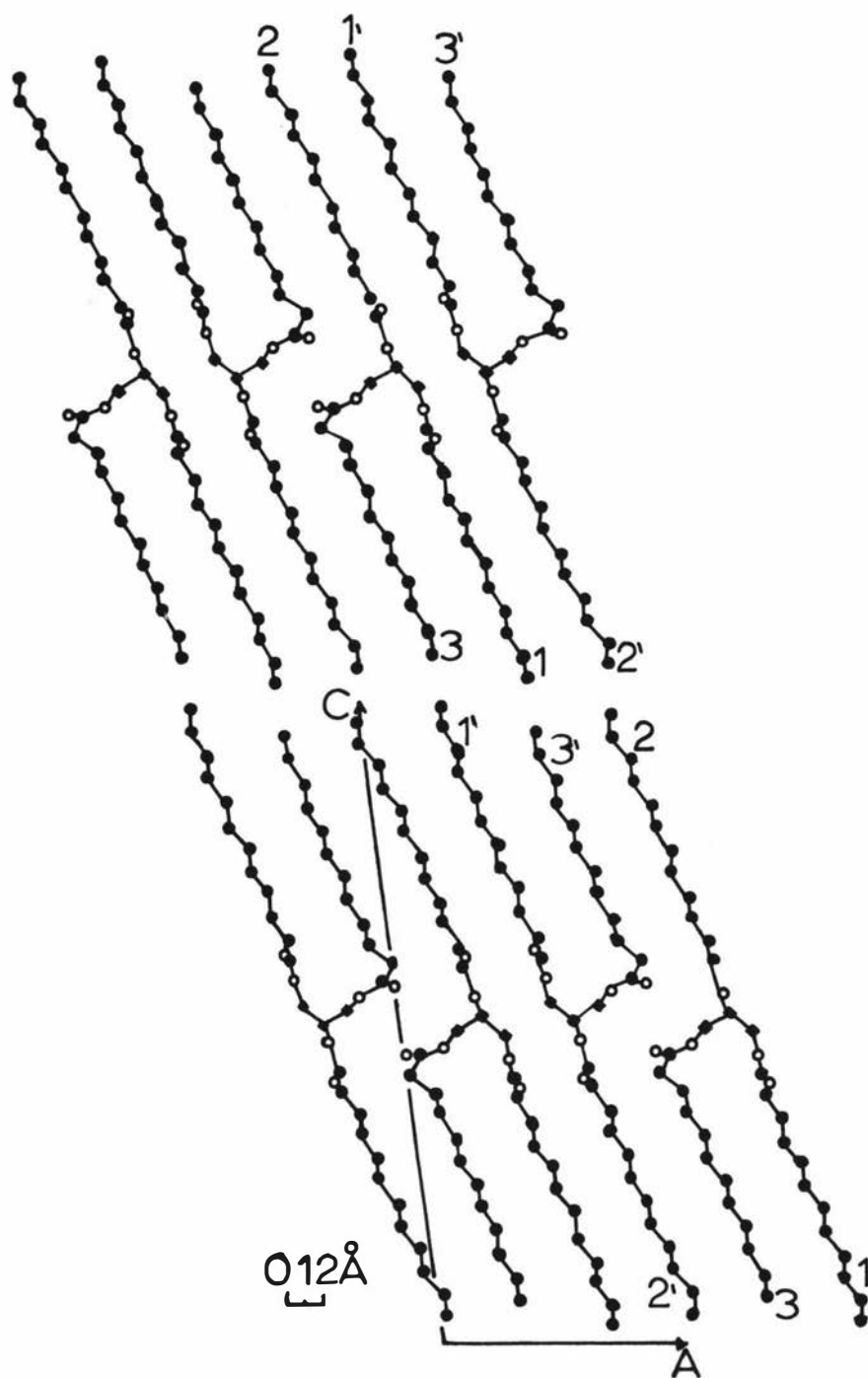


FIG.1-4 MOLECULAR ARRANGEMENT OF TRILAURIN  
 B - AXIS PROJECTION  
 ( LARSSON , 1963 )

Key: ■ glyceryl carbon atom, ● acyl carbon atom,  
 O oxygen atom .

An unusual feature of the TG structure is that the methyl end groups form terraces while in most other long chain structures the terminal groups lie in one plane or in two parallel planes (Larsson, 1964a). In the layer boundary classification the occurrence of terraces is indicated by a fractional Miller index, thus the classification for the  $\beta$  form is  $(1/3\ 0\ 1)$ . The terraced structure has an important influence on the stability of the  $\beta$  form of TGs containing fatty acids of different chain lengths (Larsson, 1972).

Although the structures of the  $\alpha$  and  $\beta'$  forms of simple TGs are not known in such detail as that of the  $\beta$  form, it is probable that the tuning-fork conformation occurs in both polymorphs (Larsson, 1964b). Some incomplete single crystal studies of  $\beta'$  by Larsson (1964b, 1971) and Webb (private communication to Lutton, 1972) have shown that the

molecules are packed in a double chain layer with a change in the direction of tilt at the glycerol residue. The chain tilt alternates between opposite directions in successive double layers so that chains on opposite sides of the layer boundary are parallel. Thus the chain axes are arranged in a zig-zag pattern with a repetition period of four chain layers. According to Larsson (1966a), the  $\beta'$  end group structure,  $O\perp(111)$ , can readily accommodate different chain lengths and this partly explains the increased stability of the  $\beta'$  form in mixed TGs and fats.

(c) Liquid State

Close packing considerations suggest that the tuning-fork structure probably persists above the melting point since conformations in which the third chain is not folded back parallel to the first two are very much less compact. Both nuclear magnetic resonance (NMR) (Callaghan, 1977) and X-ray diffraction (Larsson, 1971; 1972) studies of TG melts are consistent with this tuning-fork liquid state model, and Larsson has proposed a short-range lamellar arrangement formed by the lateral interlocking of these units (Fig. 1-5). In general, simple lipid molecules such as fatty acids do not possess a lamellar structure in the liquid state, although such structures are found in the mesomorphic forms of more complex lipids (Lutton, 1972).

Since the structures of the TG melt and the loosely packed  $\alpha$  form are so similar, crystallisation of the  $\alpha$  form is kinetically favoured over that of the more tightly packed  $\beta'$  or  $\beta$  form. Larsson (1971) has suggested that natural fats show similar solidification behaviour to simple TGs because glycerides with different chain lengths can readily be accommodated in the same liquid lamellar structure units adopted by

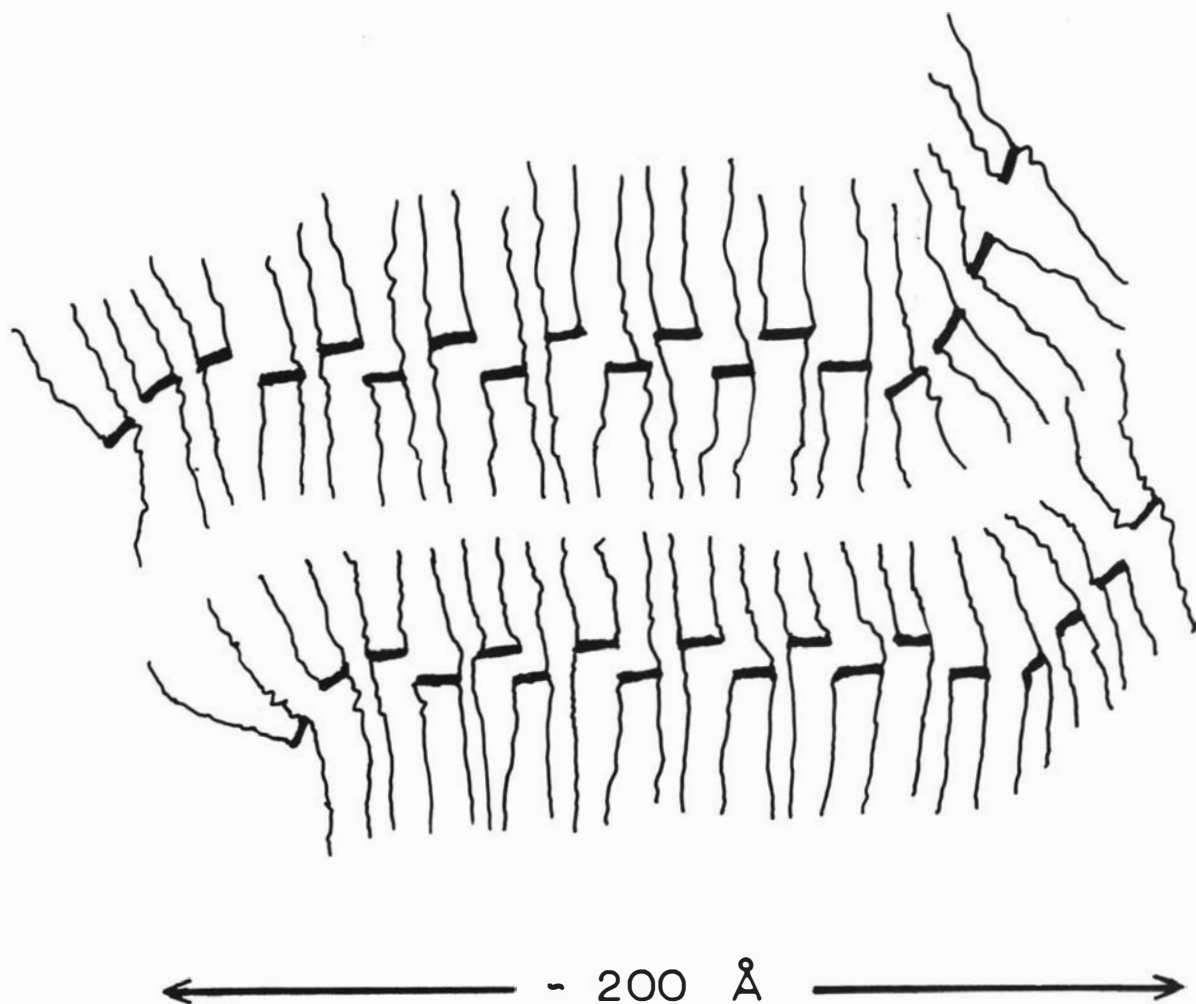


FIG.1-5 TRIACYLGLYCEROLS IN THE LIQUID STATE  
PROPOSED LAMELLAR STRUCTURE  
( LARSSON, 1972 )

monoacid TGs.

(d) Additional Forms

On cooling the  $\alpha$  form, the chain oscillation is progressively reduced permitting tighter packing of the chains within the lattice. At sufficiently low temperatures ( $-50$  to  $-70^{\circ}\text{C}$  for tristearin; Chapman, 1962; Larsson, 1964b), a gradual and reversible transition to the  $\text{O}\perp$  subcell is observed with no change in long spacing. The continuous enantiotropic nature of the transition suggests that it is second order (Chapman, 1962; Larsson, 1964b), although no accurate heat capacity data have yet been reported to confirm this. The transformation was first reported by Jackson and Lutton (1950) who called the low-temperature form 'sub- $\alpha$ '. Larsson (1966a) has suggested that this term should be avoided because the form is not strictly a separate phase. However the name will be used here as it is convenient for describing spectral patterns.

In addition to sub- $\alpha$  and the three main forms occurring in simple TGs, there is evidence for the existence of at least one other form. In a survey of the thermal behaviour of saturated and unsaturated monoacid TGs, Hagemann, Tallent and Kolb (1972) noted that the saturated TGs showed two endothermic transitions intermediate between the least stable ( $\alpha$ ) and most stable ( $\beta$ ) polymorphs. Hagemann *et al.* attributed these transitions to the melting of multiple  $\beta'$  forms, which, in accordance with Larsson's nomenclature (Table 1.1), were labelled  $\beta'_1$ ,  $\beta'_2$  in order of decreasing melting point. Perron, Petit and Mathieu (1969) had earlier reported a sub- $\beta'$  form ( $\beta'_2$  according to Larsson's nomenclature) for the mixed TGs PSS, PPS and PSP, although their evidence, based on differential thermal analysis, was less convincing than that of Hagemann. Contrary to Hagemann *et al.* (1972), these workers did not detect a  $\beta'_2$  form for SSS and PPP. The structure of the  $\beta'_2$  form is unknown although presumably it is closely related to the structure of the main  $\beta'_1$  form.

1.1.4 Unsaturated Triacylglycerols

Glycerides containing unsaturated fatty acids show similar chain packings ( $\alpha$ ,  $\beta'$  and  $\beta$ ) to those of the saturated TGs (Chapman, 1962). However, the presence of the double bond, particularly if it is cis, introduces a distortion which reduces the chain packing density and hence lowers the melting point of the unsaturated TG compared with the corresponding saturate. Trans-unsaturated TGs show similar thermal behaviour to their saturated counterparts which is a consequence of the relative ease with which the saturated chain zig-zag can accommodate a trans-

double bond. The only major difference shown by trans-TGs is that the  $\beta'$  form is frequently absent (Minor and Lutton, 1953; Hagemann *et al.*, 1972, 1975). In contrast to the trans-isomers, cis-unsaturated TGs, particularly the monoenes, show additional polymorphic complexity compared with the simple saturates.

(a) Monooleoyl Triacylglycerols

The most studied of the unsaturated TGs are the disaturated 1- and 2-oleoyl glycerides, mainly because of their practical importance in confectionary and enrobing fats (Lutton, 1972). Although there is general agreement on the stable forms, the number of polymorphic forms for these TGs is still in doubt and there is a wide diversity of melting point data, particularly for the three TGs SOS, POS and POP. In spite of the variety of results reported, the consensus would appear to favour the work of Lutton (Lutton, 1946, 1951; Lutton and Jackson, 1950; Wille and Lutton, 1966). It is significant that the very complete study of Lavery (1958) on all seven racemic monoene TGs of oleic, palmitic and stearic acids showed substantial agreement with Lutton's results. A summary of the polymorphism of these TGs based on the results of Lutton and Lavery is presented in Table 1.2.

The most characteristic feature of the polymorphism of the TGs OXY and XOY (where X and Y are palmitoyl or stearyl) is the occurrence of triple chain length structures (denoted by the suffix '-3' following the chain packing designation, Lutton, 1950). Fig. 1-6 shows the triple chain length (TCL) structure postulated by Larsson (1972) for the stable  $\beta$ -3 form of SOS, which is isomorphous with the stable forms of POS, POP and cocoa butter (Wille and Lutton, 1966). Although the tuning-fork conformation is still present, the chains are sorted into two equivalent saturated layers with the unsaturated layer sandwiched between. This 'chain sorting' allows the most efficient chain packing for each type of chain, i.e. T// for the saturated chains and O'// for the unsaturated chains. The latter subcell is adopted by the low-melting form of oleic acid and is apparently well suited for accommodation of a cis-double bond into the chain packing (Abrahamsson and Ryderstedt-Nahringbauer, 1962). The proposed molecular arrangement is supported by diffraction and spectral data, both of which show contributions from the two subcells (Larsson, 1972; Chapman, 1962).

Long spacing data for the stable forms of the OXY TGs show that they also have TCL structures, although the short spacings and IR spectra are consistent with a  $\beta'$  packing rather than the  $\beta$  packing adopted by the

Table 1.2: The Polymorphs of 1-Oleoyl and 2-Oleoyl  
Disaturated Triacylglycerols

- 1) Polymorphs<sup>a</sup> of SOS, POS and POP in order of decreasing melting point<sup>b</sup> (°C) (from Lutton, 1951; Lavery, 1958; Wille and Lutton, 1966).

SOS		POS		POP	
$\beta$ -3	44.3	$\beta$ -3	37.3	$\beta$ -3	38.3
sub- $\beta$ -3	36.2				
$\beta$ '-3 <sup>c,e</sup>	35	$\beta$ '-3	33		
		$\beta$ '-2 <sup>c</sup>	25.5	$\beta$ '-2	33.5
				sub- $\beta$ '-2 <sup>c</sup>	26.5
				sub- $\beta$ -3 or $\beta$ " <sub>M</sub> <sup>d</sup>	26.7
$\alpha$ -3	22.4	$\alpha$ -2	18.2	$\alpha$ -2	18.1
sub- $\alpha$ -3 <sup>c</sup>		sub- $\alpha$ -3 <sup>c</sup>		sub- $\alpha$ -3 <sup>c</sup>	

- 2) Polymorphs<sup>a</sup> of OSS, OSP, OPS and OPP' in order of decreasing melting point<sup>b</sup> (°C) (from Lutton, 1951; Lavery, 1958).

OSS		OSP		OPS		OPP	
$\beta$ '-3	43.5	$\beta$ '-3 <sup>e</sup>	39.8	$\beta$ '-3 <sup>e</sup>	40.2	$\beta$ '-3	35.2
		$\beta$ '-2	40.2				
				sub- $\beta$ '-3	37		
		(?) <sup>d</sup>	30.6				
$\alpha$ -3	30.4	sub- $\alpha$ -2 <sup>c</sup>	26.3	$\alpha$ -2	25.3	$\alpha$ -3	18.5
sub- $\alpha$ -3		sub- $\alpha$ -3 <sup>d</sup>	25.5	sub- $\alpha$ -2		no sub- $\alpha$ observed	

a Lutton's nomenclature is used throughout (see Table 1.1)

b melting points are primarily those reported by Lutton (1951)

c observed by Lutton only

d observed by Lavery only

e from solvent only

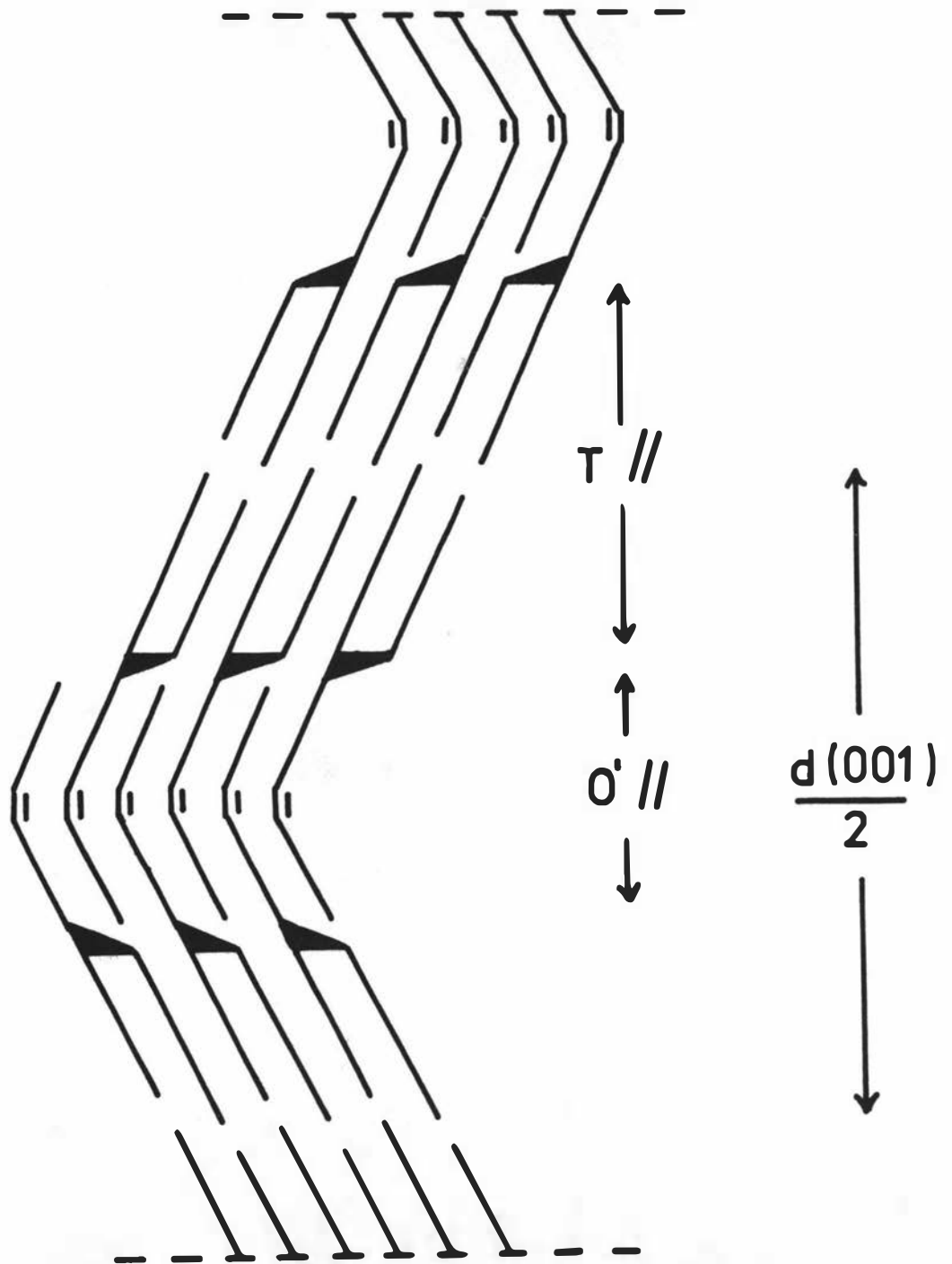


FIG.1-6 TRIPLE CHAIN STRUCTURE OF THE  $\beta$  STABLE FORM OF 2-OLEOYLDISTEAROYLGLYCEROL (LARSSON, 1972)

KEY. CHAIN AXIS ———, GLYCERYL RESIDUE ,  
OLEOYL CHAIN 

stable forms of the XOY TGs. The glycerol conformation of the OXY stable form must be different from that of the tuning-fork model because chain sorting in the TCL forms of OXY TGs can only occur if the primary and secondary saturated chains pack alongside each other leaving the oleoyl primary chain extended in the opposite direction (the so-called 'chair' conformation; Lutton, 1948). In the tuning-fork conformation both primary chains are packed together with the secondary chain extended away from them.

In addition to the subcell differences in the saturated chain layers of the stable forms of XOY and OXY TGs, there are clear differences in the oleoyl chain packings of the two forms. For example, a strong band at  $690\text{cm}^{-1}$ , attributed to the C-H out-of-plane deformation of the cis-group (Bellamy, 1975), occurs in the IR spectrum of the  $\beta$ -3 stable form of SOS but not in the spectrum of the  $\beta'$ -3 stable form of OSS (Chapman, 1956). Furthermore, NMR studies suggest that the oleoyl chains in the 1-isomer have greater mobility than those in the 2-isomer (Chapman, Richards and Yorke, 1960).

Although TCL structures are predominant in the polymorphism of XOY and OXY TGs (Table 1.2), double chain length (DCL) structures also exist. They are distinguished by the suffix '-2'. In these DCL forms the oleoyl chain must pack alongside the saturated chains and, whether the chains are extended or bent (Sundaralingham, 1972; Huang, 1977a,b), there must be considerable distortion of the packing around the cis-double bond. Presumably this chain distortion is best accommodated by the  $\beta'$  subcell since no  $\beta$ -2 forms occur (Table 1.2).

The monooleoyl TGs show unusual crystallisation behaviour. Thus OSP is reported to crystallise directly in the sub- $\alpha$  form, transforming on heating to  $\beta'$ -2 (Lutton, 1951) or a  $30^\circ\text{C}$ -melting-form (Lavery, 1958) without the intermediacy of an  $\alpha$  form. Moreover, there is some uncertainty about the chain multiplicity of sub- $\alpha$  OSP since Lavery reported a sub- $\alpha$ -3 form whereas Lutton found sub- $\alpha$ -2. OSS and OPS show conventional  $\alpha$  forms,  $\alpha$ -3 and  $\alpha$ -2 respectively, but the reversible transition to the sub- $\alpha$  form occurs at much higher temperatures (about  $0^\circ\text{C}$ ) than the corresponding transition in saturated TGs (Lutton, 1951; Lavery, 1958; Chapman, 1962). The solidification behaviour of SOS, POS and POP is particularly puzzling. On very rapid cooling of the melt, the TGs crystallise into a fleetingly stable, low-melting state with sub- $\alpha$  short spacings and long spacings which are suggestive of a TCL form (Wille and Lutton, 1966). These so-called 'sub- $\alpha$ ' forms transform irreversibly to

the conventional  $\alpha$  forms,  $\alpha$ -3 for SOS and  $\alpha$ -2 for POS and POP, even if held at temperatures well below their melting points. This behaviour is obviously contrary to that of normal sub- $\alpha$  forms.

(b) Dioleoyl Triacylglycerols

Dioleoyl TGs containing palmitic or stearic acid are important components of many fats. They show somewhat similar polymorphism to the monooleoyl TGs discussed above. Thus the symmetrical compounds, OXO, have  $\alpha$ ,  $\beta$ '-2 and stable  $\beta$ -3 forms (compare XOY) while the unsymmetrical compounds, OOX, have only  $\alpha$  and stable  $\beta$ '-3 forms (compare OXY) (Lutton, 1966). The TCL stable forms of the dioleoyl TGs are analogous to the corresponding forms of the monooleoyl TGs except that the layer arrangements are reversed so that the diene structures consist of a layer of saturated chains sandwiched between two equivalent unsaturated chain layers. Comparison of the melting points of the stable forms of mono- and dioleoyl TGs shows that the presence of the additional oleoyl chain in the latter TGs lowers the melting points by approximately 20°C ( $\beta$ -3 SOS 44.3°C, OSO 25.4°C;  $\beta$ '-3 OSS 43.5°C, OOS 24.5°C; Lutton, 1951, 1966).

1.1.5 Diacid Saturated Triacylglycerols

The phase behaviour of mixed saturated TGs is best illustrated by an analysis of the polymorphism of diacid TGs. In general, these glycerides behave like tristearin with three DCL polymorphs,  $\alpha$ ,  $\beta$ ' and  $\beta$  in order of increasing stability. However, depending on the symmetry of the TG and the difference in chain lengths, three variations from this scheme may be observed: (1) a reversal of the relative stabilities of  $\beta$ '-2 and  $\beta$ -2, (2) the absence of a  $\beta$ -2 form and (3) the presence of a  $\beta$ -3 form similar to the TCL structures which occur in the oleoyl TGs (Lutton and Fehl, 1972). The nature of the polymorphism of a given TG is primarily determined by the end group structures of the possible forms (Larsson, 1972). Thus close polymorphic similarity occurs for mixed TGs in which the chain length differences ( $\Delta$ ) between the three positions are the same (Malkin, 1954), e.g.  $C_{14} C_{14} C_{18}$  and  $C_{18} C_{18} C_{22}$  (Lutton and Fehl, 1972).

(a) Diacid Triacylglycerols with a Chain Length Difference of 2 CH<sub>2</sub> Units

Consider first the case of TGs containing both palmitoyl and stearoyl chains, i.e. diacid TGs with a chain length difference of two methylene units ( $\Delta = 2$ ). If the  $\beta$ -2 forms of the four possible isomeric TGs (PSS, PPS; PSP, SPS) are as nearly isomorphous as possible with the

$\beta$ -2 forms of trilaurin and rac-2-(11-bromoundecanoyl)-1,3-dicaproyl-glycerol (an analogue of  $C_{10} C_{12} C_{10}$ ), then there are two possible terrace arrangements of the methyl end groups (Lutton, 1971a; Larsson, 1972). The unsymmetrical glycerides with one primary chain shorter or longer than the other two (PSS, PPS) have the same end group structure as mono-acid TGs (left hand diagram in Fig. 1-7). However, the symmetrical TGs (PSP, SPS) show a much steeper terrace arrangement (right hand diagram in Fig. 1-7) in which the methylene groups of one layer are almost in van der Waals contact with the methyl groups in the opposite layer, an unfavourable situation as mentioned in Section 1.1.2. Thus the  $\beta$ -2 polymorphs of  $C_n C_{n+2} C_n$  TGs form limits for the possibilities of isomorphism (Larsson, 1972). As a general rule, glycerides such as  $C_n C_{n-2} C_{n+4}$  for which an isomorphous  $\beta$ -2 form would have steeper terraces than this limiting case either show no  $\beta$  form or show only a TCL structure for this chain packing. It is noteworthy that of all the palmitoyl-stearoyl TGs, only PSP and SPS have stable  $\beta'$  forms, the remainder being  $\beta$ -stable. However,  $\beta'$  SPS (like  $\beta$  PSP) is only obtained with difficulty (Lutton and Hugenberg, 1960; Hugenberg and Lutton, 1963).

(b) Diacid Triacylglycerols with a Chain Length Difference of 4  $CH_2$  Units

As the chain length difference increases to four or more methylene units, it is not possible to obtain close packing in the methyl end group region of any DCL form with extended chains. If, for example, one chain is much shorter than the other two, the two surfaces of the unit layer will have an empty space in one out of three chain positions and no chain penetration to fill up these spaces is possible. In the  $\alpha$  and  $\beta'$  forms of such glycerides, therefore, close packing near the chain terminus is achieved by a bend in each of the two longer chains at the position of the shorter chain methyl group, so that these two chains are close packed in the same lateral space as is occupied by all three chains in the inner chain region (Lutton, 1950; Larsson, 1972). Such an arrangement, which is independent of the symmetry of the glyceride, is apparently more readily accommodated by the H and O $\perp$  subcells than by the T// subcell. Thus many diacid TGs for which  $\Delta \geq 4$  show both  $\alpha$ -2 and  $\beta'$ -2 but no  $\beta$ -2 form (e.g.  $C_{22} C_{22} C_{16}$  and  $C_{22} C_{18} C_{22}$ ; Jackson and Lutton, 1950; Lutton and Fehl, 1972). In other cases,  $\beta$ -2 is present but is less stable than  $\beta'$ -2 (e.g.  $C_{22} C_{18} C_{18}$ ; Lutton and Fehl, 1972).

However, most of these TGs show another structural variant,  $\beta$ -3, which is invariably the most stable polymorph. This TCL form allows

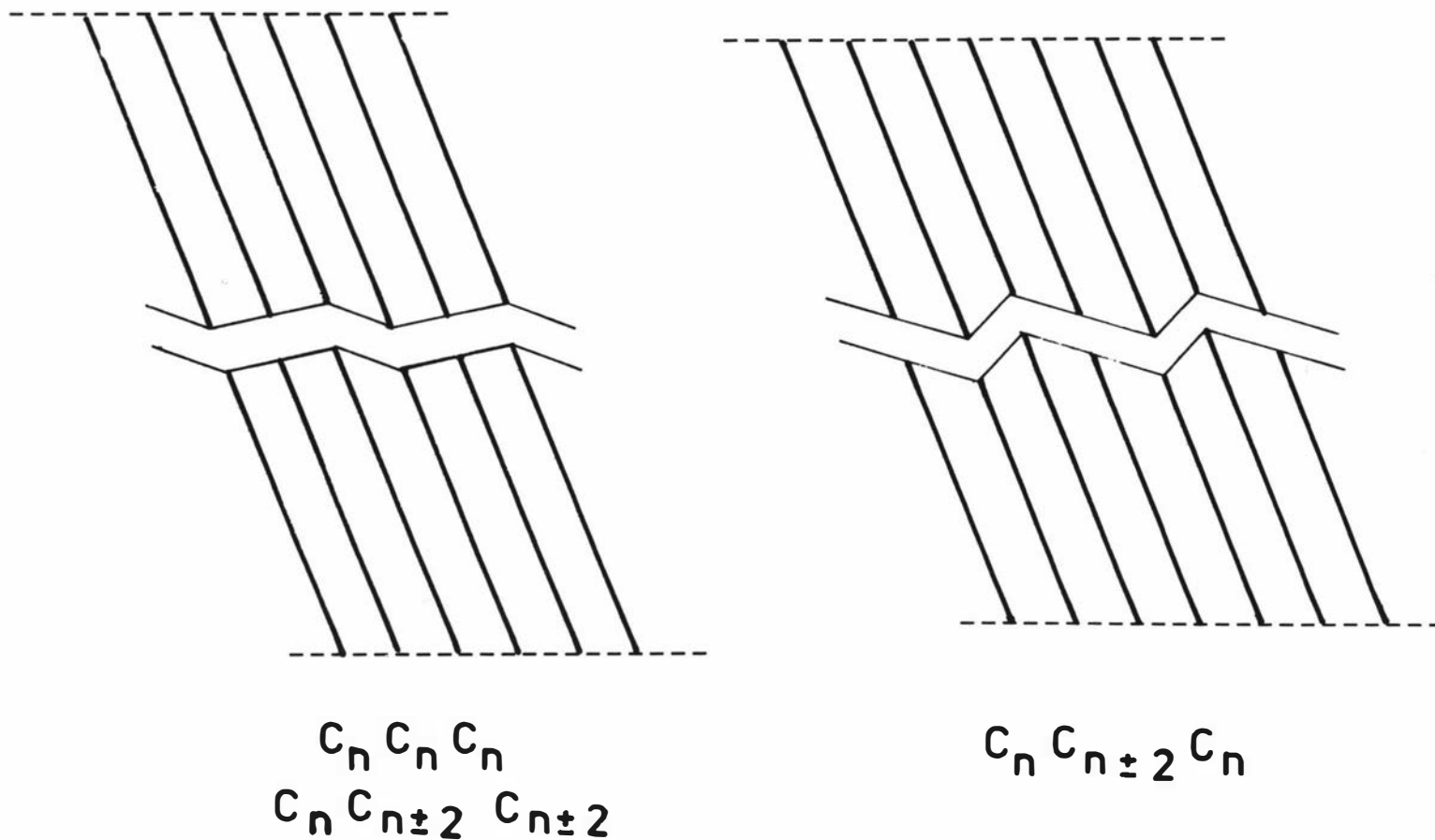


FIG.1-7 LAYER STACKING OF METHYL END GROUPS IN THE  $\beta$ -FORMS OF  $C_n/C_{n\pm 2}$  TRIACYLGLYCEROLS SHOWING THE TWO TERRACE STRUCTURES (LUTTON, 1971).

CHAIN AXIS ——— ; LAYER BOUNDARY - - - - .

closer packing than the DCL forms because extended chains can be accommodated without any empty space in the end group region. As in mono- and dioleoyl glycerides only the symmetrical diacid saturated TGs (e.g.  $C_n C_n \pm 4 C_n$ ) can give chain sorting (of the  $C_n \pm 4$  chains) in a TCL structure with the favoured tuning-fork conformation. However, in contrast to the unsaturated TG series, unsymmetrical diacid TGs of the type  $C_n C_n C_n \pm 4$  also show TCL forms with the  $\beta$  packing (Lutton and Fehl, 1972). In further contrast to the unsaturated TGs, diacid saturated TGs do not generally show  $\alpha$  and  $\beta'$  TCL structures unless the difference in chain lengths becomes very large ( $\Delta \geq 10$ ; Jackson and Lutton, 1952).

(c) Diacid Triacylglycerols with a Chain Length Difference of  
 $\sim 10 \text{ CH}_2$  Units

The polymorphism of glycerides containing both long and very short chains has been much studied (Jackson, Wille and Lutton, 1951; Jackson and Lutton, 1952; Menz, 1975). These glycerides exhibit unusual and markedly individual behaviour, especially in respect of the  $\alpha$  forms (Chapman, 1962). This presumably results from the relatively large structural role played by the carbonyl portions of the short acyl groups compared with their polymethylene chains (Jackson *et al.*, 1951). The investigations have generally concentrated on TG types which do not occur naturally, for example the diacetyl TGs, which were considered to have possible applications as coating fats (Baur, 1954). The polymorphism of the short chain TGs that occur in bovine milkfat has not been reported in the literature.

1.1.6 Enantiomeric Triacylglycerols

The preceding sections have dealt with the polymorphism of racemic TGs, but many fats (e.g. milkfat) contain unsymmetrical TGs which represent one or other of the two antipodes rather than the racemate. Surprisingly, no comparison of the polymorphic behaviour of corresponding enantiomeric and racemic TGs has yet been reported, although other lipids are known to show differences in the polymorphism of chiral and racemic forms (e.g. 1-acylglycerols, Larsson, 1964b; 1-stearoylpropylene glycol, Stauffer, 1967). Enantiomeric TGs have in fact been synthesised by a number of workers (Baer and Fischer, 1939b; Tattrie, Bailey and Kates, 1958; Schlenk, 1965; Quinn, 1967; Gronowitz, Herslof, Ohlson and Töregard, 1975; Lok, Ward and van Dorp, 1976), but in general only the melting points of the stable forms were determined. In most cases, the melting points were approximately equal to those of the equivalent

racemic forms, particularly where both determinations were made in the same laboratory (Schlenk, 1965; Quinn, 1967). However, Schlenk did find distinct differences in the X-ray diffraction patterns of the stable forms of corresponding rac- and sn-TGs. For the three TGs whose diffraction patterns were reported (LPP, PPS and POS), the racemates all had  $\beta$  stable forms while the stable forms of the enantiomers showed spacings more characteristic of  $\beta'$  than  $\beta$ . Unfortunately, Schlenk did not confirm these apparent subcell differences by IR spectroscopy, nor did he further characterise the polymorphism of the TGs.

## 1.2 Infrared Spectroscopy of Triacylglycerols in the Solid State

Infrared (IR) spectroscopy has proved a valuable complementary technique to X-ray powder diffraction in the study of the polymorphism of lipids. Its use by Chapman (1955-1965) conclusively confirmed Lutton's controversial description of TG polymorphism (Section 1.1.1). IR spectroscopy is less direct than X-ray powder diffraction because of the overlapping effects of polymorphism and chemical structure but it is capable of giving structural information which is not obtainable by the X-ray technique.

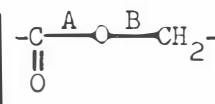
### 1.2.1 Assignments of Characteristic Absorption Bands

The most important characteristic bands in the solid state spectra of TGs are presented in Table 1.3 together with their assignments. Some vibrational modes give rise to a single band (e.g. the carbonyl stretching frequency at  $1740\text{cm}^{-1}$ ) while others cause a number of related bands (e.g. the methylene wagging and rock-twist modes at  $1385\text{-}1185\text{cm}^{-1}$  and  $1060\text{-}720\text{cm}^{-1}$  respectively). The term 'band progression' is applied to the absorption bands which belong to a single vibrational mode in a particular compound (de Ruig, 1971).

For the interpretation of their IR spectra, TG molecules can be thought of as consisting of a number of independent units or 'diatheses', each generating characteristic band progressions or sets of normal vibrations (de Ruig, 1971; Dijkstra and de Ruig, 1973; de Ruig and Dijkstra, 1975). A 'diathesis' is defined as a group of atoms joined together in a spatial arrangement so that at least one vibrational mode exists in which all atoms are involved. In saturated TGs in the solid state each all-trans-polymethylene chain constitutes a separate diathesis because the carbonyl group is the only barrier to vibrational coupling. Hence in a di- or triacid solid TG, two or three different chain diatheses are present resulting in a superposition of two or three band progressions for each mode.

Table 1.3: Characteristic Bands in the Solid State Spectra of Triacylglycerols (from de Ruig, 1971)

Approximate Frequency/cm <sup>-1</sup>	Intensity	Assignment
2925	very strong	methylene asymmetric stretching
2850	very strong	methylene symmetric stretching
1740	very strong	carbonyl stretching
1475	strong	methylene scissoring
[ 1470 1460-1440	[ strong some shoulders	[ combination of methylene scissoring and methyl asymmetric deformation
1415	medium	α-methylene scissoring
1385	strong	methyl symmetric deformation
1385-1185 <sup>a</sup>	strong to medium	methylene wagging
1180	very strong	C <sup>A</sup> -O stretching of
1115	strong	C <sup>B</sup> -O stretching of
890	medium	methyl rocking
1060-720 <sup>a</sup>	medium to weak	methylene rocking-twisting
720	very strong	principal methylene rocking band



a regular band progression

Table 1.4 gives the methylene wagging band progressions generated by palmitoyl, stearoyl, oleoyl and elaidoyl diatheses in monoacid TGs in the  $\alpha$  phase (de Ruig and Dijkstra, 1975). For the oleoyl chain, the same diathesis is present as in the  $C_9$  chain (although shifted by  $-12\text{cm}^{-1}$ ), i.e. only that part of the chain between the carbonyl and cis-double bond shows its band progression in the spectrum. For the diathesis between the double bond and the terminal methyl group, the methylene wagging bands are not intensified by the inductive effect of the carbonyl group (which is blocked by the cis-bond) and cannot therefore be observed alongside the wagging bands due to the first diathesis. Thus, in triolein, the cis-double bond acts as a barrier for the normal vibrations of the polymethylene chains. By contrast, in trielaidin, the trans-double bond only forms a partial barrier for the chain vibrations, so that the  $C_{18}$  diathesis generates the methylene wagging frequencies above  $1251\text{cm}^{-1}$  and the  $C_9$  diathesis generates those at  $1251$  and  $1207\text{cm}^{-1}$ . As a result, the  $\alpha$  spectrum of trielaidin is similar to  $\alpha$  triolein between  $1200$  and  $1260\text{cm}^{-1}$  and to  $\alpha$  tristearin between  $1260$  and  $1360\text{cm}^{-1}$  (de Ruig and Dijkstra, 1975).

In the liquid state, a long chain compound primarily displays conformations in which two sections of all-trans-single bonds are joined by a cis-single bond (i.e. a gauche arrangement) in various places along the chain (Horowitz *et al.*, 1973). The cis-bond in the chain acts as a barrier for normal vibrations so each all-trans-part forms one diathesis. The net effect is that in the liquid state there are many more diatheses than in the solid, causing many more different band progressions in the IR spectrum. These overlap to give a spectrum with very few significant features, in effect the spectrum of a complex mixture of diatheses (de Ruig, 1971; de Ruig and Dijkstra, 1975).

### 1.2.2 Spectral Differences Between Polymorphic Forms

The effect of the polymorphic state of a TG on its IR spectrum is a second order one and these interchain or intermolecular effects are not so well understood as the intramolecular effects discussed above. Nevertheless, spectra of the same TG in different polymorphic forms show marked differences, the most important of which are summarised in Table 1.5. The main methylene rocking band near  $720\text{cm}^{-1}$  has proved to be especially characteristic of the three principal chain arrangements,  $\alpha$ : singlet at  $720\text{cm}^{-1}$ ;  $\beta'$ : doublet at  $726$  and  $719\text{cm}^{-1}$ ;  $\beta$ : singlet at  $717\text{cm}^{-1}$ . The  $\beta$ -specific band at  $\sim 900\text{cm}^{-1}$  and the  $\beta'$ -specific bands

Table 1.4: Methylene Wagging Band Distributions for the Alpha Forms of the Monoacid Triacylglycerols of Elaidic, Oleic, Palmitic and Stearic Acids (from de Ruig, 1971 and de Ruig and Dijkstra, 1975)

Acyl Group	Methylene Wagging Band Distribution/cm <sup>-1</sup>					
16 : 0	1348	1331	1311	1286	1266	1243
	1220	1196				
18 : 0	1358	1346	1327	1314	1293	1273
	1254	1233	1214	1193		
18 : 1 <u>trans</u> -9	1358	1346	1327	1314	1293	1251
	1207					
18 : 1 <u>cis</u> -9	1330	1295	1251	1207		

Table 1.5: Comparison of the Spectra of  $\alpha$ ,  $\beta'$  and  $\beta$  Polymorphs of Monoacid Saturated Triacylglycerols (from de Ruig, 1971)

	$\alpha$	$\beta'$	$\beta$
Number of bands	less bands	more bands	still more bands
Appearance of bands	less sharp	more sharp	still more sharp
[CH <sub>2</sub> scissoring + CH <sub>3</sub> asymmetric deformation	1470-1450	ditto <sup>a</sup>	ditto <sup>a</sup>
		1436 extra band	1439 extra band
$\alpha$ -CH <sub>2</sub> scissoring	1418m	1415s	1425-1415m doublet or triplet
CH <sub>3</sub> symmetric deformation	1380 <sup>a</sup> broad	1395 sharp 1380 <sup>a</sup> broad or doublet	1395 <sup>a</sup> sharp
CH <sub>2</sub> wagging	1385-1185	ditto	ditto
	regular progression	splitting up	more splitting up
CO-O stretching	1178	1175 <sup>a</sup>	1180
			~1160 extra band
CH <sub>2</sub> rocking	720	726 and 719	717
Other characteristic bands of unknown assignment	~950	~975m	
		~950m	
		~925m	
		~835m	
			~900s
		~635	~635
		~610 weakest	~610 strongest
~575 strongest	~600 weakest		

a Shoulders or weak bands at the lower frequency side of the band.

at 835, 925, 950 and  $975\text{cm}^{-1}$  have also proved useful for identification purposes (de Ruig, 1971). In addition to these characteristic differences, the transition sequence  $\alpha \rightarrow \beta' \rightarrow \beta$  results in a general sharpening of all absorption bands in the  $1500$  to  $600\text{cm}^{-1}$  region of the IR spectrum and a progressive increase in band splitting and other irregularities, particularly in the methylene wagging band progression.

The  $\alpha$ ,  $\beta'$  and  $\beta$  polymorphs of natural fats show similar spectral differences to the corresponding polymorphs of monoacid TGs although the spectra are generally less well defined. Hence the  $\beta'$  form can be distinguished by the presence of a doublet near  $720\text{cm}^{-1}$  and two absorption bands of medium intensity at 922 and  $835\text{cm}^{-1}$  which are absent in the  $\beta$  form. Similarly, the spectrum of the  $\beta$  form of fats shows a sharp singlet at about  $720\text{cm}^{-1}$  and a strong band at  $890\text{cm}^{-1}$ . The  $\alpha$  form is easy to recognise from the appearance of the whole spectrum, having fewer and broader bands than the spectra of the  $\beta'$  and  $\beta$  forms (de Ruig, 1971).

### 1.3 Melting and Solidification of Fats

#### 1.3.1 Technical Importance of the Phase Behaviour of Fats

Apart from flavour and nutritional aspects, fats are important food constituents because of the way their physical properties influence the texture of foods. The most important properties in this regard are those which govern the phase behaviour of fats. A major part of the technology of edible fats is therefore concerned with the production of glyceride mixtures which have specific phase properties, for example mixtures which will either soften and melt or remain plastic and workable within a given temperature interval.

#### 1.3.2 Polymorphism of Fats

Although fats are complex mixtures of TGs differing in chain lengths and degree of unsaturation, they often behave physically as a single component or a simple mixture of two or three components (Bailey, 1950). Furthermore, many fats display the same polymorphic forms and phase relations as simple TGs (e.g. milkfat; Woodrow and de Man, 1968). According to Larsson (1971), such behaviour occurs because fats in the solid state adopt similar lattice arrangements to the polymorphic forms of simple TGs. However, in fats the end group structure is disordered so that chains of various lengths can be accommodated. Thus, when a fat crystallises from the melt in the  $\alpha$  form, the randomly distributed chains form bimolecular layers in which the various chain lengths are extended as far as possible in the regular  $\alpha$  packing but are disordered in the

end group region to obtain the closest local contact distance across the layer boundary. Two types of disorder probably occur, bending of longer chains near the ends of adjacent shorter chains and interpenetration of the longer chains into adjacent lamellae.

The process of transformation from the vertical  $\alpha$  form or the lamellar melt to a crystal form with tilted chains ( $\beta'$  or  $\beta$ ) is greatly facilitated if the two chain layers of the lamellae adopt opposite tilt positions as in the  $\beta'$  structure (Section 1.1.3). The  $\alpha \rightarrow \beta'$  phase transition involves an accordian-like contraction of the double layer with little displacement of the end groups along the layer boundary. However, in the  $\alpha \rightarrow \beta$  or  $\beta' \rightarrow \beta$  transitions it is necessary for the methyl groups on opposite sides of the boundary to slide horizontally in relation to each other, because there is only one chain tilt direction in the  $\beta$  form. In fats this process would be impeded by the interpenetration of chains between adjacent lamellae. Accordingly, for complex glyceride mixtures the transition  $\alpha \rightarrow \beta'$  is usually more facile than the transitions  $\alpha \rightarrow \beta$  and  $\beta' \rightarrow \beta$  so that the  $\beta'$  form is more stable in mixtures than in pure monoacid TGs (Larsson, 1971). However, fats in which the chain lengths show little variation, e.g. hydrogenated soybean oil, are  $\beta$ -tending. When blended with liquid oil to make shortenings, such fats confer different rheological properties on the product than do  $\beta'$ -tending fats (e.g. hydrogenated cottonseed oil) because of the different crystal habits of the two forms (Lutton, 1972).

### 1.3.3 Solid Miscibility of Fats

The melting behaviour of fats is not only dependent on their polymorphism but also on their pronounced tendency to solid miscibility (Bailey, 1950). The two phase phenomena invariably occur together, although polymorphism is more evident in sharp melting fats which consist of a small number of TGs (e.g. cocoa butter), while solid miscibility is more apparent in complex fats with a broad melting range (e.g. milkfat).

Substitutional solid solutions occur when molecules of one type in a crystal lattice can be replaced at random by molecules of a second type. The extent of solid miscibility is governed by the degree to which the molecules are isomorphous and by the ability of the lattice to accommodate distortion. In lipids, this accommodating power increases in the order  $\beta < \beta' < \alpha$  (Chapman, 1962).

In fats, TGs belonging to a single structural type, such as the long chain saturates, are generally miscible in the solid state regardless of the distribution of the fatty acids among the TG molecules. The

different chain lengths are accommodated in solid solution by disorder in the end group region (Larsson, 1971; Knoester, de Bruijne and van den Tempel, 1972). The limits to solid solution formation in fats, although ill-defined, appear to be formed by relatively gross differences in molecular structure, the most important of which is the structural dichotomy between saturated and cis-unsaturated chains. Thus the tendency is for trisaturated glycerides to form a separate solid solution from the disaturated glycerides and so on. However, the extent of inter-solubility should increase as the molecular complexity and resultant lattice distortion increase. As a result, TG classes would be expected to show increasing overlap in solid miscibility as they become more unsaturated. To a first approximation, then, solid fats behave like a simple mixture, each component of which is a solid solution containing TGs from one or more classes. In practical terms, the solid solutions formed by the tri- and disaturated glyceride classes are particularly important components of plastic fats because they determine the rheological properties of these materials over the temperature range of domestic use.

Because of the bulk of TG molecules, the formation of their solid solutions is subject to diffusional delays and thus the composition of the mixed crystals is dependent on the rate of cooling (Bailey, 1950; Mulder, 1953; Hannewijk, Haighton and Hendrikse, 1964). Since polymorphism is also dependent on temperature history, the thermal behaviour of fats is particularly complex.

#### 1.3.4 Melting and Solidification of Milkfat and Milkfat Fractions

##### (a) Composition of Milkfat

Although bovine milkfat contains an extraordinary number of unusual fatty acids, almost 90 mole % is accounted for by 10 major acids comprising the long chain saturates (14:0, 16:0 and 18:0), the short chain saturates (4:0, 6:0, 8:0, 10:0 and 12:0) and the cis- and trans-monoenes (18:1). As a consequence of ruminant physiology, bovine milkfat has an unusual abundance of short chain acids and a relatively high trans-content, but is low in polyunsaturated fatty acids.

Stereospecific analyses of milkfat fractions have shown that the fatty acids in milkfat are distributed in a highly selective manner (Breckenridge and Kuksis, 1968, 1969; Taylor and Hawke, 1975b). Thus, 4:0 and 6:0 are esterified almost entirely at position sn-3, 14:0 is concentrated at position sn-2 and 16:0 is preferentially esterified at positions sn-1 and sn-2. In low molecular weight TGs, 18:0 and 18:1

are preferentially esterified at position sn-1, while in high molecular weight TGs they are concentrated at both sn-1 and sn-3 positions.

Fig. 1-8 summarises the results reported by Taylor and Hawke (1975a,b) for New Zealand milkfat and shows the major TG types present in classes separated according to molecular weight and degree of unsaturation. Of the TG types represented, only those of high molecular weight have been characterised with regard to their polymorphism.

(b) Phase Behaviour of Milkfat Fractions

The relatively homogeneous fractions of milkfat separated by fractional crystallisation or chromatography show clear evidence of polymorphism and solid miscibility. For example, the high-melting glyceride (HMG) fraction of milkfat, obtained by crystallisation from acetone (Patton and Keeney, 1958), exhibits polymorphic behaviour typical of the  $\beta$ -stable palmitoyl-stearoyl TGs (Woodrow and de Man, 1968). Such behaviour is a consequence of the relative homogeneity of the HMG fraction, which contains very high proportions of palmitic and stearic acids (Patton and Keeney, 1958). However, when the HMG is subdivided by further acetone fractionation, the subfractions show a progressive  $\beta'$  tendency as their melting points decrease (Barbano, 1973). The increasing stability of the  $\beta'$  form is probably the result of the greater heterogeneity of chain lengths in the lower melting subfractions.

Solid solution formation between fractions of milkfat was first demonstrated by Sherbon and Coulter (1966), using an adiabatic calorimeter. Comparison of the thermograms obtained for a mixture containing equal parts of high- and low-melting fractions to the thermogram calculated on the basis of no interaction of the two components showed that the low-melting fraction melted at a higher temperature in the mixture than it did alone, whereas the high-melting fraction melted at a lower temperature than it did alone. Such thermal behaviour is consistent with the occurrence of partial solid miscibility for the two fractions.

Taylor (1973) has reported on the thermal behaviour of fractions which were separated from milkfat according to molecular weight and degree of unsaturation (cf. Fig. 1-8). The saturated TGs of high, medium and low molecular weight showed clear evidence of polymorphic transformation, although no phase assignments were made. Comparison of the melting thermogram of the low molecular weight fraction with those of its saturated and unsaturated subfractions indicated that little solid solution formation occurred between the two subfractions. In other

	<u>SATURATED TGS</u>	<u>MONOENE TGS</u>	<u>DIENE TGS</u>	<u>TRIENE TGS</u>
<u>HIGH MOL.WT TGS</u>				
% in Milkfat	13.1	17.0	7.2	4.0
Major Type	L — [ L L	L — [ 18:1 L	18:1 — [ 18:1 16:0	18:1 — [ 18:1 18:1
<u>MEDIUM MOL.WT TGS</u>				
% in Milkfat	7.9	5.3	1.6	1.3
Major Type	L — [ L 6:0	16:0 — [ 18:1 6:0	18:1 — [ 18:1 6:0	
<u>LOW MOL.WT TGS</u>				
% in Milkfat	22.8	13.6	3.8	2.4
Major Type	L — [ L 4:0	16:0 — [ 18:1 4:0	18:1 — [ 18:1 4:0	
<u>KEY</u>	L = 14:0, 16:0 or 18:0		[ = TG SKELETON	

**FIG.1-8 TRIACYLGLYCEROLS OF MILKFAT (TAYLOR,1973)**

words, the structural difference between the saturated and unsaturated TGs of low molecular weight was sufficiently large to prevent significant solid miscibility. However, the saturated and unsaturated TGs of the high molecular weight fraction showed greater overlap of their melting ranges on mixing than would be expected on the basis of no interaction between the two components. This result is somewhat surprising in view of the fact that the high-melting fractions separated by crystallisation contain little if any unsaturated fatty acids. The latter observation is consistent with the earlier comment (Section 1.3.3), that the saturated TGs of fats show a general tendency to form a separate solid solution from the unsaturated TGs.

(c) Phase Behaviour of Milkfat

Because of the variation in both molecular weight and degree of unsaturation of its component TGs, milkfat has a wide melting range ( $-40$  to  $40^{\circ}\text{C}$ ). NMR measurements on a sample of New Zealand summer milkfat tempered at  $20^{\circ}\text{C}$  showed that approximately 37% melted below  $0^{\circ}\text{C}$ , 37% between 0 and  $20^{\circ}\text{C}$  and the remaining 26% above  $20^{\circ}\text{C}$  (Norris and Taylor, 1977). The results of Taylor (1973) suggest that the fraction melting below  $0^{\circ}\text{C}$  consists primarily of unsaturated TGs, especially those of low molecular weight, that melting between 0 and  $20^{\circ}\text{C}$  consists of saturated TGs of low molecular weight or monoene TGs of high molecular weight, and that melting above  $20^{\circ}\text{C}$  consists of saturated TGs of high molecular weight.

In 1953, Mulder noted the possibility of solid miscibility in milkfat and discussed the consequences of such phase behaviour on the melting and solidification of milkfat. In particular, Mulder showed that a larger proportion of fat would be expected to crystallise on rapid cooling than on slow cooling. Later workers confirmed Mulder's observations (e.g. de Man and Wood, 1959; Vasic and de Man, 1966).

Mulder (1953) was also one of the first investigators to describe polymorphism in milkfat. He observed a double melting point for milkfat which had been rapidly cooled to  $0^{\circ}\text{C}$ . More recently, a number of workers (e.g. Woodrow and de Man, 1968; de Ruig, 1971; van Beresteyn, 1972) have demonstrated by means of X-ray diffraction and IR spectroscopy that  $\alpha$ ,  $\beta'$  and  $\beta$  polymorphs can all occur in milkfat. According to Woodrow and de Man (1968), milkfat which had been slowly cooled from  $40^{\circ}\text{C}$  to  $0^{\circ}\text{C}$  indicated the presence of  $\beta'$  and  $\beta$  forms, but rapidly cooled milkfat crystallised predominantly in the  $\alpha$  form. On subsequent holding at  $5^{\circ}\text{C}$ , the  $\alpha$  form slowly transformed to the  $\beta'$  and  $\beta$  forms. A possible inter-

pretation of this work is that the proportion of milkfat melting between 0°C and 40°C consists of at least two solid solutions, one  $\beta$ -stable (presumably the HMG fraction melting between 20 and 40°C) and the other(s)  $\beta'$ -stable (presumably the TG fraction melting between 0 and 20°C).

Obviously, a good deal more work is required to relate the phase behaviour and rheological properties of milkfat and other fats to the phase behaviour of their component TGs.

#### 1.4 Aim of the Present Work

The aim of this investigation was to synthesise a series of racemic and enantiomeric TGs representative of the major milkfat glyceride classes and to characterise their phase behaviour by differential scanning calorimetry and IR spectroscopy. Initially, it had been anticipated that binary systems would be studied but this proved too ambitious. The investigation was therefore limited to a thorough analysis of the polymorphism of the selected TGs.

##### 1.4.1 Selection of Triacylglycerols for Synthesis

Most TGs were synthesised from four of the major fatty acids occurring in milkfat, i.e. butyric, oleic, palmitic and stearic acids. With these starting materials, 22 of the 40 possible racemic TGs were selected for preparation (Table 1.6). In addition, three trans-monoenes were also synthesised, i.e. SES, ESS and BES. Elaidic acid, trans-9-octadecenoic acid, was used for the preparation of these glycerides because of the difficulty in obtaining trans-11-octadecenoic acid, the most abundant of the trans-isomers in milkfat (Hay and Morrison, 1970; Parodi, 1976). However, the monoacid TGs of these two acids have very similar thermal properties (Hagemann *et al.*, 1972, 1975), suggesting that the 9-isomer is a suitable analogue for the 11-isomer.

In general, the selected TGs were representative of, or isomeric to, the most important glyceride classes in milkfat (Fig. 1-8). However, no attempt was made to synthesise glycerides such as OXO and BXO with low-melting residues in both primary glycerol positions, because of the difficulty in purifying their partial glyceride intermediates (Mattson and Volpenhein, 1962).

To allow a comparison of the polymorphism of antipode and racemate, enantiomeric TGs complementary to three of the racemic TGs listed in Table 1.6 were also prepared. Because of the difficulty of synthesis, the selection was limited to TGs representative of the two most abundant TG

Table 1.6: Selection of Triacylglycerols for Synthesis

TG Type		Symmetrical <sup>a</sup>				Unsymmetrical <sup>a</sup>			
Unsaturation	Molecular Weight	SSS	SPS	PSP	PPP	PSS	PPS		
saturated	high	SSS	SPS	PSP	PPP	PSS	PPS		
saturated	low	SBS				BSS <sup>b</sup>	BSP	BPS	BPP
<u>cis</u> -monoene	high	SOS	POS <sup>a</sup>	POP		OSS <sup>b</sup>	OSP	OPS	OPP <sup>b</sup>
<u>trans</u> -monoene	high	SES				ESS			
<u>cis</u> -monoene	low					BOS	BOP		
<u>trans</u> -monoene	low					BES			
<u>cis</u> -diene	high					OOS	OOP		

Key: B butyryl; E elaidoyl; O oleoyl; P palmitoyl; S stearoyl  
 BSP rac-1-butryl-2-stearoyl-3-palmitoylglycerol

Note: a Symmetry with respect to 1 and 3 positions. For POS, P and S are sufficiently similar to each other and different from O that the TG may be considered symmetrical.

b Enantiomers of these three TGs were also prepared.

classes, i.e. saturated low molecular weight (sn-SSB) and cis-monoene high molecular weight (sn-SSO and sn-PPO).

## Chapter 2

MATERIALS AND METHODSA. Analytical and Synthetic Methods2.1 Materials

Unless otherwise stated, all chemicals were supplied by British Drug Houses Ltd. (Poole, England) or by May and Baker Ltd. (Dagenham, England).

2.1.1 Solvents

Reagent grade acetone was dried by distillation from  $\text{CaSO}_4$ . Diethyl ether and 2-methoxyethanol were dried and rendered peroxide-free by passage through a column of activated alumina (2l/100g) and were then distilled. Dry pyridine was obtained by reflux and distillation over NaOH pellets. Reagent grade N,N'-dimethylformamide was dried with  $\text{CaSO}_4$ , distilled under reduced pressure and stored over  $\text{CaSO}_4$ . N-dibutyl ether was synthesised from n-butanol and p-toluenesulphonyl chloride (Schorigin and Makarov-Zemlianskii, 1932), dried with alumina and distilled. Chloroform for esterification reactions was washed with concentrated sulphuric acid (3 x 0.1 vol.) to remove ethanol, with water (3 x 0.5 vol.) to remove acid, partially dried with  $\text{Na}_2\text{SO}_4$  and then distilled from  $\text{P}_2\text{O}_5$ . Either butanol (100 ppm) or 2,6-di-t-butyl-4-methylphenol (BHT, 50 ppm; Eastman Kodak, Rochester, U.S.A.) was added to the chloroform to prevent formation of phosgene during storage. Analytical grade acetone, benzene and methanol were used without purification.

2.1.2 Reagents

Powdered  $\text{H}_3\text{BO}_3$ , anhydrous  $\text{Na}_2\text{SO}_4$  and granulated silica gel were dried at  $110^\circ\text{C}$ , while  $\text{CaSO}_4$  and Union Carbide Molecular Sieves Type 4A were dried at  $240^\circ\text{C}$  and  $300^\circ\text{C}$  respectively. Chromatographic grade neutral alumina was activated at  $500^\circ\text{C}$  overnight.

Analytical grade glycerol was dried by heating to  $160^\circ\text{C}$  for 15 min and then used directly (Hartman, 1957). Reagent grade thionyl chloride was purified by the method of Friedman and Wetter (1967).

Analytical grade oxalyl chloride, p-toluenesulphonic acid, D-mannitol and anhydrous sodium acetate,  $\text{ZnCl}_2$  and  $\text{K}_2\text{CO}_3$  were used as received. Reagent grade lead tetraacetate and  $\text{NaBH}_4$  were also used directly.

### 2.1.3 Fatty Acids

Butyric acid and "specially pure grade" palmitic and stearic acid were supplied by BDH. If necessary, batches of the latter two fatty acids were recrystallised from acetone to a final purity of at least 99% when measured by gas-liquid chromatography (GLC). A second lot of stearic acid (> 99.5% by GLC; Fluka A.G., Buchs, Switzerland) was used without further purification. Elaidic acid from the Sigma Chemical Company (Saint Louis, U.S.A.) was checked by GLC (> 99% 18:1) and silver ion thin-layer chromatography (TLC) (> 98% trans-monoene), then used as received.

Oleic acid was prepared from olive oil according to the procedure of Rubin and Paisley (1960) with some modifications. Fig. 2-1 gives a flow sheet for the preparation. The final product (yield 192g, 15% based on olive oil fatty acids) contained > 99.5% 18:1 by GLC, and no trans-acid could be detected by either silver ion TLC or IR spectroscopy. The position of the double bond was determined by the ozonolysis and GLC procedure of Stein and Nicolaidis (1962). Comparison with an oleic acid standard (99%, Sigma Chemical Company) confirmed that more than 99% of the double bonds in the product were in the 9-10 position.

### 2.1.4 Storage of Glycerides and Synthetic Intermediates

Prior to analysis, all glycerides were dried in vacuo at 20°C and stored in airtight screwcap jars. Saturated TGs were stored at 0°C while unsaturated TGs, acyl chlorides, partial glycerides and all other intermediates were stored at -20°C.

## 2.2 Analytical Methods

### 2.2.1 Thin-Layer Chromatography

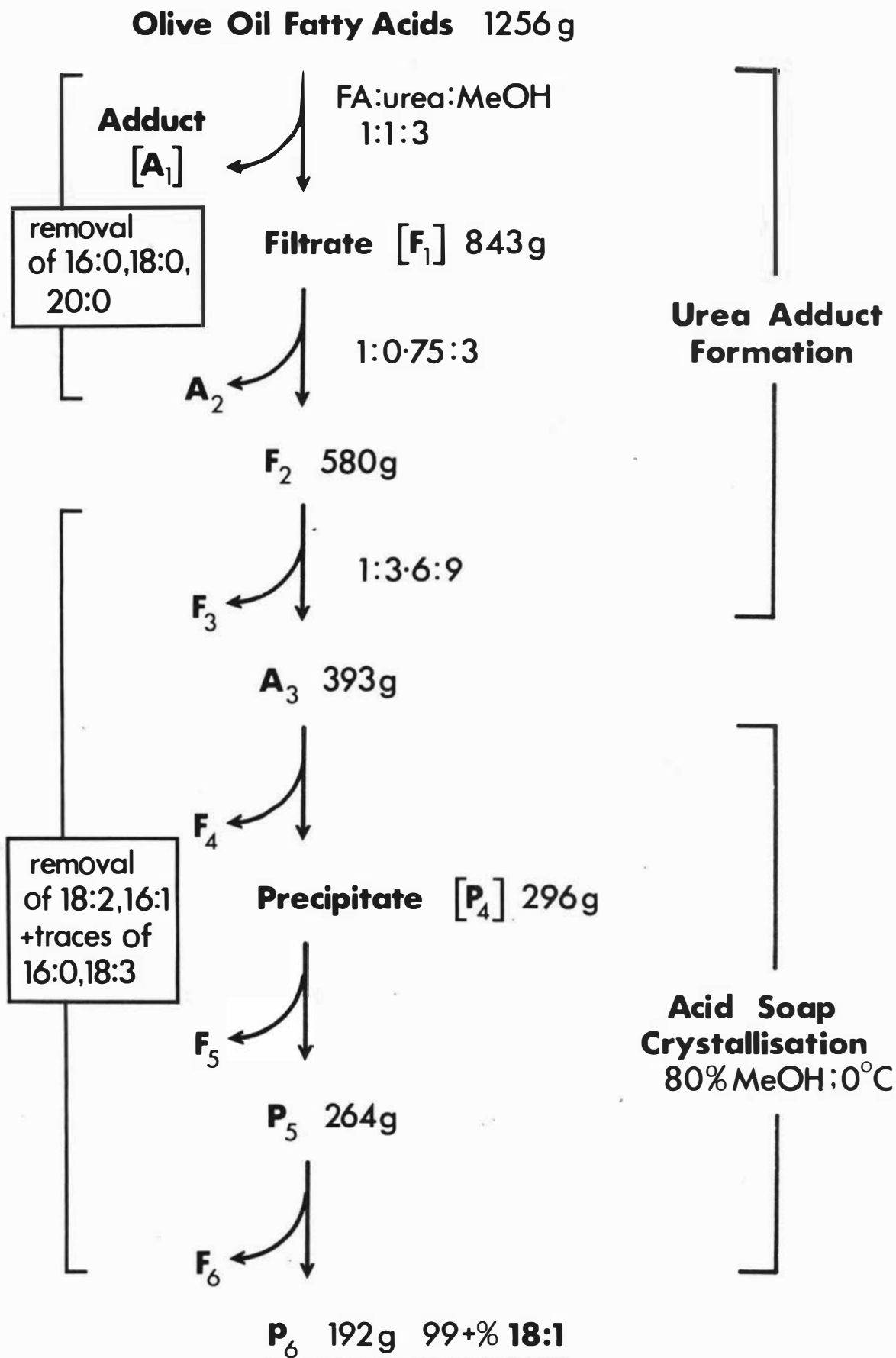
Thin-layer chromatography (TLC) was used for following the course and extent of reactions and for checking the identity and purity of products.

Thin-layers of silica gel G were prepared by slurring the adsorbent with water (1:2 w/v) or a solution of boric acid (35g/l) and spreading onto glass plates (20 x 20cm) to a thickness of 0.3mm. After air-drying for 30 min, the layers were activated by heating at 110°C for 2h.

Thin-layers impregnated with AgNO<sub>3</sub> were prepared from a slurry of 30g silica gel G and 65ml of a solution of AgNO<sub>3</sub> (100g/l).

Samples were applied as spots with a 30µl syringe and the plates

**Fig.2-1 Scheme for the Preparation of Oleic Acid**  
 – adapted from Rubin and Paisley [1960]



were developed by the ascending method in saturated chromatographic tanks. Partial glycerides were separated on silica gel G layers impregnated with  $H_3BO_3$  using a solvent system of hexane-diethyl ether (50:50) or chloroform-methanol (150:3). For TGs the thin layers were developed in either hexane-diethyl ether (85:15 and 50:50) or dichloromethane. Lipids were detected by fluorescence (spray reagent: 2g/l of 2,7-dichlorofluorescein in methanol) or charring (50% (v/v) sulphuric acid; 150°C for 1h). The dichlorofluorescein spray reagent was mainly used for the detection of fatty acids, which are not stained by the sulphuric acid spray.

For the determination of glyceride purity, conditions were chosen so that expected impurities could be detected at the 1% level. This detection level was confirmed by the examination of pure standards to which increasing levels of specific impurities had been added.

### 2.2.2 Column Chromatography

With the exception of saturated TGs of high molecular weight, all TGs were purified by column chromatography on alumina according to the convenient procedure of Jensen et al. (1966).

Column chromatography was also used to separate unreacted 1-stearoylglycerol from 1-butyryl-3-stearoylglycerol since the two compounds were not readily separated by crystallisation (cf. Feuge and Lovegren, 1956). To prepare the adsorbent, chromatographic grade neutral alumina (90g) was added to a solution of  $H_3BO_3$  in methanol (10g in 200ml) in a 2l fluted flask and the suspension was evaporated to dryness on a rotary vacuum evaporator at 35-40°C. After 30 min the free-flowing powder was transferred to a beaker, dried overnight at 110°C and then stored in a dessicator. The column was packed by adding the adsorbent (2g/g of compound) in successive small amounts to a chromatographic tube (2.5cm i.d.) filled with developing solvent (hexane-diethyl ether 25:75). The crude 1,3-diacylglycerol, dissolved in 1 vol. of developing solvent, was applied to the top of this column and then rapidly eluted (<15 min) with 20 vol. of developing solvent. Examination of the eluant by TLC showed that all the 1-acylglycerol had been retained on the column and that little further isomerisation of the 1,3-diacylglycerol had occurred. Based on the original mass of the reaction product applied to the column, the recovery of the partially purified 1-butyryl-3-stearoylglycerol was 88%.

### 2.2.3 Gas-Liquid Chromatography

Gas-liquid chromatography (GLC) was used to determine the purity of the fatty acid starting materials and the fatty acid composition of the synthetic TGs and their lipolysis products. Analyses of fatty acid methyl esters were performed on a Varian Aerograph (Walnut Creek, California, U.S.A.) Series 1520 chromatograph fitted with a flame ionisation detector and a linear temperature programmer. Long chain glycerides and fatty acids were converted to methyl esters by the method of Van Wijngaarden (1967) while butyryl TGs were interesterified by the procedure of Shehata, de Man and Alexander (1970). Methyl esters were analysed on a stainless steel column (2.4m x 3.2mm i.d.) packed with 12% diethylene glycol succinate on Chromosorb W (60-80 mesh, acid washed and DMCS treated). Gas flow rates were 25, 250 and 20 ml/min of nitrogen carrier gas, air and hydrogen respectively. Injector and detector temperatures were 230 and 250°C and the column oven was operated isothermally at ~190°C (long chain esters) or programmed from ~60 to 190°C at 10°C/min (mixtures of short and long chain esters). Peak areas were measured by triangulation (height x width at half height) or by an electronic integrator (Varian Model 480) and the relative proportions of esters were obtained using experimental weight response factors (Shehata et al., 1970).

Butyric acid was analysed for purity by chromatography of the free acid on a glass column (2.4m x 3.2mm i.d.) packed with 10% (w/w) diethylene glycol adipate and 2% (w/w) phosphoric acid on 60-80 mesh Chromosorb W (acid-washed and DMCS treated). The oven was maintained at 100°C. The gas flow rates were the same as those for the methyl ester column although a formic acid bubbler was fitted in the carrier gas line to reduce tailing of the peaks.

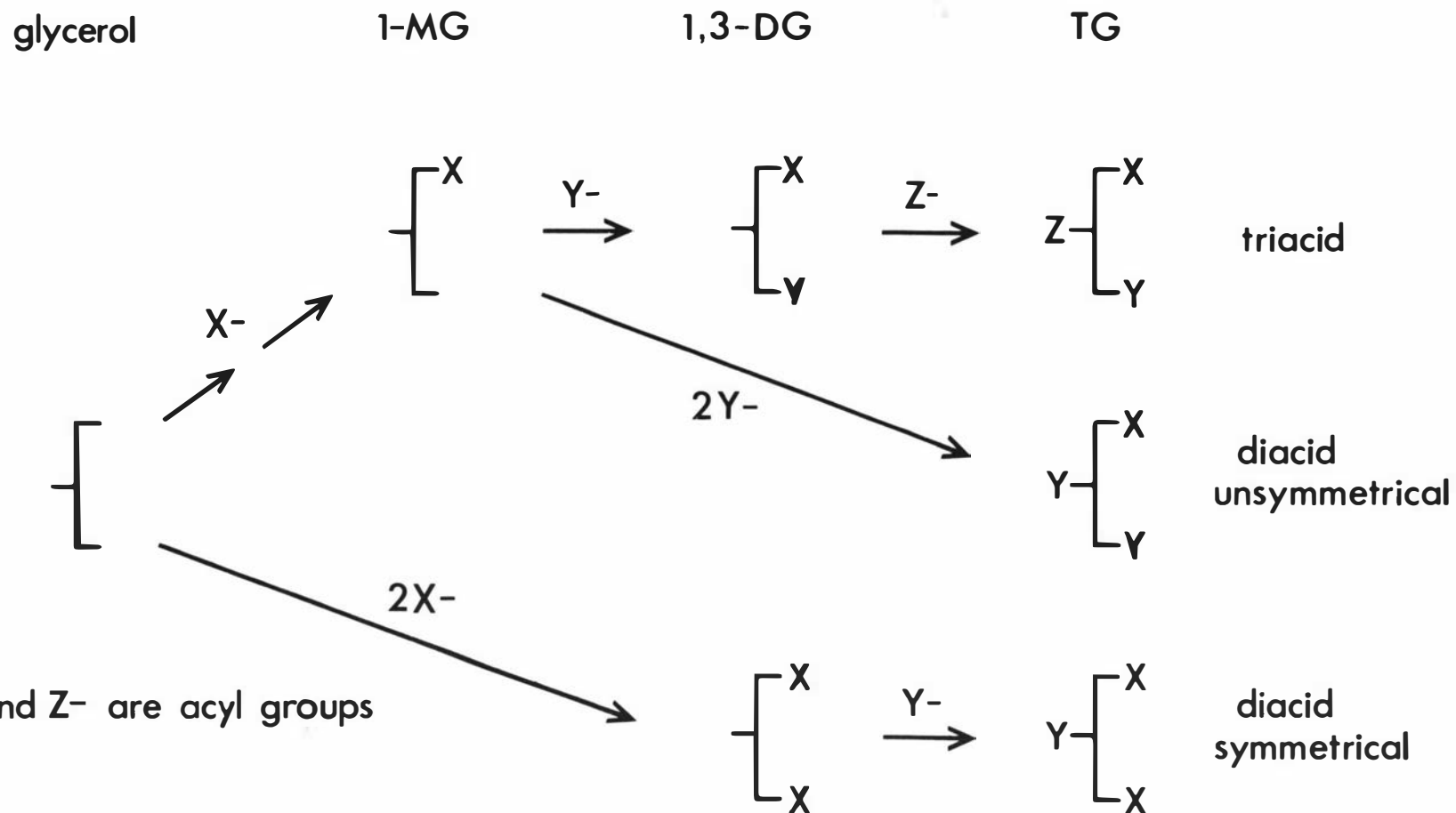
### 2.2.4 Structural Analysis of Triacylglycerols

Positional and stereospecific analyses were performed on selected TGs by Dr I. Morrison at Massey University (Ph.D. Thesis, 1976). The procedures were essentially those described by Luddy et al. (1964) and Christie and Moore (1969).

### 2.3 Preparation of Racemic Triacylglycerols

The general scheme adopted for the preparation of racemic TGs is shown in Fig. 2-2. Triacid TGs were synthesised via 1-(mono)acylglycerol (1-MG) and 1,3-diacylglycerol (1,3-DG) by direct esterification with the appropriate acyl chloride (Hartman, 1957; Mattson and Volpenhein, 1962;

Fig.2-2 General Scheme for the Synthesis of Racemic Triacylglycerols [Hartman,1957]



Note: X-,Y- and Z- are acyl groups

Quinn, Sampagna and Jensen, 1967; Jensen, 1972). Rac-1-MGs were prepared from 1,2-isopropylidene glycerol (Quinn et al., 1967) according to the reaction scheme shown in Fig. 2-3 (scheme 1).

Unsymmetrical, diacid rac-TGs were synthesised by complete esterification of 1-MGs while symmetrical diacid TGs were synthesised from monoacid 1,3-DGs. The latter compounds were prepared by direct esterification of glycerol (Hartman, 1957). However, there were several exceptions to the scheme for the preparation of diacid TGs. OOP and OOS were prepared from 1-oleoylglycerol via the 1,3-DGs; ESS and PSS were synthesised from rac-1,2-distearoylglycerol; BPP and BSS were synthesised from 1-palmitoyl- and 1-stearoylglycerol via the 1,3-DG.

### 2.3.1 Acyl Chlorides

Palmitoyl and stearoyl chlorides were prepared using thionyl chloride as the chlorinating reagent, while oleoyl and elaidoyl chlorides were prepared using oxalyl chloride (Quinn et al., 1967). Butyryl chloride was synthesised with phosphorus trichloride (Cason and Rapoport, 1970) and the crude product was distilled through a 15 x 1.5cm i.d. column packed with 3mm single-turn glass helices (b.p. 100-102°C).

All acyl chlorides were checked for the presence of unreacted fatty acid by IR spectroscopy (Youngs, Epp, Craig and Sallans, 1957); samples with more than 1-2% of fatty acid were reacted with fresh chlorinating reagent and the work-up repeated.

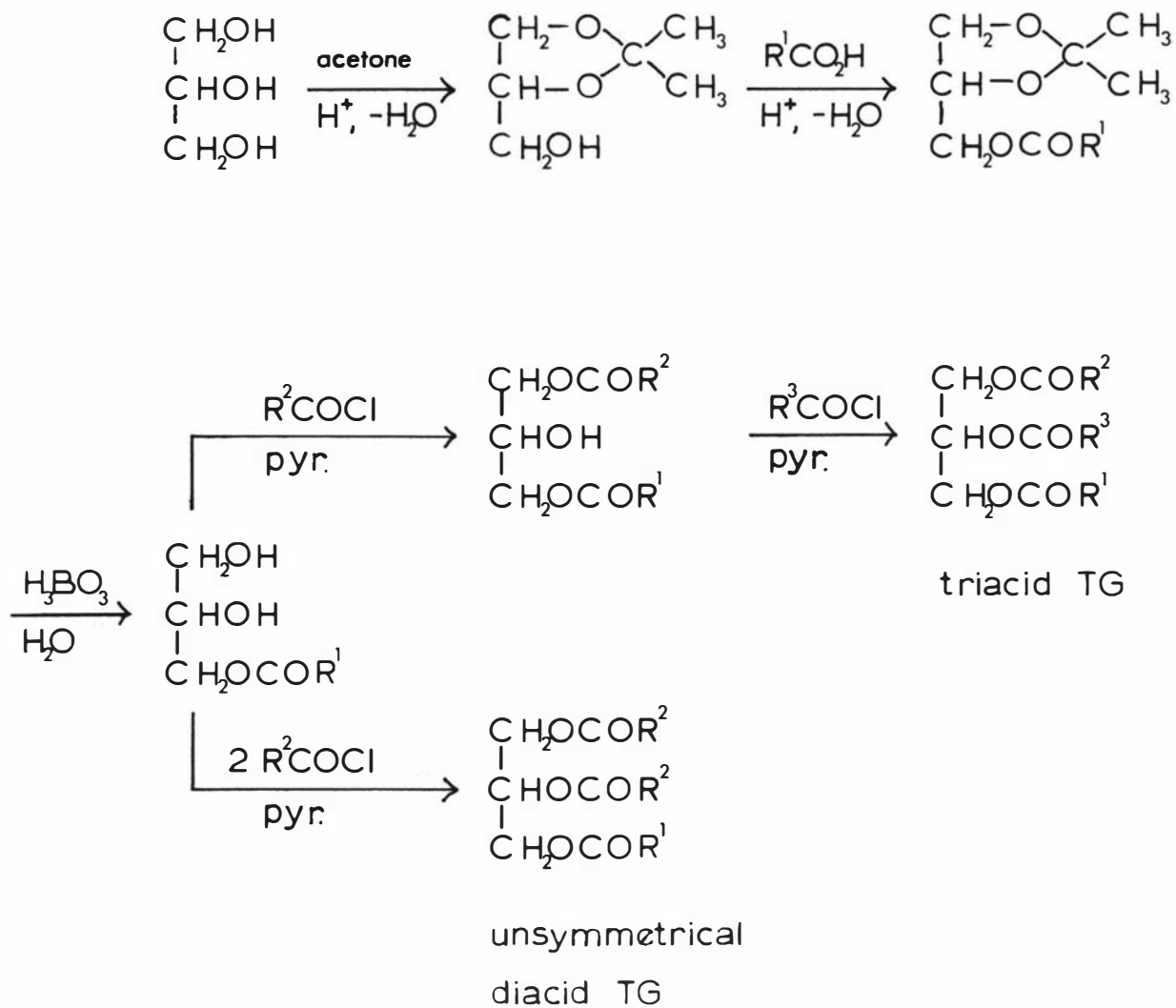
### 2.3.2 1-Acylglycerols

Preparation of rac-1-MGs was the first step in the synthesis of triacid and unsymmetrical diacid TGs (Figs. 2-2 and 2-3 scheme 1).

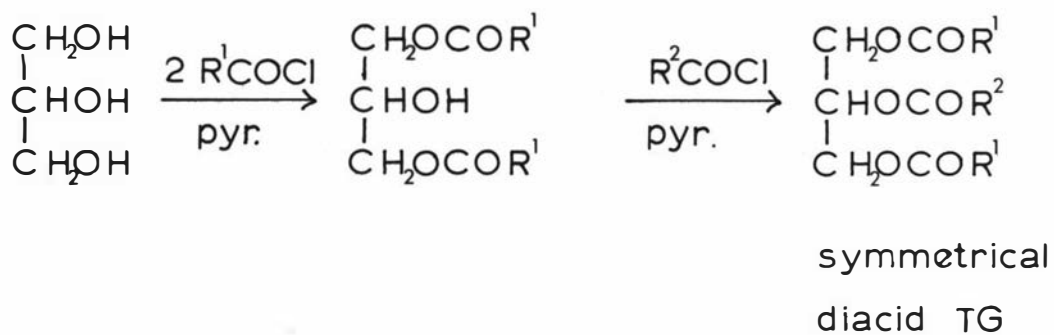
Racemic 1-MGs were prepared (Fig. 2-3 scheme 1) by a modification (Quinn et al., 1967) of Hartman's procedure (1960). Glycerol (0.72 mol), acetone (1.44 mol), p-toluene sulphonic acid hydrate (0.01 mol) and 500ml of benzene were refluxed in a 2l flask fitted with a Dean-Stark trap and a condenser. At the cessation of water formation (10-12h), 0.24 mol of fatty acid (palmitic, stearic or oleic) was added and the refluxing continued for a further 12-16h until water formation had again stopped. The acid catalyst was then neutralised by shaking the flask contents with powdered anhydrous sodium acetate (0.03 mol). After filtering, the solution was washed with water to remove excess isopropylidene glycerol, dried with anhydrous Na<sub>2</sub>SO<sub>4</sub> and then evaporated to dryness under reduced pressure.

FIG. 2-3 SYNTHESIS OF RACEMIC TRIACYLGLYCEROLS

## Scheme 1



## Scheme 2



Note: pyr. = pyridine

The ketal blocking group was removed by borate replacement; the acyl acetone glycerol was reacted with boric acid (2.4 mol) in 400ml of 2-methoxyethanol for 1.5 h at 100°C. The reaction was carried out with careful exclusion of water in a 2l flask fitted with an air condenser, a silica gel drying tube and a magnetic stirrer bar. At the completion of the reaction the flask contents were allowed to cool and were then filtered. The boric acid precipitate was washed repeatedly with a total of 2l of diethyl ether-chloroform (3:1) and the combined filtrates were extracted with water (4 x 1l) and dried with anhydrous Na<sub>2</sub>SO<sub>4</sub>. Most of the solvent was removed under reduced pressure at 30-35°C and the crude 1-MG was then crystallised two or three times from 10-15 vol. of diethyl ether-hexane (6:4) at 20°C for the saturated 1-MGs and -20°C for 1-oleoylglycerol. Examination of the recrystallised products by TLC showed that only traces of the 2-isomer were present. Furthermore, IR spectroscopy of the methyl ester prepared from 1-oleoylglycerol demonstrated that no detectable isomerisation of the double bond had occurred.

<u>rac</u> -1-palmitoylglycerol	m.p. observed	75-76°C
	literature	76.5°C (Lutton, 1971b)
	yield	73% based on fatty acid
<u>rac</u> -1-stearoylglycerol	m.p. observed	80-81°C
	literature	81.6°C (Lutton, 1971b)
	yield	71%
<u>rac</u> -1-oleoylglycerol	yield	66%

### 2.3.3 1,3-Diacylglycerols

#### (a) Monoacid 1,3-Diacylglycerols

The preparation of monoacid 1,3-diacylglycerols (1,3-DGs) was the first step in the synthesis of symmetrical diacid TGs (Figs. 2-2 and 2-3 scheme 2).

1,3-Dipalmitoyl- and 1,3-distearoyl-glycerol were prepared by the direct esterification of glycerol in an homogeneous reaction system (Hartman, 1957). Anhydrous glycerol (0.05 mol) was dissolved in N,N'-dimethylformamide (10ml), chloroform (75ml) and pyridine (25ml) in a dry stoppered flask. Stearoyl or palmitoyl chloride (0.11 mol) in chloroform (150ml) was then added dropwise to the magnetically stirred solution. If necessary, more pyridine or dimethylformamide was added at this stage to ensure that the flask contents were homogeneous. After 4-16h, methanol (10ml) was added to react with unchanged acyl chloride and the

clear solution was then evaporated to dryness at 30-35°C. Examination of the crude reaction product by TLC showed that the chief impurities were methyl ester, TG, 1,2-DG and 1-MG. The oily solid was then crystallised successively from 300ml of absolute ethanol and 250ml of hexane at 20°C. This procedure removed pyridine, dimethylformamide and most lipid contaminants except for TG. The latter was removed by two further recrystallisations from 10 vol. of hexane at 35°C. TLC of the final product showed no detectable impurities.

1,3-dipalmitoylglycerol	m.p. observed	73.5-74.0°C
	literature	73.5-74.0°C (Hartman, 1957)

yield 51% based on glycerol

1,3-distearoylglycerol	m.p. observed	79-80°C
	literature	80°C (Hartman, 1957)

yield 56%

(b) Recovery of Triacylglycerol from 1,3-Diacylglycerol Preparation

The combined 35°C hexane filtrates from the 1,3-DG purification were evaporated to dryness and the resultant solid was recrystallised twice from absolute ethanol-hexane (1:1) and then twice from chloroform-hexane (1:5). TIC of the recrystallised TG showed no detectable impurities.

tripalmitoylglycerol	m.p. observed	65.8-66.2°C
	literature	66.4°C (Lutton and Fehl, 1970)

yield 15% based on glycerol

tristearoylglycerol	m.p. observed	71.5-72.5°C
	literature	73.5°C (Lutton and Fehl, 1970)

yield 6%

(c) Diacid 1,3-Diacylglycerols

Diacid rac-1,3-diacylglycerols were intermediates in the synthesis of all triacid TGs and the diacid TGs, BPP, BSS, OOP and OOS (Figs. 2-2 and 2-3 scheme 1).

(i) Diacid 1,3-Diacylglycerols of High Molecular Weight

Rac-1-oleoyl-3-stearoylglycerol and rac-1-oleoyl-3-palmitoylglycerol were prepared by the esterification of rac-1-oleoylglycerol (100g/l in chloroform) with an equimolar quantity of stearoyl or palmitoyl chloride in the presence of excess pyridine (Hartman, 1957). After

standing overnight, methanol was added to react with any remaining acyl chloride and the solution was evaporated under reduced pressure at 30-35°C. The resultant solid was taken up in ether and the solution was then extracted four times with water to remove pyridine and evaporated to dryness at 30-35°C. Finally, the crude 1,3-diacylglycerol was crystallised from 95% ethanol (10 vol; 0°C), followed by two recrystallisations from hexane (10 vol.; 0°C). No impurities could be detected in the products by TLC. Based on 1-MG, the yields of 1,3-DG were 70 and 64% for rac-1-oleoyl-3-stearoylglycerol and 1-oleoyl-3-palmitoylglycerol respectively.

1-Palmitoyl-3-stearoylglycerol was recovered as a by-product from the preparation of the TG PPS. 1-Stearoylglycerol (0.05 mol) was incompletely esterified by reaction with palmitoyl chloride (0.10 mol) for 24h and the TG recovered by 4 crystallisations of the crude reaction mixture from acetone-chloroform-hexane (4 : 1 : 1). The first two filtrates were then combined and recrystallised three times from hexane (10-15 vol.) at 35°C to yield 9% (based on 1-MG) of the pure 1,3-DG.

(ii) Diacid 1,3-Diacylglycerols of Low Molecular Weight

Monobutyryl 1,3-DGs were prepared from palmitoyl or stearoyl 1-MGs because of the difficulty of synthesising pure 1-butyrylglycerol.

Rac-1-stearoylglycerol (100g/l in chloroform) was esterified with butyryl chloride (1 : 1.05 molar ratio) in the presence of excess pyridine. After leaving overnight, the solution was evaporated in vacuo at 30-35°C to remove chloroform, pyridine and any remaining butyryl chloride. Examination of the crude product by TLC showed that the main impurities were pyridine hydrochloride, unreacted 1-MG, 1,2-DG and TG.

Pyridine hydrochloride was removed by dissolving the crude solid in warm hexane (5 vol.), cooling to 20°C and filtering through a Millipore membrane filter under positive nitrogen pressure. (Pyridine hydrochloride could not readily be removed by extraction with water because of the very stable emulsions formed when organic solutions of the crude DG were shaken with water. Presumably DGs containing short and long chain fatty acids are effective emulsifiers). The clear hexane solution was evaporated to dryness at 30-35°C and the resultant solid was chromatographed on a column of aluminium oxide-boric acid to remove 1-MG and remaining traces of pyridine hydrochloride (Section 2.2.2). Finally, to remove TG and 1,2-DG, the product was crystallised twice from 15 vol. of hexane at -5°C. The overall yield of rac-1-butyryl-3-stearoylglycerol was 61% (based on 1-MG) and no impurities could be detected in the product by TLC.

Rac-1-butyryl-3-palmitoylglycerol was prepared in a similar manner, although the overall yield was much lower (29% based on 1-MG) because of the higher molar ratio of acyl chloride to 1-MG (1.5 : 1) and the loss of material during repeated attempts to remove 1-MG by extraction, crystallisation and, finally, column chromatography. Because of the large excess of acyl chloride, the TG BBP accounted for about half of the crude reaction product. It was recovered from the final two hexane filtrates and purified by column chromatography on alumina (Jensen et al., 1966). The yield of pure BBP was 32% based on 1-MG.

#### 2.3.4 1,2-Distearoylglycerol

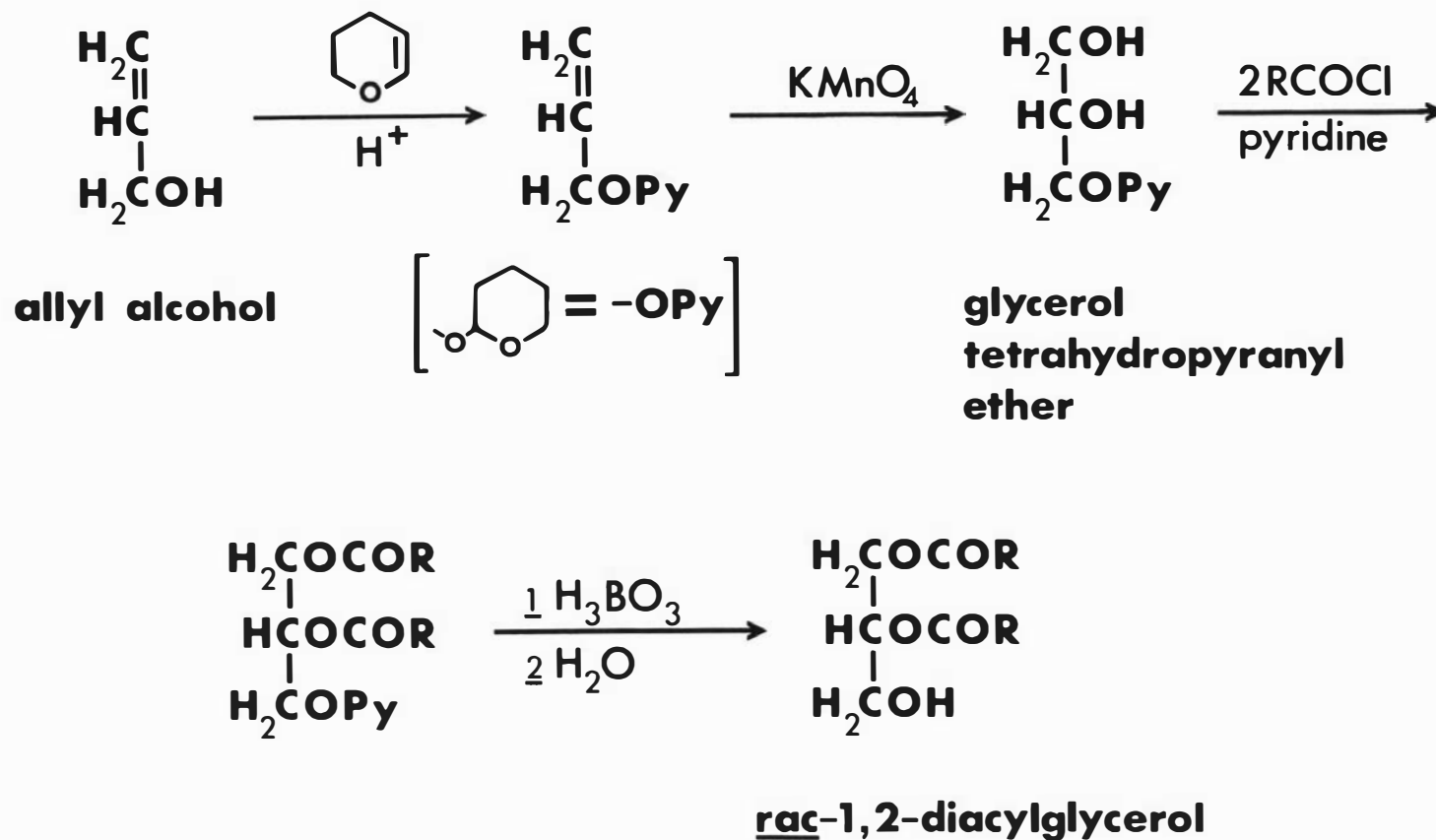
Rac-1,2-distearoylglycerol, an intermediate in the preparation of the TGs ESS and PSS, was synthesised according to the scheme shown in Fig. 2-4.

Glycerol-1-tetrahydropyranyl(THP) ether (Barry and Craig, 1955) was esterified with stearoyl chloride (10% molar excess) in a one phase system containing chloroform, N,N'-dimethylformamide and excess pyridine. After 10 days, methanol was added and the solution was evaporated in vacuo at 35-40°C. The resultant slurry was taken up in ether, and the solution was washed with water (to remove pyridine and N,N'-dimethylformamide), dried with anhydrous Na<sub>2</sub>SO<sub>4</sub> and evaporated to dryness in vacuo.

The THP group was removed from the crude rac-1,2-distearoyl-3-(tetrahydropyranyl)-glyceryl ether by a modification of the procedure of Gigg and Gigg (1967) which utilised the cleavage and protective properties of boric acid (compare the removal of the isopropylidene group in the preparation of rac-1-MGs). Boric acid (0.54 mol) and rac-1,2-distearoyl-3-(tetrahydropyranyl)-glyceryl ether (0.0189 mol) in 140ml of 2-methoxyethanol were placed in a round-bottom flask fitted with an air condenser, a silica gel drying tube and a magnetic stirrer bar. The flask was transferred to a boiling water bath and the contents were vigorously stirred for 1.5h. After cooling to 20°C, the slurry was diluted with dichloromethane and filtered to remove boric acid. The clear filtrate was washed with water and then evaporated to dryness at 35-40°C. Examination of the crude reaction product by TLC showed that the main impurities were: 1-MG, 1-(mono)stearoyl-3-(tetrahydropyranyl)-glyceryl ether, stearic acid and (running together) methyl stearate and unchanged 1,2-distearoyl-3-(tetrahydropyranyl)glyceryl ether. Only a trace (<1%) of 1,3-DG was present with the 1,2-DG, which formed the majority of the reaction product. The 1,2-DG was purified by crystallisation of the crude product from 20 vol. of acetone-methanol (1 : 1) at

**Fig. 2-4 SYNTHESIS OF RACEMIC 1,2 - DIACYLGLYCEROL**

Adapted from Krabisch and Borgstrom [1965]



0°C followed by two recrystallisations from chloroform-hexane (1 : 10) at -5°C. No impurities in the final 1,2-DG could be detected by TLC.

<u>rac</u> -1,2-distearoylglycerol	m.p. observed	70-72°C
	literature	71°C (Howe and Malkin, 1951)
	yield	47% based on glycerol-1-tetrahydropyranyl ether

### 2.3.5 Triacylglycerols

TGs were prepared by esterification of the appropriate partial glyceride according to the scheme outlined in Fig. 2-2. The partial glyceride was dissolved in chloroform and reacted with acyl chloride in the presence of excess pyridine. To ensure maximum TG yield, a 50% molar excess of acyl chloride was normally used (Quinn *et al.*, 1967), but this was reduced to a 10% excess for the butyryl TGs to avoid possible difficulties in purification. After reaction times (at 20°C) of 4-16h for 1,2-DG or 3-7 days for 1-MG and 1,3-DG, methanol was usually added to react with excess acyl chloride and the solution was evaporated to dryness at < 35°C. Purification was then carried out as follows:-

- 1) Saturated TGs of high molecular weight were first recrystallised once or twice from either absolute ethanol-acetone (4 : 1) or absolute ethanol-hexane (1 : 1) to remove methyl ester, partial glycerides and pyridine hydrochloride, and then 1 to 3 times from acetone-hexane (4 : 1) to remove fatty acid. (Unless otherwise stated, all crystallisations were from 10-15 vol. of solvent at 20°C.)
- 2) Monobutyryl saturated TGs were recrystallised twice from acetone-methanol (2 : 1) at 20-25°C, chromatographed on alumina (Jensen *et al.*, 1966) and finally recrystallised from acetone or acetone-hexane (4 : 1) at -5°C.
- 3) Crude SES and ESS were taken up in hexane, washed with 95% ethanol and evaporated to dryness. The oily solids were crystallised from acetone-methanol (2 : 1) at 12°C, chromatographed on alumina (at 30°C) and finally recrystallised from 15 vol. of acetone at -5°C.
- 4) Monooleoyl TGs of high molecular weight were crystallised twice from acetone or acetone-hexane (4 : 1) at 0°C or -5°C, chromatographed on alumina and then recrystallised from 15 vol. of acetone at -5°C.
- 5) Crude BES was taken up in hexane and washed several times with 95% methanol. The hexane solution was then evaporated to dryness and

chromatographed on alumina. After evaporation of the eluant, the slowly solidifying oil was crystallised twice from 40 vol. of acetone-methanol (2 : 1) at  $-18^{\circ}\text{C}$ .

6) TGs which are liquid at or near room temperature (BOP, BOS, OOP and OOS) were taken up in hexane and extracted with water. After evaporation of the hexane solution in vacuo, the oils were purified by chromatography on alumina. The products were not purified by crystallisation because of their high solubility.

All crystallisations were monitored by TLC of both filtrate and precipitate. With the exception of BES, the purified TGs contained no impurities detectable by TLC. However, the chromatographic examination of BES showed a trace of an impurity which ran slightly ahead of the main band on a TLC plate developed in dichloromethane. The closeness of the  $R_f$  values suggested the possibility that the impurity was isomeric with BES, for example EBS.

Yields of the pure TGs based on the partial glycerides were approximately 65% for the butyryl TGs and 75% for the others.

#### 2.4 Preparation of Enantiomeric Triacylglycerols

The general scheme adopted for the preparation of chiral TGs is shown in Fig. 2-5. 1,2-Dipalmitoyl- and 1,2-distearoyl-sn-glycerol were synthesised from the key intermediate, 1,2-isopropylidene-sn-glycerol (Baer and Fischer, 1939a), using the trichloroethylcarbonate group to block the sn-3-position (Rakhit, Bagli and Deghenghi, 1969; Pfeiffer, Miao and Weisbach, 1970). The sn-TGs were then prepared by esterification of the sn-1,2-DGs with the appropriate acyl chloride.

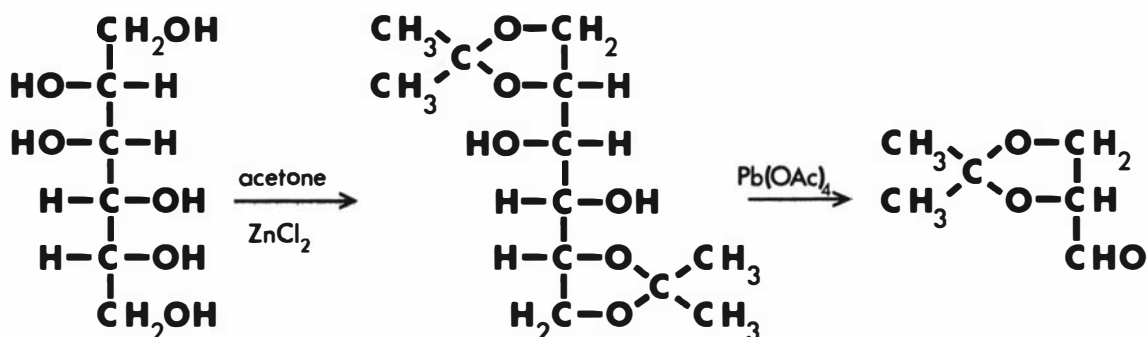
Although this procedure involves two additional steps compared with the alternative synthesis via sn-3-MG (cf. Fig. 2-3, Scheme 1) the removal of the carbonate blocking group occurs under particularly mild conditions and causes little or no acyl migration. Thus, only a trace (< 2%) of the 1,3-DG isomer was present in the crude sn-1,2-DG prepared by the above method; by contrast, 5-10% of the 2-MG isomer was present in trial preparations of crude sn-3-MG. Since acyl migration leads to racemisation, the former synthetic scheme was chosen in preference to the latter.

##### 2.4.1 1,2-Isopropylidene-sn-glycerol

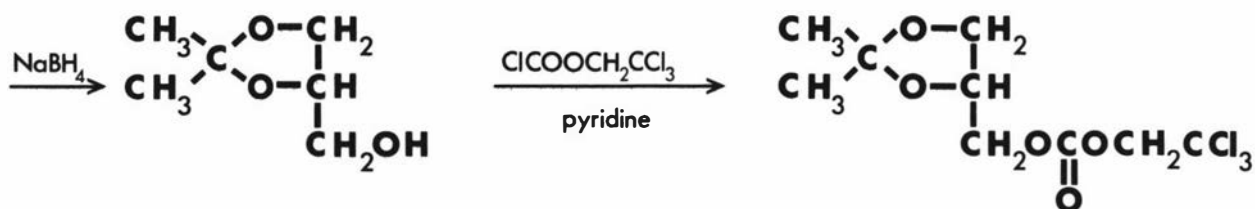
This key intermediate was prepared by the procedure of Baer (1952) except that sodium borohydride was used for the reduction of 1,2-isopropy-

**FIG. 2-5 SYNTHESIS OF ENANTIOMERIC TRIACYLGLYCEROLS**

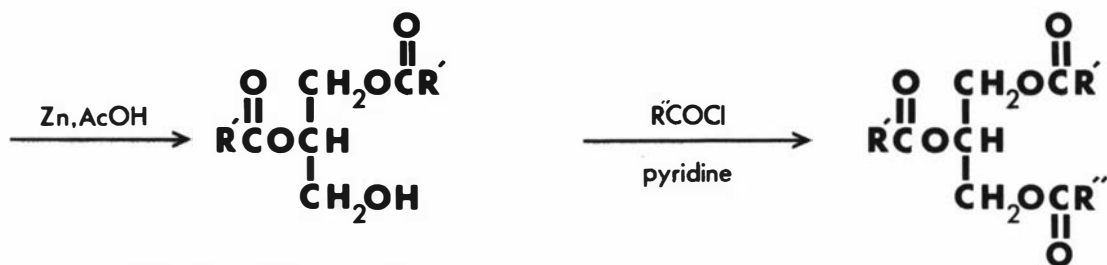
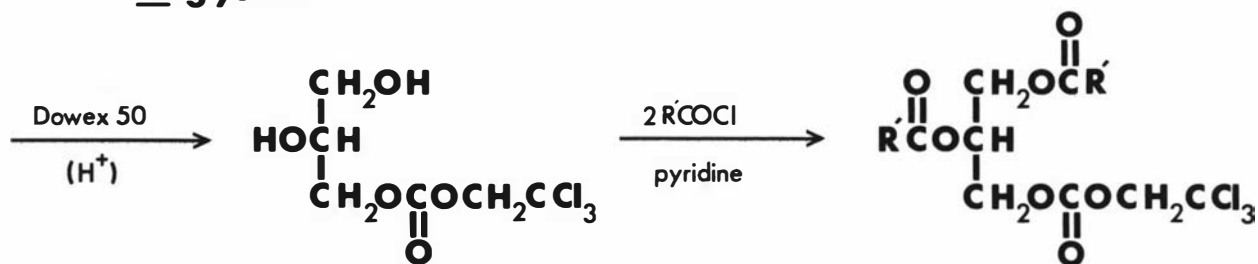
[Rakhit *et al.*, 1969]



**D-mannitol**



**1,2-isopropylidene-sn-glycerol**



**1,2-diacyl-sn-glycerol**

**diacid sn-TG**

lidene-sn-glyceraldehyde (Fig. 2-5).

A solution of the aldehyde (0.2 mol) in methanol (5 vol.) was added dropwise to sodium borohydride (0.1 mol) in water (25ml). The magnetically stirred reaction mixture was maintained at  $\sim 20^{\circ}\text{C}$  during the addition (30 min) and for a subsequent 2h period. The solution was then refluxed for 30 min to decompose excess sodium borohydride, evaporated under reduced pressure to half its volume, saturated with  $\text{K}_2\text{CO}_3$  and extracted with ether (3 x 100ml). The ether extracts were combined, dried with anhydrous  $\text{Na}_2\text{SO}_4$  and concentrated in a rotary evaporator at  $30\text{-}35^{\circ}\text{C}$ . Distillation of the resultant syrup gave a middle fraction, b.p.  $80\text{-}84^{\circ}\text{C}/12$  mm Hg. The purity of the product, 1,2-isopropylidene-sn-glycerol, was confirmed by comparison of its GLC behaviour with an authentic sample of rac-1,2-isopropylidene-glycerol (DEGS column at  $105^{\circ}\text{C}$ ).

#### 1,2-isopropylidene-sn-glycerol

	observed	literature (Baer, 1952)
$n_{20}^D$	1.4348	1.4347
$[\alpha]_D^{20}$	$14.08 \pm 0.07^{\circ}$	$13.8^{\circ}$
	in substance	

#### 2.4.2 1,2-Diacyl-sn-glycerols

1,2-Distearoyl- and 1,2-dipalmitoyl-sn-glycerol were prepared by the method of Rakhit et al. (1969) according to the scheme shown in Fig. 2-5. Treatment of 1,2-isopropylidene-sn-glycerol with  $\beta,\beta,\beta$ -trichloroethoxycarbonyl chloride gave the corresponding carbonate. A solution of this carbonate in 90% (v/v) methanol was then passed through a column of Dowex 50 ( $\text{H}^+$ ) ion exchange resin resulting in the hydrolysis of the isopropylidene group and formation of 3-( $\beta,\beta,\beta$ -trichloroethyl-carbonate)-sn-glycerol. After removal of solvent, the crude diol was fully esterified with a 10% molar excess of palmitoyl or stearoylchloride and the resulting 1,2-diacylcarbonate was treated with zinc powder in acetic acid-diethyl ether (1:1) to remove the blocking group.

The crude sn-1,2-DG, which contained only a trace of 1,3-DG, was crystallised from 10 vol. of acetone/methanol (1:1) at  $-5^{\circ}\text{C}$  and then recrystallised twice from chloroform-hexane (1:10) at  $20^{\circ}\text{C}$ . Examination of the product by TLC showed only one spot up to the overload limit of the plate.

1,2-dipalmitoyl- <u>sn</u> -glycerol	m.p. observed	67-68°C
	literature	67-67.5°C (Sowden and Fischer, 1941) 68-69°C (Baer and Kates, 1950)
	yield	43% based on 3-(β,β,β-trichloroethyl-carbonate)- <u>sn</u> -glycerol
1,2-distearoyl- <u>sn</u> -glycerol	m.p. observed	74-75.5°C
	literature	74-74.5°C (Sowden and Fischer, 1941) 76-77°C (Baer and Kates, 1950)
	yield	48%

### 2.4.3 Triacylglycerols

Diacid sn-TGs were prepared by esterification of 1,2-dipalmitoyl- and 1,2-distearoyl-sn-glycerol with butyryl or oleoyl chloride. The sn-1,2-DG (0.001 mol) was dissolved in chloroform and esterified with a 10% molar excess of the oleoyl chloride or a 20% molar excess of the butyryl chloride in the presence of excess pyridine. After a reaction time of 30h at 20°C, purification was carried out as follows:-

#### 1) sn-SSB

The reaction mixture was evaporated to dryness at 30-35°C and taken up in 25ml of diethyl ether. The solution was extracted with water (4 x 10ml) and dried with anhydrous Na<sub>2</sub>SO<sub>4</sub>. After removal of the solvent, the crude solid was crystallised from acetone-methanol (2 : 1) at 20°C, chromatographed on alumina and finally recrystallised from acetone at -5°C.

#### 2) sn-SSO

The reaction mixture was worked up similarly to that of sn-SSB except that the crude TG was chromatographed without prior crystallisation. The resultant solid was recrystallised from acetone at -5°C.

#### 3) sn-PPO

Methanol was added to the reaction mixture which was then evaporated to dryness at 30-35°C. The crude solid was taken up in hexane and successively washed with 2M-HCl, M-NaHCO<sub>3</sub> and water. After evaporation of the hexane solution, the strongly-coloured oil was crystallised from 15 vol. of acetone at -5°C, chromatographed on alumina and recrystallised as before.

No impurities could be detected by TLC in the recrystallised products.

## B. Physical Methods

### 2.5 Melting Point Determination

Melting points above 30°C were determined with a calibrated Koffler hot stage microscope to an accuracy of  $\pm 0.5^\circ\text{C}$ .

### 2.6 X-Ray Powder Diffraction

#### 2.6.1 Apparatus

Diffraction patterns of all solvent crystallised phases were obtained using a Philips goniometer (model PW 1050) and an X-ray generator (PW 1010) with a cobalt target ( $K\alpha_1$ ;  $\lambda = 1.789\text{\AA}$ ). Short spacing data were collected by scanning from  $2\theta$  values of  $17^\circ$  to  $32^\circ$  ( $6.05\text{\AA}$  to  $3.25\text{\AA}$ ) at  $2^\circ/\text{min}$ . No long spacings were determined because of the obscuring effect of the high background at low  $2\theta$  values.

#### 2.6.2 Preparation of Samples

Powder films of high-melting TGs were prepared by depositing a few drops of a dichloromethane solution of the TG on a diffractometer slide and allowing the solvent to evaporate. This technique was unsuccessful with low-melting TGs and in such cases the solid was ground with the minimum of silica gel H necessary to give a non-caking, fine powder and then spread as a uniform film on a vaseline-smeared sample slide. The addition of silica gel H was found essential to permit effective grinding and thereby prevent spurious 'preferred orientation' effects (cf. Klein and Wilcox, 1971). Comparison between diffraction patterns obtained for ESS, SES and SOS by the two methods of sample preparation showed that although the use of silica gel H gave patterns with a convex baseline, it did not significantly obscure or distort the TG short spacings.

#### 2.6.3 Identification of Polymorphs

Polymorphic forms examined by X-ray diffraction were classified according to the criteria of Lutton (Table 1.1). Thus, a form showing two strong short-spacing lines near  $4.2$  and  $3.8\text{\AA}$  was called  $\beta'$ , while a form with a strong line near  $4.6\text{\AA}$  was termed  $\beta$ .

## 2.7 Infrared Spectroscopy

### 2.7.1 Apparatus

Solid state infrared spectra of TGs were recorded on a Beckman (Fullerton, California, U.S.A.) IR-20 spectrophotometer. Under standard conditions, the instrument was scanned at  $240\text{cm}^{-1}/\text{min}$  from  $1500$  to  $600\text{cm}^{-1}$ , the most useful region for the identification of polymorphic forms (de Ruig, 1971). Where closer examination of the  $720\text{cm}^{-1}$  band was required, the instrument was scanned from  $800$  to  $600\text{cm}^{-1}$  at  $60\text{cm}^{-1}/\text{min}$  with fourfold scale expansion of the abscissa. Wave number accuracy was better than  $2\text{cm}^{-1}$  (calibrated) and  $10\text{cm}^{-1}$  (uncalibrated) over the entire range and resolution was better than  $5\text{cm}^{-1}$  at  $720\text{cm}^{-1}$ .

Solvent crystallised phases were examined as KBr discs which were prepared in a Wilks (South Norwalk, Connecticut, U.S.A.) Minipress using BDH KBr "specially prepared for IR spectroscopy".

The polymorphism of rac-TGs containing butyrate, elaidate or oleate was investigated using a Variable Temperature Chamber Model 104 (Barnes Engineering, Stamford, Connecticut, U.S.A.). The chamber temperature was measured to an accuracy of  $\pm 0.5^{\circ}\text{C}$  by a calibrated copper/constantan thermocouple pair connected to a digital voltmeter.

### 2.7.2 Investigation of Polymorphism

A few drops of molten TG were placed between KBr plates and the cell was loaded in the variable temperature chamber and equilibrated at  $10$ - $20^{\circ}\text{C}$  above the melting point of the stable form. After recording the spectrum of the melt, the chamber was cooled rapidly to  $\sim 0^{\circ}\text{C}$  to produce the  $\alpha$  form. The  $\alpha$  spectrum was recorded and the temperature further reduced to  $-30^{\circ}\text{C}$ , the lower limit of the chamber, to investigate possible formation of the sub- $\alpha$  phase. TGs with  $\alpha$  forms melting below  $0^{\circ}\text{C}$  were cooled directly to  $-30^{\circ}\text{C}$ .

The sample was then slowly heated to the  $\alpha$  melting or transition temperature and held isothermally until successive spectra showed no further change. After recording the spectrum of the new form, the procedure was repeated at each successive transition point until the stable form was obtained (de Ruig, 1971). Finally, the sample was melted as before and then crystallised  $1$ - $2^{\circ}\text{C}$  above the  $\alpha$  melting point; the spectrum of the form so obtained was compared with the corresponding spectra recorded during the heating cycle. This procedure was repeated for each of the transition points found previously. Thus, the form or

forms intermediate between  $\alpha$  and the stable form were normally obtained both by transformation of lower melting forms and by crystallisation from the melt. Comparison of the spectra obtained in these two ways provided a useful check on phase purity.

### 2.7.3 Identification of Polymorphs

Polymorphs were identified by comparison of their spectra with those of the  $\alpha$ ,  $\beta'$  and  $\beta$  phases of monoacid TGs (Chapman, 1965; de Ruig, 1971; Table 1.5). In particular, the following criteria were used:-

- $\alpha$  - a form crystallising from the melt and displaying a single band at  $720\text{cm}^{-1}$ .
- $\beta'$  - a form exhibiting a doublet in the  $720\text{cm}^{-1}$  region ( $\sim 719$  and  $726\text{cm}^{-1}$ ); other characteristic bands are often present at  $\sim 835$ ,  $925$ ,  $950$  and  $975\text{cm}^{-1}$ .
- $\beta$  - a form displaying a single sharp band near  $717\text{cm}^{-1}$ ; often a strong band near  $890\text{-}900\text{cm}^{-1}$  is also present.

The term 'sub- $\alpha$ ' was retained for any phase which was reversibly obtained by cooling the  $\alpha$  form and which exhibited a doublet in the  $720\text{cm}^{-1}$  region of the IR spectrum ( $\sim 719$  and  $726\text{cm}^{-1}$ ).

Where possible, confirmation of the above assignment was sought by comparison of phase preparation, transition temperature or transformation relationships with either the literature or an analogous form of a related TG.

## 2.8 Thermal Analysis

### 2.8.1 Apparatus

Thermal analysis was performed using a Perkin-Elmer (Norwalk, Connecticut, U.S.A.) DSC 1-b differential scanning calorimeter (DSC). Sealed sample pans and sample holder covers were used for all runs. The sample mass was generally 3-6mg for liquids and 1-3mg for solids. To ensure good thermal contact, solid samples were tightly confined in the base of the pan with an aluminium foil inner liner. The analyser unit was operated in a dry box to permit more convenient sub-ambient operation (Currie and Doyle, 1968) and liquid nitrogen was used as a coolant for all samples except indium. The sample compartment was flushed with dry nitrogen gas at a flow rate of 30ml/min (measured at the outlet at a cell temperature of  $100^\circ\text{C}$  with no coolant).

Data from the DSC was recorded on paper tape by a Hewlett Packard

(Palo Alto, California, U.S.A.) data acquisition system consisting of a coupler-controller (model 2575A) interfaced to a teleprinter (12801A) and a digital voltmeter (3480A).

### 2.8.2 Calibration

Power calibration, thermal resistance and average and differential temperature calibration were checked daily using 99.999% indium (K and K Laboratories, Plainview, New York, U.S.A.) weighed on a Mettler (Zurich, Switzerland) M5A microbalance. The heat of fusion of indium was taken as 29.2J/g (Richardson and Savill, 1975), rather than the older value of 28.4J/g which has been widely used in DSC literature. Previously reported heats of fusion of TGs which are presented here have been adjusted in accordance with the new value. It was found that the power calibration constant relating raw ordinate data (mV) to the true heat flow rate (W) showed little variation over a period of several months. For example, the constant had a coefficient of variation of 2.7% for 150 determinations made over an eleven month period. Consequently, a mean value of the constant, which was averaged over the entire period during which TGs were analysed, was used in the calculation of the heats of fusion of TGs. Similarly, an average value for the thermal resistance was used in the correction for thermal lag.

At approximately three-monthly intervals, the DSC temperature axis was calibrated over the range  $-60^{\circ}\text{C}$  to  $80^{\circ}\text{C}$ , using melting point standards (James Hinton, Newport News, Virginia, U.S.A.) according to the procedure of Thermal Analysis Newsletter No. 5 (Perkin-Elmer, 1966). For each scan rate, the relationship between true temperature and DSC dial temperature was approximated by a quadratic regression, which was subsequently used to correct the temperature axis of recorded thermograms.

### 2.8.3 Presentation of Data

Conventions for the presentation of thermal analysis data are shown in Fig. 2-6. In differential scanning calorimetry, the sample is heated or cooled at a linear scan rate and the heat flow rate to or from the sample is recorded as a function of temperature. Phase transitions appear as peaks superimposed on the scan baseline of the resultant graph, which is called a thermogram. In the present work, raw data corresponding to the uncorrected thermogram were collected and stored on paper tape prior to computer processing. In the subsequent analysis, a straight line was fitted to the initial linear portion of the melting curve. As the data were scanned the first point with a residual greater than three

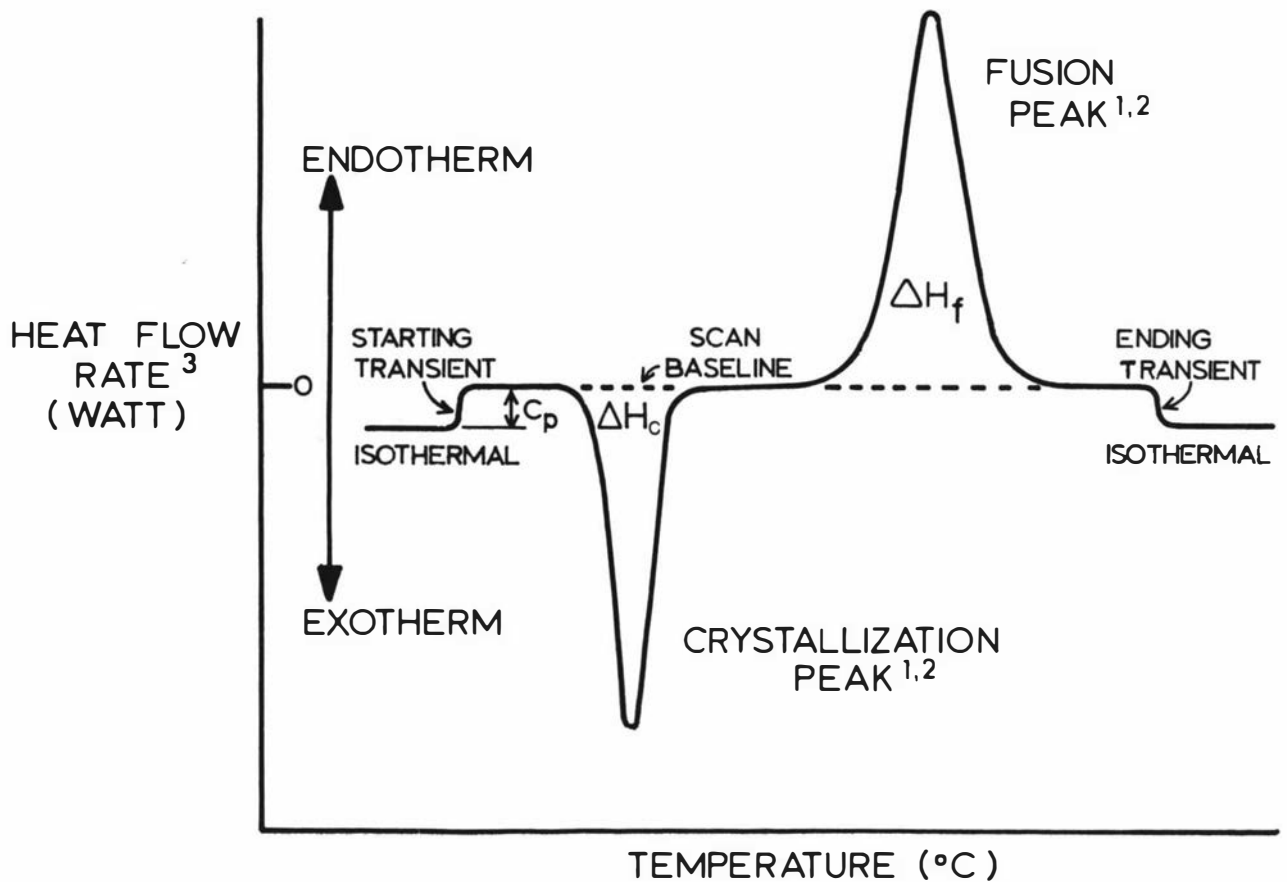


FIG. 2-6 CONVENTIONS FOR THE PRESENTATION OF THERMAL ANALYSIS DATA

- Note
1. Heats of transition are determined from peak areas.
  2. Transition temperatures are determined from peak temperatures corrected for thermal lag.
  3. Ordinate data in this thesis are presented in either specific heat flow rate units (W/g) or apparent specific heat capacity units (J/(gK)) with the scan baseline arbitrarily defined as zero.

standard deviations about the regression line was taken as the start-of-melting. The end-of-melting was determined in a similar manner. The program then determined the area between the melting curve and the straight line connecting the start- and end-of-melting. After corrections for thermal lag and the temperature and power calibration, the computer determined the heat of fusion and the peak temperature (melting point) and plotted a corrected melting curve.

In this thesis, a group of thermograms illustrating the polymorphic behaviour of a single TG or a set of related TGs are presented on common axes. For the sake of clarity, only the transition curves are shown. The y-scale may be regarded as 'floating' with the zero y-value for each thermogram arbitrarily defined by the horizontal line connecting the start- and end-of-transition (i.e. the contribution of the sample's heat capacity to its heat flow rate is arbitrarily set at zero). Normally, the ordinate data of these comparative diagrams are presented in the conventional heat flow rate units (W/g). However, in the comparison of thermograms recorded at different scan rates, the ordinate data are presented in units of apparent heat capacity (J/(gK)), obtained by dividing the heat flow rate values (W/g), of a particular thermogram by the scan rate (K/s). The advantage of using apparent heat capacity units is that the transition area is then independent of scan rate, allowing a more meaningful comparison of thermograms recorded at different rates.

#### 2.8.4 Investigation of Polymorphism

The aim of the thermal analysis was to isolate all the polymorphs of each TG and to determine their melting points and heats of fusion. To this end, the following sequence of thermograms was recorded for all TGs solid at room temperature:-

- 1) solvent crystallised form  $\longrightarrow$  melt
- 2) melt  $\longrightarrow$   $\alpha$
- 3)  $\alpha$   $\longrightarrow$  melt
- 4) intermediate form(s)  $\longrightarrow$  melt

The melting thermogram of the solvent crystallised (stable) form was recorded at a heating rate of 4°C/min from about 20°C below the melting point of the form to about 10°C above. The resultant melt was cooled, usually at 4°C/min, from above the stable form melting point to about 30°C below the main ( $\alpha$ ) crystallisation exotherm. From these two thermograms the thermal properties of the stable and  $\alpha$  forms were determined

and the temperature range of polymorphism defined.

Melting thermograms of the  $\alpha$  form from 2) were recorded from below the  $\alpha$  freezing point to above the stable form melting point at different heating rates. Slower scan rates (typically 2, 4 or 8°C/min) were used to elucidate the  $\alpha$  transformation sequence (and determine melting or transition temperatures) while faster rates (16 or 32°C/min) were employed to determine the heat of fusion of the  $\alpha$  form. The particular choice of scan rates depended principally on the transformation rate of the  $\alpha$  form; the slower the transformation rate, the slower the scan rate required.

Most TGs showed only one major polymorph intermediate in stability between  $\alpha$  and the stable form. This intermediate form was prepared either by isothermal transformation of  $\alpha$  at (or slightly below) its melting point or by crystallisation of the melt at (or slightly above) the same temperature. The minimum time required for each transformation was determined either by monitoring the isothermal heat flow rate (which returned to a constant value at the completion of the transition) or, better, by recording cooling thermograms at increasing time intervals after the start of the transformation (no  $\alpha$  crystallisation exotherm occurred on cooling when the transformation to the intermediate form was complete). Once determined, these minimum times were used for all subsequent preparations. Longer times were avoided because of the possibility of transformation of the intermediate form itself.

Heating thermograms of the intermediate form were recorded using a similar procedure to that described for the  $\alpha$  form. Where the thermogram showed two or more intermediate forms, attempts were made to isolate the higher melting form by transformation of the lower melting form at its melting point, again for the minimum time required for complete transformation. A heating thermogram was then recorded as above. Unfortunately, rapid transformation, partial melting during conversion and overlapping melting ranges often prevented an accurate determination of the heat of fusion of intermediate forms.

Where possible, the stable form was prepared by transformation of  $\alpha$  or the highest melting intermediate form and a heating thermogram was recorded under the same conditions as that for the solvent crystallised form.

With the exception of the solvent crystallised thermogram, a similar set of thermograms was recorded for those TGs which were liquid

at room temperature. The temperature range of their polymorphism was defined by exploratory cooling and heating runs between 35°C and -100°C.

For each TG, replicate thermograms were recorded with different samples and the results averaged. For solvent crystallised forms, the determinations of melting point and heat of fusion had standard deviations of about 0.5°C and 1.5% respectively.

#### 2.8.5 Identification of Polymorphs

Since the DSC can give no structural information, the assignment of the polymorphs present in a thermogram was necessarily indirect. The basic assumption was that for a given thermogram there is a one-to-one correspondence between the number of 'sharp' endothermic transitions and the number of polymorphs.

A single endotherm was classified by comparison of its transition temperature with that of the similarly tempered form examined by IR spectroscopy (or, in some cases, reported in the literature). The same procedure was used to identify the phases present in more complex thermograms but transformational relationships were also invoked in the identification of intermediate forms.

#### 2.9 Preparation of $\beta$ PSP and $\beta'$ SPS

The  $\beta$  form of PSP and the  $\beta'$  form of SPS, which are not accessible by normal tempering procedures, were prepared by the methods of Lutton and Hugenberg (1960, 1963).

$\beta$  PSP was prepared by crystallisation of a 20g/l hexane solution at 16°C (Hugenberg and Lutton, 1963) or of a 50g/l hexane solution at ~26°C in the presence of 1g/l of finely powdered succinic acid (Lutton and Hugenberg, 1960). A further preparation was obtained by evaporation of a dichloromethane solution on a diffractometer slide.

$\beta'$  SPS was prepared by crystallisation of a 100g/l hexane solution in the presence of 2g/l of finely powdered succinic acid at ~34°C for 20 days (Hugenberg and Lutton, 1963). The fine-grained  $\beta$  crystals which formed initially slowly transformed on standing to the spherulitic  $\beta'$  crystals.

The preparations containing succinic acid as nucleating agent were filtered and washed successively with hexane (to remove mother liquor) and methanol (to remove succinic acid) and then dried in vacuo.

## Chapter 3

RESULTS

For ease of reference, the Tables and Figures for this Chapter are collected together on pages 83-92 and 93-119 respectively.

3.1 Structural Analysis of Triacylglycerols

Representative racemic and enantiomeric TGs were subjected to hydrolysis by pancreatic lipase to check their isomeric purity. The results agreed closely with those expected for the composition of position 2 of these TGs (Table 3.1).

The 1,2(2,3)-DGs produced from the hydrolysis of sn-SSB by pancreatic lipase, and from the hydrolysis of sn-SSO by a Grignard reagent, were subjected to stereospecific analysis as a check on the enantiomeric purity of the two glycerides. The fatty acid composition of positions 1, 2 and 3 of sn-SSO and sn-SSB (Table 3.2) was close to that expected for the particular enantiomeric forms, and was therefore consistent with a high optical purity for both TGs.

3.2 Polymorphism of Racemic Triacylglycerols

Comparative results for the polymorphism of structurally related TGs are presented in the following sections of this Chapter, while thermograms and IR spectra of the polymorphs of the individual TGs are shown in the Appendix.

3.2.1 Palmitoyl-Stearoyl and Elaidoyl-Stearoyl Triacylglycerols(a) Solvent Crystallised Forms

Short spacing data for the solvent crystallised forms of SSS, PPP, PSS, PPS, SES and ESS are presented in Table 3.3 and the corresponding X-ray diffraction patterns are shown in Fig. 3-1. As expected, each TG crystallised in the  $\beta$  form, which shows a strong spacing near  $4.6\text{\AA}$ . Furthermore, there was a close similarity between the diffraction patterns of the saturated and unsaturated TGs. The IR spectra of the forms were also characteristic of the  $\beta$  phase, with strong bands at  $716$  and  $890\text{cm}^{-1}$  (e.g.  $\beta$  SES and ESS, Fig. 3-11).

In contrast to the above TGs, the symmetrical glycerides SPS and PSP could be crystallised from solvent in either the  $\beta'$  or  $\beta$  forms. Short spacing data for the normal solvent crystallised forms,  $\beta$  SPS and  $\beta'$  PSP, and the less accessible forms,  $\beta'$  SPS and  $\beta$  PSP (prepared by the methods of Lutton and Hugenberg; 1960, 1963), are also presented in

Table 3.3 and the respective diffraction patterns are shown in Fig. 3-2. Corresponding patterns for the  $\beta$  and  $\beta'$  forms of SPS and PSP were very similar although the  $\beta$  patterns differed somewhat from those of the other palmitoyl-stearoyl TGs (Fig. 3-1). The X-ray assignments were confirmed by IR spectroscopy. DSC results (see below) showed that both SPS and PSP are  $\beta'$ -stable in contrast to the other TGs in this group, which are all  $\beta$ -stable.

(b) Thermal Analysis

All solvent crystallised forms showed a single sharp melting endotherm typical of compounds of high purity (Appendix, Figs. 1 to 7, 9). On cooling the melt at  $4^{\circ}\text{C}/\text{min}$ , the  $\alpha$  form was obtained for all TGs except PSP, which gave a mixture of  $\alpha$  and  $\beta'$ . The pure  $\alpha$  form of PSP was only obtained by cooling at  $16^{\circ}\text{C}/\text{min}$  or higher. The  $\alpha$  form transformed on heating at  $4^{\circ}\text{C}/\text{min}$  to the  $\beta$  form in the case of SSS, SPS, PPP and SES (Fig. 3-3), to the  $\beta'$  form in the case of PSP and PSS and successively to the  $\beta'$  and  $\beta$  forms in the case of ESS (Fig. 3-4). At a heating rate of  $4^{\circ}\text{C}/\text{min}$  the  $\alpha$  form of PPS melted without transformation to a higher form, but at  $1^{\circ}\text{C}/\text{min}$  successive transformation to  $\beta'$  and  $\beta$  forms occurred (Appendix, Fig. 3). Transformation rates varied quite markedly from the very unstable  $\alpha$  PSP, which transformed without melting at a heating rate of  $4^{\circ}\text{C}/\text{min}$ , to the relatively stable  $\alpha$  PPS, which melted without transformation to a higher form at the same scan rate.

The  $\beta'$  forms of all TGs except SPS were readily obtained from the melt by crystallising at a temperature just above the  $\alpha$  melting point. The unsymmetrical TGs (PSS, PPS and ESS) and the  $\beta'$ -stable PSP also gave the  $\beta'$  form by isothermal transformation of the  $\alpha$  form at or just above its melting point. Under these conditions SSS, PPP and SES transformed to the  $\beta$  form.

Figs. 3-5 and 3-6 show the melting thermograms of the  $\beta'$  forms of all TGs except SPS and PSP. The thermograms were recorded at a heating rate of  $4^{\circ}\text{C}/\text{min}$  and all forms except  $\beta'$  PPS were obtained by crystallisation of the melt. All the thermograms showed the presence of two  $\beta'$  forms, that is two forms with melting points intermediate between the  $\alpha$  and  $\beta$  melting points. In each case, on momentarily tempering at the lower peak temperature, the lower melting form,  $\beta'_{2}$ , transformed irreversibly to the  $\beta'_{1}$  form. The stability of the  $\beta'_{1}$  forms was dependent on TG symmetry. Thus the  $\beta'$  form of the symmetrical TGs, SSS, PPP and SES, transformed readily to the stable  $\beta$  form (Fig. 3-5) while the  $\beta'$  forms of the unsymmetrical TGs, PSS, PPS and ESS, melted without transformation

to  $\beta$  (Fig. 3-6). Comparable behaviour was shown by the  $\alpha$  forms, which transformed directly to  $\beta$  in the case of symmetrical TGs, other than PSP, but which transformed to or via  $\beta'$  in the case of the unsymmetrical TGs.

The exceptional nature of the  $\beta'$  forms of SPS and PSP is emphasised by Fig. 3-7 which shows the melting endotherms of  $\beta'$  and  $\beta$  forms of the two TGs, all recorded at  $4^\circ\text{C}/\text{min}$ . All forms melted without transformation to another solid phase and no  $\beta'_2$  forms were evident. The  $\beta'$  forms are clearly higher melting than the  $\beta$  forms.

Table 3.4 gives the melting points of the polymorphic forms of the palmitoyl-stearoyl and elaidoyl-stearoyl TGs, the heats of fusion of the solvent crystallised forms and the heats of crystallisation of the  $\alpha$  forms. With the exception of  $\beta'$  SPS and PSP, the heats of fusion of the  $\beta'$  forms could not be determined as accurately as those of the  $\alpha$  and  $\beta$  forms because of the rapid conversion of  $\beta'$  to  $\beta$ , the overlapping melting of  $\beta'_2$  and  $\beta'_1$  or the wide variation in the heats of transition for replicate phase preparations. The  $\beta'$  heats of fusion reported in Table 3.4 are estimates based on the assumption that only a single phase was present prior to recording the melting thermogram.

The molar heats of fusion of all forms increase in the same order as their melting points. Except for SPS and PSP, the values show an increase in the order  $\alpha < \beta' < \beta$  and a general increase with molecular weight. Thermal data for the corresponding polymorphs of SES and ESS were very similar, in contrast to the differences found between their cis-counterparts, SOS and OSS. From the data presented in Table 3.4, SPS is obviously  $\beta'$ -stable as the  $\beta$  form has the lower heat of fusion and melting point ( $\beta'$ : 206.6kJ/mol,  $68.6^\circ\text{C}$ ;  $\beta$ : 192.9kJ/mol,  $67.6^\circ\text{C}$ ). In the case of PSP, however, the heats of fusion of the  $\beta'$  and  $\beta$  forms are practically identical and only the lower  $\beta$  melting point confirms that  $\beta'$  is the stable form ( $\beta'$ : 178.8kJ/mol,  $67.7^\circ\text{C}$ ;  $\beta$ : 179.5kJ/mol,  $64.6^\circ\text{C}$ ). The molar heats of fusion of the  $\beta$  forms of these two TGs are comparable with those of their unsymmetrical counterparts ( $\beta$  PSS: 190.0kJ/mol;  $\beta$  PPS: 174.4kJ/mol) but the heats of fusion of  $\beta'$  SPS and PSP are very much higher than the corresponding values for PSS ( $\beta'$ : 140kJ/mol) and PPS ( $\beta'$ : 134kJ/mol).

### 3.2.2 1-Butyryl-2-Oleoyl and 1,2-Dioleoyl Triacylglycerols

The polymorphic behaviour of OOS, OOP, BOS and BOP is summarised below. Since the stable forms of these TGs melt at or below room temperature, no solvent crystallised forms were examined.

(a) Variable Temperature IR Spectroscopy

These two sets of TGs were grouped together primarily because the IR spectra of their stable forms were surprisingly similar (Fig. 3-8). The spectra were unusual in that they exhibited bands specific for the  $\beta'$  form at 835, 940 and  $980\text{cm}^{-1}$ , but rather than the expected doublet at  $720\text{cm}^{-1}$ , they showed a diffuse singlet, even at  $-30^\circ\text{C}$ . In addition to the  $\beta'$  stable phases, the IR study of OOS, BOS and BOP showed the existence of sub- $\alpha$  and  $\alpha$  forms (Appendix, Figs. 12, 16 and 18). Sub- $\alpha$  was obtained by cooling the melt to  $-30^\circ\text{C}$  and on heating transformed, reversibly, to  $\alpha$ . However, no  $\alpha$  form of OOP could be obtained as the stable form crystallised even with the most rapid cooling to  $-30^\circ\text{C}$ . This reflects the lower stability of the  $\alpha$  form of OOP compared with the  $\alpha$  forms of the other TGs. The  $\alpha$  spectra were more diffuse than those of higher melting TGs, although methylene wagging band progressions contributed by the palmitoyl or stearoyl diatheses were discernible. Transformation of  $\alpha$  or crystallisation of the melt at or just above the  $\alpha$  melting point gave the stable  $\beta'$  form.

(b) Thermal Analysis

Heating thermograms of the rapidly crystallised melt showed that the  $\alpha$  forms of OOS and OOP were much less stable (with respect to transformation to  $\beta'$ ) than those of BOS and BOP. For example, at a heating rate of  $16^\circ\text{C}/\text{min}$  the  $\alpha$  form of BOP melted without transformation to  $\beta'$  while the  $\alpha$  form of OOP transformed readily even at  $64^\circ\text{C}/\text{min}$  (Fig. 3-9). In keeping with the behaviour of other homologues, the  $\alpha$  forms of the palmitoyl TGs transformed more rapidly than those of the corresponding stearoyl TGs.

Both sets of TGs showed a reversible, low energy transition, here called  $\alpha_2$ , involving the main  $\alpha$  form,  $\alpha_1$ . For OOS and OOP the  $\alpha_2$  transitions, not shown in Fig. 3-9, occurred at  $-60^\circ\text{C}$  and  $-57^\circ\text{C}$  respectively and the heat of transition was  $\sim 15\%$  of the heat of fusion of the main  $\alpha_1$  form in both cases. For BOS and BOP, the  $\alpha_2$  transitions occurred at  $-11^\circ\text{C}$  and  $-25^\circ\text{C}$  respectively but the heat of transition was only  $\sim 2\%$  of the  $\alpha_1$  heat of fusion. There was evidence in some thermograms for a form intermediate between  $\alpha$  and  $\beta'$  in the case of OOS and OOP but not in the case of BOS and BOP.

Table 3.5 summarises the thermal properties of OOS, OOP, BOS and BOP. As expected, the melting points and heats of fusion were the lowest of the TG classes studied, reflecting the presence of two low-melting acyl residues per molecule. The molar heats of fusion of the  $\beta'$  forms

increased with increasing molecular weight, i.e. in the order: BOP < BOS < OOP < OOS. The large differences in the values for corresponding dioleoyl and butyryl-oleoyl TGs ( $\sim 22\text{kJ/mol}$ ) suggest that the contribution to the packing of the stable form made by an oleoyl chain in position 1 is greater than that made by a butyryl chain. The molar heats of crystallisation of the  $\alpha$  forms also increased with molecular weight, but the differences between the values for corresponding dioleoyl and butyryl-oleoyl TGs were relatively small ( $\sim 3\text{-}4\text{kJ/mol}$ ). The melting points of the  $\beta'$  forms showed a similar trend to the heats of fusion, but the melting points of  $\alpha_1$  BOS and BOP were higher than those of  $\alpha_1$  OOS and OOP respectively.

For  $\alpha$  BOP and BOS, the heat of fusion was equal to the heat of crystallisation within experimental error. The heats of fusion of  $\alpha$  OOP and OOS could not be determined accurately because of the very rapid transformation rate of these forms.

### 3.2.3 1,2-Dibutyryl-3-palmitoylglycerol

The only dibutyryl glyceride studied was BBP, a by-product in the synthesis of rac-1-butyryl-3-palmitoylglycerol. BBP is a liquid at room temperature and therefore no solvent crystallised form was prepared.

#### (a) Thermal Analysis

The DSC cooling curve showed one main exotherm at  $-1^\circ\text{C}$ , corresponding to the crystallisation of the  $\alpha_1$  form, and two minor transitions at  $-11^\circ\text{C}$  and  $-25^\circ\text{C}$ , which were labelled  $\alpha_2$  and  $\alpha_3$  in order of decreasing temperature (Appendix, Fig. 19). The transitions were all reversible and the heating curve was a mirror image of the cooling curve. In neither curve did the heat flow rate between the transitions return to the baseline level, suggesting that a continuous structural change accompanies the discrete transformations which occur at the transition temperatures. The molar heat of transition for the entire transformation sequence  $\alpha_3 \rightarrow \text{melt}$  ( $43\text{kJ/mol}$ ) was approximately equal to the molar heat of fusion of the  $\alpha_1$  form of BOS ( $42.7\text{kJ/mol}$ ) and the  $\alpha_1$  melting points of the two TGs were also similar (Table 3.5). However, in contrast to BOS, no stable form was obtained for BBP in spite of prolonged tempering of the  $\alpha$  form.

#### (b) Variable Temperature IR Spectroscopy

IR spectra obtained during stepwise cooling from the melt are shown in the Appendix (Fig. 20). The spectrum of liquid BBP had several bands not normally found in the spectra of TG melts, for example at  $750$ ,

800 and  $960\text{cm}^{-1}$ . The broad band at  $960\text{cm}^{-1}$  also occurred in the spectrum of liquid SBS but was weak or absent in the spectra of the other butyryl glycerides.

On cooling to  $-2^{\circ}\text{C}$ , a new spectrum appeared which was characteristic of a loosely packed  $\alpha$  form. Compared with the spectrum of the liquid, the band at  $720\text{cm}^{-1}$  had intensified and a weak methylene wagging band progression was present. Further cooling over the temperature range of the  $\alpha_1$  to  $\alpha_3$  transitions resulted in a gradual transformation to sub- $\alpha$ . Thus at  $-16^{\circ}\text{C}$ , intermediate between the  $\alpha_2$  and  $\alpha_3$  transitions, the spectrum showed a partial splitting of the  $720\text{cm}^{-1}$  band, while on subsequent cooling to  $-32^{\circ}\text{C}$ , i.e. below the  $\alpha_3$  transition, the band transformed further to a symmetrical doublet and splitting of the  $1470\text{cm}^{-1}$  band was now also apparent. These spectral changes, which were accompanied by a general sharpening of the bands as the temperature was lowered, were reversed on heating. BBP was the only glyceride to show an obvious parallel between spectral and thermal transitions involving the  $\alpha$  phase.

#### 3.2.4 2-Oleoyl Triacylglycerols

The polymorphism of SOS, POS and POP was particularly complex and highly individual. In spite of the large number of  $\beta'$  and  $\beta$  polymorphs, only the stable form was common to all three TGs, although two forms were common to two different pairs of TGs. The following sections should therefore be read with reference to Fig. 3-15, which provides a schematic summary of the polymorphism.

##### (a) Solvent Crystallised Forms

Fig. 3-10 gives the X-ray diffraction patterns and Table 3.6 the corresponding short spacing data for the solvent crystallised forms of SOS, POS and POP. As expected, the patterns showed a very strong spacing near  $4.6\text{\AA}$  and the forms were therefore classified as  $\beta$ . The IR spectra, shown in Fig. 3-11, confirmed this assignment (strong singlets at  $715$  and  $890\text{cm}^{-1}$ ) and revealed close parallels between the  $\beta$  stable forms of SOS, SBS and SES (or ESS).

##### (b) Variable Temperature IR Spectroscopy

Phase assignments determined by IR spectroscopy are summarised in Fig. 3-15. The symbols in brackets refer to forms that were only detected by thermal analysis.

On cooling the melt to  $0^{\circ}\text{C}$ , typical  $\alpha$  spectra were obtained for

all three TGs (Appendix, Figs. 23, 25, 27). In contrast to the behaviour of the 1-oleoyl TGs, the sub- $\alpha$  form was not obtained even on direct cooling to  $-30^{\circ}\text{C}$ . The  $\alpha$  spectra were similar to one another and to the  $\alpha$  spectra of SES and OSS (Appendix, Figs. 3 and 42). In particular, the methylene wagging band progressions for  $\alpha$  POP and SOS showed clear contributions from the palmitoyl and stearoyl diatheses, although the contributions from the oleoyl diatheses were not well resolved. The methylene wagging band progression for  $\alpha$  POS was less distinct because of the overlap of the palmitoyl and stearoyl contributions.

On heating  $\alpha$  POS to its melting point (or by crystallisation of the melt at the same temperature), a  $\beta'$  form was obtained (doublet at  $720\text{cm}^{-1}$ ) which was analogous to the  $\beta'$  form of SOS (q.v.) with common spectral bands at 910,  $950 + 960$ , 1005, 1025 and  $1055 + 1065\text{cm}^{-1}$  (Fig. 3-12). The spectra of these forms were unusual in showing a marked splitting of the  $\text{CH}_2\text{-O}$  stretching band (doublet at 1090,  $1110\text{cm}^{-1}$ ). After tempering at  $30^{\circ}\text{C}$  for several days,  $\beta'$  POS transformed to the stable  $\beta$  form, which had an identical spectrum to that of the solvent crystallised form.

On heating to their melting points,  $\alpha$  SOS and POP transformed to analogous  $\beta_2$  forms (Fig. 3-12). The same forms were also obtained by crystallisation of the melt at the  $\alpha$  melting points. In contrast to the spectrum of the stable  $\beta_1$  form, the  $\beta_2$  spectrum showed no band at  $690\text{cm}^{-1}$ , suggesting that the oleoyl chains are packed differently in the two polymorphs (the band at  $690\text{cm}^{-1}$  is sensitive to the geometry of the double bond, Bellamy, 1975). At  $37^{\circ}\text{C}$ ,  $\beta_2$  SOS transformed via the melt to a  $\beta'$  form whose spectrum corresponded with that of  $\beta'$  POS (Fig. 3-12). On cooling to  $-26^{\circ}\text{C}$ , the resolution of the  $\beta'$  spectrum was markedly enhanced and a band appeared at  $690\text{cm}^{-1}$  (Appendix, Fig. 23), indicating a change in the oleoyl chain packing. Tempering  $\beta'$  SOS at  $30^{\circ}\text{C}$  resulted in a gradual transformation to the stable  $\beta_1$  form.

At  $27^{\circ}\text{C}$ ,  $\beta_2$  POP transformed to a  $\beta'$  form with a spectrum (Fig. 3-12) different from that of the  $\beta'$  forms of SOS and POS discussed above. At room temperature, the spectrum showed a diffuse singlet band near  $720\text{cm}^{-1}$ , but on cooling to  $-32^{\circ}\text{C}$ , the band was asymmetrically broadened on the high frequency side, indicating the presence of an unresolved doublet (Appendix, Fig. 27). The  $\beta'$  assignment was confirmed by the presence of four bands specific for the  $\beta'$  form at 830, 920, 950 and  $980\text{cm}^{-1}$ . These bands were especially prominent in the sharply resolved spectrum recorded at  $-32^{\circ}\text{C}$ . As Fig. 3-12 shows, the spectrum of  $\beta'$  POP

was similar to that of  $\beta'$  PSP. At its melting point  $\beta'$  POP transformed to the stable  $\beta_1$  form.

(c) Thermal Analysis

The thermal behaviour of POP was the most complex of the TGs studied and there was evidence for six forms, four of which were characterised by IR spectroscopy (Fig. 3-15). Accurate heats of fusion could only be determined for the  $\alpha$  and  $\beta_1$  forms (Table 3.7).

In contrast to the behaviour of SOS and POS, only a single exotherm was observed on cooling POP from the melt and the area of this peak was equivalent to the heat of fusion of the  $\alpha$  form (72.6kJ/mol).

The shape of the  $\alpha$  melting thermogram was particularly dependent on heating rate. Thus, at 16°C/min the  $\alpha$  form melted with very little transformation to higher forms, whereas at 4°C/min the  $\alpha$  melting process was less dominant and a complex transformation sequence was displayed with endotherms at 16.0, 22.7, 27.4, 31.7 and 32.7°C (Fig. 3-13). The  $\alpha$  melting thermogram recorded at 2°C/min showed similar polymorphic transformations to that of the 4°C/min thermogram, except that the transition near 23°C was absent and the two highest endotherms were more clearly resolved (Appendix, Fig. 26). By comparison with the melting points and transformation relationships of the forms characterised by IR spectroscopy, the transitions at 16.0, 27.4, 31.7 and 32.7°C were assigned to the melting of the  $\alpha$ ,  $\beta_2$ ,  $\beta'$  and  $\beta_1$  forms respectively. The transition at ~23°C was not detected by IR spectroscopy, possibly because of its transient nature.

Fig. 3-14 shows the melting thermogram of the solid obtained by crystallisation of the POP melt at ~16°C for 5 min. The thermogram was similar to the melting thermogram of the  $\alpha$  form (Fig. 3-13) except that the  $\alpha$  melting endotherm and accompanying exotherm were absent, an additional endotherm was present at about 25.1°C and the two highest endotherms were merged into a single broad endotherm at 32-33°C. The relative intensity of the two endotherms at 25.1 and 27.1°C was sensitive to variation in the tempering conditions but not to heating rate, suggesting that the preparations initially contained a mixture of both forms. The major endotherm at 27.1°C in Fig. 3-14 corresponds with the major endotherm at 27.4°C in Fig. 3-13, both being correlated with the melting of the  $\beta_2$  form. The additional endotherm at 25.1°C in Fig. 3-14 did not correspond with any form observed in the IR study, but comparison with the results of Lutton and Jackson (1950) suggests a correlation with their  $\beta'_2$  (sub- $\beta'$ -2) form (Table 1.2). The heat of fusion determined

from thermograms in which the  $\beta'_2$  and  $\beta_2$  endotherms were predominant was almost independent of the relative proportions of the two phases. It was concluded that the heats of fusion of  $\beta'_2$  and  $\beta_2$  were approximately equal (Table 3.7).

The melting thermogram of the  $\beta'_1$  form, prepared by tempering the lower forms of POP at 30°C for 15 min, showed a single broad endotherm with a peak temperature of 32.2°C. The wide melting range indicated that the form was incompletely stabilised or that two forms were present (i.e.  $\beta'_1$  and  $\beta_1$ ), so that the value for the heat of fusion (112kJ/mol) must be regarded as tentative.

The existence of the  $\alpha$ ,  $\beta_2$ ,  $\beta'$  and  $\beta_1$  forms of SOS characterised by IR spectroscopy was confirmed by thermal analysis. An additional transition intermediate between  $\alpha$  and  $\beta_2$  at 28°C was also detected (Fig. 3-15). In common with the solvent crystallised forms of POS and POP, the solvent crystallised form of SOS exhibited the sharp melting endotherm typical of a pure phase (Appendix, Fig. 21). However, on rapid cooling of the melt (16°C/min), the TG crystallised in a complex manner, the thermogram showing an extended transition with two distinct exotherms rather than the single sharp exotherm typically obtained (Appendix, Fig. 22). The phenomenon was not reversible and on rapid heating (16°C/min) of the resultant solid a single endotherm was obtained, presumably the  $\alpha$  melting transition, with approximately the same total heat change.

On slow heating of the  $\alpha$  form at 4°C/min, SOS showed three distinct endotherms at 24.4, 36.0 and 37.0°C, corresponding to the melting of the  $\alpha$ ,  $\beta_2$  and  $\beta'$  phases respectively (Fig. 3-13). The presence of two exotherms at 25.2 and 28.5°C suggests the possibility of a fourth form, melting point  $\sim$ 28°C, intermediate between the  $\alpha$  and  $\beta_2$  forms. The  $\alpha$  melting thermogram of POP displayed a similar low-energy transition occurring between the  $\alpha$  and  $\beta_2$  melting transitions.

The phases obtained by crystallisation of the SOS melt at 24°C or by transformation of  $\alpha$  at the same temperature showed identical thermal behaviour. The heating thermograms of these preparations were essentially equivalent to the  $\alpha$  heating thermogram from  $\sim$ 30°C on, with  $\beta_2$  and  $\beta'$  endotherms at 36.5 and 37.6°C (compare Fig. 3-14 with Fig. 3-13 or see Fig. 21 in the Appendix). The overlapping melting ranges of the two forms precluded accurate determination of the heat of fusion of the  $\beta_2$  form because it was impossible to determine the proportion of the two phases present in the initial preparation. However, the heat of fusion

of different preparations was surprisingly uniform in spite of differences in the relative intensities of the two peaks. This suggests that either the preparations contained only  $\beta_2$  initially and  $\beta'$  was produced by transformation concurrent with the melting of  $\beta_2$ , or that the heat of fusion of the two forms is approximately equal. In either case, the heat of fusion of  $\beta_2$  is equal to the total heat of fusion of the double endotherm, i.e. 118kJ/mol.

The polymorphic behaviour of SOS is summarised in Fig. 3-15. Melting points of all forms and the heats of fusion of  $\alpha$ ,  $\beta_2$  and the solvent crystallised  $\beta_1$  form are given in Table 3.7.

Thermograms illustrating the polymorphic behaviour of POS were simpler than those of POP and SOS because there were only three main forms,  $\alpha$ ,  $\beta'_1$  and  $\beta$  and both  $\alpha$  and  $\beta'$  were relatively stable to transformation (Figs. 3-13 and 3-14). The results confirmed the transition temperatures obtained by IR spectroscopy, although two additional low-energy transitions intermediate between  $\alpha$  and  $\beta'_1$  were also detected (Fig. 3-15).

On cooling the melt of POS at 4°C/min a broad exotherm was obtained with a poorly defined end-of-transition. The peak area accounted for only about 60% of the heat of fusion of the  $\alpha$  form which was determined in a subsequent melting thermogram (78.9kJ/mol). This anomalous behaviour was similar to that occurring in the crystallisation of the 1-oleoyl TGs.

The  $\alpha$  form of POS was more stable than  $\alpha$  POP or SOS and melted without transformation to a higher form at a heating rate of 4°C/min (Fig. 3-13). However, the form produced by shock-cooling at >32°C/min differed from that produced by slow cooling (4°C/min) in showing a second smaller endotherm, peak temperature 20.7°C, only partially resolved from the main  $\alpha$  melting endotherm, peak temperature 19.4°C. There was no significant difference in the heats of fusion of the two preparations. This cooling rate dependence is a further example of the unusual crystallisation behaviour of POS.

The  $\beta'$  form of POS was prepared by crystallisation of the melt or transformation of the  $\alpha$  form at its melting point. In the latter case, particularly for short tempering periods of 10-15 min, the melting thermogram recorded at 4 or 8°C/min showed two small endotherms at 20.7°C and 22.6°C preceding the main  $\beta'$  endotherm at 31.1°C (Fig. 3-14). Following the convention of Hagemann et al. (1972), the three endotherms

were designated as  $\beta'_3$ ,  $\beta'_2$  and  $\beta'_1$  in order of increasing melting point. The  $\beta'_3$  melting point was identical with the peak temperature of the transition associated with the melting of the shock-cooled  $\alpha$  form, so it is possible that these two transitions are the same. In several thermograms exotherms were observed between  $\beta'_3$ ,  $\beta'_2$  and  $\beta'_2$ ,  $\beta'_1$ , clearly confirming that the transition sequence was monotropic.

The polymorphic behaviour of POS is summarised in Fig. 3-15. Melting points of all forms and heats of fusion of  $\alpha$ ,  $\beta'_1$  and the solvent crystallised  $\beta$  form are given in Table 3.7.

### 3.2.5 2-Butyryl-1,3-distearoylglycerol

#### (a) Solvent Crystallised Form

The X-ray short spacings (Table 3.6, Fig. 3-10) and IR spectrum (Fig. 3-11) of the stable  $\beta$  form of SBS were analogous to the corresponding data of  $\beta$  SOS, which suggests that the stearyl chain packings in the two polymorphs are equivalent.

#### (b) Thermal Analysis

A heating thermogram of the phase produced by quickly cooling the melt showed a rapid sequence of transformations with endotherms at approximately 29, 34, 39 and 53°C (Appendix, Fig. 28). By comparison with the crystallisation temperature of the slowly cooled melt,  $\sim 31^\circ\text{C}$ , and the melting point of the solvent crystallised form,  $54.2^\circ\text{C}$ , the forms melting at 34 and  $53^\circ\text{C}$  were identified as  $\alpha_1$  and  $\beta$  respectively. The minor transition at  $29^\circ\text{C}$ , which appeared to be reversibly associated with  $\alpha_1$ , was labelled  $\alpha_2$ . The  $\alpha_1$  and  $\beta$  assignments were confirmed by IR spectroscopy although the transitions at 29 and  $39^\circ\text{C}$  could not be so characterised.

Thermal data for SBS is presented in Table 3.7. Because of the very rapid transformation rate of  $\alpha_1$ , the heats of crystallisation and fusion for this form could not be determined accurately (cf.  $\alpha$  PSP). Similarly, only an estimate could be made for the heat of fusion of the transient  $39^\circ\text{C}$  form, which was obtained by transformation of  $\alpha_1$  at  $33\text{--}34^\circ\text{C}$  for 1-3 min.

#### (c) Variable Temperature IR Spectroscopy

Only (sub) $\alpha$  and  $\beta$  forms were characterised by IR spectroscopy. The  $\alpha$  form was obtained by rapid cooling of the melt to  $\sim 0^\circ\text{C}$  and further cooling to  $-30^\circ\text{C}$  resulted in a reversible transformation to a sub- $\alpha$  form (partially resolved doublet near  $720\text{cm}^{-1}$ , Appendix, Fig. 29). As expected,

the (sub) $\alpha$  spectrum showed a well-defined methylene wagging band distribution in which the contribution of the stearyl diathesis was clearly evident. The unusual presence of several relatively intense bands in the  $1050\text{-}600\text{cm}^{-1}$  region of this spectrum would seem to indicate either a special structural feature of  $\alpha$  SBS or a contribution from another form.

The stable  $\beta$  form was obtained by transformation of  $\alpha$  or crystallisation of the melt at the  $\alpha$  melting point. The spectrum of this phase was identical with that of the solvent crystallised form. No spectrum corresponding to the  $39^\circ\text{C}$  form was observed during the variable temperature IR investigation, presumably because transformation to the stable form occurred too readily.

### 3.2.6 1-Butyryl Triacylglycerols

#### (a) Solvent Crystallised Forms

IR spectra of the stable  $\beta'$  forms of BSS, BSP, BPS and BPP displayed a striking similarity to the spectra of the stable forms of the corresponding oleoyl TGs (Fig. 3-16). The  $\beta'$  spectra of BSS, BPS, and BPP were closely analogous to those of OSS, OPS and OPP respectively, and all spectra exhibited a symmetrical doublet at  $717, 727\text{cm}^{-1}$  and characteristic bands at  $860, 940$  and  $1030\text{cm}^{-1}$ . In contrast, the  $\beta'$  spectra of BSP and OSP showed a diffuse singlet at  $719\text{cm}^{-1}$  and common bands at  $870, 925$  and  $980\text{cm}^{-1}$ . The latter two spectra were also unusual in showing an apparent splitting of the  $\text{CH}_2\text{-O}$  stretching band (doublet at  $1080, 1110\text{cm}^{-1}$ ; cf.  $\beta'$  POS, SOS) and a marked temperature dependence. Thus, on cooling from  $25^\circ\text{C}$  to  $-30^\circ\text{C}$  the single bands at  $1470$  and  $720\text{cm}^{-1}$  split into doublets (Appendix, Figs. 34 and 44). This reversible change was analogous to that accompanying the  $\alpha$  to sub- $\alpha$  transition.

Although the X-ray short spacing data could be classified on the same structural basis as the IR spectra, the differences between BSS, BPS and BPP on the one hand and BSP on the other were not so pronounced (Table 3.8 and Fig. 3-17). Similarly, while the X-ray diffraction patterns of analogous 1-butyryl and 1-oleoyl TG stable forms were related (Fig. 3-17), the correspondence was not as clear-cut as that of the IR spectra. As expected, the solvent crystallised forms of the homologous TGs BSS and BPP showed very similar diffraction patterns with strong short spacings at  $3.74, 3.81, 4.04$  and  $4.17\text{\AA}$ . The corresponding polymorph of BPS exhibited similar spacings although the intensity distribution was different. The diffraction pattern for the solvent crystallised form of BSP was even more distinctive; the spacings near  $4.04$  and  $3.74\text{\AA}$  were weak and absent respectively and a new spacing was present at

4.33Å. By Lutton's criteria, all phases were  $\beta'$  (strong spacings near 3.8 and 4.2Å).

(b) Variable Temperature IR Spectroscopy

Spectra of the  $\alpha$  forms (obtained by crystallisation of the melt at 0°C) were similar to those of other high-melting TGs, displaying more and sharper bands than the  $\alpha$  spectra of low-melting TGs such as BOS and BOP. Contributions from the palmitoyl and stearoyl chains to the methylene wagging band progressions were particularly well resolved for the spectra of  $\alpha$  BPP and BSS. On cooling to -30°C, the  $\alpha$  forms of BSS and BSP underwent a partial transformation to the sub- $\alpha$  form, both spectra showing an unsymmetrical doublet near  $720\text{cm}^{-1}$ . The transition was reversible.

The stable  $\beta'$  forms were produced by transformation of the  $\alpha$  form or crystallisation of the melt at the  $\alpha$  melting point. The minor spectral differences, particularly in the shape of the  $720\text{cm}^{-1}$  bands, between the different  $\beta'$  preparations were eliminated by tempering at room temperature for several hours or just below the  $\beta'$  melting point for a few minutes. The spectra of such 'stabilised' forms were identical with those of the solvent crystallised forms.

(c) Thermal Analysis

In addition to the  $\alpha$  and  $\beta'$  phases characterised by IR spectroscopy, thermal analysis showed the existence of intermediate melting forms for all four TGs.

BPP, BPS and BSP solvent crystallised forms each displayed a single sharp melting endotherm typical of a high purity phase. In contrast, the corresponding melting thermogram of BSS (Appendix, Fig. 31) had two endotherms, one melting at 47.0°C and the other at 50.5°C, although the lower melting phase contributed only a few percent of the total heat of fusion (cf. OPS). The lower melting phase was readily transformed to the stable form by momentarily tempering at 47.0°C. The resultant thermogram showed only a single endotherm at 51.6°C.

Thermal data for the stable form of BSP were at variance with the corresponding data for the other TGs. Thus, while both the melting point and molar heat of fusion of  $\beta'$  BPS were approximately midway between those of BPP and BSS, the melting point of  $\beta'$  BSP (50.0°C) was only a little lower than that of BSS (51.6°C) but the molar heat of fusion of  $\beta'$  BSP (120kJ/mol) was only a little higher than that of BPP (116kJ/mol) (Table 3.9).

The four TGs showed normal crystallisation behaviour in that the transition between liquid and  $\alpha$  solid was completed within the relatively narrow temperature range of the exotherm (contrast SOS) and the measured heats of crystallisation and fusion of the  $\alpha$  form were identical within experimental error. Melting thermograms of the  $\alpha$  forms recorded at a heating rate of  $4^{\circ}\text{C}/\text{min}$  are shown in Fig. 3-18. The  $\alpha$  forms of BPP and BSS were relatively stable and melted without transformation to a higher form. Under the same conditions,  $\alpha$  BPS and BSP transformed readily, each thermogram showing two forms intermediate between the  $\alpha$  and  $\beta'_1$  endotherms. The shape of the melting thermogram of  $\alpha$  BPS was dependent on the rate at which the melt was cooled (Appendix, Fig. 35). In contrast to other butyryl TGs and to the corresponding 1-oleoyl TGs, none of these TGs showed any evidence of an  $\alpha_2$  transition, emphasising the regular thermal behaviour of their  $\alpha$  forms. Melting points and molar heats of fusion of the  $\alpha$  forms are given in Table 3.9. Both properties showed the same trend, increasing in the order: BPP < BPS < BSP < BSS. The molar heats of fusion showed surprisingly close agreement with those of the  $\alpha$  forms of the corresponding 1-oleoyl TGs. However, the  $\alpha$  melting point of the butyryl TGs were  $6-7^{\circ}\text{C}$  higher than their oleoyl counterparts (cf.  $\alpha$  SBS, SOS; BOS, OOS etc.)

Intermediate forms were prepared by transformation of  $\alpha$ , the ease of transformation decreasing in the order: BSP > BPS > BPP > BSS. Fig. 3-19 shows the melting thermograms of the forms obtained in this way. For BPP, BPS and BSP there were two intermediate forms, tentatively designated  $\beta'_3$  and  $\beta'_2$  in order of increasing peak temperature, while for BSS there was only one such form,  $\beta'_2$ . The intermediate forms could not be obtained free of the stable  $\beta'_1$  form and because of this association and the generally inadequate resolution between endotherms, it was impossible to determine their heats of fusion.

In contrast to the behaviour of saturated TGs of high molecular weight, it was difficult to obtain pure stable forms by transformation of the intermediate forms of the 1-butyryl TGs. The phases so produced had wide melting ranges and lower heats of fusion than the corresponding forms obtained by solvent crystallisation.

### 3.2.7 1-Butyryl-2-elaidoyl-3-stearoylglycerol

#### (a) Solvent Crystallised Form

In view of the close similarity between the polymorphism of SES and SSS, BES had been expected to show analogous polymorphic behaviour to BSS. In fact the polymorphism of the two TGs was quite different.

In particular, the IR spectrum and X-ray diffraction pattern of the solvent crystallised form of BES were similar to those of BSP (and OSP) and distinctly different from those of BSS, BPS and BPP (Figs. 3-16 and 3-17; Table 3.8).

(b) Thermal Analysis

Thermal data for BES is presented in Table 3.9. Heats of fusion and melting points of the  $\alpha_1$  and stable  $\beta'$  forms were approximately midway between the corresponding data for BSS and BOS but in other respects BES resembled the latter TG more closely. Thus, in common with BOS and BOP, BES showed no forms intermediate in melting between  $\alpha_1$  and  $\beta'$ . Furthermore, like BOS and in contrast to BSS, BES exhibited a reversible  $\alpha_2$  transition occurring immediately before the main  $\alpha_1$  melting transition (Appendix, Fig. 38). However, the  $\alpha_2$  transition of BES involved a much greater heat change than  $\alpha_2$  BOS, accounting for about 25% of the total heat of fusion of the  $\alpha$  forms.

(c) Variable Temperature IR Spectroscopy

Only (sub) $\alpha$  and  $\beta'$  forms were detected in the IR spectroscopic examination (Appendix, Fig. 39). The  $\alpha$  form was obtained by crystallisation of the melt at 0°C and further cooling to -30°C resulted in a partial transformation to sub- $\alpha$ . On heating, no change other than the sub- $\alpha$  to  $\alpha$  transition occurred until at 18-19°C the  $\alpha$  form melted and the melt slowly recrystallised into a form identical with the solvent crystallised form. The  $\alpha_2$  transition observed by thermal analysis could not be resolved from the main  $\alpha$  melting transition in the variable temperature IR cell.

### 3.2.8 1-Oleoyl Triacylglycerols

As mentioned in Section 3.2.6, the solvent crystallised forms of OPP, OPS, OSP and OSS showed a remarkable correspondence with the solvent crystallised forms of the structurally analogous 1-butyryl TGs, BPP, BPS, BSP and BSS. In other respects, however, the polymorphism of the 1-oleoyl TGs was rather more complex than that of the 1-butyryl TGs, particularly with regard to the thermal behaviour of the  $\alpha$  forms and the greater individuality of the intermediate forms. A schematic summary of the polymorphic behaviour of the 1-oleoyl TGs is given in Fig. 3-24, reference to which provides a guide to the following sections.

(a) Solvent Crystallised Forms

Short spacing data for the solvent crystallised forms of these TGs are presented in Table 3.10. As expected, OSS and OPP had similar X-ray diffraction patterns (Fig. 3-17) with principal spacings at 3.76, 4.04, 4.17, 4.27 and 4.38Å. The solvent crystallised form of OPS had lines in common with these (except the 4.27Å spacing which was absent) although the intensity distribution of the pattern was different and two additional spacings were present at 3.70 and 4.08Å. However, in contrast to the rather complex diffraction patterns of OPP, OSS and OPS, the pattern for the solvent crystallised form of OSP was very simple with only three main spacings at 3.78, 4.01 and 4.21Å (Fig. 3-17). Similar structural dichotomy was demonstrated by the stable forms of BPP, BSS, BPS and BSP and the two exceptional TGs, BSP and OSP, showed diffraction patterns that were clearly analogous. By comparison, short spacing data for the other TG analogues, for example OSS and BSS, showed many differences although the stable forms of all eight TGs had strong lines near 3.8 and 4.2Å and the forms were therefore classified as  $\beta'$ .

The IR spectra of the solvent crystallised forms of the 1-oleoyl TGs followed the same structural classification as the short spacing data with OSP again the exceptional TG. Spectral correspondence with the stable forms of the analogous 1-butyryl TGs was more obvious than the similarities in their diffraction patterns, presumably because the contributions of the oleoyl chains are masked by those of the saturated chains in the IR spectra but not in the diffraction patterns. Thus, ignoring the obvious differences in the methylene wagging band progressions, the spectra of  $\beta'$  OSS, OPS and OPP were very similar to each other and to the spectra of  $\beta'$  BSS, BPS and BPP (Fig. 3-16). In particular, a symmetrical doublet was present at 717, 727 $\text{cm}^{-1}$  in all spectra. Similarly, the exceptional spectra of OSP and BSP were closely related, particularly with regard to their temperature dependence. On cooling the stable form of OSP from  $\sim 25^\circ\text{C}$  to  $-34^\circ\text{C}$ , the diffuse singlet at 720 $\text{cm}^{-1}$  split into a doublet which was just resolved (717; 723 $\text{cm}^{-1}$ ;  $\Delta_{720} = 6\text{cm}^{-1}$ ) and the methylene scissoring band at  $\sim 1470\text{cm}^{-1}$  was asymmetrically broadened on the low frequency side, indicating the presence of a doublet not clearly resolved (Appendix, Fig. 44). These changes, which were reversed on heating to room temperature again, were analogous to, but less pronounced than, those shown by the stable form of BSP (for which  $\Delta_{720}$  and  $\Delta_{1470}$  were 8 and 9 $\text{cm}^{-1}$  respectively at  $-33^\circ\text{C}$ ).

(b) Variable Temperature IR Spectroscopy

On rapid cooling of the melt to  $-30^\circ\text{C}$  ( $0^\circ\text{C}$  for OSS), all four TGs

crystallised in the sub- $\alpha$  form (unsymmetrical doublet near  $720\text{cm}^{-1}$ ). On heating, the sub- $\alpha$  form OSS, OPS and OPP showed a gradual (and reversible) transition to the  $\alpha$  form (symmetrical singlet at  $720\text{cm}^{-1}$ ). For OSP the transformation of sub- $\alpha$  to  $\alpha$  was accompanied by a simultaneous transformation to the  $\beta'_1$  form which made it impossible to check the reversibility of the transition. The spectra were typical of the  $\alpha$  forms of higher melting TGs and sub- $\alpha$  OPP, OSP and OSS exhibited distinct methylene wagging band progressions in which the contributions of the saturated chains were well resolved. In contrast, the methylene wagging band progression of sub- $\alpha$  OPS was rather diffuse although the band positions still matched the expected values fairly well.

Transformation of  $\alpha$  or crystallisation of the melt near the  $\alpha$  melting point gave a form identical with the solvent crystallised form for OSS but resulted in intermediate  $\beta'_2$  forms for OPP and OPS. In the case of OSP, the two tempering procedures gave different forms, the stable  $\beta'_1$  form by transformation of  $\alpha$  and  $\beta'_2$  by crystallisation of the melt.

The spectrum of the intermediate form of OPP showed an unresolved doublet at  $720\text{cm}^{-1}$  and bands at  $\sim 830, 920, 940$  and  $970\text{cm}^{-1}$  which are characteristic of the  $\beta'$  form. In other respects, however, the  $\beta'_2$  spectrum was difficult to classify because of the general diffuseness of the bands and the possible presence of the stable form in some preparations. On tempering overnight at  $20^\circ\text{C}$  or for 30 min at  $\sim 30^\circ\text{C}$ ,  $\beta'_2$  transformed to  $\beta'_1$ , the spectrum of the latter displaying only minor differences from that of the solvent crystallised form.

For OPS, the spectrum of the form obtained by transformation of  $\alpha$  or crystallisation of the melt was very similar to that of the solvent crystallised form, although the comparison was restricted by the poor quality of the latter spectrum. However, consideration of the thermal analysis results showed that the two forms were in fact different. Thus the form obtained by transformation, the lower melting of the two, was labelled  $\beta'_2$  and the solvent crystallised form,  $\beta'_1$ .

On heating,  $\alpha$  OSP underwent a ready transformation to a form whose spectrum was essentially identical with that of the solvent crystallised form. On the other hand, crystallisation of OSP melt at  $\sim 28^\circ\text{C}$  for  $\sim 60$  min produced a  $\beta'$  form whose spectrum was quite different from that of the solvent crystallised form. Initially, the spectrum displayed rather diffuse bands but after tempering overnight at  $\sim 30^\circ\text{C}$ , the resolution was much improved. The sharpness of the bands was still

further improved by cooling to  $-30^{\circ}\text{C}$ . The spectrum of the tempered form showed an unsymmetrical doublet at  $720\text{cm}^{-1}$  and four bands at 830, 920, 950 and  $980\text{cm}^{-1}$  which in the spectra of monoacid TGs are specific for the  $\beta'$  form. The spectrum of this  $\beta'_2$  form bore a close resemblance to that of  $\beta'$  PSP and showed several features in common with the spectrum of  $\beta'$  POP (Fig. 3-12).

(c) Thermal Analysis

The solvent crystallised forms of OPP, OSP and OSS each showed a sharp melting endotherm typical of a pure compound. The corresponding thermogram for OPS was unusual in showing two endotherms, although the lower melting of these, labelled  $\beta'_2$ , accounted for only 2-3% of the total heat of fusion (Appendix, Fig. 45). The higher melting form could be obtained free of  $\beta'_2$  by tempering at the  $\beta'_2$  peak temperature ( $37.6^{\circ}\text{C}$ ) for 2 min. Melting points and molar heats of fusion of the solvent crystallised forms increased in the order  $\text{OPP} < \text{OPS} < \text{OSS}$ , while the solvent crystallised form of OSP had a higher heat of fusion but lower melting point than that of OPS (Table 3.11). Thermal data for the 1-butyryl TGs showed a similar trend although the solvent crystallised form of BSP had a lower heat of fusion and higher melting point than that of BPS (Table 3.9).

In contrast to the  $\alpha$  forms of the 1-butyryl TGs, the  $\alpha$  forms of all four 1-oleoyl TGs exhibited anomalous crystallisation and melting behaviour. Thus on cooling the melt, a single crystallisation exotherm was observed but the end of the transition was often ill-defined and the heat of crystallisation was always much lower than the heat of fusion obtained from a subsequent heating thermogram (cf. POS). For example, the estimated heat of crystallisation of  $\alpha$  OSS was only  $63\text{kJ/mol}$ , while the heat of fusion of the resultant solid was  $77\text{kJ/mol}$  (Table 3.11). Furthermore, at the appropriate heating rate, melting thermograms of the  $\alpha$  forms showed a low-energy endotherm occurring immediately before the main  $\alpha$  melting endotherm (Fig. 3-20). The main  $\alpha$  transition, which was identified by comparison of its melting point with the crystallisation temperature determined by DSC and the  $\alpha$  melting point determined by IR spectroscopy, was labelled  $\alpha_1$  and the low-energy transition associated with it was labelled  $\alpha_2$ . The  $\alpha_2$  transition (accounting for  $\sim 6\%$  of the total  $\alpha$  heat of fusion for OPP, OSP and OSS) was irreversible. Thus, if the form produced by rapid cooling of the melt was tempered at the  $\alpha_2$  peak temperature for 0-2 min and then cooled, a subsequent heating thermogram showed no  $\alpha_2$  transition (Fig. 3-21).

There were no thermal transitions corresponding to the reversible  $\alpha$  to sub- $\alpha$  transformations characterised by IR spectroscopy, and conversely, there were no spectral changes corresponding to the irreversible  $\alpha_2$  transformations.

Fig. 3-22 shows  $\alpha$  melting thermograms recorded at heating rates of 2°C/min (OSP and OPP) and 4°C/min (OPS and OSS). With the exception of OSS, polymorphic transformation accompanied the melting of all the  $\alpha_1$  forms, in contrast to the behaviour for higher scan rates (Fig. 3-20) at which only  $\alpha_1$ OPS transformed. (The rapid transformation of  $\alpha$  OPS prevented an accurate determination of its heat of fusion.) By inspection of Fig. 3-22, it can be seen that the transformation rates of  $\alpha_1$  increased in the order: OSS  $\ll$  OSP  $\lesssim$  OPP  $<$  OPS. By comparison, the  $\alpha$  transformation rates of the corresponding butyryl TGs were: BSS  $<$  BPP  $\ll$  BPS  $<$  BSP. Overall, the transformation of the butyryl TGs was slower than that of the oleoyl series. In contrast to the  $\alpha_1$  form,  $\alpha_2$  of OPS was surprisingly stable since it was clearly evident in the 4°C/min heating thermogram (Fig. 3-22).

The  $\alpha$  melting thermograms of OPP, OPS and OSP showed that in addition to the  $\alpha$  forms, OPP and OPS displayed two forms and OSP three. The same forms were also obtained by transformation of  $\alpha$  at its melting point or crystallisation of the melt at the same temperature (Fig. 3-23), although different preparations gave different proportions of the phases. The 28 and 31°C endotherms of OPP obviously corresponded with the  $\beta'_2$  and  $\beta'_1$  forms characterised by IR spectroscopy (same melting points and transformation relationships). Similarly, the spectroscopic examination of OPS showed that the phase obtained by transformation of  $\alpha$  had a very similar spectrum to that of the solvent crystallised form, suggesting that the two forms melting at 37.5 and 38.0°C in Fig. 3-23 are closely related and may therefore be assigned as  $\beta'_2$  and  $\beta'_1$ .

For OSP, the lowest melting of the three endotherms shown in Fig. 3-23 (29.8°C) was denoted by a question mark because it was too fleeting to be characterised by IR spectroscopy. The two highest melting forms of OSP were assigned as  $\beta'_2$  and  $\beta'_1$  by comparison with the spectroscopic results, although the DSC melting points were somewhat lower than those obtained in the variable temperature cell (DSC 33.7, 35.5°C; IR cell 35-38, 38-39°C). As mentioned earlier, in the spectroscopic examination different forms of OSP were obtained by crystallisation of the melt and by transformation of  $\alpha$ , whereas in the DSC the same thermogram was obtained for the two tempering methods. It is possible that this difference was due to the different thermal response of the two

instruments.

Because of the overlapping melting ranges of  $\beta'_2$  and  $\beta'_1$  for OPP, OPS and OSP (Fig. 3-23), it was impossible to determine if a single phase was present initially and transformed during the course of the thermogram or if a mixture of phases was produced by the tempering procedures. However, estimates of the heat of fusion of  $\beta'_2$  of OPP and OPS were made on the assumption that only the  $\beta'_2$  phase was present at the start of the thermogram (Table 3.11). Since the 29.8°C form of OSP was well separated from  $\beta'_2$  and  $\beta'_1$ , it could be examined at high heating rates without the complete loss of resolution which occurs for overlapping forms. At a heating rate of 16°C/min, the 29.8°C endotherm accounted for ~80% of the total heat of fusion of the phase(s) obtained by transformation of  $\alpha$  (5 min) or crystallisation of the melt (15 min) at the  $\alpha$  melting point. Thus, a reliable estimate of the heat of fusion of this form could be obtained (Table 3.11).

The heats of fusion and melting points of the  $\beta'_1$  forms obtained by transformation were significantly lower than those of the solvent crystallised forms. The differences were typically 5-15% for the heat of fusion and 1.5-3.5°C for the melting point. This disparity and the corresponding spectral variations previously noted were presumably due to incomplete equilibration of the phases obtained by transformation.

A schematic summary of the polymorphism of OSS, OSP, OPS and OPP is presented in Fig. 3-24. The figure gives phase assignments, melting or transition points and transformation relationships. Correspondence with the phases reported in the literature is also indicated.

### 3.3 Polymorphism of Enantiomeric Triacylglycerols

#### 3.3.1 Comparison of the Polymorphism of Corresponding Enantiomeric and Racemic Triacylglycerols

Three enantiomeric TGs were prepared, sn-SSB, SSO and PPO, and the polymorphism of these glycerides was investigated in relation to that of their racemates.

##### (a) Solvent Crystallised Forms

The IR spectra of the solvent crystallised forms of equivalent enantiomeric and racemic TGs were essentially identical (Fig. 3-25). All spectra showed a symmetrical doublet near 720cm<sup>-1</sup> and the forms were therefore assigned as  $\beta'$  phases. X-ray diffraction patterns of the solvent crystallised forms are shown in Fig. 3-26 and the corresponding short spacings are listed in Table 3.12. In contrast to the spectroscopic

results, there were obvious differences between the X-ray patterns of the racemates and their antipodes. While the short spacings of the racemic TGs were distinct, the short spacing patterns of the enantiomers were diffuse and relatively few spacings were resolved. Similar patterns were obtained for the stable forms prepared by transformation. However, all patterns showed strong spacings near  $3.8$  and  $4.2\text{\AA}$ , confirming the  $\beta'$  assignments made by IR spectroscopy.

(b) Thermal Analysis

Representative thermograms for sn- and rac-SSB, SSO and PPO are presented in the Appendix (Figs. 30, 31; 40, 41; and 47, 48 respectively). The corresponding melting points and heats of fusion are summarised in Table 3.13. In general, equivalent enantiomeric and racemic TGs exhibited similar polymorphic behaviour except that the  $\alpha$  forms of the antipodes transformed more rapidly than the  $\alpha$  forms of the racemates. Thus, while the  $\alpha$  form of rac-SSB melted without transformation to a higher form at a heating rate of  $4^\circ\text{C}/\text{min}$ , the  $\alpha$  form of sn-SSB transformed readily to  $\beta'_2$  and  $\beta'_1$  under the same conditions (Fig. 3-27). Similarly, at a heating rate of  $8^\circ\text{C}/\text{min}$  the  $\alpha$  form of rac-SSO melted without transformation to a higher form, but at the same rate the  $\alpha$  form of sn-SSO transformed without melting (Fig. 3-27). Although the corresponding thermograms for PPO are not presented in Fig. 3-27, the  $\alpha$  forms of rac- and sn-PPO showed analogous behaviour to those of SSO except that the transformation of  $\alpha$  sn-PPO was even more rapid (Appendix, Fig. 47).

With the exception of the  $\beta'_2$  form of rac-PPO, for every polymorph of a racemic TG there was an equivalent polymorph for the corresponding antipode. Melting points and heats of fusion of the equivalent polymorphs were very similar although not identical (Table 3.13). For example, the melting point and heat of fusion of the solvent crystallised form of rac-SSB were  $51.6^\circ\text{C}$  and  $131.5\text{kJ}/\text{mol}$ , while the corresponding values for the solvent crystallised form of sn-SSB were  $51.8^\circ\text{C}$  and  $129.4\text{kJ}/\text{mol}$  respectively.

Because of the rapid transformation of the enantiomeric glycerides, they were not investigated by variable temperature IR spectroscopy.

Table 3.1: Positional Analysis of Synthetic Triacylglycerols

TG	Fatty Acid Composition (mole %)							
	TG Composition				2-MG Composition <sup>a</sup>			
	4:0	16:0	18:0	18:1	4:0	16:0	18:0	18:1
<u>rac-PPS</u>	-	67.1	32.9	-	-	96.8	2.1	1.1 <sup>b</sup>
<u>rac-POP</u>	-	66.7	tr. <sup>c</sup>	33.3	-	2.8	0.8 <sup>b</sup>	96.4
<u>rac-OPP</u>	-	66.4	-	33.6	-	96.6	1.1 <sup>b</sup>	2.3
<u>rac-OOS</u>	-	-	33.4	66.6	-	2.5 <sup>b</sup>	1.2	96.3
<u>rac-OSP</u>	-	34.0	33.0	33.0	-	1.0	99.0	-
<u>sn-SSB</u>	33.7	-	66.3	tr.	-	0.6 <sup>b</sup>	99.4	tr.
<u>sn-SSO</u>	-	0.5	66.3	33.2	-	2.2 <sup>b</sup>	97.8	tr.

a position 2

b fatty acids present in the 2-MG but not in the TG were derived from the lipid associated with the crude pancreatic lipase.

c tr. = trace

Table 3.2: Stereospecific Analysis of sn-SSO and sn-SSB

		Fatty Acid Composition (mole %)			
		4:0	16:0	18:0	18:1
<u>sn-SSO</u>	TG	-	0.5	66.3	33.2
	TG (Recalc) <sup>g</sup>	-	2.3	66.9	30.8
	position 1 <sup>a</sup>	-	2.0	96.6	1.4
	2 <sup>b</sup>	-	2.2	97.8	tr.
	2 <sup>c</sup>	-	1.9	98.1	tr.
	3 <sup>d</sup>	-	-2.7	4.5	98.2
	3 <sup>e</sup>	-	2.6	6.4	91.0
	3 <sup>f</sup>	-	0.0	5.5	94.6
<u>sn-SSB</u>	TG	33.7	-	66.3	tr.
	TG (Recalc) <sup>g</sup>	31.0	1.6	66.4	0.9
	position 1 <sup>a</sup>	5.9	1.5	92.5	tr.
	2 <sup>b</sup>	-	0.6	99.4	tr.
	3 <sup>d</sup>	95.2	-2.1	7.0	tr.
	3 <sup>e</sup>	87.2	2.8	7.4	2.6
	3 <sup>f</sup>	91.2	0.4	7.2	1.3

a sn-1 = lysophospholipid (1-PL) from phospholipase A hydrolysis

b sn-2 = monoacylglycerol (2-MG) from pancreatic lipase hydrolysis

c sn-2 = fatty acid from phospholipase A hydrolysis

d sn-3 = 3 (original TG)-(1-PL)-(2-MG)

e sn-3 = 2(unhydrolysed phospholipid (2,3-PL))-(2-MG)

f average of two calculations for position 3

g recalculated composition = (2(2,3-PL) + (1-PL))/3

Table 3.3: X-Ray Short Spacings of the Solvent Crystallised Forms of Palmitoyl-Stearoyl and Elaidoyl-Stearoyl Triacylglycerols

TG	Form <sup>a</sup>	Principal Short Spacings/Å				
SSS	$\beta$	3.67s <sup>b</sup>	3.83s	4.54vs		
PPP	$\beta$	3.66s	3.82s	4.54s		
		3.68s	3.84s	4.61vs <sup>1</sup>		
PSS	$\beta$	3.66s	3.81s	4.54vs <sub>1</sub>		
		3.67s	3.87s	4.61vs <sup>1</sup>		
PPS	$\beta$	3.67s	3.82s	4.54vs <sub>1</sub>		
		3.67s	3.85s	4.61vs <sup>1</sup>		
SPS	$\beta$	3.70vs	3.79s	4.54vs(db)		
		3.72s	3.81s	4.57vs <sup>1</sup>		
PSP	$\beta^c$	3.71s	3.79m	4.55s (db)		
		3.73s	3.82w	3.96w	4.59s <sup>2</sup>	
SES	$\beta$	3.68s	3.84s	4.55s <sub>3</sub>		
		3.75s	3.90s	4.61s <sup>3</sup>		
ESS	$\beta$	3.68s	3.85s	4.55s		
SPS	$\beta^d$ (stable)	3.72s	3.94m	4.09vs	4.22s	4.41w
		3.75s	3.95w	4.10vs	4.23m	4.37vw <sup>4</sup>
PSP	$\beta'$ (stable)	3.75s	3.99m	4.14s	4.28m	
		3.81s	4.07m	4.23vs	4.57m <sup>1,2</sup>	

Notes:

- a  $\beta$ , strong spacing near 4.6Å  
 $\beta'$ , strong spacings near 3.8 and 4.2Å
- b vs = very strong intensity, s = strong, m = medium, w = weak, vw = very weak, db = doublet
- c prepared according to references 2 or 4
- d prepared according to reference 4

References:

- 1 Lutton, Jackson and Quimby (1948)
- 2 Lutton and Hugenberg (1960)
- 3 Minor and Lutton (1953)
- 4 Hugenberg and Lutton (1963)

Table 3.4: Melting Points and Heats of Fusion of the Polymorphic Forms<sup>a</sup> of Palmitoyl-Stearoyl and Elaidoyl-Stearoyl Triacylglycerols

TG	Previous Reports						Present Work						
	Melting Point/°C				$\Delta H_f$ /kJ mol <sup>-1</sup>		Melting Point/°C				Heat of Fusion/kJ mol <sup>-1</sup>		
	$\alpha$	$\beta'_2$	$\beta'_1$	$\beta^b$	$\beta^b$		$\alpha$	$\beta'_2$	$\beta'_1$	$\beta^b$	$\alpha$	$\beta'$	$\beta^b$
SSS	54.7	61 <sup>2</sup>	63.2	73.5 <sup>1</sup>	197 <sup>2</sup>	193 <sup>8</sup>	55.6	62.5	65.4	72.8	113.6 + 2.2(4) <sup>c,d</sup>	144(2) <sup>e</sup>	193.7 + 1.5(4)
PSS	50.6	? <sup>4</sup>	60.8 <sup>4</sup>	65.2 <sup>3</sup>	179 <sup>9</sup>		51.1	56.8	60.5	64.5	109 + 4 (9) <sup>d</sup>	140 + 5 (11) <sup>e</sup>	190.0 + 2.6(5)
PPS	47.4	? <sup>4</sup>	57.1 <sup>4</sup>	62.7 <sup>3</sup>	168 <sup>9</sup>		47.5	53.7	56.4	62.2	108.4 + 2.7(6) <sup>d</sup>	134(2) <sup>e</sup>	174.4 + 2.6(5)
PPP	44.7	53 <sup>2</sup>	56.6	66.4 <sup>1</sup>	170 <sup>2</sup>	171 <sup>8</sup>	46.4	52.8	57.1	66.2	94.5(2) <sup>d</sup>	125 + 6(8) <sup>e</sup>	171.4(2)
SPS	51.8	- <sup>g</sup>	69.0 <sup>5</sup>	68.5 <sup>5</sup>	168 <sup>9</sup>		50.6	- <sup>g</sup>	68.6 <sup>b</sup>	67.6	117.3 + 1.8(7) <sup>f</sup>	206.6 + 1.6(5) <sup>b</sup>	192.9 + 2.4(4)
PSP	47.0	? <sup>4</sup>	68.7 <sup>6</sup>	65.5 <sup>6</sup>	166 <sup>9</sup>	( $\beta'$ )	45.9	-	67.7 <sup>b</sup>	64.6	~104(11) <sup>d</sup>	178.8 + 0.9(4) <sup>b</sup>	179.5 + 2.0(8)
SES	42.9	-	47.0	59.5 <sup>7</sup>	-		42.0	46.5	50.0	60.9	103 + 4(4) <sup>d</sup>	129 + 5(5) <sup>e</sup>	182.3 + 3.3(6)
ESS							41.0	48.3	51.8	59.4	106.7 + 1.7(9) <sup>f</sup>	128 + 8(11) <sup>e</sup>	184.5 + 3.6(7)

Notes:

- a all forms were classified according to Larsson's nomenclature (Table 1.1)  
 b solvent crystallised form  
 c mean + standard deviation (number of results)  
 d heat of crystallisation  
 e tentative heat of fusion based on the assumption that only one form was present initially  
 f mean of heats of fusion and crystallisation  
 g -, not found

References:

- 1 Lutton and Fehl (1970)  
 2 Hagemann, Tallent and Kolb (1972)  
 3 Lutton, Jackson and Quimby (1948)  
 4 Perron, Petit and Mathieu (1969) ( $\beta'_2$  was reported for PSS, PPS and PSP but no melting points were given)  
 5 Hugenberg and Lutton (1963)  
 6 Lutton and Hugenberg (1960)  
 7 Minor and Lutton (1953)  
 8 Hampson and Rothbart (1969)  
 9 Knoester, de Bruijne and van den Tempel (1972).  $\Delta H_f$  of  $\beta$  SSS and PPP was reported as 180 and 168 kJ mol<sup>-1</sup> respectively

Table 3.5: Melting Points and Heats of Fusion of the Polymorphic Forms<sup>h</sup> of OOS, OOP, BOS, BOP and BBP

TG	Melting Point/ $^{\circ}$ C				Heat of Fusion/ $\text{kJ mol}^{-1}$	
	$\alpha_3^a$	$\alpha_2^a$	$\alpha_1$	$\beta',^b$	$\alpha$	$\beta',^b$
OOS <sup>1</sup>	- <sup>c</sup>	-60	-1.6	25.3	$45.9 \pm 1.1(4)^{d,e}$	$107.4 \pm 3.5(5)$
OOP <sup>1</sup>	-	-57	-13.6	19.7	$41.7(2)^e$	$99.4 \pm 2.2(4)$
BOS	-	-11.0	3.3	20.3	$42.7 \pm 0.6(8)^f$	$85.2 \pm 2.0(7)$
BOP	-	-25.3	-9.7	13.9	$37.9 \pm 1.2(4)^f$	$77.7 \pm 1.8(3)$
BBP <sup>2</sup>	-23	-10	1	-	$43.2 \pm 1.8(7)^g$	-

Notes:

a reversible transitions

b stable form by transformation

c -, not found

d mean  $\pm$  standard deviation (number of results)

e heat of crystallisation ( $\Delta H_c$ ) of  $\alpha_1$  form; heat of transition of  $\alpha_2$  was  $\sim 15\%$  of  $\alpha_1 \Delta H_c$

f mean of heat of fusion and heat of crystallisation for  $\alpha_1$  and  $\alpha_2$  together;  $\alpha_2$  accounted for 2-3% of the total heat of transition

g mean of heat of fusion and heat of crystallisation for  $\alpha_1$ ,  $\alpha_2$  and  $\alpha_3$

h all forms were classified according to Larsson's nomenclature (Table 1.1)

References:

- Lutton (1966)  
OOS m.p.  $\alpha$   $2.5^{\circ}\text{C}$   $\beta'$   $24.5^{\circ}\text{C}$   
OOP m.p.  $\alpha$   $-13^{\circ}\text{C}$   $\beta'$   $19.5^{\circ}\text{C}$

- Jackson and Lutton (1952)  
BBP m.p.  $\alpha$   $2.9^{\circ}\text{C}$

Table 3.6: X-Ray Short Spacings of the Solvent Crystallised Forms of SOS, POS, POP and SBS

TG	Form <sup>a</sup>	Principal Short Spacings/Å						
SOS	β	3.65m <sup>b</sup>	3.74w	3.86m	3.97m		4.55s	5.39m
		3.68s	3.79ms		4.02ms		4.59s <sup>1</sup>	
POS	β		3.70m	3.82m	3.93m		4.53s	5.32w
			3.68s	3.87ms		4.05ms	4.59vs <sup>1</sup>	
POP	β	3.61w	3.72m	3.80m	3.93m	4.05m	4.57vs	5.43w
			3.73m			4.05m	4.56vs	5.40w <sup>1</sup>
SBS	β	3.58m	3.70m	3.84m	4.01m		4.53vs	
		3.54m	3.69m	3.85s	4.04s		4.60vs <sup>2</sup>	

Notes:

a β, strong spacing near 4.6Å

b vs = very strong intensity, s = strong,  
m = medium, w = weak, vw = very weak

References:

- 1 Lavery (1958)
- 2 Jackson, Wille and Lutton (1951)

Table 3.7: Melting Points and Heats of Fusion of the Polymorphic Forms<sup>a</sup> of SOS, POS, POP and SBS

TG	Previous Reports				Present work									
	Melting Point/°C				Melting Point/°C					Heat of Fusion/kJ mol <sup>-1</sup>				
SOS <sup>1</sup>	α	β'	β <sub>2</sub>	β <sub>1</sub> <sup>b</sup>	α	? <sup>c</sup>		β <sub>2</sub>	β'	β <sub>1</sub> <sup>b</sup>	α	β <sub>2</sub> <sup>h,i</sup>	β <sub>1</sub> <sup>b</sup>	
	22.4	35	36.2	44.3	24.3	~28		36.5	37.4	41.9	78.5 ± 0.7(3) <sup>d,e</sup>	118 ± 2(9) <sup>h,i</sup>	167.5(2)	
POS <sup>1,2</sup>	α	β' <sub>2</sub>	β' <sub>1</sub>	β <sup>b</sup>	α	β' <sub>3</sub> <sup>c</sup>	β' <sub>2</sub> <sup>c</sup>		β' <sub>1</sub>	β <sup>b</sup>	α	β' <sub>1</sub> <sup>h</sup>	β <sup>b</sup>	
	18.2	25.5	33	37.3	19.4	20.7	22.6		31.1	36.0	78.9 ± 2.6(10) <sup>e</sup>	113 ± 2(8) <sup>h</sup>	159.2 ± 1.5(7)	
POP <sup>1,5</sup>	α	β' <sub>2</sub>	β' <sub>1</sub>	β <sub>1</sub> <sup>b</sup>	α	? <sup>c</sup>	β' <sub>2</sub> <sup>c</sup>	β <sub>2</sub>	β' <sub>1</sub>	β <sub>1</sub> <sup>b</sup>	α	β <sub>2</sub> <sup>h,j</sup>	β' <sub>1</sub> <sup>h</sup>	β <sub>1</sub> <sup>b</sup>
	18.1	26.5	33.5	38.3	15.8	22.6	25.1	27.1	31.4	36.1	72.6 ± 1.4(11) <sup>f</sup>	97 ± 1(3) <sup>h,j</sup>	112(2) <sup>h</sup>	150.7 ± 2.7(7)
3		β <sub>2</sub>												
		26.7												
SBS <sup>4</sup>	α	'super-α'	β <sup>b</sup>		α <sub>2</sub>	α <sub>1</sub>		? <sup>c</sup>		β <sup>b</sup>	α	? <sup>c</sup>	β <sup>b</sup>	
	33.4	42.7	54.8		~29	33.8		39.2		54.2	76.1 ± 1.0(3) <sup>g</sup>	93(2) <sup>h</sup>	144.4 ± 3.4(5)	

Notes:

- a all forms are classified according to Larsson's nomenclature (Table 1.1)
- b solvent crystallised form
- c assignment unknown or uncertain
- d mean ± standard deviation (number of results)
- e apparent heat of crystallisation of SOS and POS was 55 and 49kJ mol<sup>-1</sup> respectively at a cooling rate of 4 C/min

- f mean of heats of fusion and crystallisation
- g heat of crystallisation
- h tentative heat of fusion based on the assumption that only one form was present initially
- i heats of fusion of β<sub>2</sub> and β'SOS are probably similar
- j heats of fusion of β'<sub>2</sub> and β<sub>2</sub>POP are probably similar

References:

- Lutton (1951)
- Wille and Lutton (1966)
- Lavery (1958)
- Jackson, Wille and Lutton (1951)
- Lovegren, Gray and Feuge (1971, 1976) reported the following data for POP:-

m.p./°C	α	? <sup>c</sup>	β <sub>2</sub>	β'	β <sub>1</sub>
ΔH <sub>f</sub> /kJ mol <sup>-1</sup>	69.5	-	90-97	104.3	132.6

Table 3.8: X-Ray Short Spacings of the Solvent Crystallised Forms of BSS, BSP, BPS, BPP and BES

TG	Form <sup>a</sup>	Principal Short Spacings/Å				
BSS	β'	3.74s <sup>b</sup>	3.80s	4.04s	4.16s	
BPS	β'	3.69m	3.81m	4.02m	4.15s	
BPP	β'	3.74s	3.82s	4.03s	4.17s	
BSP	β'		3.80s	4.01w	4.13s	4.33m
BES	β'		3.86s		4.16s	4.32w 5.43w

a β', strong spacings near 3.8 and 4.2Å

b s = strong intensity, m = medium, w = weak

Table 3.9: Melting Points and Heats of Fusion of the Polymorphic Forms of BSS, BSP, BPS, BPP and BES

TG	Melting Point/°C					Heat of Fusion/kJ mol <sup>-1</sup>	
	α <sub>2</sub>	α <sub>1</sub>	β' <sub>3</sub>	β' <sub>2</sub>	β' <sub>1</sub> <sup>a</sup>	α	β' <sub>1</sub> <sup>a</sup>
BSS	- <sup>b</sup>	37.0	-	45.1	51.6	77.3 ± 0.8(13) <sup>c,d</sup>	131.5 ± 1.6(8)
BSP <sup>1</sup>	-	31.9	38.9	45.8	50.0	75.0 ± 2.1(5) <sup>e</sup>	120.4 ± 1.1(6)
BPS <sup>1</sup>	-	29.5	43.4	45.5	48.3	70.0 ± 1.6(8) <sup>e</sup>	126.8 ± 1.8(7)
BPP	-	24.2	33.8	37.7	43.1	64.1 ± 1.2(8) <sup>d</sup>	116.3 ± 1.6(4)
BES	15.9 <sup>f</sup>	17.9	-	-	31.4	56.0 ± 0.7(7) <sup>g</sup>	101.7 ± 2.0(4)

Notes:

a solvent crystallised form

b -, not found

c mean ± standard deviation (number of results)

d mean of heat of fusion and heat of crystallisation

e heat of crystallisation

f reversible transition

g combined heat of fusion of α<sub>1</sub> and α<sub>2</sub> forms; α<sub>2</sub> accounted for ~25% of the total heat of fusion

Reference:

- 1 Verkade (1943) reported stable form melting points of 49.5 - 50.0°C and 47.5 - 48.0°C for BSP and BPS respectively

Table 3.10: X-Ray Short Spacings of the Solvent Crystallised Forms of OSS, OSP, OPS and OPP

TG	Form <sup>a</sup>	Principal Short Spacings/Å						
OSS	$\beta'$	3.76s <sup>b</sup>		4.05s	4.17m	4.27m	4.37m	4.63w <sup>1</sup>
		3.79s		4.06s		4.23w	4.39w	4.64m <sup>1</sup>
OPS <sup>c</sup>	$\beta'$	3.70m	3.79m	4.01w	4.08m	4.17s		4.42m
		3.66m	3.78m	4.02w		4.17vs	4.23m	4.66w <sup>1</sup>
OPP	$\beta'$	3.76s		4.03s	4.16s	4.26m	4.38s	4.64m <sup>1</sup>
		3.77s		4.05s		4.20w	4.42w	4.65m <sup>1</sup>
OSP	$\beta'$		3.78s	4.01m		4.21vs		
		3.56w	3.82s	4.03m		4.20vs	4.38m <sup>1</sup>	

Notes:

a  $\beta'$ , strong spacings near 3.8 and 4.2Å

b vs = very strong intensity, s = strong, m = medium, w = weak

c thermal analysis showed that the solvent crystallised form of OPS contained a small proportion of  $\beta'_2$ , which may account for the spacing at 4.08Å

Reference:

1 Lutton (1951)

Table 3.11: Melting Points and Heats of Fusion of the Polymorphic Forms<sup>k</sup> of OSS, OSP, OPS and OPP

TG	Previous Reports				Present Work								
	Melting Point/°C				Melting Point/°C					Heat of Fusion/kJ mol <sup>-1</sup>			
	$\alpha$	? <sup>a</sup>	$\beta'_2$	$\beta'_1$ <sup>b</sup>	$\alpha_2$ <sup>c</sup>	$\alpha_1$	? <sup>a</sup>	$\beta'_2$	$\beta'_1$ <sup>b</sup>	$\alpha$	? <sup>a</sup>	$\beta'_2$	$\beta'_1$ <sup>b</sup>
OSS <sup>1</sup>	30.4	- <sup>d</sup>	-	43.5	23.0	30.3	-	-	43.7	79.2 ± 1.2(4) <sup>e,f</sup>	-	-	142.7 ± 1.1(8)
OSP <sup>1</sup>	26.3	-	40.2 <sup>i</sup>	39.8 <sup>j</sup>	18.1	24.5	29.3	33.7	37.9	73.9 ± 1.2(4) <sup>g</sup>	102 ± 1(4) <sup>h</sup>	-	141.2 ± 3.3(6)
2	25.5	30.6	37.2	36.1									
OPS <sup>1</sup>	25.3	-	37 <sup>i</sup>	40.2 <sup>j</sup>	16.2	22.2	-	37.6	40.0	63.4 ± 2.9(3) <sup>g</sup>	-	119 ± 1(10) <sup>h</sup>	136.7 ± 1.9(7)
OPP <sup>1</sup>	18.5	-	-	35.2	14.0	18.2	-	28.2	35.5	63.3 ± 1.8(6) <sup>f</sup>	-	93 ± 3(13) <sup>h</sup>	124.9 ± 2.1(10)

Notes:

- a ?, assignment unknown  
 b solvent crystallised form  
 c irreversible transition  
 d -, not found  
 e mean ± standard deviation (number of results)  
 f  $\alpha_1$  heat of fusion determined after tempering at  $\alpha_2$  peak temperature; combined heat of fusion of  $\alpha_1$  and  $\alpha_2$  = 76.6 ± 2.1(7) for OSS and 61.8 ± 2.4(6) for OPP; apparent heat of crystallisation = 63.4 ± 1.0(8) for OSS and 50.6 ± 1.4(4) for OPP at a cooling rate of 4 °C/min

- g combined heat of fusion of  $\alpha_1$  and  $\alpha_2$   
 h tentative heat of fusion based on the assumption that only one form was present initially  
 i apparently stable form obtained by transformation  
 j from solvent only  
 k all forms are classified according to Larsson's nomenclature (Table 1.1)

References:

- 1 Lutton (1951)  
 2 Lavery (1958)

**Table 3.12: X-Ray Short Spacings of the Solvent Crystallised Forms of Corresponding Racemic and Enantiomeric Triacylglycerols**

TG	Form <sup>a</sup>	Principal Short Spacings/Å						
SSO	<u>rac-</u>	β'	3.76s <sup>b</sup>	4.05s	4.17m	4.27m	4.37m	4.63w
	<u>sn-</u>	β'	3.75s	4.12s (dif.)		4.22w	4.36w	4.63w
PPO	<u>rac-</u>	β'	3.76s	4.03s	4.16s	4.26m	4.38s	4.64m
	<u>sn-</u>	β'	3.75m	4.10s (dif.)		4.24w	4.37w	4.65w
SSB	<u>rac-</u>	β'	3.74s	3.80s	4.04s	4.16s		
	<u>sn-</u>	β'	3.74s		4.09s (dif.)			

a β', strong spacings near 3.8 and 4.2Å<sup>0</sup>  
b s = strong intensity, m = medium, w = weak, dif. = diffuse

**Table 3.13: Melting Points and Heats of Fusion of the Polymorphic Forms<sup>a</sup> of Corresponding Racemic and Enantiomeric Triacylglycerols**

TG	Melting Point/°C				Heat of Fusion/kJ mol <sup>-1</sup>		
	α <sub>2</sub>	α <sub>1</sub>	β' <sub>2</sub>	β' <sub>1</sub> <sup>b</sup>	α <sub>1</sub>	β' <sub>1</sub> <sup>b</sup>	
SSO	<u>rac-</u>	23.0	30.3	- <sup>c</sup>	43.7	79.2 ± 1.2(4) <sup>d</sup>	142.7 ± 1.1(8)
	<u>sn-</u>	24.5	29.2	-	45.4	* <sup>e</sup>	138.2 ± 1.2(6)
PPO <sup>1</sup>	<u>rac-</u>	14.0	18.2	28.2	35.5	63.3 ± 1.8(6)	124.9 ± 2.1(10)
	<u>sn-</u>	13.4	15.6	-	36.8	*	121.8 ± 2.7(7)
SSB <sup>1</sup>	<u>rac-</u>	-	37.0	45.1	51.6	77.3 ± 0.8(13) <sup>f</sup>	131.5 ± 1.6(8)
	<u>sn-</u>	-	37.7	47.4	51.8	77.7 ± 0.8(6) <sup>f</sup>	129.4 ± 0.4(3)

**Notes:**

- a all forms are classified according to Larsson's nomenclature (Table 1.1)  
b solvent crystallised form  
c -, form not detected  
d mean ± standard deviation (number of results)  
e \*, α transformation rate was too rapid for the determination of the heat of fusion or crystallisation  
f mean of heats of fusion and crystallisation

**Reference:**

- 1 Lok, Ward and van Dorp (1976) report stable form melting points of 37°C and 49°C for sn-OPP and sn-SSB respectively

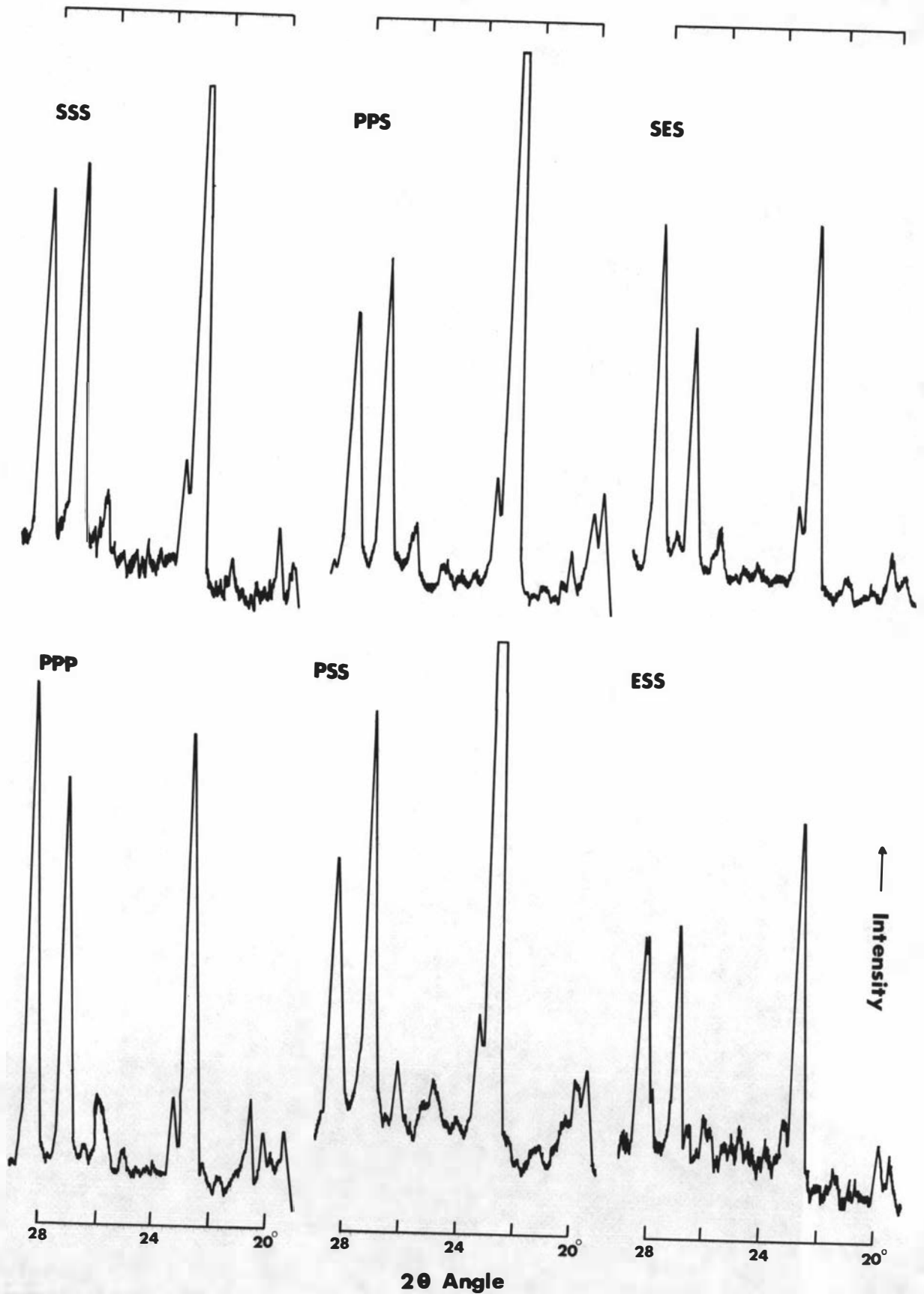


**Fig.3-1 X-ray diffraction patterns of  $\beta$  stable forms of PS & ES TGs**  
 $\lambda$  [Cobalt  $K\alpha_1$ ] = 1.79 Å

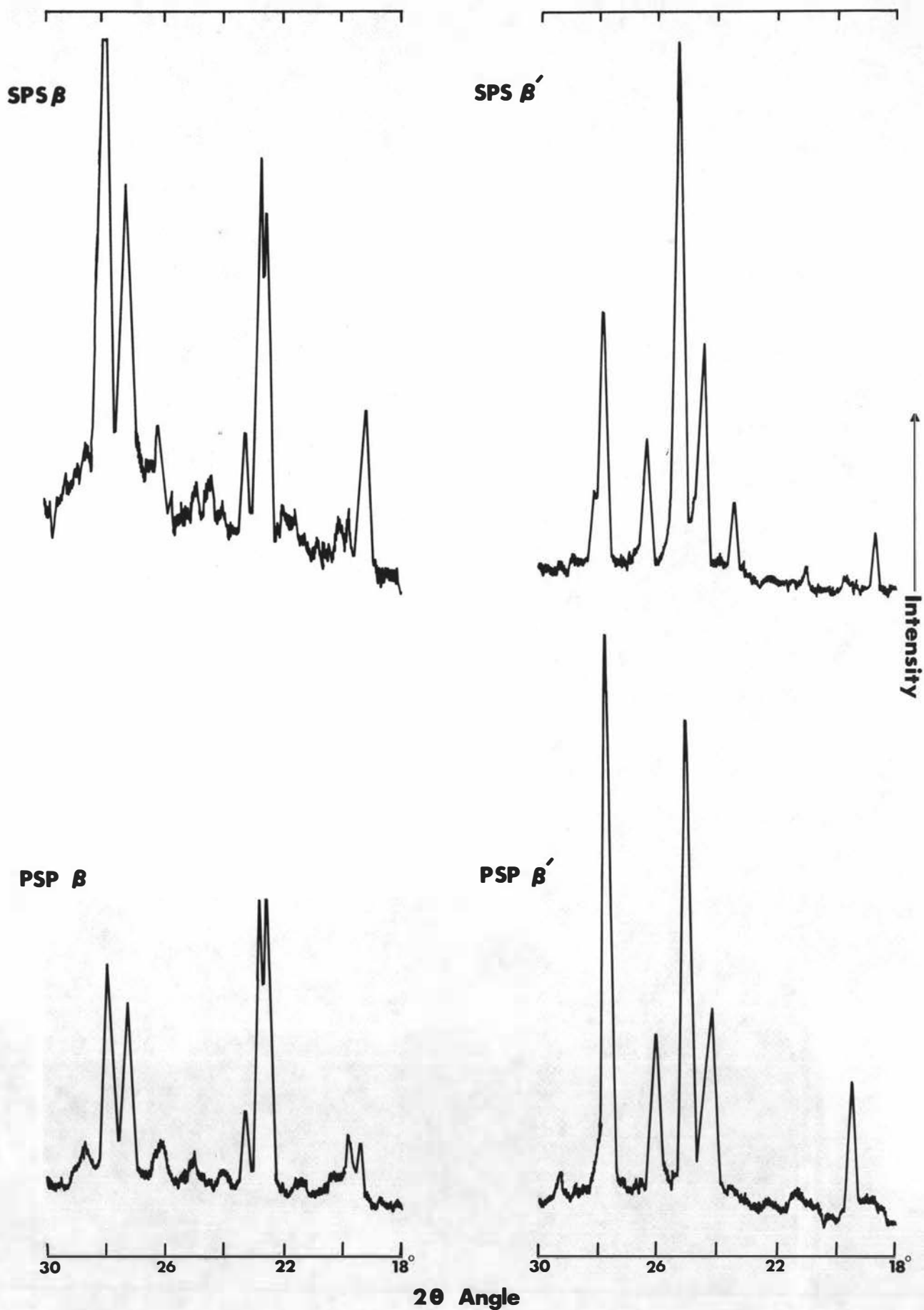


**Fig.3-2 X-ray diffraction patterns of  $\beta$  &  $\beta'$  forms of PSP & SPS**

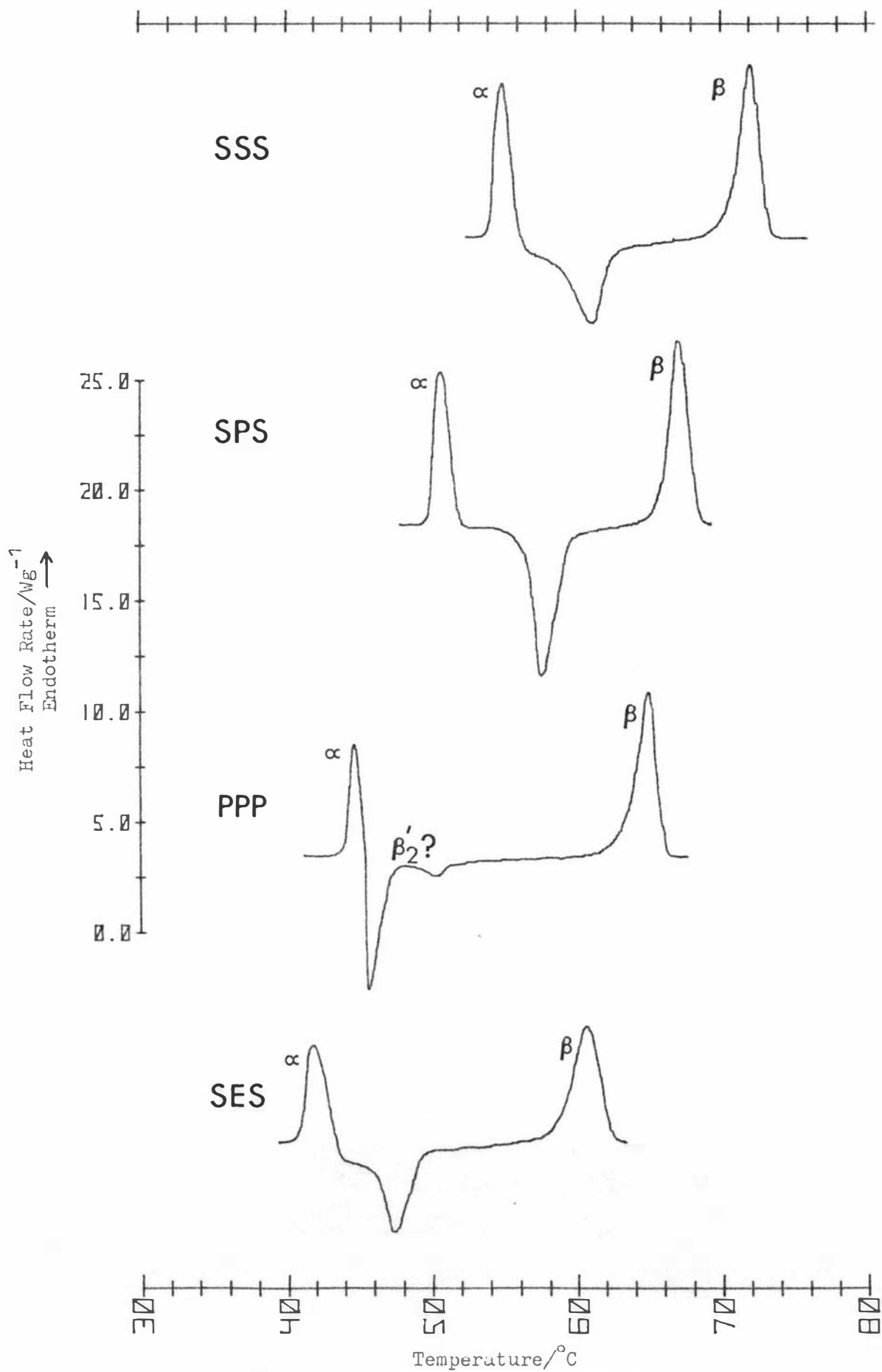


Fig. 3-3: Melting thermograms of  $\alpha$  SSS, SPS, PPP and SES, heating rate  $4^{\circ}\text{C}/\text{min}$ .

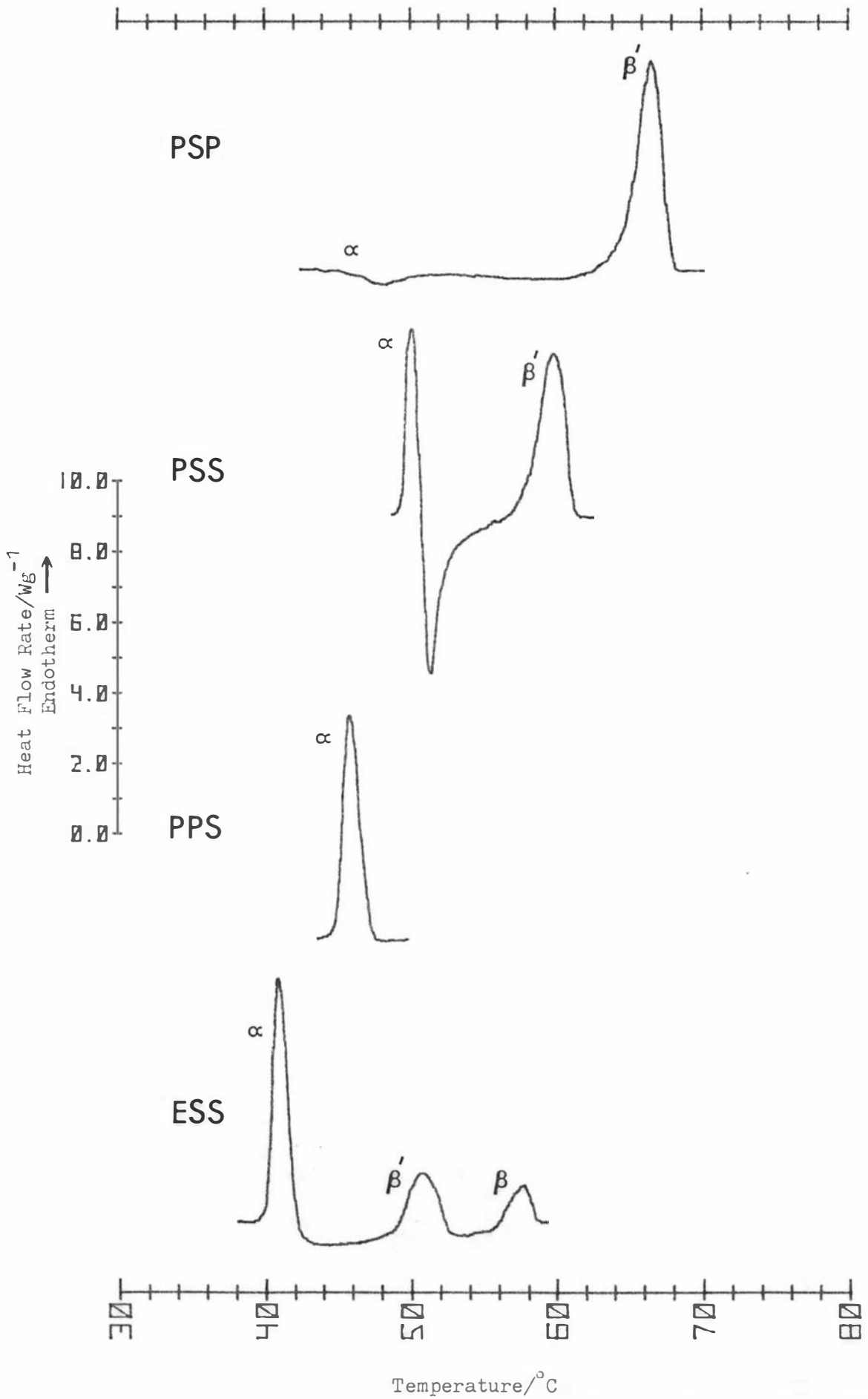


Fig. 3-4: Melting thermograms of  $\alpha$  PSP, PSS, PPS and ESS, heating rate  $4^{\circ}\text{C}/\text{min}$ .

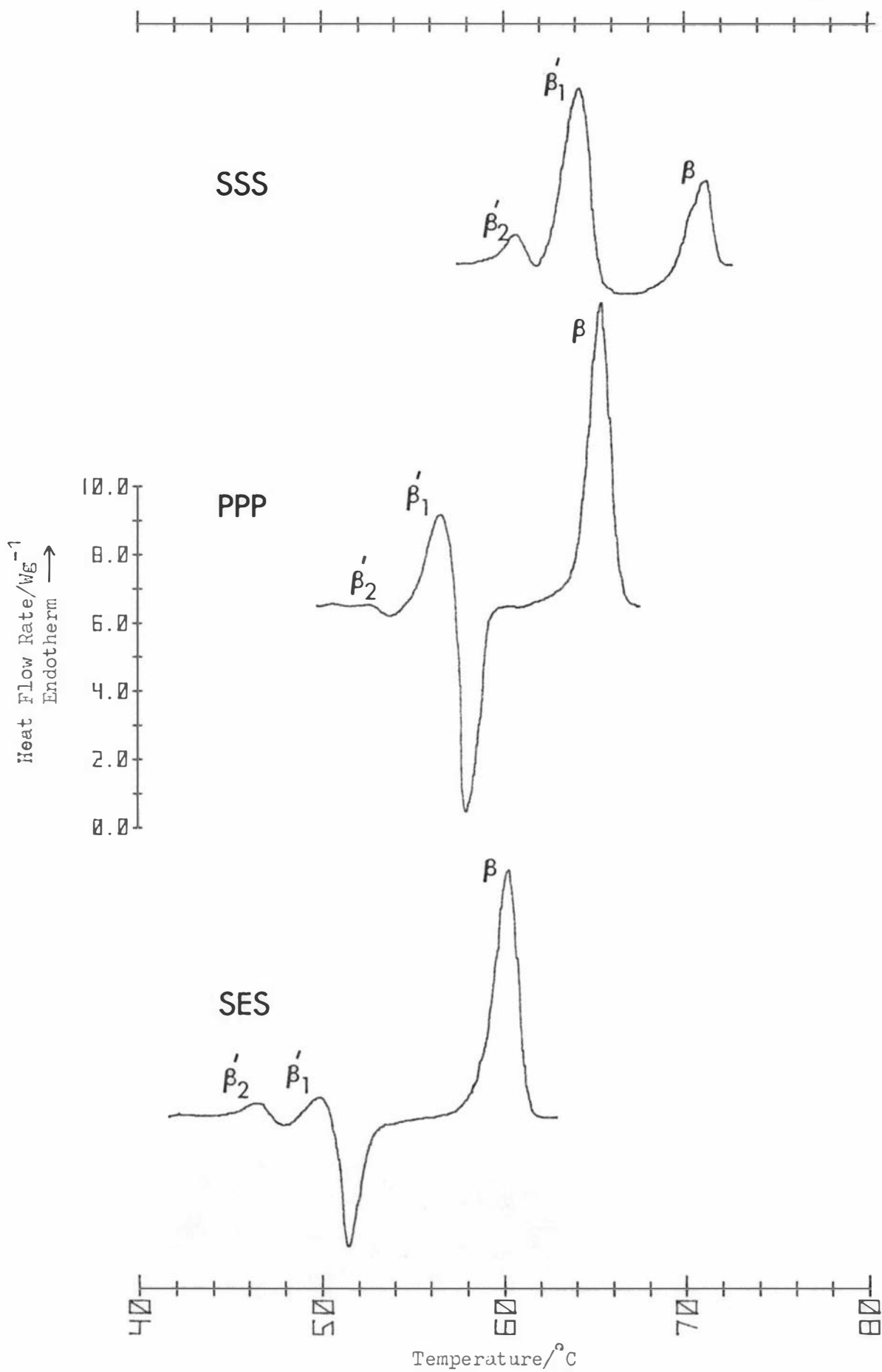


Fig. 3-5: Melting thermograms of  $\beta'$  SSS, PPP and SES, prepared by crystallisation of the melt near the  $\alpha$  melting point for 15, 7.5 and 20 min respectively, heating rate  $4^{\circ}\text{C}/\text{min}$ .

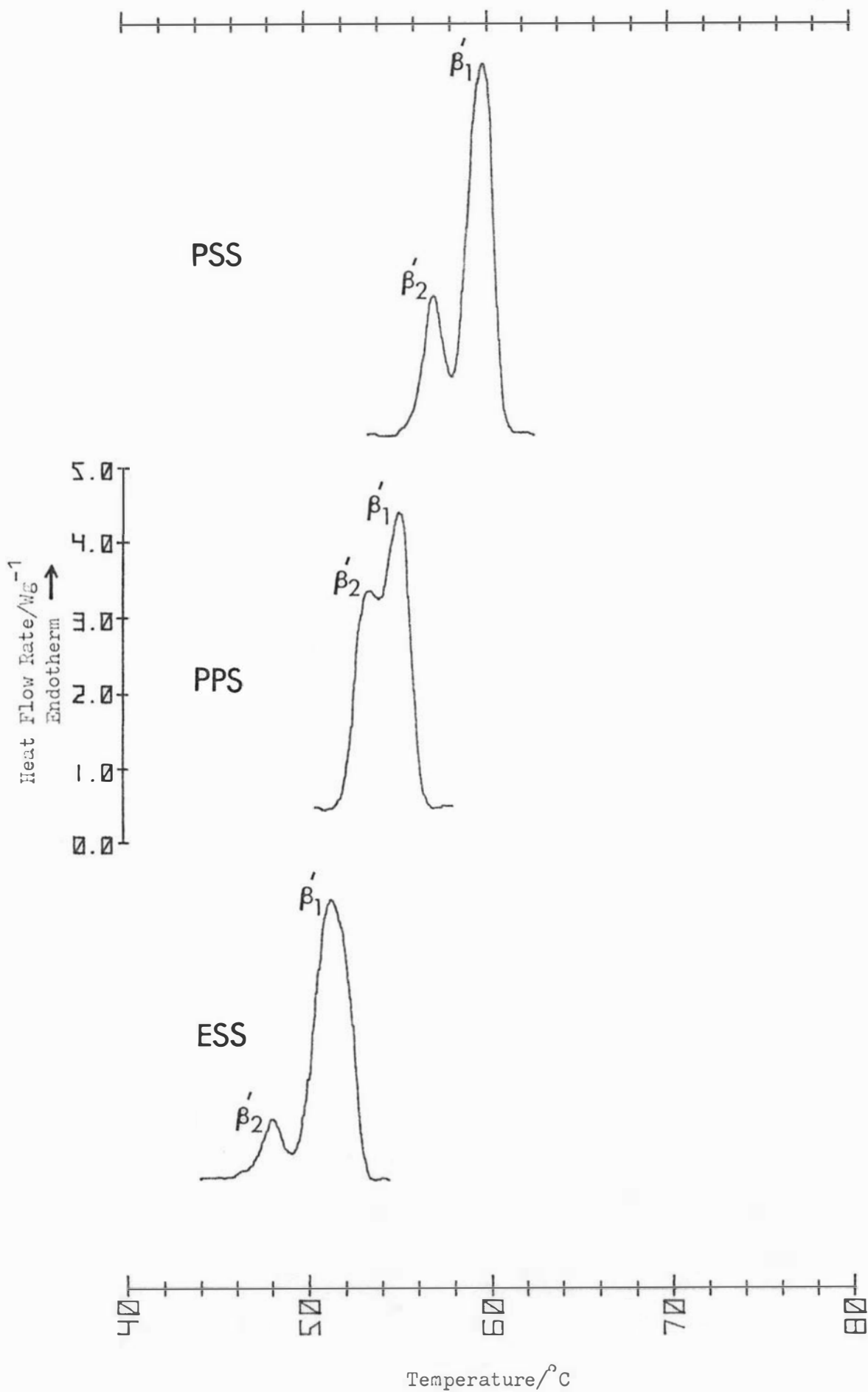


Fig. 3-6: Melting thermograms of  $\beta'$  PSS, PPS and ESS, prepared by crystallisation of the melt near the  $\alpha$  melting point for 30 min (PSS and ESS) or transformation of  $\alpha$  near its melting point for 30 min (PPS), heating rate  $4^{\circ}\text{C}/\text{min}$ .

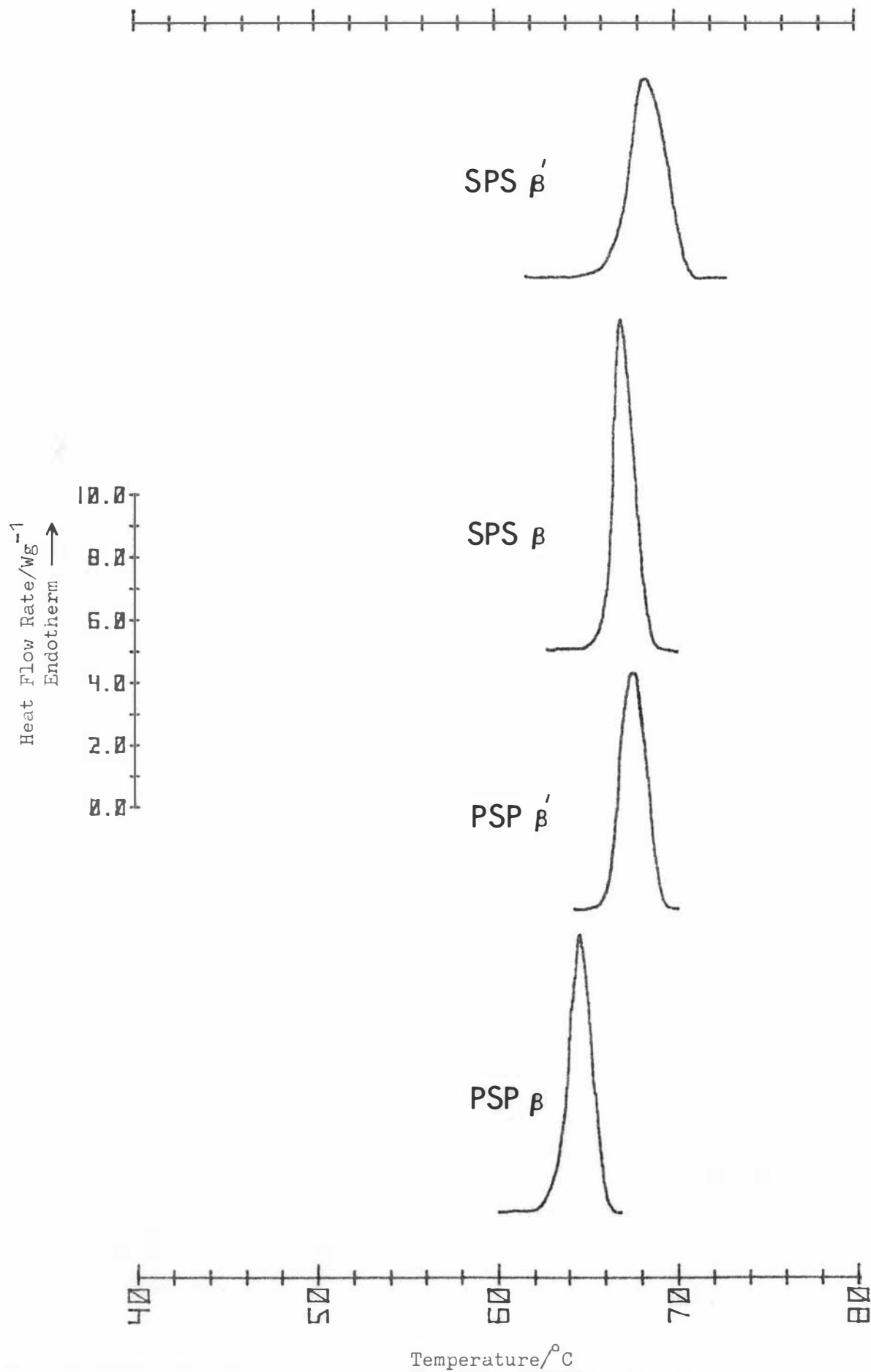
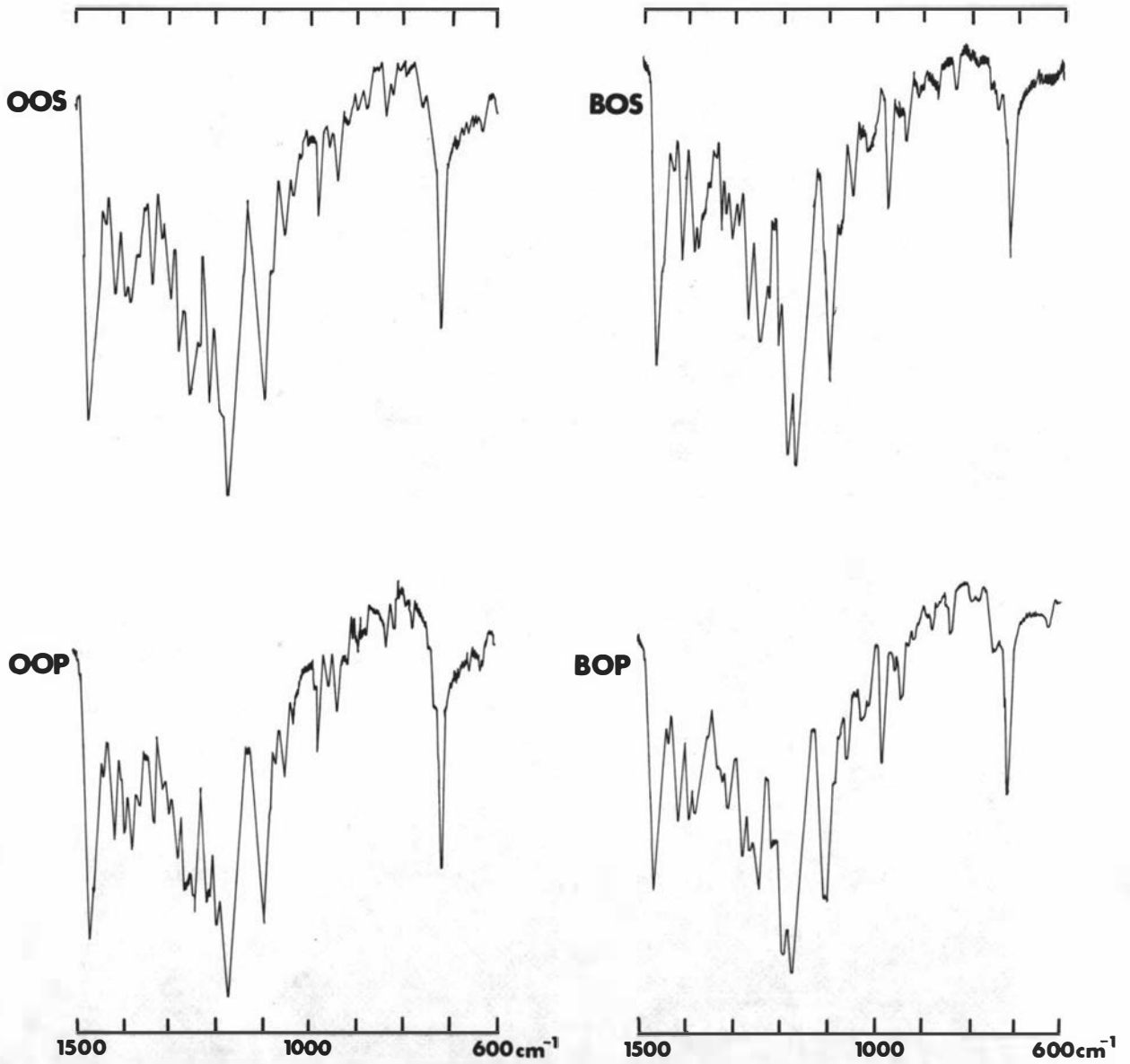


Fig. 3-7: Melting thermograms of the solvent crystallised  $\beta'$  and  $\beta$  forms of SPS and PSP, heating rate  $4^\circ\text{C}/\text{min}$ .



**Fig.3-8 IR Spectra of  $\beta'$  stable forms of XOO and XOB TGs**

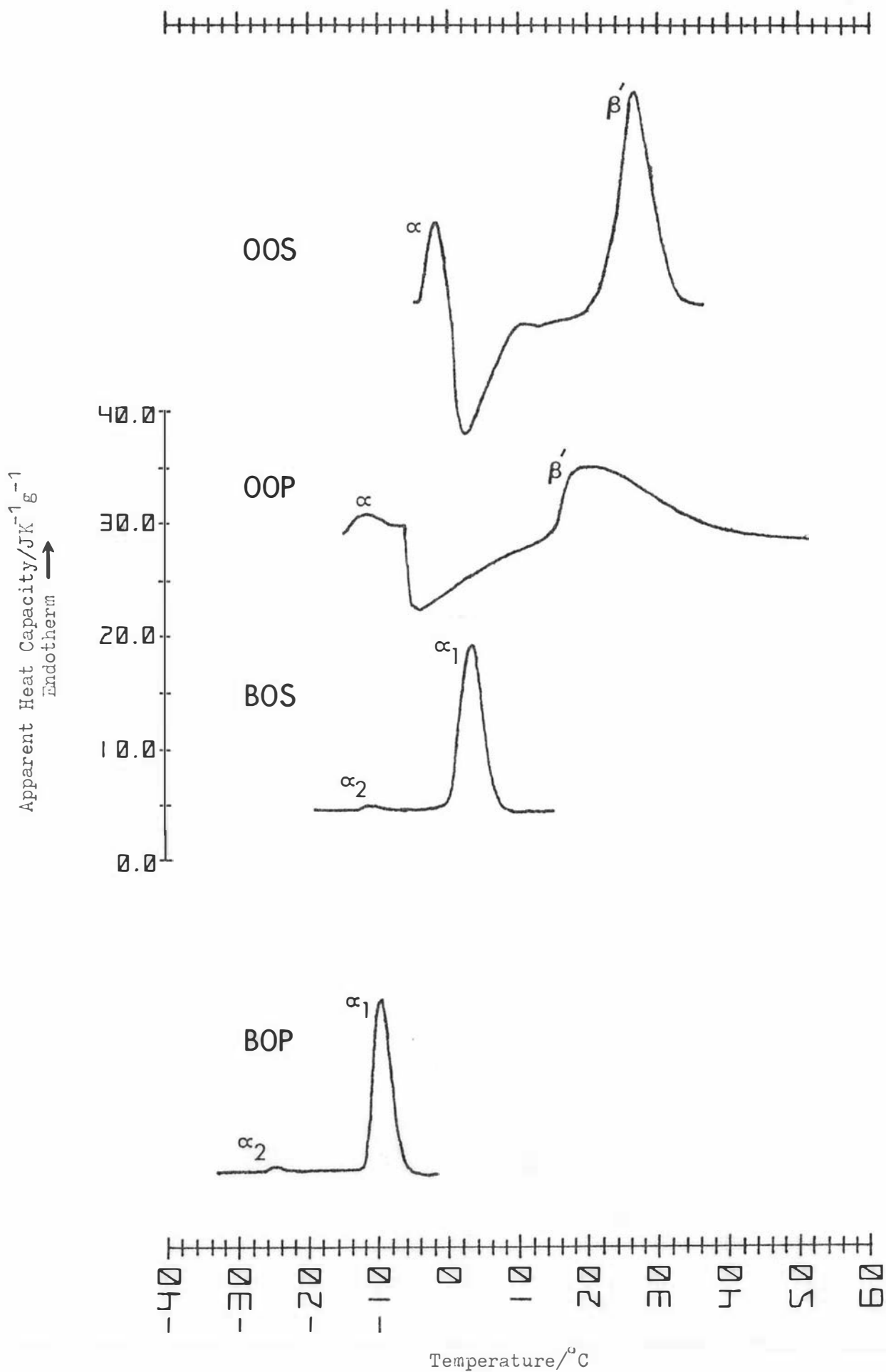


Fig. 3-9: Melting thermograms of  $\alpha$  OOS, OOP, BOS and BOP, heating rate  $64^{\circ}\text{C}/\text{min}$  for OOP and  $16^{\circ}\text{C}/\text{min}$  for the others.

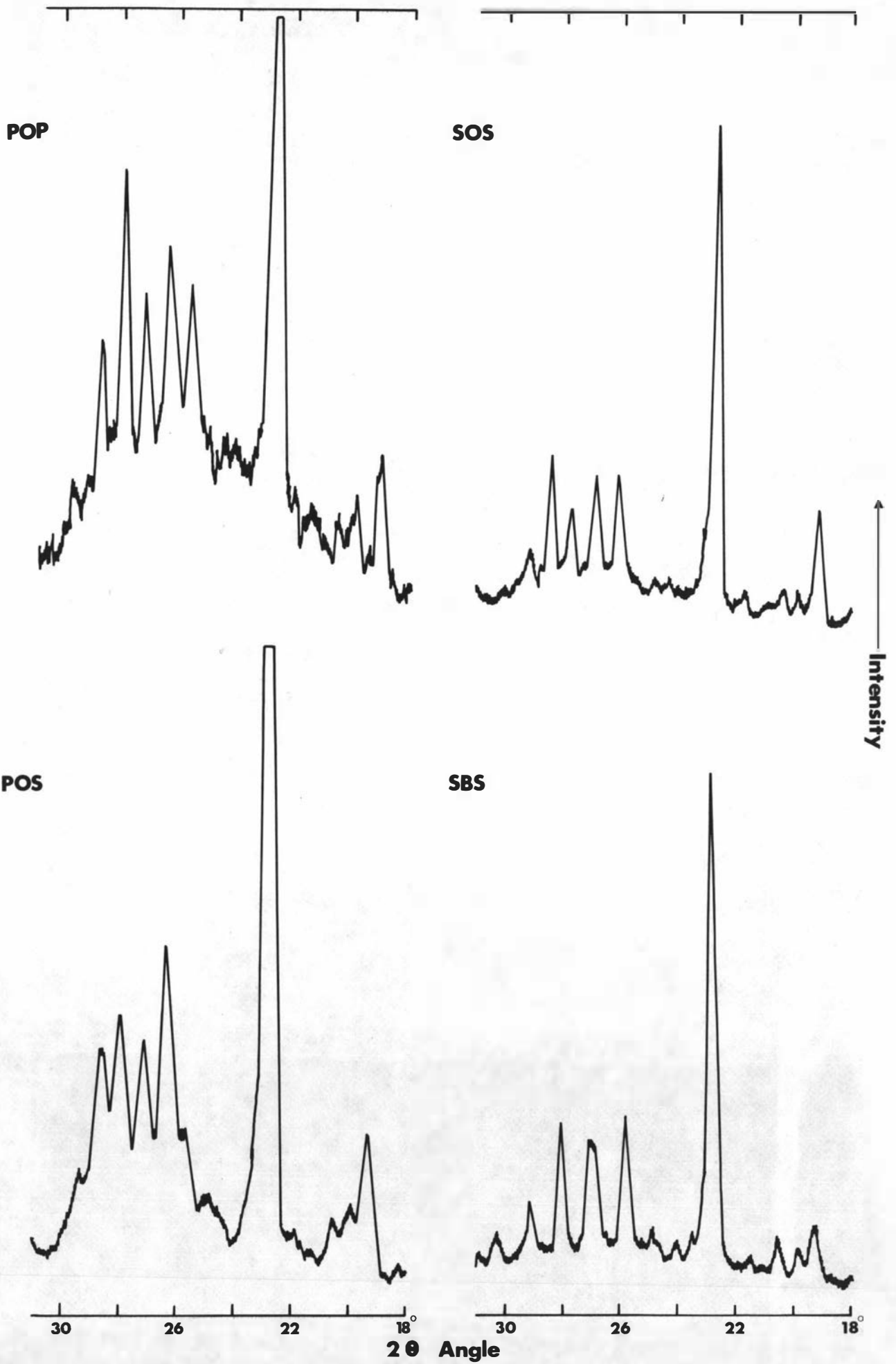
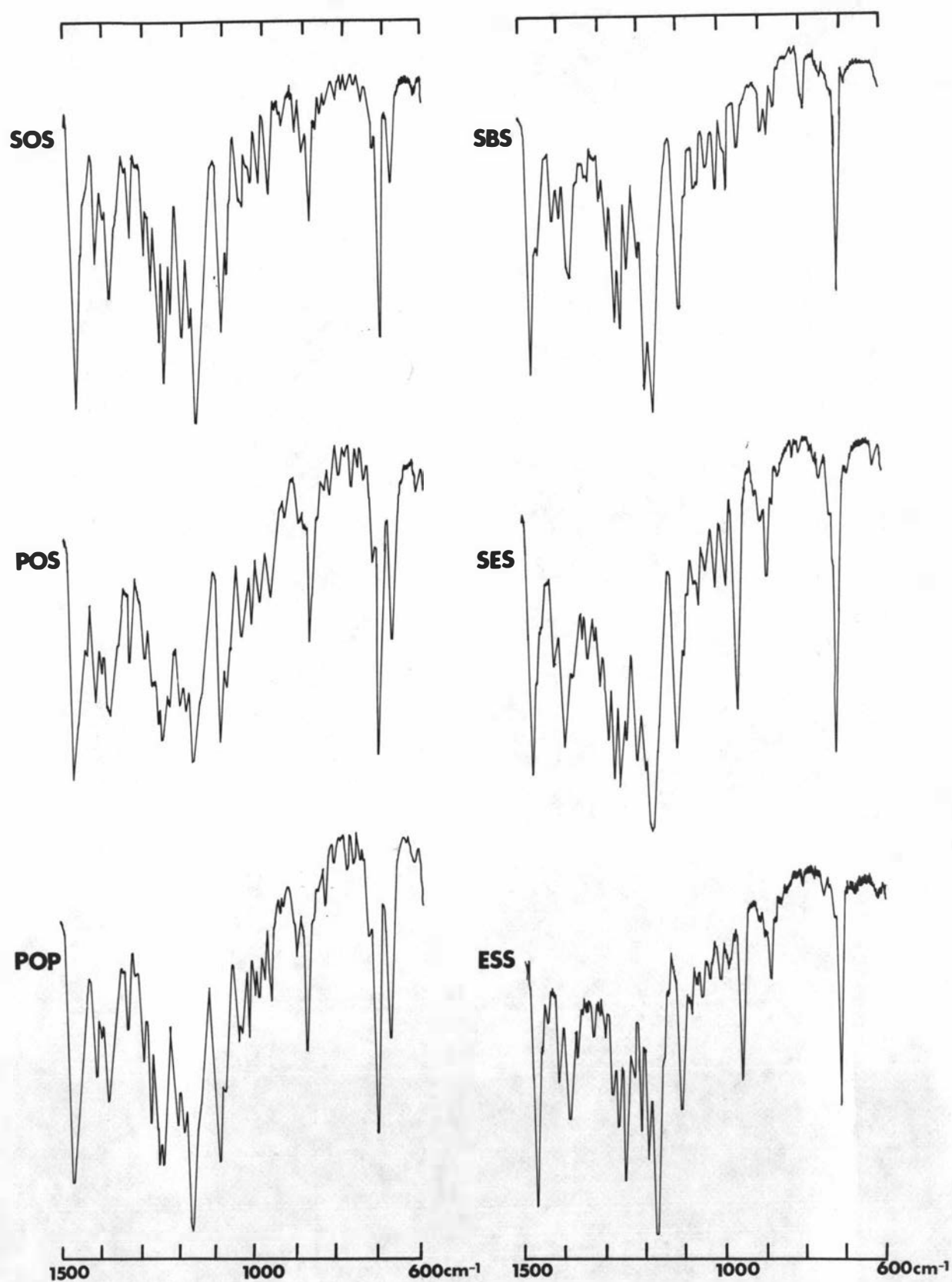


Fig.3-10 X-ray diffraction patterns of  $\beta$  stable forms of XOY & SBS TGs



**Fig. 3-11** IR Spectra of  $\beta$  stable forms of XOY, SBS, SES and ESS TGs

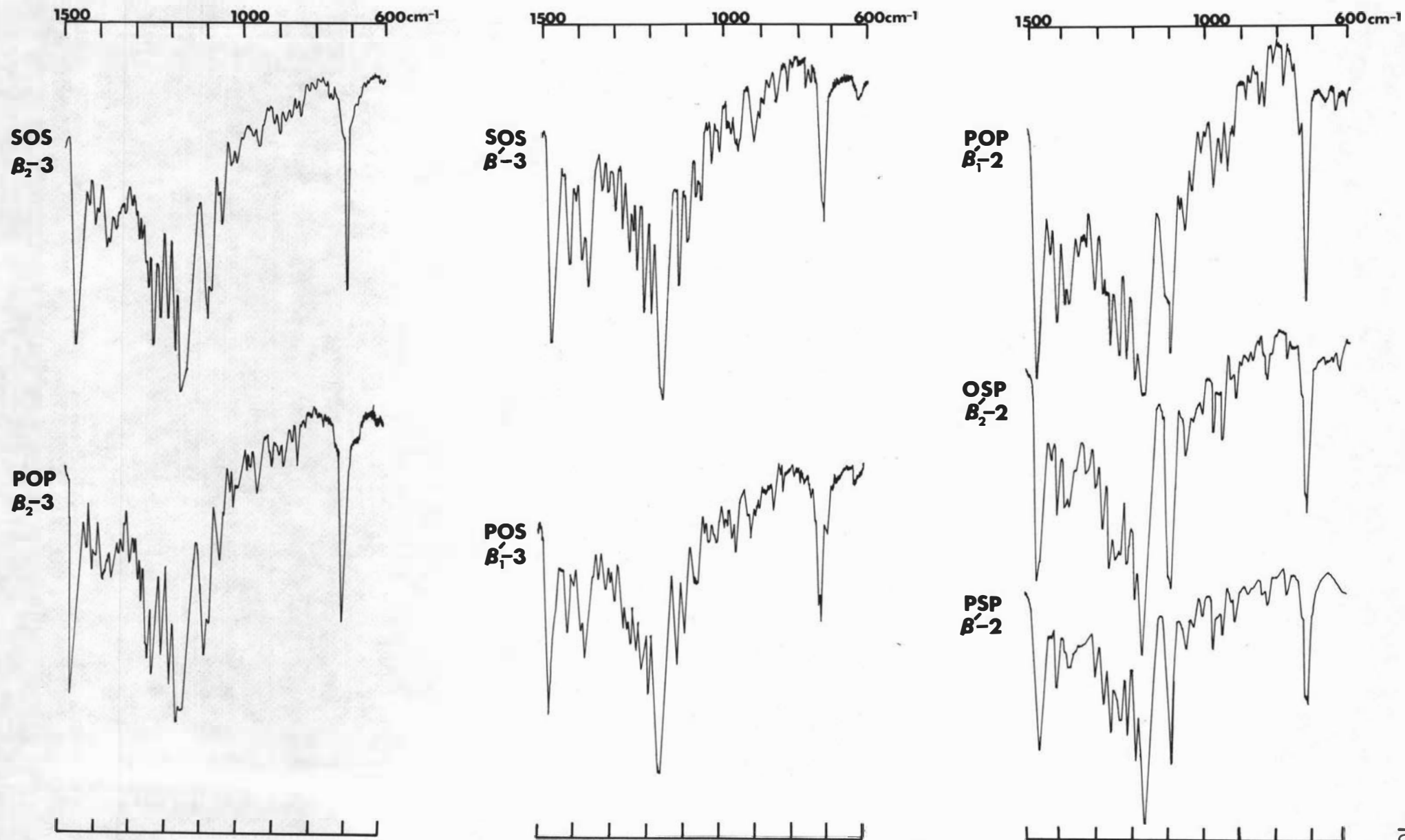


Fig.3-12 IR Spectra of comparative  $\beta_2$  and  $\beta'_1$  polymorphs of SOS, POS, and POP TGs

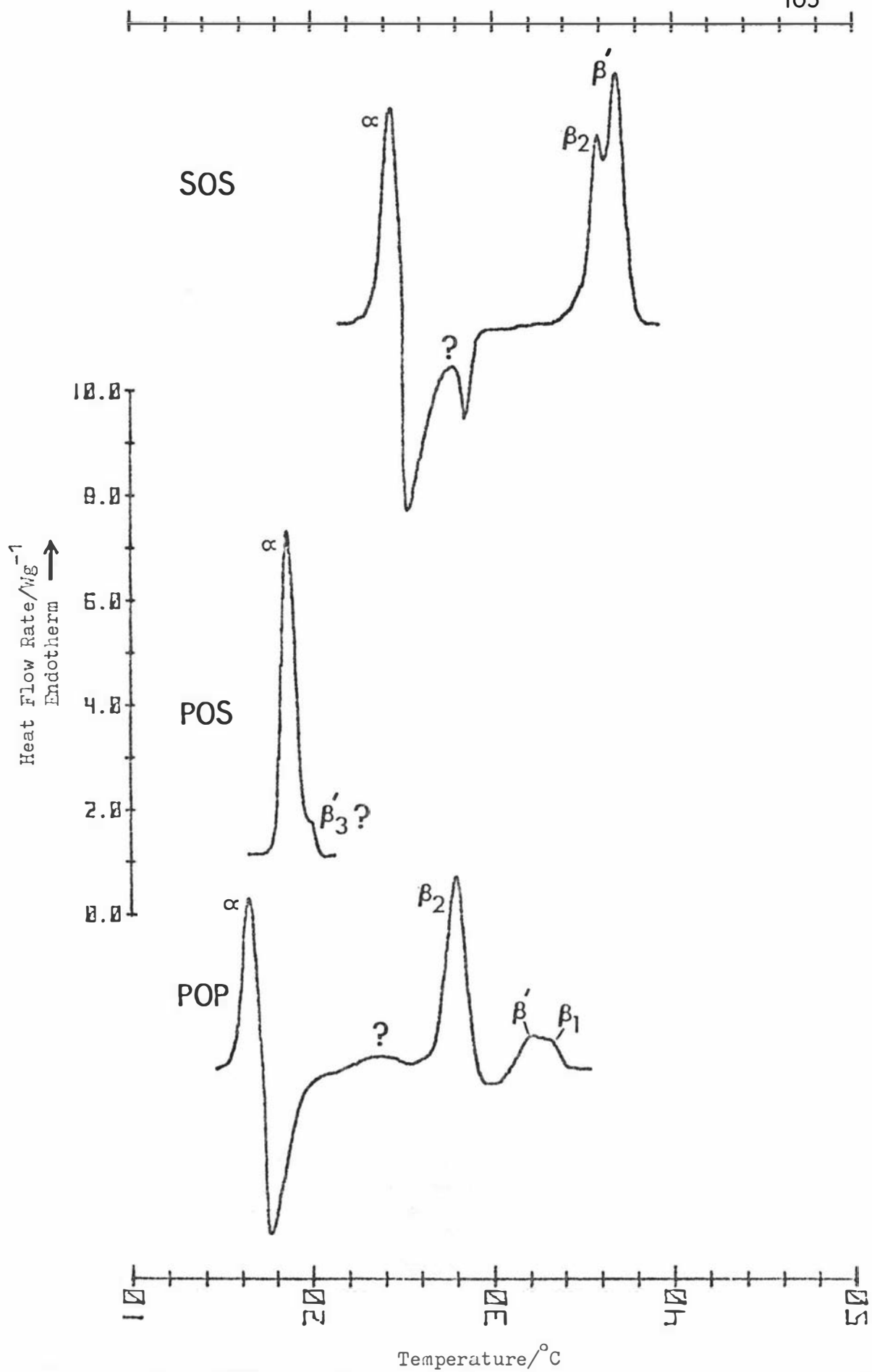


Fig. 3-13: Melting thermograms of  $\alpha$  SOS, POS and POP, heating rate  $4^{\circ}\text{C}/\text{min}$ .

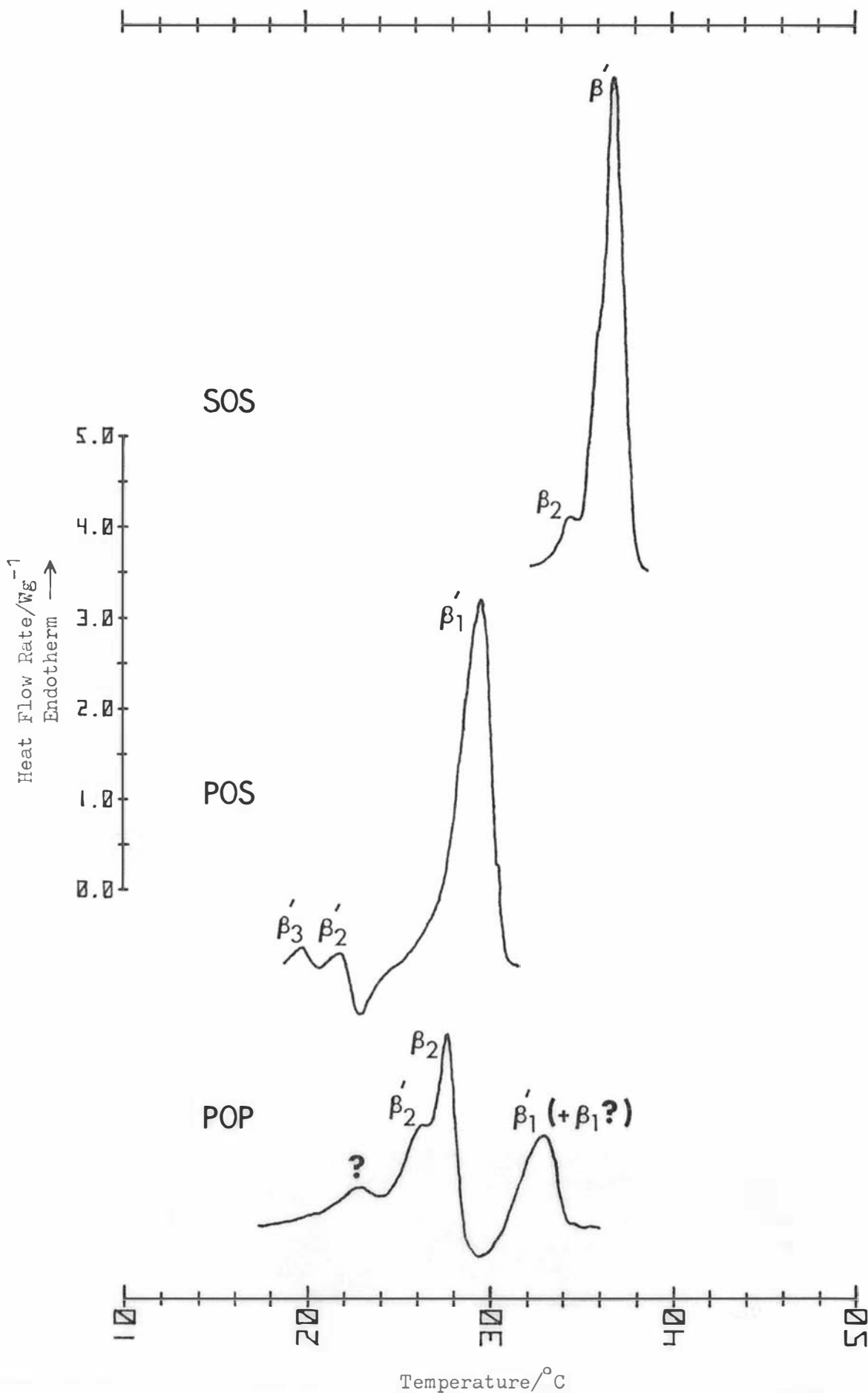
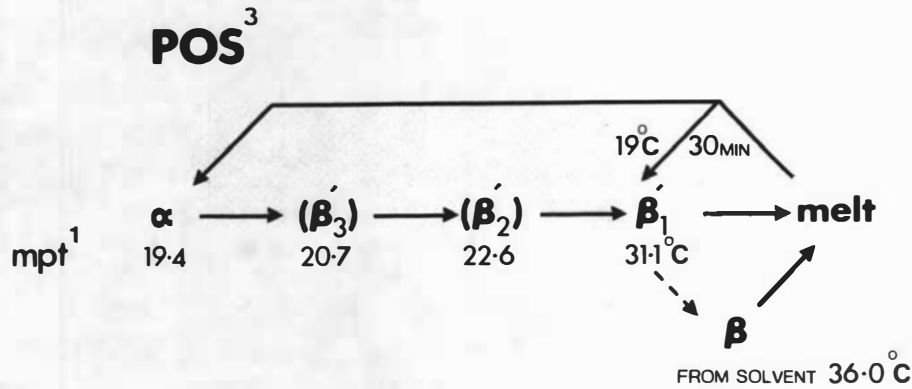
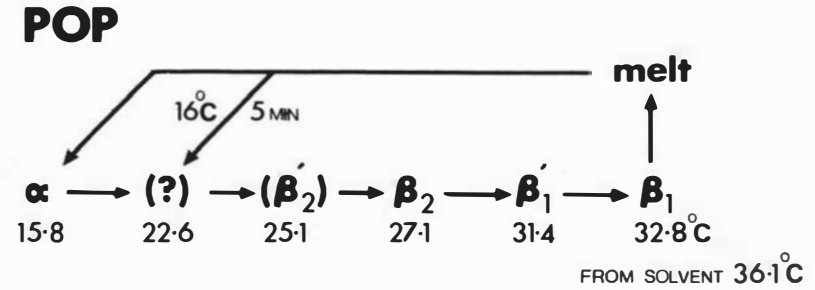
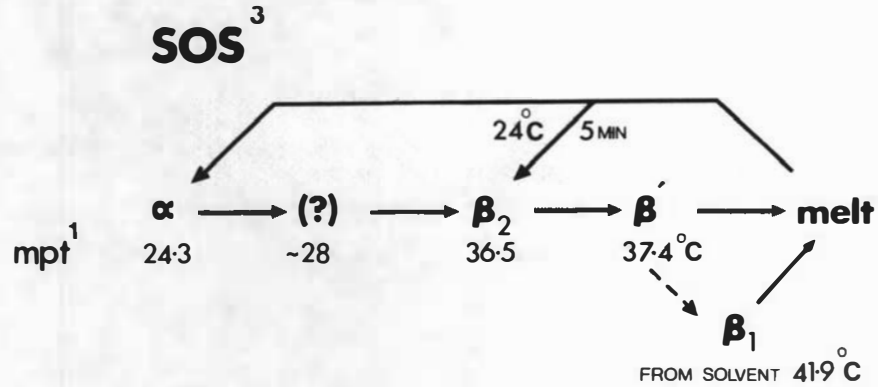


Fig. 3-14: Melting thermograms of the intermediate forms of SOS, POS and POP prepared by crystallisation of the melt (SOS, POP) or transformation of  $\alpha$  (POS) at the  $\alpha$  melting point, heating rate 4°C/min.

**Fig. 3-15 Polymorphism of SOS, POS and POP**



Equivalent Forms			
SOS	POS	POP	
$\beta_1$	$\beta$	$\beta_1$	$\beta-3^4$
$\beta'$	$\beta'_1$	-	$\beta'-3$
-	-	$\beta'_1$	$\beta'-2$
$\beta_2$	-	$\beta_2$	sub $\beta-3$ , $\beta''_M$
-	-	( $\beta_2$ )	sub $\beta'-2?$

**Note** 1 Mpts and phase assignments were determined by DSC and IR spectroscopy respectively. Assignments in brackets were made from DSC [Hagemann et al., 1972].

2 ----->, slow transition ; ----->, fast transition

3 SOS and POS crystallise in a very unstable form not shown above [see text].

4 Forms reported by Wille and Lutton [1966] and Lavery [1958]

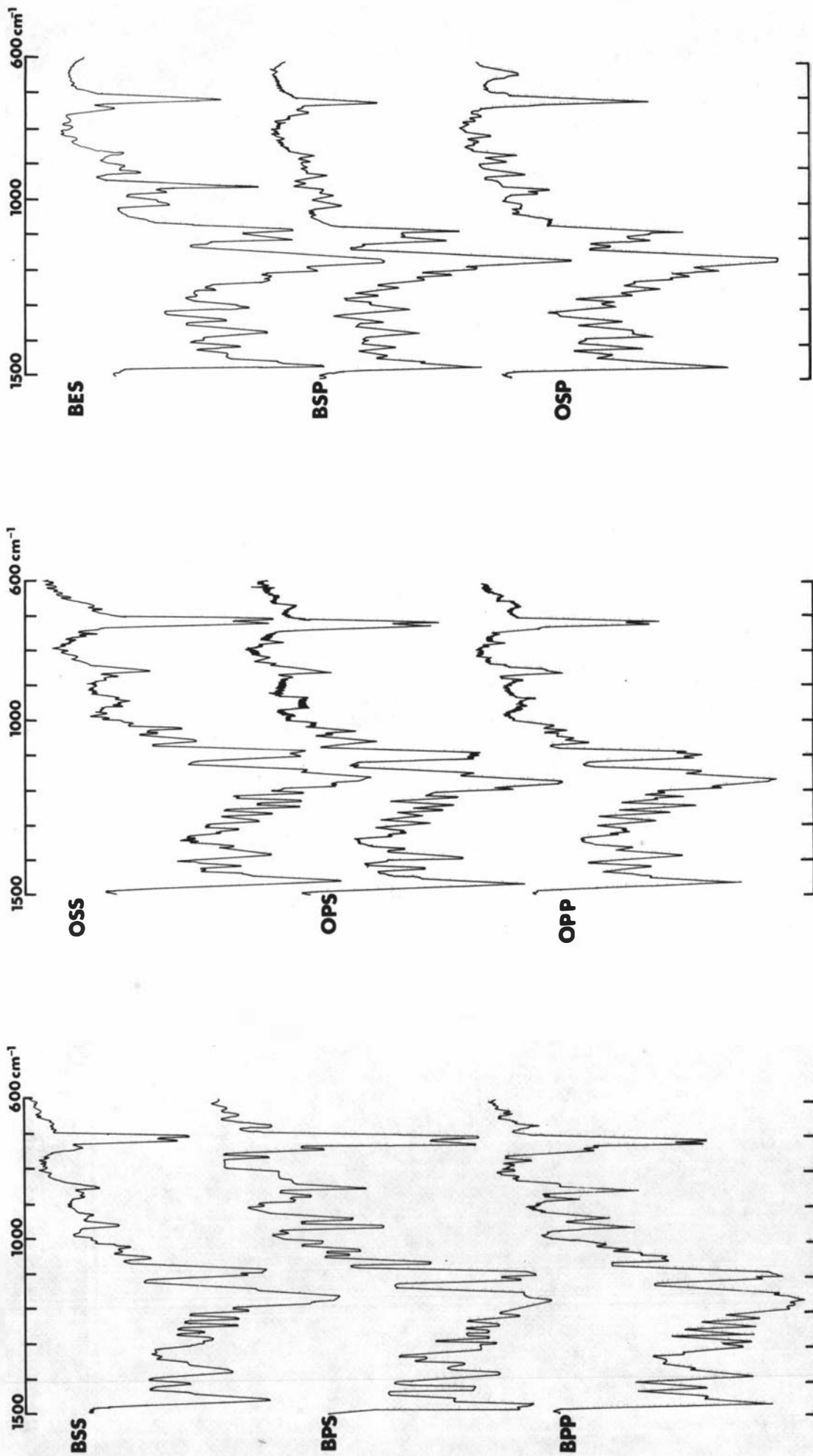


Fig.3-16 IR Spectro of  $\beta'$  stable forms of OXY and BXY TGs at 25°C

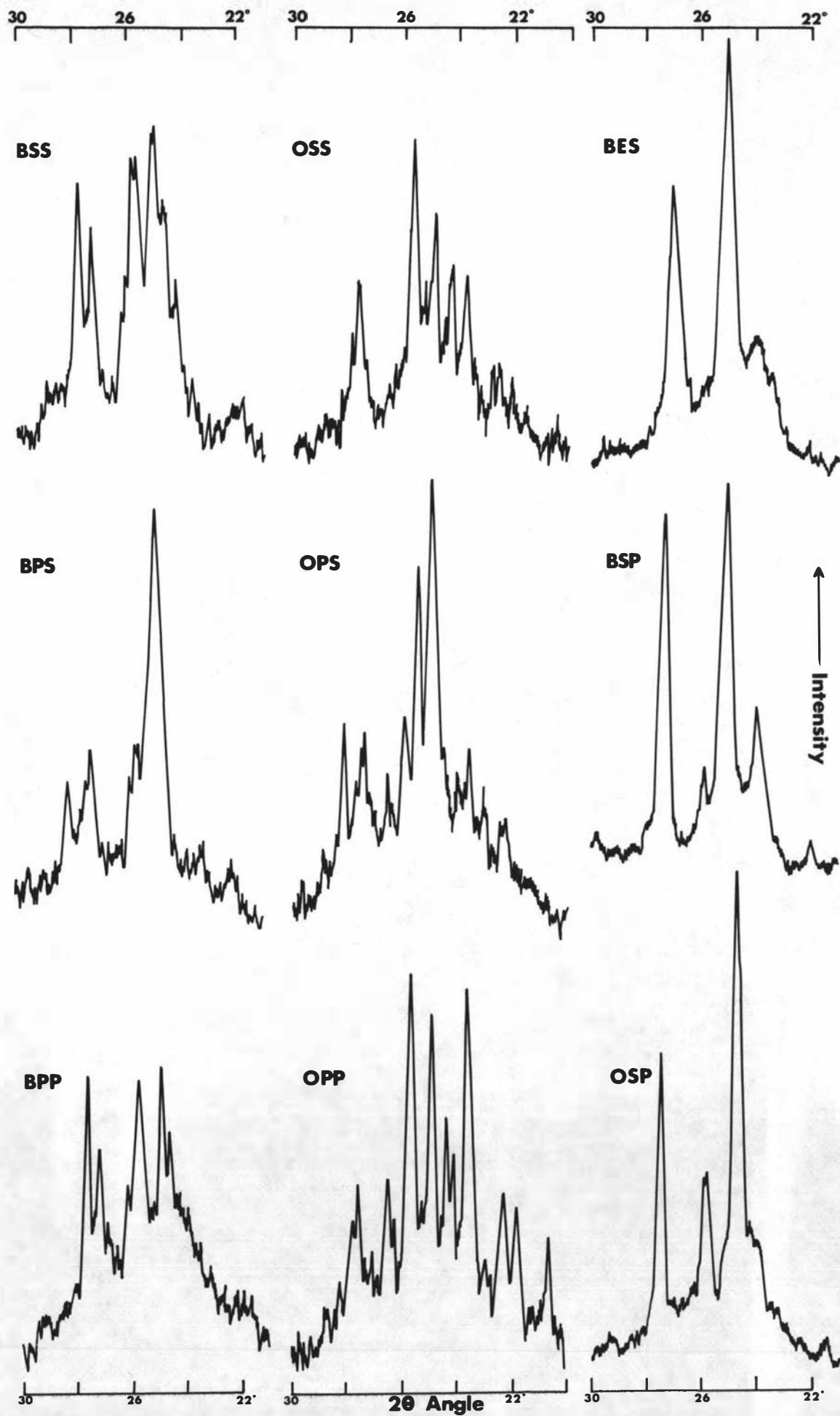


Fig. 3-17 X-ray diffraction patterns of  $\beta'$  stable forms of OXY & BXY TGs

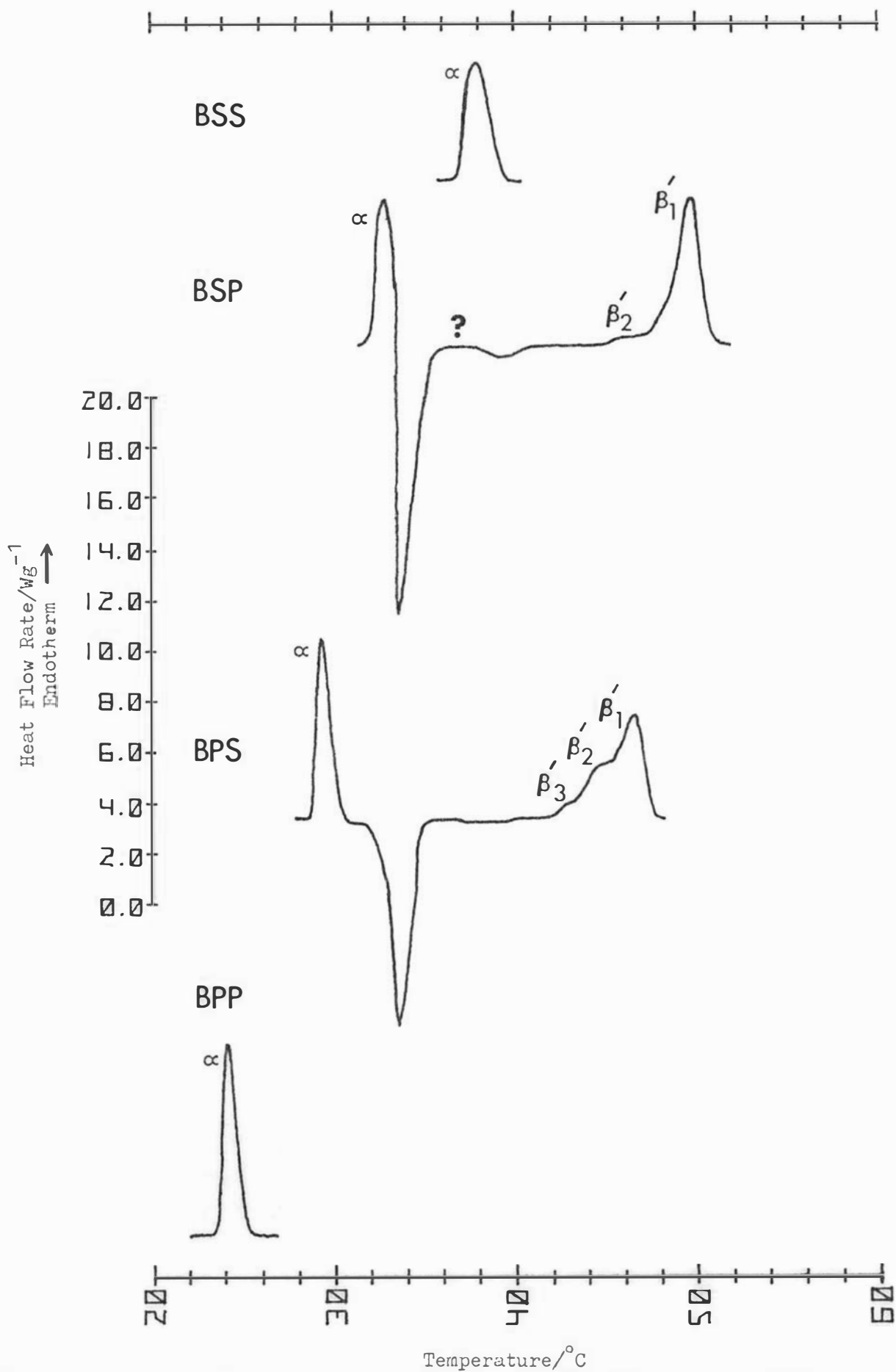


Fig. 3-18: Melting thermograms of  $\alpha$  BSS, BSP, BPS and BPP, heating rate  $4^{\circ}\text{C}/\text{min.}$

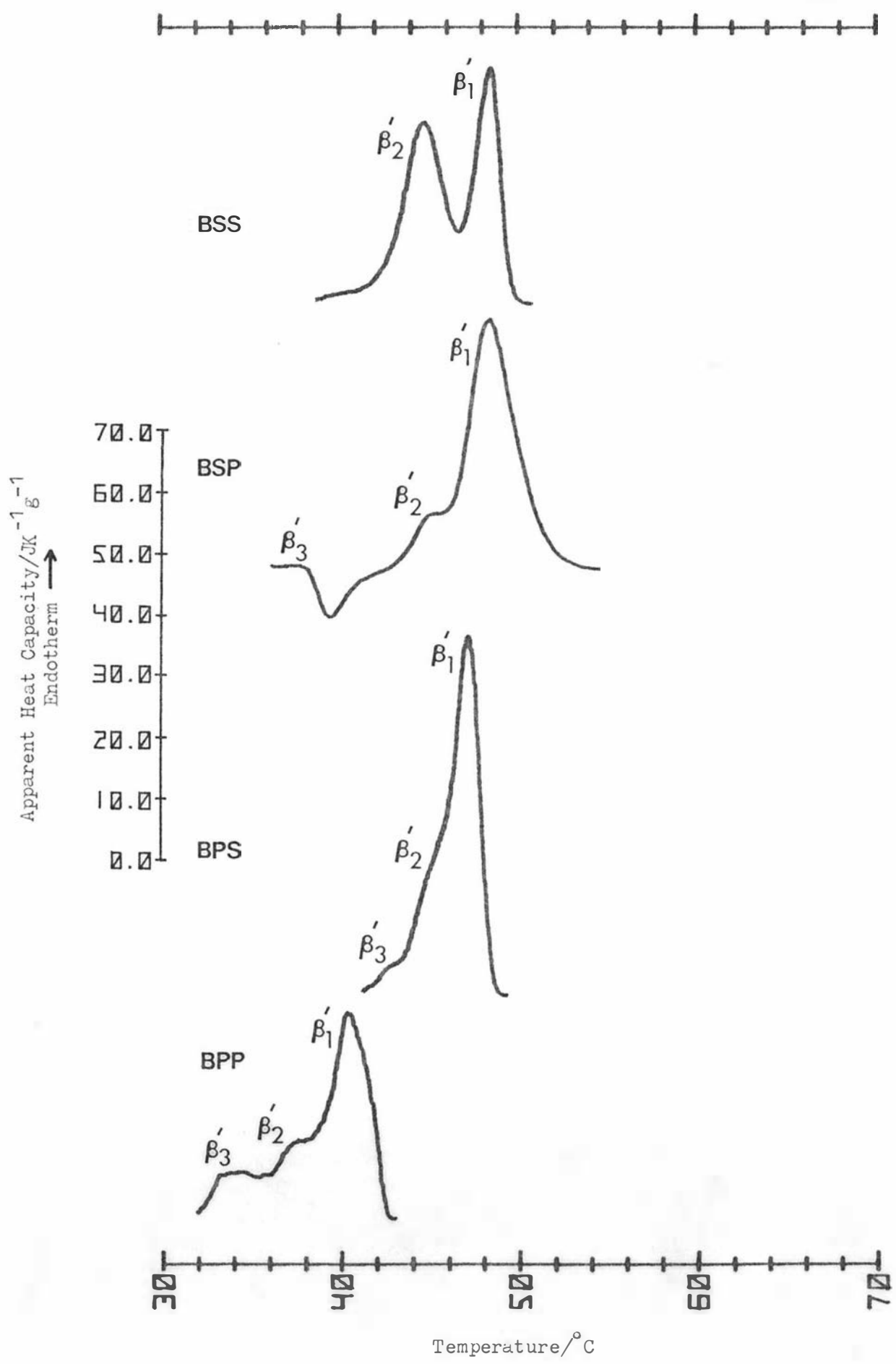


Fig. 3-19: Melting thermograms of the intermediate forms of BSS, BSP, BPS and BPP prepared by transformation of  $\alpha$  near its melting point for 45, 2, 10 and 15 min. respectively, heating rate 16°C/min for BSP and 4°C/min for the others.

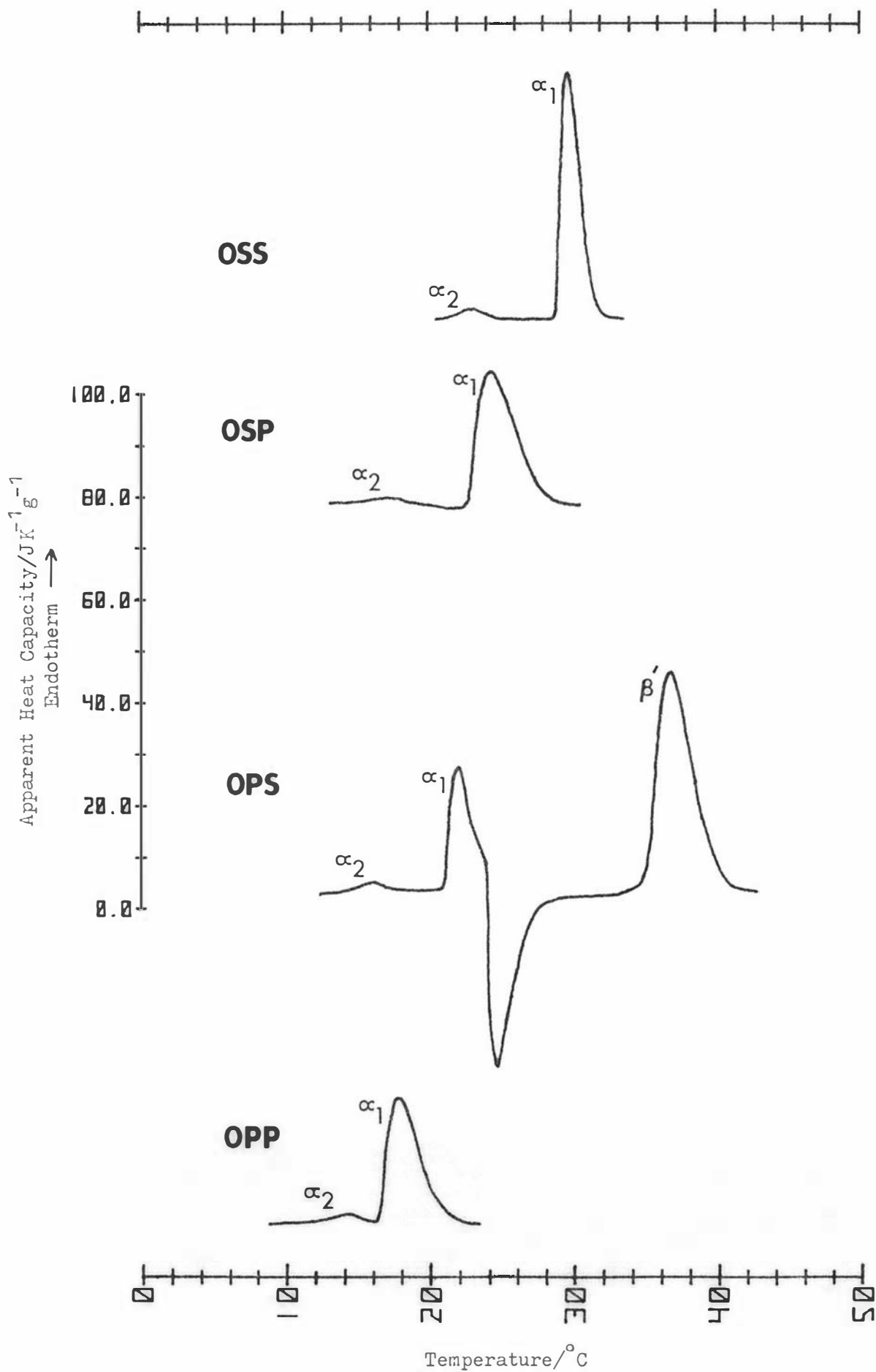


Fig. 3-20: Melting thermograms of  $\alpha$  OSS, OSP, OPS and OPP showing the presence of the  $\alpha_2$  form at high heating rates, 8°C/min for OSS and 16°C/min for the others.

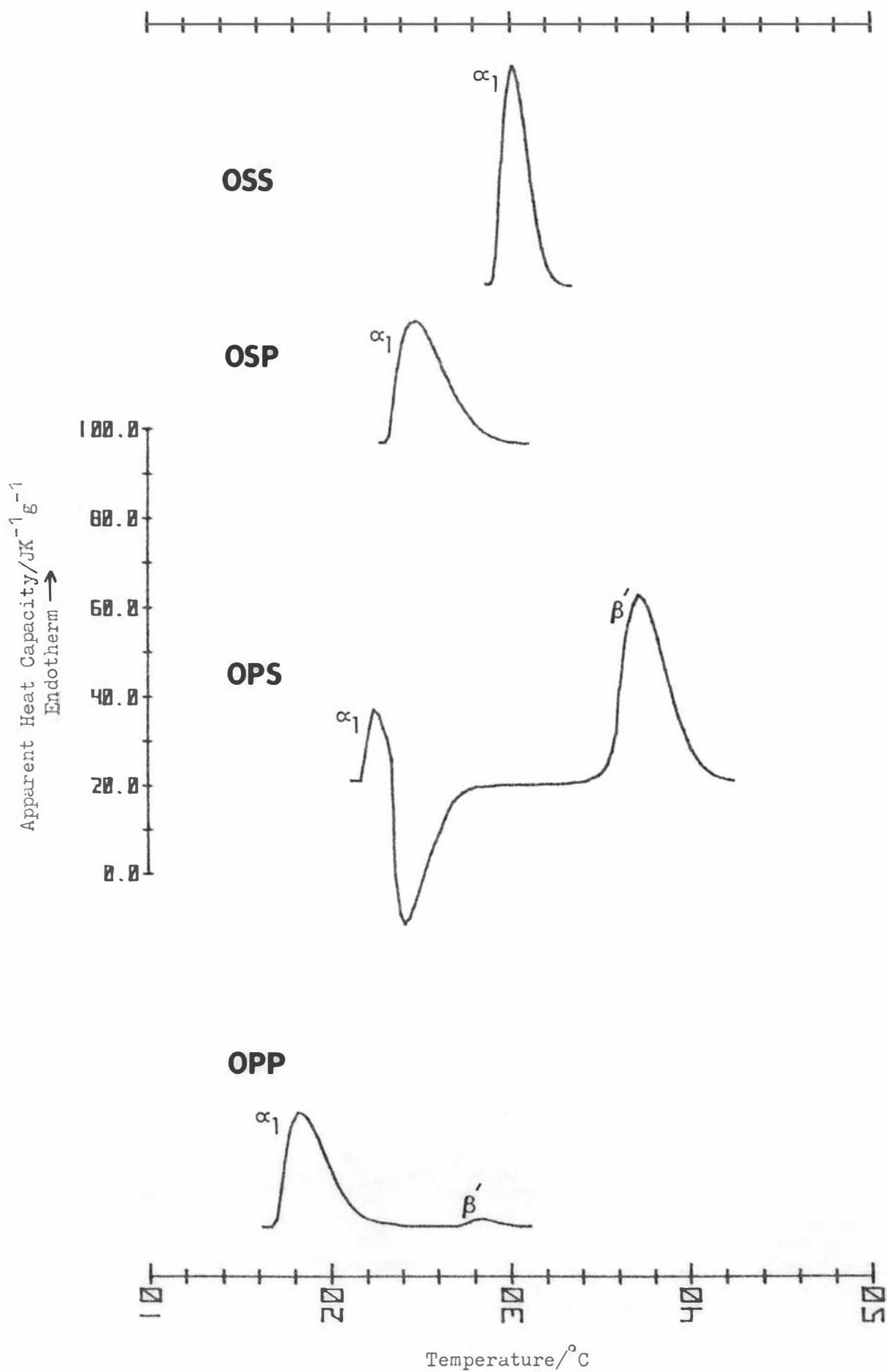


Fig. 3-21: Melting thermograms of  $\alpha$  OSS, OSP, OPS and OPP recorded after tempering at the  $\alpha_2$  peak temperature for 5, 2, 2 and 5 min. respectively. The heating rate was  $8^{\circ}\text{C}/\text{min}$  for OSS and  $16^{\circ}\text{C}/\text{min}$  for the others.

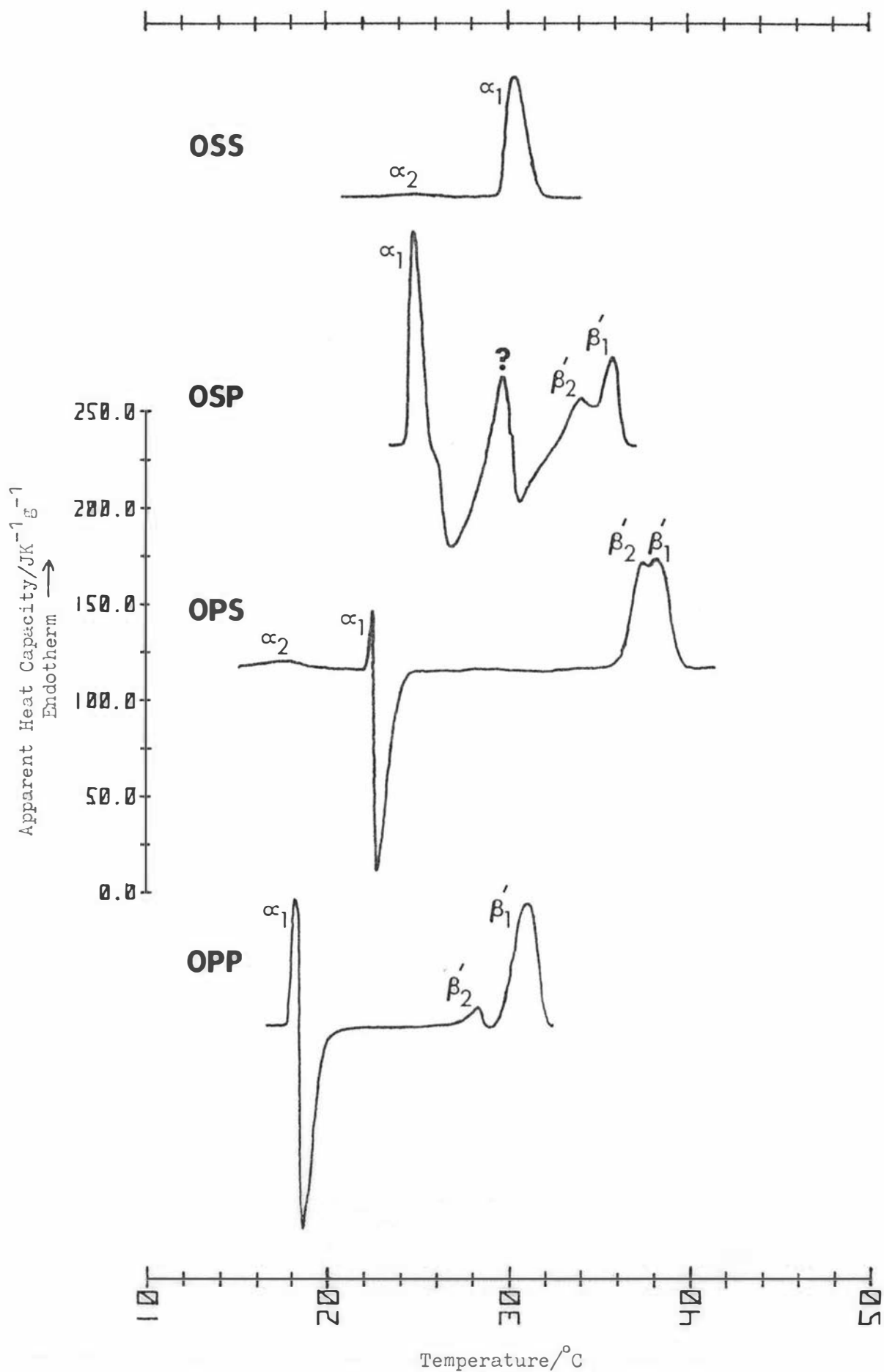


Fig. 3-22: Melting thermograms of  $\alpha$  OSS, OSP, OPS and OPP recorded at the low heating rates of 4, 2, 4 and 2  $^{\circ}\text{C}/\text{min}$  respectively.

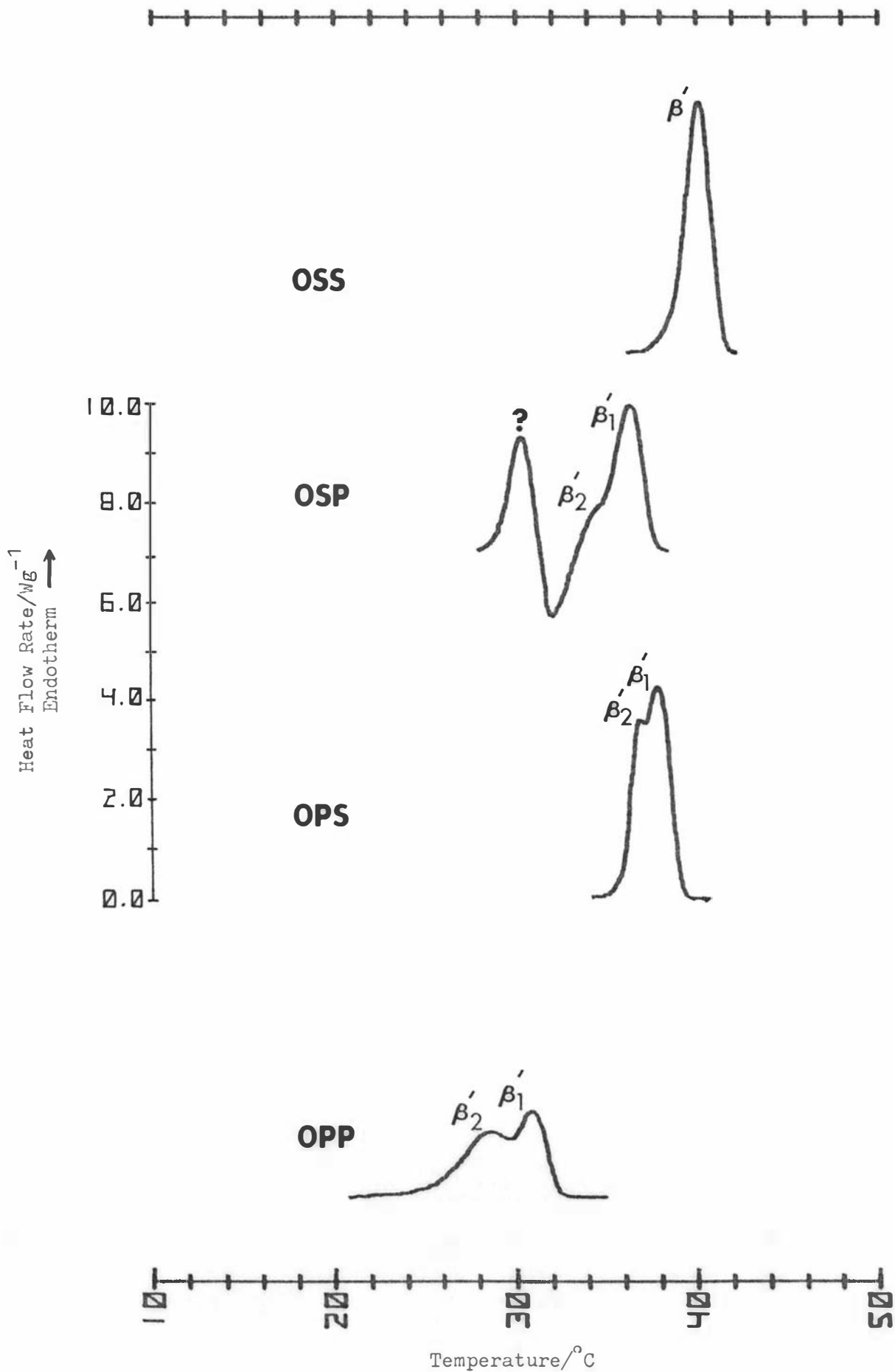
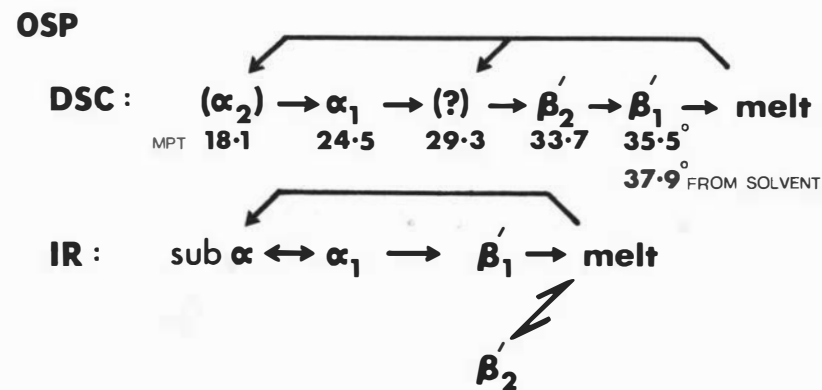
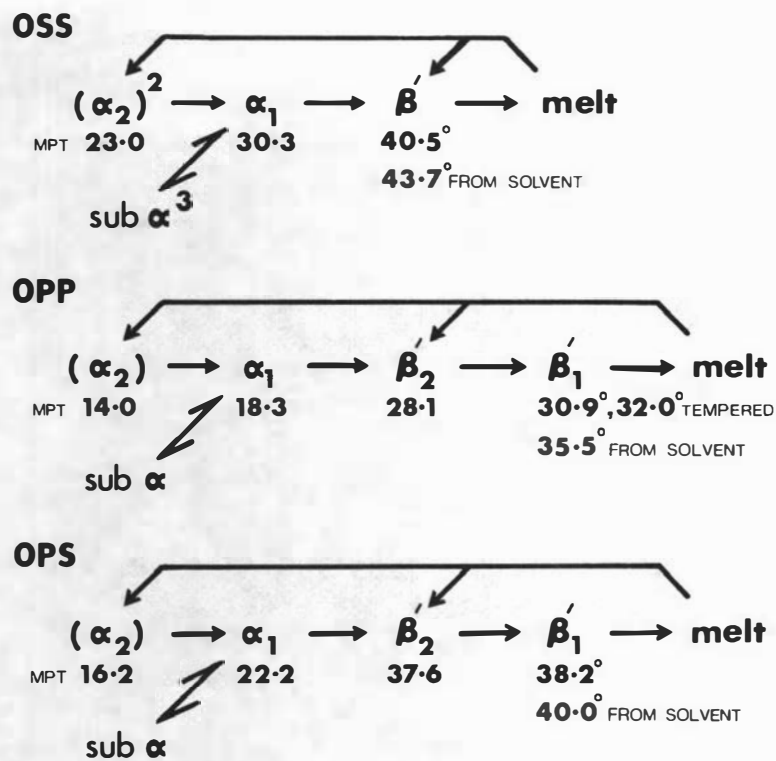


Fig. 3-23: Melting thermograms of the intermediate forms of OSS, OSP, OPS and OPP prepared by crystallisation of the melt (OPS, 3 min; OPP, 25 min) or transformation of  $\alpha$  (OSS, 10 min; OSP, 5 min) at the  $\alpha$  melting point, heating rate 4°C/min.

**Fig. 3 - 24 Polymorphism<sup>1</sup> of OSS, OSP, OPS and OPP.**



Equivalent Forms				
OSS	OSP	OPS	OPP	
$\beta'$	$\beta_1$ <sup>5</sup>	$\beta_1$	$\beta_1$	$\beta'-3$ <sup>4</sup>
-	$\beta_2$	-	-	$\beta'-2$
-	-	$\beta_2$	-	sub $\beta'-3$
-	-	-	$\beta_2$	-
-	(?)	-	-	(?)

Note

- 1 Phase melting points (°C) and assignments were determined by DSC and IR spectroscopy respectively.
- 2 Polymorphs in brackets were not detected by IR spectroscopy.
- 3 The sub  $\alpha \leftrightarrow \alpha$  transition was not observed in the DSC study.
- 4 Polymorphs reported by Lutton (1951) and Lavery (1958).
- 5 The stable form of OSP was not isostructural with the other stable forms.

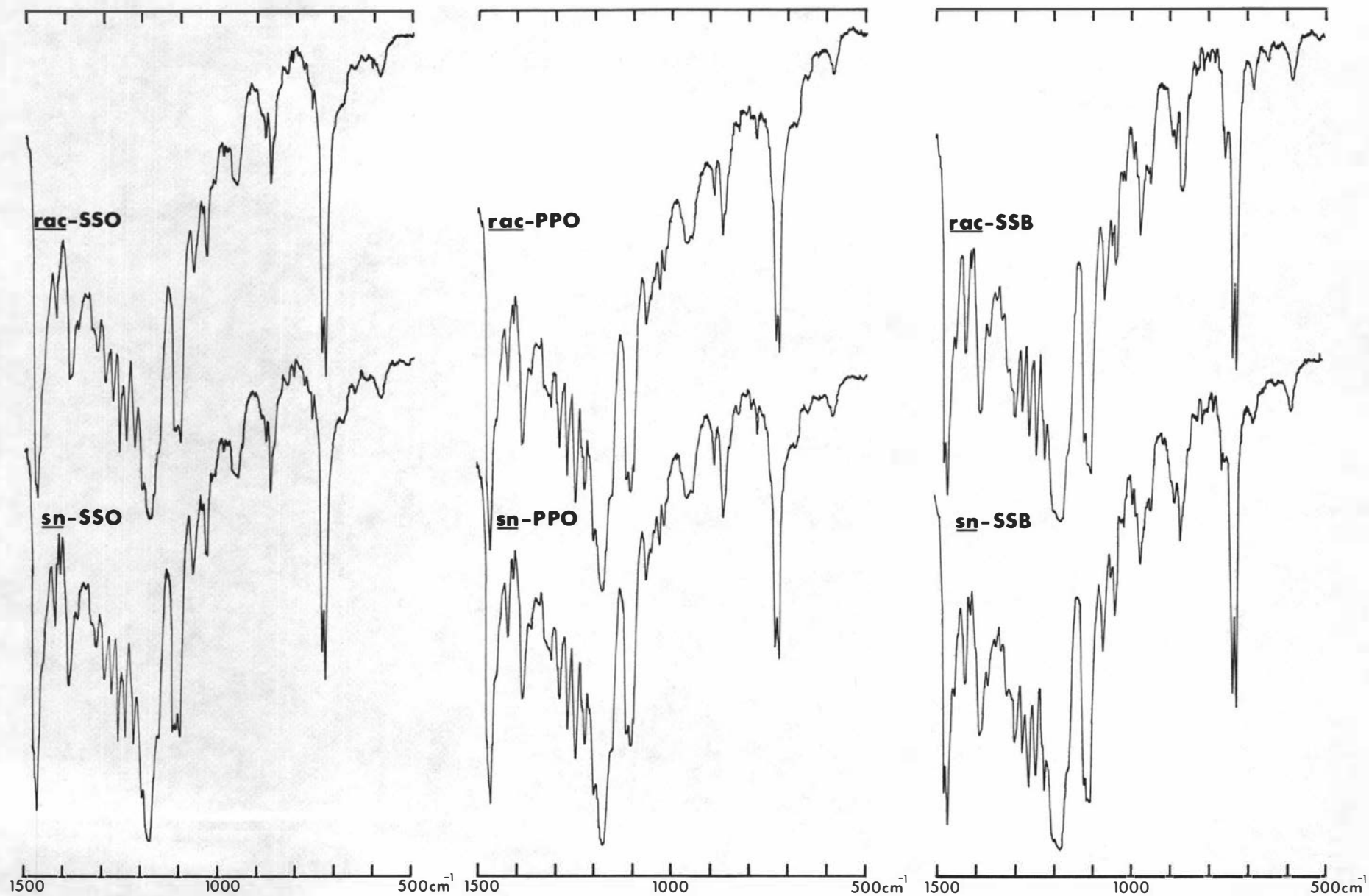


**Fig.3-25 IR Spectra of the  $\beta'$  stable forms of racemic and enantiomeric triacylglycerols**

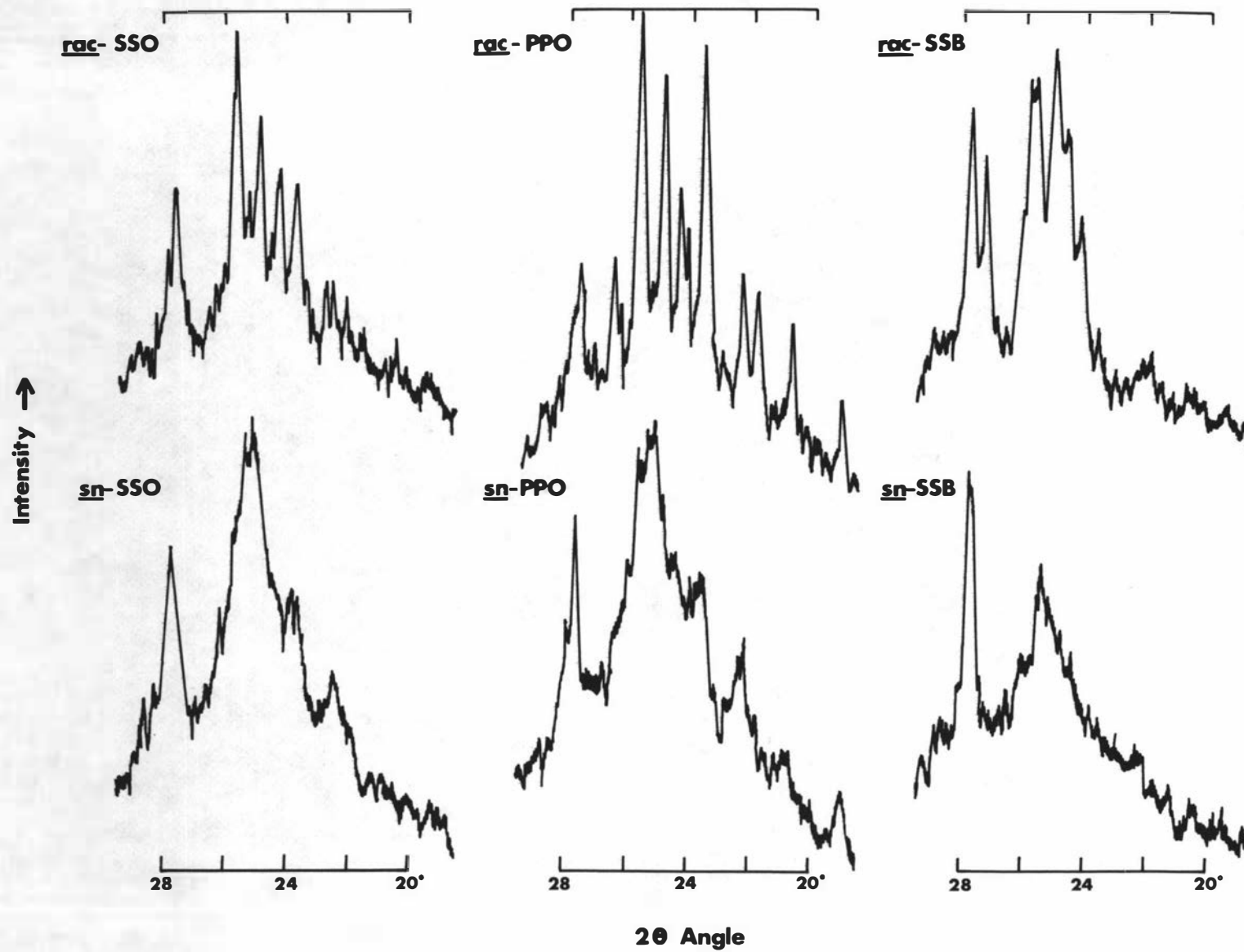


Fig.3-26 X-ray diffraction patterns of the stable forms of corresponding rac- and sn-TGs

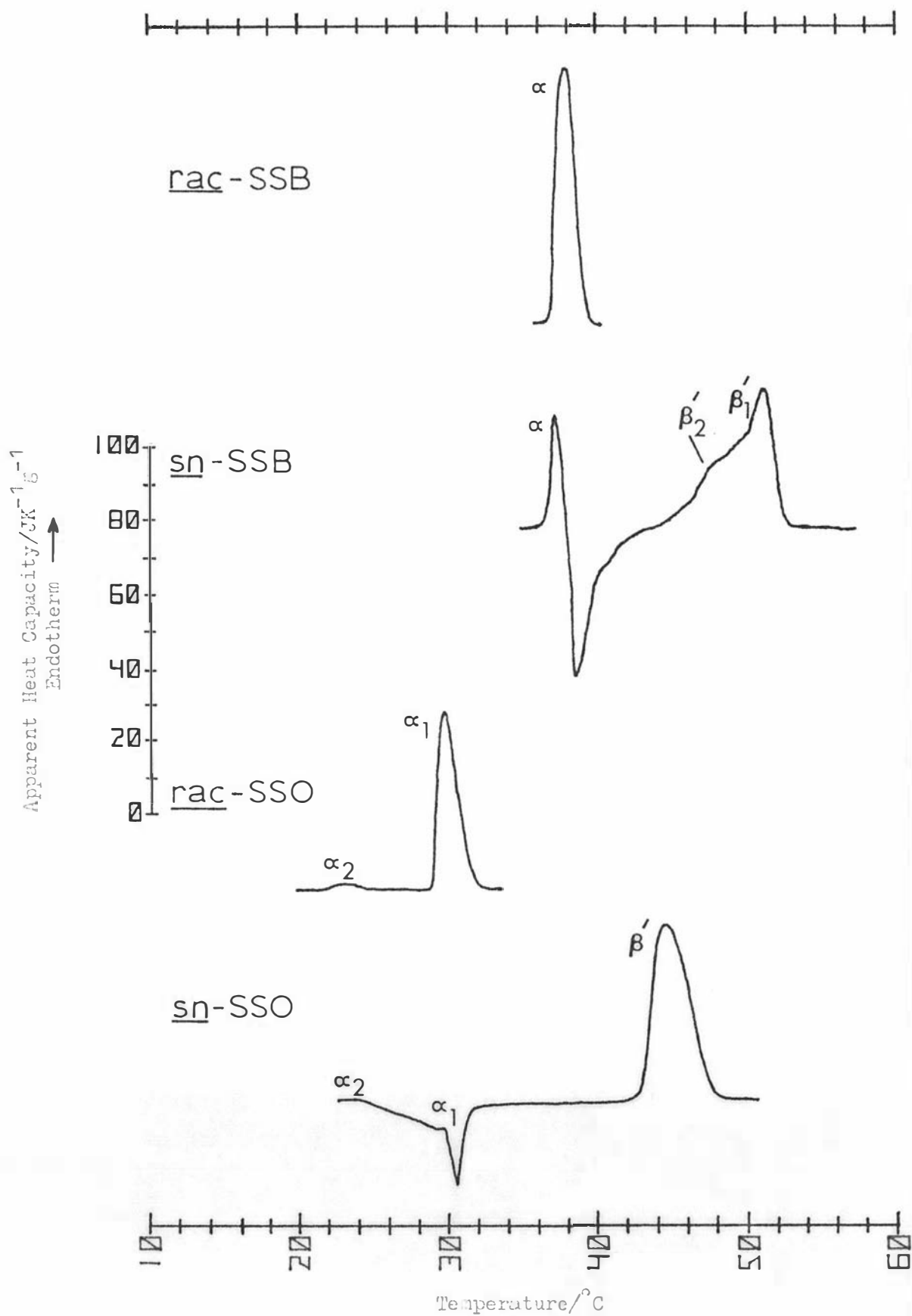


Fig. 3-27: Melting thermograms of the  $\alpha$  forms of rac- and sn-SSB (heating rate 4°C/min) and SSO (8°C/min) showing the more rapid transformation of the antipodes.

## Chapter 4

DISCUSSION4.1 Polymorphism of Racemic Triacylglycerols4.1.1 Palmitoyl-Stearoyl and Elaidoyl-Stearoyl Triacylglycerols

In general, the results obtained for the thermal behaviour of these TGs were consistent with the published data (Table 3.4). The DSC melting points showed good agreement with those reported by Lutton and others (Lutton *et al.*, 1948; Minor and Lutton, 1953; Chapman, 1957; Lutton and Hugenberg, 1960; Hugenberg and Lutton, 1963; Perron *et al.*, 1969). Similarly, the heats of fusion for  $\beta$  SSS and PPP agreed well with the DSC data of Hagemann *et al.* (1972) and Hampson and Rothbart (1969), while the heats of fusion of  $\beta$  PPS and PPP were within 3% of the corresponding values determined by Knoester *et al.* (1972) using differential thermal analysis. However, the heats of fusion of the stable forms of SSS, PSS, SPS and PSP reported by Knoester *et al.* were significantly lower than the present values (by 6 to 13%).

The presence of  $\beta'_2$  forms was confirmed for SSS and PPP (Hagemann *et al.*, 1972) and for PPS and PSS (Perron *et al.*, 1969), but contrary to the results of the latter workers no  $\beta'_2$  form was detected for PSP. Both the elaidoyl TGs, SES and ESS, showed a  $\beta'_2$  form (reported here for the first time), which further demonstrated their similarity to the saturated TGs.

The unusual stability of the  $\beta'$  forms of SPS and PSP is difficult to understand in terms of the geometric concepts of molecular packing outlined in Section 1.1.5. According to Larsson (1964b), the  $\beta'$  forms of PSP and simple TGs like PPP or SSS are essentially isostructural, differing only in the end group region. But drawings of the end group region of  $\beta'$  PSP, based on the projection given by Larsson (1966b) for the  $\beta'$  form of simple TGs, show no features which can account for the very large difference in the heat of fusion of the respective forms (e.g.  $\Delta H_f$  of  $\beta'$  SPS = 207 kJ/mol;  $\Delta H_f$  of  $\beta'$  SSS = 144 kJ/mol; see Table 3.4). Similarly, although Larsson (1972) claims that the terraces in the end group region of the  $\beta$  forms of PSP and SPS are sufficiently steep to form the limits to isomorphism (Section 1.1.5), these polymorphs have comparable heats of fusion to the  $\beta$  forms of SSS, PSS etc. (e.g.  $\Delta H_f$  of  $\beta$  SPS = 193 kJ/mol;  $\Delta H_f$  of  $\beta$  SSS = 194 kJ/mol; Table 3.4) which possess a flatter and supposedly more favourable terrace structure (Fig. 1-7).

In summary, although the palmitoyl-stearoyl TGs display considerable individuality, there are similarities in their polymorphism which parallel the structural classifications (Hugenberg and Lutton, 1963). Three molecular types may be distinguished, each with characteristic thermal behaviour, namely monoacid, unsymmetrical diacid and symmetrical diacid (Lutton, 1967). For the first group (SSS, PPP), both  $\alpha$  and  $\beta'$  transform on heating to  $\beta$ , but for the second group (PSS, PPS)  $\alpha$  transforms to  $\beta'$ , which melts without transformation to  $\beta$ . The  $\alpha$  forms of the symmetrical diacid TGs, PSP and SPS, transform to  $\beta'$  and  $\beta$  respectively, but both TGs have stable  $\beta'$  forms (although  $\beta'$  SPS cannot be obtained from the melt) whereas all the other TGs are  $\beta$  stable. The two elaidoyl TGs, SES and ESS, may be accommodated in this scheme with only a minor modification. Thus, SES behaves as a monoacid TG rather than a symmetrical diacid TG, while ESS behaves, as expected, like an unsymmetrical diacid TG.

#### 4.1.2 1-Butyryl-2-Oleoyl and 1,2-Dioleoyl Triacylglycerols

##### (a) 1,2-Dioleoyl Triacylglycerols

As shown in Table 3.5, the phase assignments and melting points for OOS and OOP agreed well with the data of Lutton (1966) who characterised the polymorphism of these TGs by capillary melting point and X-ray diffraction. Quinn (1967) also reported melting points for the stable forms in close agreement with the present data.

Both glycerides showed reversible  $\alpha_2$  transitions, but in contrast to the  $\alpha_2$  transitions of other TGs reported here, they occurred at much lower temperatures than the main  $\alpha_1$  melting endotherms. The heats of transition of  $\alpha_2$  OOS and OOP were also somewhat larger than normal ( $\sim 15\%$  of the heat of crystallisation of the  $\alpha_1$  form). Thermal transitions of the  $\alpha_2$  type, which did not occur for any of the saturated TGs except BBP and SBS, have not previously been reported for unsaturated TGs. However, similar transitions have been reported for long chain esters (Lundquist, 1970, 1971), 1-MGs (Lutton, 1971b) and TGs containing two short and one long chain (Menz, 1975). In such cases, the transitions are thought to involve a stepwise change in the hindered rotation of the chains (Menz, 1975) and presumably the same structural change is responsible for the  $\alpha_2$  transition of OOS and OOP. Unfortunately, this could not be checked by IR spectroscopy as the transitions occurred below the lower temperature limit of the variable temperature cell.

As discussed in Section 1.1.4, the  $\beta'$  stable form of OOS and OOP probably has a TCL structure with a middle layer of saturated chains and

two outer layers of oleoyl chains. Because the TGs are unsymmetrical, chain sorting can only occur if the glycerol group has the chair conformation rather than the more usual tuning-fork arrangement (Section 1.1.4). OOS and OOP follow what appears to be the general rule that stable forms of TGs for which a TCL chair structure would be expected are  $\beta'$  while stable forms of TGs for which a TCL tuning-fork structure would be expected are  $\beta$ . In other words, for TGs in which one fatty acid is very different from the other two, the position of the unusual acid determines the chain packing of the TCL stable form. If the acid is in a primary glycerol position, the TG is  $\beta'$ -stable, while if it is in the secondary position the TG is  $\beta$ -stable.

(b) 1-Butyryl-2-Oleoyl Triacylglycerols

The thermal behaviour of these glycerides has not been reported previously.

In common with other TGs containing short chain residues, BOS and BOP show relatively stable  $\alpha$  forms which have unusually high melting points (Table 3.5). The glycerides also exhibit a reversible  $\alpha_2$  transition comparable to that occurring in BBP, BES and SBS, but generalisations concerning the rôle of the short chain acid are confounded by the absence of such transitions in the TGs BSS, BSP, BPS and BPP.

From close packing considerations, the stable forms of BOS and BOP would be expected to have a TCL chair structure in which the butyryl chains form the middle layer and the oleoyl and stearyl (or palmitoyl) chains pack together in the two outer layers. This should be a more efficiently packed structure than the alternative TCL tuning-fork arrangement in which the oleoyl chains form the middle layer and the long and short saturated chains pack together in the outer layers, an unfavourable situation as discussed in Section 1.1.5. If the proposed structure of  $\beta'$  BOS and BOP is correct, then the spectral similarity between the TCL forms of  $\beta'$  BOS and  $\beta'$  OOS is analogous to the spectral similarity between the DCL forms of  $\beta'_2$  OSP (q.v.) and  $\beta'$  PSP. Such correspondence implies that oleoyl and stearyl chains may pack together in a manner which is analogous to the packing in which either chain is present alone.

Although glycerides of the structural type BSO and BOO are major components of milkfat, they were not studied in the present work because of the difficulty of synthesis (Section 1.4.1). From considerations of close packing, however, both glycerides should show a stable  $\beta'$ -3 form analogous to the structure proposed for  $\beta'$  BOS. An investigation of the polymorphism of these TGs would therefore provide an indirect check on

the suggested structure for  $\beta'$  BOS.

#### 4.1.3 1,2-Dibutyryl-3-palmitoylglycerol

In general, the thermal behaviour of BBP was similar to that of BOS and BOP except that BBP showed three transitions associated with the  $\alpha$  phase rather than two, and that the stable form of BBP was not readily accessible.

The obvious parallel between the spectral and thermal transitions of the  $\alpha$  phase of BBP suggests that the transition between  $\alpha$  and sub- $\alpha$  was not strictly second order but involved a significant heat of transition and occurred, at least in part, in a stepwise manner (i.e. via  $\alpha_2$  and  $\alpha_3$ ). A similar two stage limitation of chain rotation occurs on cooling the  $\alpha$  phase of 1,3- and 1,2-diacylglycerols which contain acetic acid and a long chain fatty acid (Martin and Lutton, 1972). The behaviour of BBP was in contrast to that of most other TGs, for which no reversible thermal transitions were observed in the temperature interval of the  $\alpha$  to sub- $\alpha$  transformations. The latter are therefore properly regarded as second order transformations.

The polymorphism of BBP has been studied by Jackson and Lutton (1952) and Feuge and Lovegren (1956). The former workers recorded only two polymorphs, sub- $\alpha$  and  $\alpha$ , with transition temperatures of  $-5$  and  $2.9^\circ\text{C}$  respectively. Feuge and Lovegren reported three forms, an  $\alpha$  form melting at  $2.8^\circ\text{C}$ , a stable form melting at  $10.5^\circ\text{C}$  and an unidentified polymorph associated with a transition at  $-34.5^\circ\text{C}$ . The stable form, which was not classified according to subcell type, was only obtained with difficulty. Of the present data, only the melting point of the  $\alpha_1$  form ( $1^\circ\text{C}$ ) shows reasonable agreement with these earlier reports.

However, more recently, Menz (1975) studied a series of short to medium chain saturated diacyl derivatives of 1-stearoyl- and 1-behenylglycerol and reported polymorphic behaviour which is very similar to that found in the present study of BBP. Thus in general, the most stable modification ( $\beta$ ) of these glycerides was only obtained with difficulty and there were two minor and reversible phase transitions, which Menz called sub- $\alpha_1$  and sub- $\alpha_2$ , adjacent to the  $\alpha$  form. The sub- $\alpha$  transitions were found to be particularly sensitive to the presence of impurities and the discrepancies between the transition temperatures earlier reported by Jackson and Lutton and those reported by Menz were attributed to the lower purity of the glyceride preparations of the former workers. Presumably the same factor is also responsible for the lack of agreement between earlier results for BBP and those reported here.

#### 4.1.4 2-Oleoyl Triacylglycerols

##### (a) Polymorphism of the Individual Triacylglycerols

The polymorphic behaviour of SOS, POS and POP is shown schematically in Fig. 3-15 together with a table indicating the equivalence between the polymorphic forms found in the present study and those reported by Lutton (Lutton, 1946, 1951; Lutton and Jackson, 1950; Wille and Lutton, 1966) and Lavery (1958).

##### (i) SOS

Melting points (Table 3.7), IR spectra (Appendix, Fig. 23), phase assignments and transformation relationships (Fig. 3-15) for the polymorphic forms of SOS generally agreed well with the literature (Lutton, 1946; Chapman, 1956; Lavery, 1958; Wille and Lutton, 1966). As expected, the  $\beta_1$ ,  $\beta'$  and  $\beta_2$  forms of SOS were spectrally equivalent to  $\beta_1$  of POS and POP,  $\beta'_1$  of POS and  $\beta_2$  of POP respectively. The heat of fusion of the solvent crystallised form, 168 kJ/mol, was in fair agreement with the figure of 175 kJ/mol determined by Hannewijk et al. (1964) from solubility data.

The  $\beta'$  form of SOS was obtained by transformation of  $\beta_2$ . However, Lutton (Lutton and Jackson, 1950; Wille and Lutton, 1966) prepared this form by rapid crystallisation from solvent and classified it as intermediate between  $\alpha$  and  $\beta_2$  (sub- $\beta$ -3), rather than intermediate between  $\beta_2$  and  $\beta_1$  as found here (Fig. 3-15). Although the unstable sub- $\alpha$  form reported by Wille and Lutton was not detected by IR spectroscopy, the existence of such a form may explain the unusual crystallisation behaviour observed in the DSC. In addition to the  $\alpha$ ,  $\beta_2$ ,  $\beta'$  and  $\beta_1$  forms of SOS, a previously unreported transition was observed at  $\sim 28^\circ\text{C}$ , intermediate between  $\alpha$  and  $\beta_2$ , although no assignment could be made.

##### (ii) POS

The melting points (Table 3.7), assignments and transformation relationships (Fig. 3-15) of the three main forms of POS,  $\alpha$ ,  $\beta'_1$  and  $\beta$ , were in good agreement with the literature (Lutton, 1951; Lavery, 1958; Wille and Lutton, 1966). The  $\beta'_1$  form (m.p.  $31.1^\circ\text{C}$ ) clearly corresponded with the  $\beta'$ -3 form reported by Lutton (1951; m.p.  $33^\circ\text{C}$ ) and Lavery (1958; m.p.  $30.8^\circ\text{C}$ ) rather than the additional  $\beta'$  form,  $\beta'$ -2, reported by Wille and Lutton (1966; m.p.  $25.5^\circ\text{C}$ ). The spectrum of  $\beta'_1$  POS showed the expected correspondence with that of  $\beta'$  SOS. In support of the findings of Lavery, no form corresponding to  $\beta'$ -2 was detected in the IR study.

Two minor transitions intermediate between  $\alpha$  and  $\beta'_1$  were observed at  $20.7^\circ\text{C}$  ( $\beta'_3$ ) and  $22.6^\circ\text{C}$  ( $\beta'_2$ ), but could not be detected by IR spectroscopy. The transitions appeared analogous to the  $\beta'_3$  and  $\beta'_2$  forms observed by Hagemann et al. (1975) for monoacid TGs of cis-octadecenoic acids, although the  $\beta'_2$  form had a similar melting point to Wille and Lutton's  $\beta'$ -2 form (m.p.  $25.5^\circ\text{C}$ ) and to the  $24.5^\circ\text{C}$  transition reported by Landmann, Feuge and Lovegren (1960). The formation of an unstable sub- $\alpha$  form from the rapidly crystallised POS melt (Wille and Lutton, 1966) may explain the discrepancy observed between the heats of crystallisation and fusion of the  $\alpha$  form.

(iii) POP

Polymorphic assignments, melting points and transformation relationships reported here (Table 3.7 and Fig. 3-15) showed general agreement with the literature (Lutton and Jackson, 1950; Lavery, 1958; Lovegren, Gray and Feuge, 1971, 1976). The different assignments previously reported for the form melting near  $27^\circ\text{C}$ , i.e. sub- $\beta'$ -2 (m.p.  $26.5^\circ\text{C}$ ; Lutton and Jackson) and sub- $\beta$ -3 ( $= \beta''_M$  m.p.  $26.7^\circ\text{C}$ ; Lavery; Lovegren et al.), were here reconciled by the observation of two forms melting near  $27^\circ\text{C}$ , one of which was  $\beta_2$  (sub- $\beta$ -3), m.p.  $27.1^\circ\text{C}$ , and the other presumably  $\beta'_2$  (sub- $\beta'$ -2), m.p.  $25.1^\circ\text{C}$ . In addition to the main forms  $\alpha$ ,  $\beta'_2$ ,  $\beta_2$ ,  $\beta'_1$  and  $\beta_1$ , a minor transition was detected at  $22.6^\circ\text{C}$ . This possibly corresponds with the  $20.8^\circ\text{C}$  polymorph,  $\beta'_M$  or  $\beta''_L$ , reported by Lovegren et al. (1971). In contrast to POS and SOS, POP showed normal crystallisation behaviour, no evidence being found for the unstable sub- $\alpha$  form reported by Wille and Lutton (1966).

Of the three TGs only POP has been investigated previously by differential scanning calorimetry. Lovegren et al. (1971, 1976) determined thermal data for  $\alpha$ ,  $\beta''_L$ ,  $\beta''_M$  ( $= \beta_2$ ),  $\beta'$ -2 ( $= \beta'_1$ ) and  $\beta$  ( $= \beta_1$ ) forms by capillary melting point, dilatometry and calorimetry. The melting points of all forms and the heats of fusion of the  $\alpha$ ,  $\beta_2$  and  $\beta'_1$  forms showed fair agreement with the present data (Table 3.7), but the heat of fusion reported by Lovegren for the solvent crystallised  $\beta_1$  form was significantly lower (133 kJ/mol versus 151 kJ/mol). However, the present value was comparable with that determined by Hannewijk et al. (1964) from solubility data (157 kJ/mol) and by Moran (1963) from differential thermal analysis (148 kJ/mol), although neither of the methods could be regarded as reliable as differential scanning calorimetry.

The thermograms obtained for POP by Lovegren et al. (1976) differed in several respects from those shown in Figs. 3-13, 3-14 and

Fig. 26 in the Appendix. For example, Lovegren's melting thermograms for the 'quickly chilled' melt showed no  $\alpha$  endotherm at heating rates of 2.5 and 5°C/min, but the  $\alpha$  endotherm was readily apparent in the present study, even at 2°C/min (Fig. 26). Such differences are probably due to the fact that Lovegren used dry ice as coolant for the DSC, necessitating a very low gas flow rate to maintain adequate heat transfer. In this work, liquid nitrogen was used as coolant following the recommendation of Ladbroke and Chapman (1969), who found liquid nitrogen necessary to maintain adequate temperature control between ambient and 100°C.

(b) Crystallisation Behaviour

SOS and POS showed anomalous crystallisation behaviour which is possibly related to the existence of the unstable sub- $\alpha$  forms reported for these TGs by Wille and Lutton (1966). On cooling the melt of SOS at 16°C/min, two exotherms were observed at 17.1°C and -2.6°C (Fig. 22 in the Appendix). A possible explanation of this behaviour is that the initial, main exotherm at 17.1°C corresponded to the crystallisation of the fleetingly stable sub- $\alpha$  form but on further cooling this phase transformed irreversibly to the normal  $\alpha$  form resulting in the second smaller exotherm at -2.6°C.

In the case of POS (and SOS) cooled at 4°C/min, the second exotherm was absent but the main exotherm was too small to account for the total crystallisation of the  $\alpha$  form. It therefore seems likely that this exotherm again represents the crystallisation of the unstable sub- $\alpha$  form, but that the transition to the  $\alpha$  form occurs as a long 'tail' on the exotherm, which accounts for the poorly defined post-peak baseline. This contribution to the heat change is easily overlooked so that the heat of crystallisation measured is not that of the  $\alpha$ -form. No sub- $\alpha$  form for SOS, POS or POP was detected during the variable temperature IR study. However, this result would be expected even if such forms do exist because of the slow thermal response of the IR cell and the relatively short lifetime of these forms near their crystallisation temperature.

POP did not show anomalous crystallisation behaviour although Wille and Lutton reported a sub- $\alpha$  form for this TG also. Possibly the transformation of this form is so rapid that it occurs simultaneously with its crystallisation at the relatively slow cooling rates of the DSC (Wille and Lutton used very rapid cooling rates obtained by quenching liquid contained in thin-wall capillary tubes).

The only other TGs to show similar crystallisation behaviour to

SOS and POS were the 1-oleoyl TGs OSS, OSP, OPS and OPP. By implication, therefore, the 'sub- $\alpha \rightarrow \alpha$ ' transformation probably involves an irreversible reorientation of the oleoyl chain.

(c) Structural Basis for the Differences in the Polymorphism of 2-Oleoyl Triacylglycerols

The complex polymorphism of SOS, POS and POP is a consequence of two factors, i.e. the presence of both saturated and unsaturated chains and the symmetrical position of the unsaturated chains. The first allows both TCL and DCL forms to exist, while the second determines the tuning-fork glycerol structure of the TCL forms. Such a structure permits both  $\beta'$  and  $\beta$  TCL forms in contrast to the chair glycerol structure of the TCL forms of unsymmetrical TGs, which do not generally show  $\beta$  forms.

Differences between the polymorphism of SOS, POS and POP may be partly ascribed to the different end group structures of equivalent forms. For isostructural TCL forms in which chain sorting occurs, the homologous TGs SOS and POP should have an identical end group arrangement, whereas POS, with two different chains in the saturated chain layers, will have a different appearance in the end group region. The absence of a  $\beta_2$ - $\beta_3$  form for POS may therefore be the result of an unfavourable end group structure (SOS and POP both show a  $\beta_2$ - $\beta_3$  form).

For DCL structures, in which the oleoyl and saturated chains must pack alongside each other, the homologous TGs SOS and POP no longer have an identical appearance in the end group region because the chain length difference between oleoyl and stearoyl is not the same as the chain length difference between oleoyl and palmitoyl. Only POP shows  $\beta'$  DCL forms, presumably because the end group structures of equivalent  $\beta'$  DCL forms for SOS and POS are unfavourable.

4.1.5 2-Butyryl-1,3-distearoylglycerol

The polymorphism of SBS was first investigated by Jackson et al. (1951) who reported  $\alpha$ , super- $\alpha$  and stable  $\beta$ - $\beta_3$  forms melting at 33.4, 42.7 and 54.8°C respectively. The unusual 'super- $\alpha$ ' form was so called because it showed the single spacing at 4.14Å characteristic of the  $\alpha$  form although its melting point was much higher than that of the normal  $\alpha$  form obtained by rapid crystallisation of the melt. The results of the present study are in general agreement with the data of Jackson et al. (Table 3.7), although unfortunately no IR assignment could be made for the phase melting near 40°C because of its rapid conversion to the stable form. In addition to the three main forms, sub- $\alpha$  and  $\alpha_2$  forms were also

found in the present study. Jackson et al. obtained the sub- $\alpha$  form but did not report the  $\alpha_2$  transition at  $\sim 29^\circ\text{C}$ .

Although SBS is not representative of any major TG type occurring in milkfat, it was selected for study in order to determine the effect of isomerism on the polymorphic behaviour of butyryl TGs. This effect is most marked with respect to the stable forms of SBS and BSS which show a surprising analogy to the stable forms of the corresponding oleoyl TGs, SOS and OSS. The symmetrical isomers, SBS and SOS, are  $\beta$ -stable while the unsymmetrical isomers, BSS and OSS, are  $\beta'$ -stable. X-ray short spacings and IR spectra show that the  $\beta$  and  $\beta'$  stearoyl chain packings in the stable forms of the butyryl TGs are equivalent to those of their oleoyl counterparts. The correspondence between these stable forms is consistent with the structures expected from close packing considerations, that is TCL structures in which the butyryl or oleoyl chains are sandwiched between two identical stearoyl chain layers. Comparison of the four polymorphs suggests that the stearoyl chain packing is independent of the nature of the intermediate chain layer and is primarily determined by the symmetry of the molecule which, in turn, determines the conformation that the glycerol group must adopt to allow chain sorting.

Although the melting point of  $\beta$  SBS ( $54.2^\circ\text{C}$ ) was higher than that of  $\beta$  SOS ( $41.9^\circ\text{C}$ ), the molar heat of fusion was lower ( $144\text{ kJ/mol}$  for SBS versus  $168\text{ kJ/mol}$  for SOS), indicating that the contribution to the packing made by the oleoyl chain is greater than that made by the butyryl chain. The thermal properties of  $\beta'$  BSS and OSS followed the same pattern.

#### 4.1.6 1-Butyryl Triacylglycerols

Although the triacid members of the series BSS, BSP, BPS and BPP were synthesised by Verkade (1943), only the melting points of the solvent crystallised forms were reported. These values showed good agreement with data for the present TGs (Table 3.9). No other thermal data has been reported for any of the four glycerides.

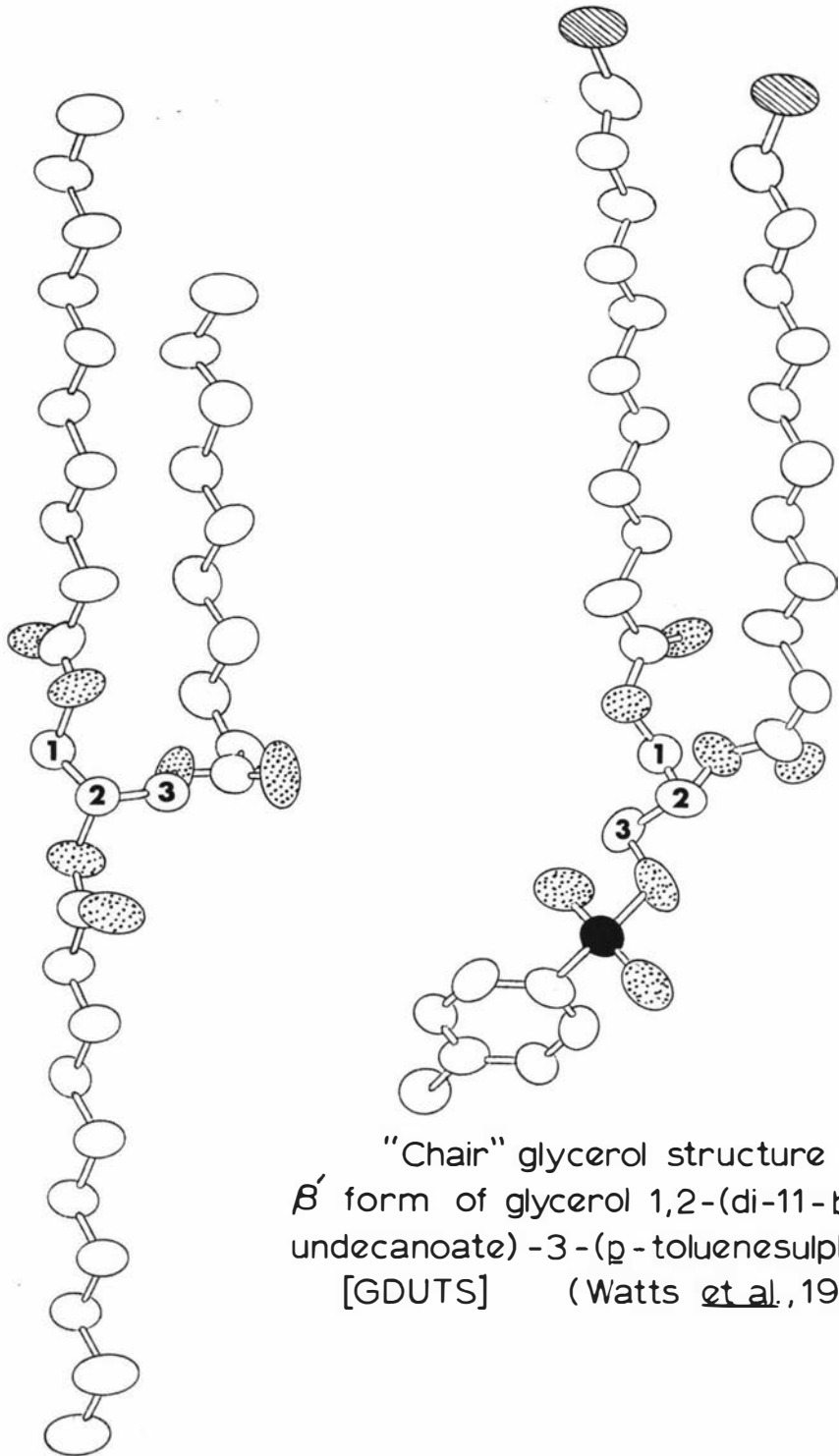
As discussed in the previous section on SBS, the correspondence between the stable forms of analogous butyryl and oleoyl TGs is probably the result of common TCL structures in which the packing of the outer chain layers is identical. The unsymmetrical 1-butyryl and 1-oleoyl TGs can only form a TCL structure in which chain sorting occurs if the glycerol group has the chair conformation. It appears to be a general rule that such structures have  $\beta'$  packing for the outer chain layers.

(Section 4.1.2). In contrast, for the TCL forms of the symmetrical 2-butyryl and 2-oleoyl TGs, chain sorting can occur with the glycerol group in the conventional tuning-fork conformation. This arrangement permits both  $\beta'$  and  $\beta$  chain packings, as in SOS and POS, although stable forms invariably show the  $\beta$  packing. The TCL stable forms of symmetrical TGs have a higher heat of fusion than the stable forms of their unsymmetrical counterparts (e.g.  $\Delta H_f$  for  $\beta$  SBS is 144 kJ/mol versus 132 kJ/mol for  $\beta'$  BSS), suggesting that the overall packing of the former structures is more efficient.

Only one structure determination has been published of a lipid in which the glycerol group adopts a chair conformation, i.e. the solvent crystallised form of rac-glycerol 1,2-(di-11-bromoundecanoate)-3-(p-toluenesulphonate) (Watts, Pangborn and Hybl, 1972). This unsymmetrical compound is structurally related to TGs like BSS in that one of the groups in the primary position (i.e. the toluenesulphonate or tosyl group) has different spatial requirements from the remaining two acyl groups. Furthermore, if we regard the tosyl moiety as a type of chain, then the crystal structure of this compound shows a chain sorting arrangement in which the tosyl 'chains' are sandwiched between two equivalent chain layers. The acyl chain packing is  $\beta'$  ( $O\perp$ ), supporting both the analogy with  $\beta'$  BSS (and OSS) and the contention that the stable forms of chair structures are generally  $\beta'$ . In Fig. 4-1 the chair structure of the model compound is compared with the conventional tuning-fork arrangement found in the  $\beta$  stable form of tricaprln (Jensen and Mabis, 1966).

The stable forms of BSP and its oleoyl counterpart, OSP, showed anomalous spectroscopic, diffraction and thermal data compared with the other 1-butyryl and 1-oleoyl TGs. For example, both the heats of fusion and melting points of the two sets of normal stable forms, BSS, BPS, BPP and OSS, OPS, OPP, showed a regular increase with increasing molecular weight, yet the stable form of BSP had a higher melting point but lower heat of fusion than that of BPS (Table 3.9). The reverse was true for OSP and OPS (Table 3.11). Furthermore, the differences in heats of fusion between the stable forms of corresponding 1-oleoyl and 1-butyryl glycerides were fairly uniform for XSS, XPS and XPP ( $X = O$  or  $B$ ), i.e. 11, 10 and 9 kJ/mol, but the difference for XSP (21 kJ/mol) was approximately twice these values. Melting point differences followed a similar pattern (i.e.  $\Delta T$  for XSS, XPS, XPP and XSP = 7.9, 8.3, 7.6 and 12.1°C respectively).

IR spectra of the stable forms of BSP and OSP showed an analogous temperature dependence to spectra of (sub) $\alpha$  forms. As the temperature was



"Chair" glycerol structure  
 $\beta'$  form of glycerol 1,2-(di-11-bromo-undecanoate)-3-(p-toluenesulphonate)  
 [GDUTS] (Watts *et al.*, 1972)

"Tuning fork" glycerol structure  
 $\beta$  form of tricaprln  
 (Jensen and Mabis, 1966)

Fig.4-1 Comparison of glycerol conformations in "tuning fork" (tricaprln) and "chair" (GDUTS) structures. GDUTS is a possible model for the  $\beta'$ -3 form of the triacylglycerols OXY and BXY (X,Y = P or S)

Key: ○ carbon ○ oxygen ● bromine ● sulphur

glycerol carbon atoms are numbered 1,3(primary) and 2(secondary) hydrogen atoms are not shown

lowered from 20 to  $-30^{\circ}\text{C}$ , the  $720\text{cm}^{-1}$  band gradually changed from a diffuse singlet to a symmetrical doublet. Since the change from doublet to singlet is correlated with an increase in chain motion for (sub) $\alpha$  (Chapman, 1962), it seems probable that the outer chain layers of  $\beta'_1$  BSP and OSP have greater motional freedom (e.g. libration) than the corresponding chains of  $\beta'_1$  BSS etc., for which the  $720\text{cm}^{-1}$  band is a well resolved doublet even at room temperatures. However other differences between the spectra of  $\beta'_1$  BSP, OSP and  $\beta'_1$  BSS, OSS etc. would seem to indicate that there are further structural distinctions between the forms.

If in fact the stable forms of BSS (BPP), BPS and BSP (or their oleoyl counterparts) were isostructural, the only difference between the forms would be in the methyl endgroup contacts. However  $\beta'$  BSP is not isostructural with the other forms and presumably this can be related directly or indirectly to the different end group contacts in the two sets of TGs. Thus, either the end group contact for a BSP form isostructural with  $\beta'_1$  BSS etc. is unfavourable, leading to a change in the structure and greater freedom of the chain packing, or BSP is the only TG in the group which can adopt a particularly favourable end group structure, albeit at the expense of a distortion in the chain packing. In either case, the increase in chain motion of  $\beta'$  BSP indicated by IR spectroscopy is the result of some perturbation of the  $0\perp$  subcell (causing it to approach the hexagonal form) introduced by its peculiar end group contacts.

In spite of the correspondence between their stable forms, 1-butyryl and 1-oleoyl TGs showed different polymorphic behaviour. For example, the latter glycerides displayed irreversible  $\alpha_2$  transitions, seemingly related to their unusual crystallisation. In contrast, the 1-butyryl TGs, like the saturated glycerides of high molecular weight, crystallised normally (i.e. the  $\alpha$  freezing transition was completed within the relatively narrow temperature range of the exotherm) and showed no  $\alpha_2$  transitions on melting. Furthermore, BSS, BPS and BPP all have one more intermediate form than the equivalent oleoyl TGs, although BSP and OSP each have two such forms. Unfortunately, the intermediate forms of BSS, BSP, BPS and BPP could not be characterised adequately and, therefore, further comparison with their 1-oleoyl counterparts was not possible.

Molar heats of fusion of the stable forms were somewhat higher for the 1-oleoyl TGs than for the 1-butyryl TGs but the reverse was true for the  $\alpha$  forms (with the exception of  $\alpha$  BSS which had a lower molar heat of fusion than  $\alpha$  OSS). Melting point data did not follow the same trend as the molar heats of fusion and in spite of the much lower molecular

weight of the butyryl glycerides, their  $\alpha$  and  $\beta'$  melting points were uniformly higher than those of their unsaturated counterparts (Tables 3.9 and 3.11). Similar relationships were observed for the thermal data of SBS and SOS. Thus in general, for corresponding stable forms, the packing contribution made by the butyryl chain is less than that made by the oleoyl group, i.e. the van der Waals interaction between adjacent butyryl chains is less than that between adjacent oleoyl chains. However, in the case of the  $\alpha$  forms, the butyryl glycerides generally show slightly more efficient packing than the equivalent oleoyl glycerides. This may reflect additional strain imposed by torsional oscillation of chains containing the bent cis-double bond compared with torsional oscillation of straight chains.

1-Butyryl and 1-oleoyl TGs of the type BXX and OXX, where X = L, P or S constitute most of the large fraction of milkfat which melts between 0 and 20°C (Taylor, 1973; Section 1.3.4). It is possible that the structural similarity between the stable forms of the two TG classes could allow some degree of solid miscibility, and that this is responsible for the relatively narrow melting range of this fraction, a characteristic which has important implications for the physical properties of milkfat (Taylor and Norris, 1977).

#### 4.1.7 1-Butyryl-2-elaidoyl-3-stearoylglycerol

In view of the close structure similarity between trans-acids and their saturated counterparts, it was anticipated that BES and BSS would show similar polymorphism (cf. SES and SSS). However, the behaviour of BES had surprisingly few features in common with that of BSS. Thus, the  $\beta'$  stable form of BES was spectrally similar to the unusual  $\beta'$  form of BSP rather than to  $\beta'$  BSS. Furthermore, like BOS, BES had no intermediate forms and showed a reversible  $\alpha_2$  transition, while BSS had one intermediate form and showed no  $\alpha_2$  transition. The polymorphism of BES has not previously been reported.

From close packing considerations, the stable form of BES should be a TCL structure with the elaidoyl and stearoyl chains packed together in the two outer layers (cf. BSS). The ratio of elaidoyl to stearoyl chains in such layers (1:1) is higher than that in the layers of the DCL stable forms of SES and ESS (1:2). It is possible that the relatively high proportion of trans-double bonds in the outer layers of the TCL  $\beta'$  form of BES can only be accommodated in the O<sub>1</sub> subcell if the packing is distorted. Such distortion could account for the appearance of the

diffuse band at  $720\text{cm}^{-1}$  in the spectrum of  $\beta'$  BES (Fig. 3-16). The possibility of a perturbation of the  $\beta'$  packing by trans-double bonds is given support by the observation that TGs containing two or three trans-acids generally show no  $\beta'$  forms (Minor and Lutton, 1953; Hagemann et al., 1972, 1975).

#### 4.1.8 1-Oleoyl Triacylglycerols

The polymorphic behaviour of OSS, OSP, OPS and OPP is shown schematically in Fig. 3-24 together with a table indicating the equivalence between the polymorphic forms found in this study and those reported by Lutton (1951) and Lavery (1958). In general, the present phase assignments and melting points showed good agreement with the earlier work although there were some differences in the respective transformation relationships.

##### (a) Solvent Crystallised Forms

X-Ray short spacing and melting point data for the stable  $\beta'$  forms of OSS, OSP, OPS and OPP (Tables 3.10 and 3.11) were in excellent agreement with the corresponding data of Lutton (1951) and Lavery (1958). Surprisingly, neither of these workers remarked on the clearly irregular diffraction pattern of  $\beta'$  OSP (Fig. 3-17). The IR spectra of  $\beta'$  OSS, OPS and OPP (Fig. 3-16) were essentially identical to those recorded by Chapman (Chapman, 1956, 1960; Chapman, Crossley and Davies, 1957), but unfortunately Chapman did not report the spectrum of  $\beta'$  OSP.

The heats of fusion of the solvent crystallised forms of OSS and OPP are about 25kJ/mol lower than the corresponding data for SOS and POP, compared with only a 13 kJ/mol difference between the heats of fusion of the stable forms of SBS and BSS (Tables 3.7, 3.9 and 3.11). The disparity between the figures for unsaturated and saturated TGs is at first surprising since corresponding oleoyl and butyryl TGs have stable forms of equivalent structure. One possibility is that the relatively large difference in lattice energy between the stable forms of 1- and 2-oleoyl TGs is related to the known difference in the packing of the oleoyl chains in the two forms (Section 1.1.4).

##### (b) Intermediate Forms

Previous workers reported only (sub) $\alpha$  and  $\beta'$  forms for the TGs OSS and OPP, no intermediate forms being observed. In the present work, however, clear thermal and spectroscopic evidence was obtained for the existence of an intermediate form for OPP ( $\beta'_2$  m.p.  $28.2^\circ\text{C}$ ), although no such form was detected for OSS. The existence of the form for only the

lower of the two homologues is seemingly analogous to the occurrence of a  $\beta'_1$ -2 form for POP but not for SOS (Section 4.1.4). If in fact  $\beta'_2$  OPP also has a DCL structure, then the absence of such a form for OSS may be the result of an unfavourable end group structure.

Like OPP, OPS showed only one intermediate form ( $\beta'_2$ , m.p.  $37.6^\circ\text{C}$ ), which was obtained by transformation of  $\alpha$  or crystallisation of the melt, and which transformed to  $\beta'_1$  on heating. Lutton and Lavery obtained an equivalent form (sub- $\beta'$ -3; m.p.  $37^\circ\text{C}$  (Lutton),  $39.8^\circ\text{C}$  (Lavery)), but this was considered to be the stable form from the melt. The discrepancy between the transformation status of  $\beta'_2$  and sub- $\beta'$ -3 is probably accounted for by the difficulty in resolving the melting of the  $\beta'_2$  and  $\beta'_1$  forms (Fig. 3-23). It is unlikely that the thermal methods of the earlier workers would have been capable of resolving the two melting transitions. The close spectral similarity of  $\beta'_2$  OPS to  $\beta'_1$  OSS, OPS and OPP suggests that the chain packing of these forms is essentially identical, at least with respect to the saturated chain layers.

Two forms intermediate in melting between the main  $\alpha$  form and the solvent crystallised form were found for OSP, one melting at  $29.3^\circ\text{C}$ , the other ( $\beta'_2$ ) at  $33.7^\circ\text{C}$ . As the question mark in Table 3.11 and Figs. 3-22, 3-23 and 3-24 implies, the lower melting form could not be characterised by IR spectroscopy, presumably because of its transient nature. (Attempts to prepare this form in the IR cell always resulted in the formation of the polymorph melting at  $34^\circ\text{C}$ ). Lavery (1958) was also unable to assign this form although its existence was clearly shown by differential thermal analysis (m.p.  $30.6^\circ\text{C}$ ). In contrast, Lutton (1951) did not report any form melting near  $30^\circ\text{C}$ , which is probably a further reflection of the form's instability.

The  $29.3^\circ\text{C}$  form of OSP was obtained during thermal analysis either by transformation of  $\alpha$  or by crystallisation of the melt at the  $\alpha$  melting point. On subsequent heating, the polymorph transformed to two further forms, one melting at  $33.7^\circ\text{C}$  and one at  $35.5^\circ\text{C}$ . Comparison with the results obtained by IR spectroscopy suggested that these two forms were  $\beta'_2$  and  $\beta'_1$  respectively. But in the IR cell  $\beta'_2$  could only be prepared by crystallisation of the melt at  $28^\circ\text{C}$ , while transformation of  $\alpha$  apparently gave  $\beta'_1$  directly (Fig. 3-24). By Occam's razor, the  $\beta'_2$  form is equivalent to the  $\beta'$ -2 form reported by Lutton (m.p.  $40.2^\circ\text{C}$ ) and Lavery (m.p.  $37.2^\circ\text{C}$ ) despite the considerable variation in melting point data (DSC m.p.  $33.7^\circ\text{C}$ , IR m.p.  $35\text{-}38^\circ\text{C}$ ). Support for the correlation between

$\beta'_2$  and  $\beta'_{-2}$  forms is provided by the close spectral similarity between  $\beta'_2$  OSP and  $\beta'_{-2}$  PSP (Fig. 3-12). However, both Lutton and Lavery regarded  $\beta'_{-2}$  as the stable form from the melt in contrast to the present thermal analysis of  $\beta'_2$ , which indicated that the form transformed to  $\beta'_1$  at its melting point. Perhaps, as in the case of OPS, this transformation could not be detected by the earlier workers because of the inferior temperature resolution of their methods.

(c) Alpha Forms

The four 1-oleoyl glycerides displayed unusual behaviour associated with the crystallisation and melting of the  $\alpha$  form. Thus, the area of the crystallisation exotherm was significantly lower than the area of the fusion endotherms of the  $\alpha$  forms so produced. Of the other TGs studied here, only SOS and POS showed similar behaviour. Furthermore,  $\alpha_2$  transitions were evident in the melting thermograms of  $\alpha$  forms of 1-oleoyl TGs, but unlike the  $\alpha_2$  transitions of other TGs (i.e. BOS, BOP, BBP, SBS and BES) they were irreversible.

The anomalous nature of the crystallisation and melting processes suggests that they are related to each other and to the structural features of this TG class. Both phenomena may be accounted for by assuming that when the 1-oleoyl TGs crystallise they do so in the unstable  $\alpha_2$  form which subsequently transforms slowly to  $\alpha_1$ . If the transformation of  $\alpha_2$  to  $\alpha_1$  is sufficiently slow, then it will not be completed within the temperature interval of the crystallisation exotherm, nor will it be detected as a second exothermic peak outside this interval. Provided that the  $\alpha_2$  form has not entirely transformed to  $\alpha_1$  prior to recording the melting thermogram, then the thermogram will show two  $\alpha$  endotherms, the lower one corresponding to the melting of the remaining  $\alpha_2$  form and the upper one to the melting of the normal  $\alpha_1$  form. Furthermore, the area of the crystallisation exotherm (representing the transition from the melt to  $\alpha_2$ ) will be smaller than the area of the  $\alpha$  endotherms (representing mainly the transition from  $\alpha_1$  to the melt) by an amount which accounts for the  $\alpha_2$  to  $\alpha_1$  transition energy (approximately 16kJ/mol for OSS and 13kJ/mol for OPP). A similar explanation accounts for the crystallisation behaviour of SOS and POS but here the transformation to the 'stable'  $\alpha_1$  form is presumably more rapid and no  $\alpha_2$  transition is evident in the melting thermogram.

## 4.2 Polymorphism of Enantiomeric Triacylglycerols

### 4.2.1 Comparison of the Polymorphism of Corresponding Enantiomeric and Racemic Triacylglycerols

#### (a) Solvent Crystallised Forms

The IR spectra of the solvent crystallised forms of sn-SSO, -PPO and -SSB were essentially identical with those of their racemates (Fig. 3-25), which suggests that the chain packings in the antipode and racemate are equivalent. The melting points and heats of fusion of the solvent crystallised forms of the corresponding enantiomeric and racemic TGs were also in close agreement (Table 3.13), showing little more variation than would be expected between two preparations of the same racemic TG. The present correlation of melting data is clearly in accord with results obtained for other enantiomeric and racemic TGs (e.g. Schlenk, 1965; Section 1.1.6). Furthermore, the melting points of sn-SSB and sn-PPO show good agreement with those reported by Lok *et al.* (1976) for sn-SSB and sn-OPP respectively (Table 3.13). Taken together, the spectral and thermal data support the conclusion that the stable forms of antipode and racemate are structurally analogous.

In contrast to the above results, significant differences were found in the corresponding X-ray diffraction patterns of the stable forms of rac- and sn-SSO, -PPO and -SSB. However, although the individual short spacings of the enantiomers were much broader than those of the racemates (Fig. 3-26), there appeared to be little change in their respective positions (Table 3.12). Such variation is probably related to differences in crystal morphology (e.g. differences in crystallite size, habit or perfection; Klug and Alexander, 1954), rather than to differences in subcell packing, because the latter would have resulted in a shift in the positions of the spacings. Consequently, both the X-ray short spacings and the IR spectra suggest that the chain packings of equivalent enantiomeric and racemic stable forms are the same. These findings contrast with those reported by Schlenk (1965) for rac- and sn-LPP, -PPS and -POS. Although Schlenk made no attempt to interpret his diffraction data according to Lutton's classification (Table 1.1), his results clearly imply that the racemic TGs are  $\beta$ -stable while the enantiomers are  $\beta'$ -stable. Obviously, independent confirmation of these results would be desirable and further work is required on chiral TGs belonging to other structural classes.

The correspondence between the solvent crystallised forms of rac- and sn-SSO, -PPO and -SSB is consistent with a structure in which glyceride

pairs of either opposite chirality (racemate) or the same chirality (antipode) can be equally well accommodated. As discussed earlier, the racemic 1-oleoyl and 1-butyryl TGs have a stable  $\beta'$  form with a TCL structure in which the oleoyl or butyryl chain layer is sandwiched between two identical layers of palmitoyl or stearoyl chain layers (cf. Fig. 1-6). From symmetry considerations and by analogy with the molecular packing of rac-glycerol 1,2-(di-11-bromoundecanoate)-3-(p-toluenesulphonate) (Pangborn, 1973), each half of the triple chain structure of the  $\beta'$  form of the racemic TG contains glycerol groups of the same chirality, but the chirality of the two 'halves' is opposite. Enantiomeric TGs should fit rather easily into this type of structure because the two 'halves' are relatively independent with respect to the glycerol groups. Thus, no major structural modification is necessary to accommodate antipodes in the same packing arrangement as the racemic TGs and it would therefore be expected that the two types of crystal would have similar physical properties.

(b) Unstable Forms

Thermal data for the other polymorphs showed the same equivalence between racemate and antipode as the data for the solvent crystallised forms (Table 3.13). Thus, with the possible exception of the  $\beta'_2$  form of rac-PPO, every polymorph of the racemic TGs had a corresponding antipode form of approximately the same melting point. Furthermore, although the  $\alpha$  forms of sn-SSO and -PPO transformed too rapidly for an accurate determination of their heat of fusion to be made, the heats of fusion of the  $\alpha$  forms of rac- and sn-SSB were in close agreement (77.3 and 77.7 kJ/mol respectively; Table 3.13). Since all the  $\alpha$  forms presumably have TCL structures, the correlation of melting data for the  $\alpha$  forms of racemate and antipode would be expected on the same basis as that of the solvent crystallised forms.

The one major difference between the polymorphic behaviour of racemic and enantiomeric TGs was that the  $\alpha$  forms of the enantiomers transformed more rapidly than the  $\alpha$  forms of their racemic counterparts. (As a consequence of the high scan rate required to follow the transformation of the  $\alpha$  form of sn-PPO (32°C/min), the  $\beta'_2$  and  $\beta'_1$  melting transitions that occur in rac-PPO would not be resolved for sn-PPO even if the  $\beta'_2$  form does exist.) In view of the similarity in thermal properties of the  $\alpha$  and  $\beta'$  forms of rac- and sn-SSO, -PPO and -SSB, the difference in the stability of the  $\alpha$  forms of racemate and antipode is particularly surprising. There seems no reasonable hope of accounting for

this unusual variation without a detailed knowledge of the crystal structures of the  $\alpha$  and  $\beta'$  forms and the conformational changes involved in the transition between these two forms.

(c) Summary

On the basis of the present work, there is little difference between the physical properties of racemic and enantiomeric TGs although it is not known how widely this generalisation holds. The differences observed in the relative stability of the  $\alpha$  forms are probably not relevant to the melting and solidification of fats, because disorder in the end group region appears to be the dominant factor controlling their polymorphic transformation (Section 1.3.2). In view of the probable structural similarity between the corresponding polymorphic forms of enantiomeric and racemic TGs, the phase behaviour of a racemic TG mixture should be little altered by substitution with one or more enantiomeric TGs. In other words, the results suggest that the optical isomerism of fats such as milkfat has only a small influence on their thermal behaviour.

4.3 Conclusion

The present study involved the synthesis of a number of TGs representative of the structural classes of milkfat and the characterisation of their phase behaviour. Principal among the TGs were the 1-butyryl and 1-butyryl-2-oleoyl glycerides, whose polymorphism had not been studied previously. In addition several TGs containing oleic, palmitic and stearic acids, which had been examined earlier, were reinvestigated. Finally, the polymorphic behaviour of two classes of enantiomeric TGs was determined here for the first time and compared with the behaviour of their racemates.

This work provides a useful compilation of spectral and thermal data for the polymorphic forms of TGs prepared from butyric, oleic, palmitic and stearic acids. Hitherto, reliable heats of fusion have only been determined for the stable forms of monoacid TGs, so the present data fill a considerable gap in our knowledge of these important compounds. Such data is essential for the thermochemical calculations of solubility and the phase boundaries of multicomponent systems.

Because of the wide variety of TGs examined, the investigation provided an opportunity for the study of phase behaviour in relation to molecular constitution and structure. Thus, on the basis of similarities between the polymorphic forms of structurally related TGs, it was found

that:-

- 1) corresponding butyryl and oleoyl TGs have analogous stable forms (e.g. BSP, OPS)
- 2) for TGs in which one fatty acid was very different from the other two (e.g. BSS, SBS, OOS), the position of the unusual acid determined the chair packing of the stable form; if the acid was in a primary position, the TG was  $\beta'$ -stable (BSS, OSS, OOS) while if it was in the secondary position, the TG was  $\beta$ -stable (SOS, SBS).

However, in terms of our understanding of TG polymorphism, the present survey represents a consolidation of experimental data rather than an explanation of the underlying structural principles. Further crystal structure determinations, particularly of TCL forms, are required to bring our knowledge of the polymorphic behaviour of mixed TGs to the level of understanding which exists for monoacid TGs.

Studies on the polymorphism of individual TGs are prerequisites for an explanation of the melting and solidification of fats. However, although the polymorphism of the major TG classes in milkfat has now been characterised, extensive investigations will be required before the properties of the components can be convincingly related to those of their composite.

APPENDIX

Representative spectral and thermal data for the polymorphic forms of the individual TGs are presented on the following pages. Unfortunately, the IR spectra for BPS were unsuitable for reproduction and are not therefore included in this compilation.

Table 1: Melting Points of the Stable Forms of Triacylglycerols

TG	Form <sup>a</sup>	Melting Point/°C <sup>b</sup>			TG	Form	Melting Point/°C		
		HSM	DSC	Lit.			HSM	DSC	Lit.
SSS	β	71.5-72.5	72.8	73.5 <sup>1</sup>	SOS	β	41.0-42.0	41.9	44.3 <sup>8</sup>
PSS	β	64.0-64.5	64.5	65.2 <sup>2</sup>	POS	β	36.0-36.5	36.0	37.3 <sup>8</sup>
PPS	β	62.0-63.0	62.2	62.7 <sup>2</sup>	POP	β	35.0-36.5	36.1	38.3 <sup>8</sup>
PPP	β	66.0-66.4	66.2	66.4 <sup>1</sup>					
					SBS	β	54.0-54.5	54.2	54.8 <sup>9</sup>
SPS	β'	- <sup>d</sup>	68.6	69.0 <sup>3</sup>					
	β	68.0-68.4	67.6	68.5 <sup>3</sup>	BSS	β'	49.5-51.0	51.6	-
PSP	β'	68.0-69.0	67.7	68.7 <sup>4</sup>	BSP	β'	49.0-49.5	50.0	49.5-50.0 <sup>10</sup>
	β	-	64.6	65.5 <sup>4</sup>	BPS	β'	47.0-48.0	48.3	47.5-48.0 <sup>10</sup>
SES	β	59.5-60.5	60.9	59.5 <sup>5</sup>	BPP	β'	42.5-43.5	43.1	-
ESS	β	59.0-60.0	59.4	-	BES	β'	-	31.4	-
OOS	β' <sup>c</sup>	-	25.3	24.5 <sup>6</sup>	OSS	β'	41.0-43.0	43.7	43.5 <sup>8</sup>
OOP	β' <sup>c</sup>	-	19.7	19.5 <sup>6</sup>	OSP	β'	37.0-39.0	37.9	39.8 <sup>8</sup>
					OPS	β'	40.0-41.0	40.0	40.2 <sup>8</sup>
BOS	β' <sup>c</sup>	-	20.3	-	OPP	β'	32.0-35.0	35.5	35.2 <sup>8</sup>
BOP	β' <sup>c</sup>	-	13.9	-					
					<u>sn</u> -SSB	β'	50.0-51.0	51.8	49 <sup>11</sup>
BBP	α <sup>c</sup>	-	1	2.9 <sup>7</sup>	<u>sn</u> -SSO	β'	45.5-46.0	45.4	-
					<u>sn</u> -PPO	β'	36.5-37.0	36.8	37 <sup>11</sup>

Notes:

- a solvent crystallised form, assignment by X-ray diffraction or IR spectroscopy
- b HSM, hot stage microscope; DSC, differential scanning calorimeter; Lit., literature melting points
- c stable form by transformation
- d -, not determined

References:

- |                                     |                                    |
|-------------------------------------|------------------------------------|
| 1 Lutton and Fehl (1970)            | 7 Jackson and Lutton (1952)        |
| 2 Lutton, Jackson and Quimby (1948) | 8 Lutton (1951)                    |
| 3 Hugenberg and Lutton (1963)       | 9 Jackson, Wille and Lutton (1951) |
| 4 Lutton and Hugenberg (1960)       | 10 Verkade (1943)                  |
| 5 Minor and Lutton (1953)           | 11 Lok, Ward and van Dorp (1976)   |
| 6 Lutton (1966)                     |                                    |

Table 2: Some Common Bands in the Infrared Spectra of Related Stable Forms

TG	Form	C.M. <sup>a</sup>	Characteristic Band Positions/cm <sup>-1</sup>												
SES ESS	}	β	2												
				890	960 ( <u>trans</u> )		990	1015	1035	1060					
SOS POS POP	}	β	3	688 ( <u>cis</u> )											
				890	955	985	1015	1035	1055						
SBS	}	β	3	800	875	890	905	960	990	1015	1040	1065			
β specific band <sup>b</sup>				~890											
BOP BOS	}	β'	3	835	880	940		980	1015	1060					
OOP OOS				}	β'	3	820	835	880	900	920	940	960	980	1035
BSS BPS BPP	}	β'	3				860		880	890	940	965	1030	1045	1060
OSS OPS <sup>c</sup> OPP				}	β'	3	860		940		1030		1060		
BSP BES OSP	}	β' <sup>d</sup>	3				870		925		980	1080	1110		
β' specific bands <sup>b</sup>				~835		~925		~950	~975						

a C.M., chain multiplicity: 2 for a double chain length structure and 3 for a triple chain length structure

b bands specific for the β and β' forms of monoacid saturated triacylglycerols (de Ruig, 1971; Table 1.5)

c β'<sub>2</sub> form of OPS, β'<sub>1</sub> form of OSS and OPP

d any two spectra showed closer agreement than the three spectra together

Table 3: Some Common Bands in the Infrared Spectra of Related  $\beta$  and  $\beta'$  Forms

TG	Form	C.M. <sup>a</sup>	Characteristic Band Positions/cm <sup>-1</sup>													
SOS POP	] $\beta_2$	3	845	920	960	980	1020	1040	1060							
SOS POS			] $\beta'$	3	910	950	960	1005	1025	1055	1065	1090	1110			
PSP POP OPS	] $\beta'_2$	2			780	830	840	870	880	920	930	950	980	1010	1035	1055
$\beta'$ specific bands <sup>b</sup>			~835					~925		~950~975						

a C.M., chain multiplicity

b bands specific for the  $\beta'$  form of monoacid saturated triacylglycerols (de Ruig, 1971; Table 1.5)

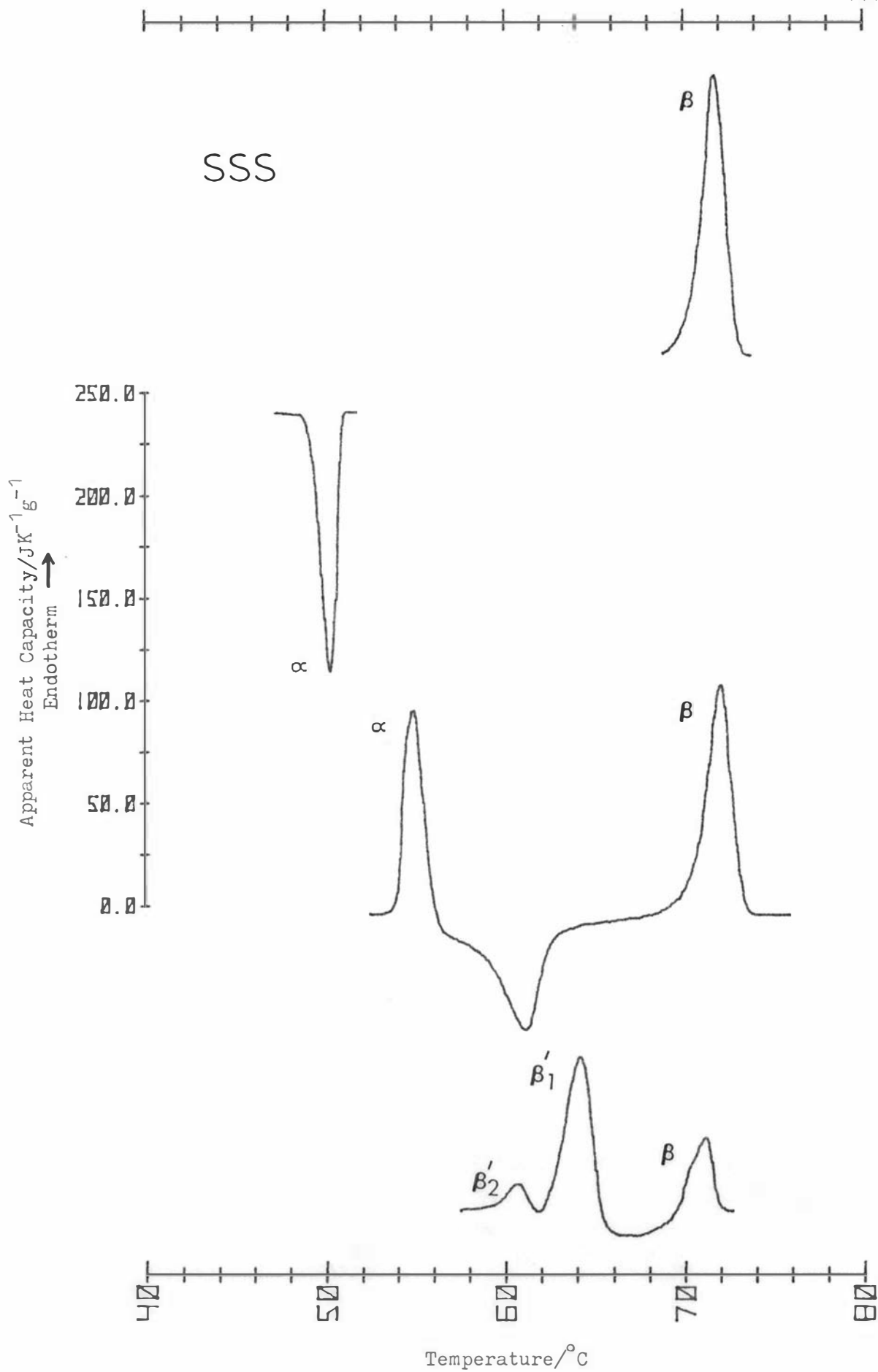


Fig. 1: Thermal behaviour of SSS.

(From top to bottom) melting of  $\beta$  from solvent; crystallisation of  $\alpha$ ; transformation of  $\alpha$ ; transformation of  $\beta'$  prepared by crystallisation of the melt at  $56^{\circ}\text{C}$  for 15 min (all recorded at  $4^{\circ}\text{C}/\text{min}$ ).

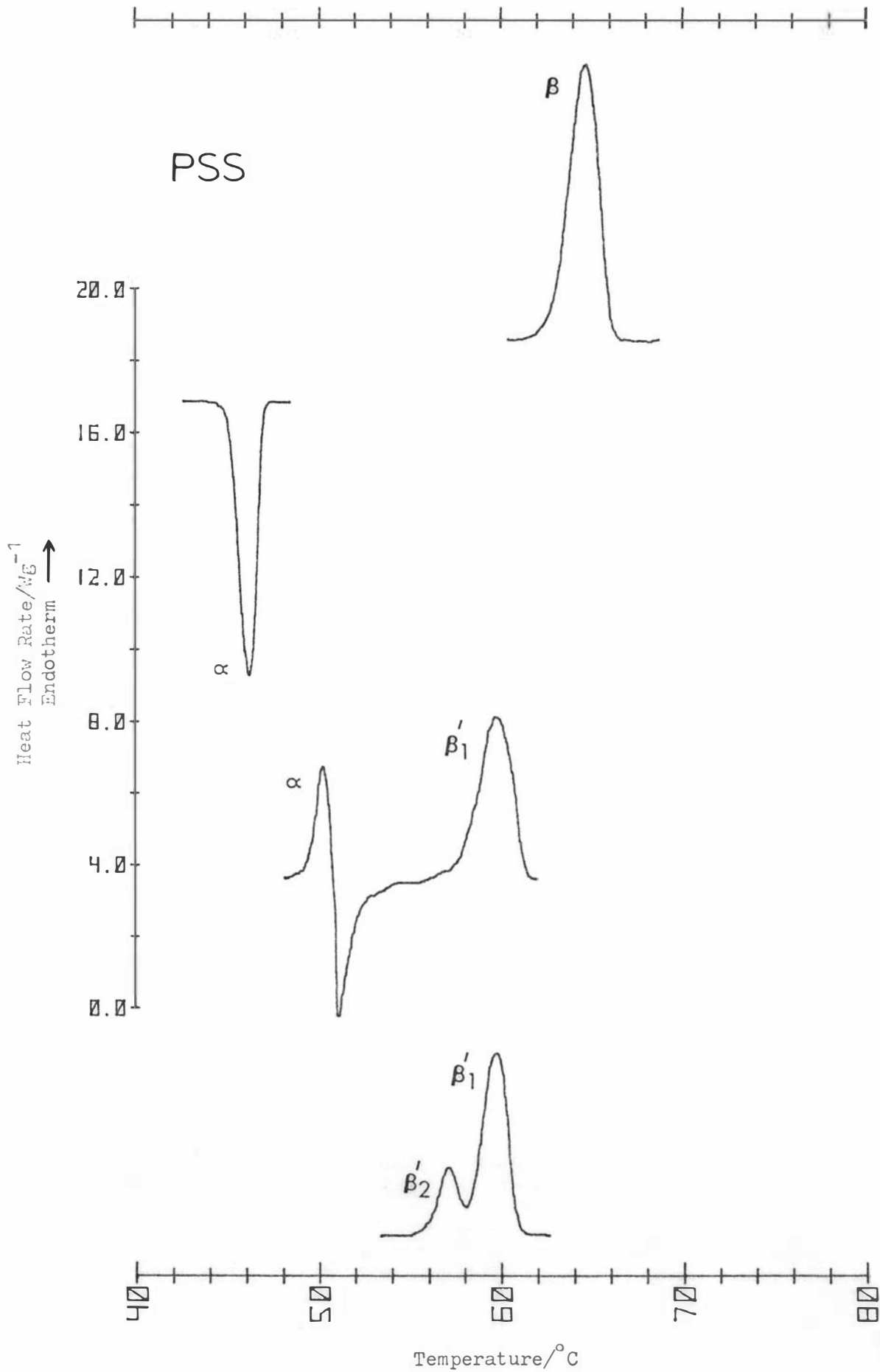


Fig. 2: Thermal behaviour of PSS.

(From top to bottom) melting of  $\beta$  from solvent; crystallisation of  $\alpha$ ; transformation of  $\alpha$ ; transformation of  $\beta'$  prepared by crystallisation of the melt at 51°C for 30 min (all recorded at 4°C/min).

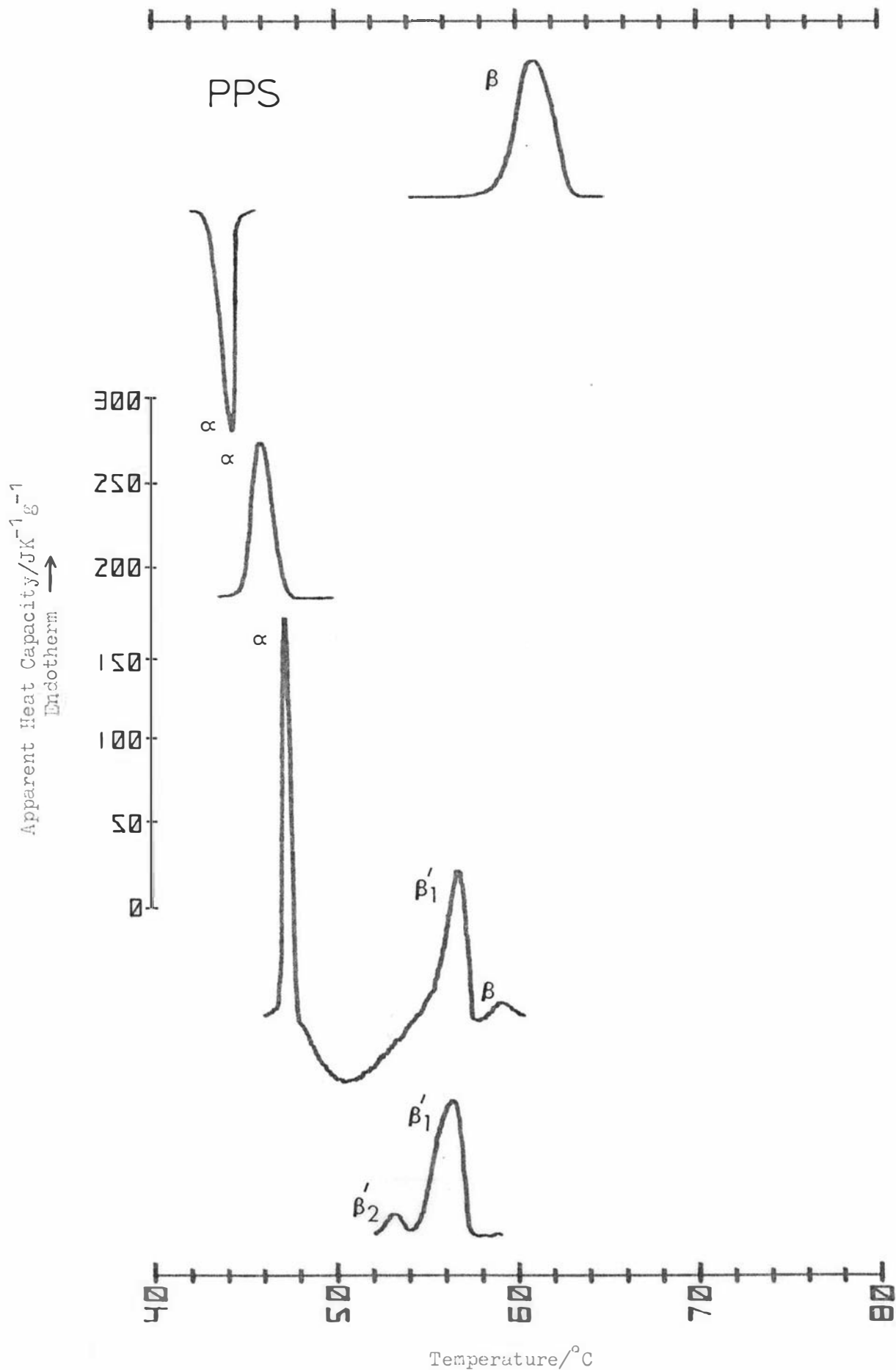
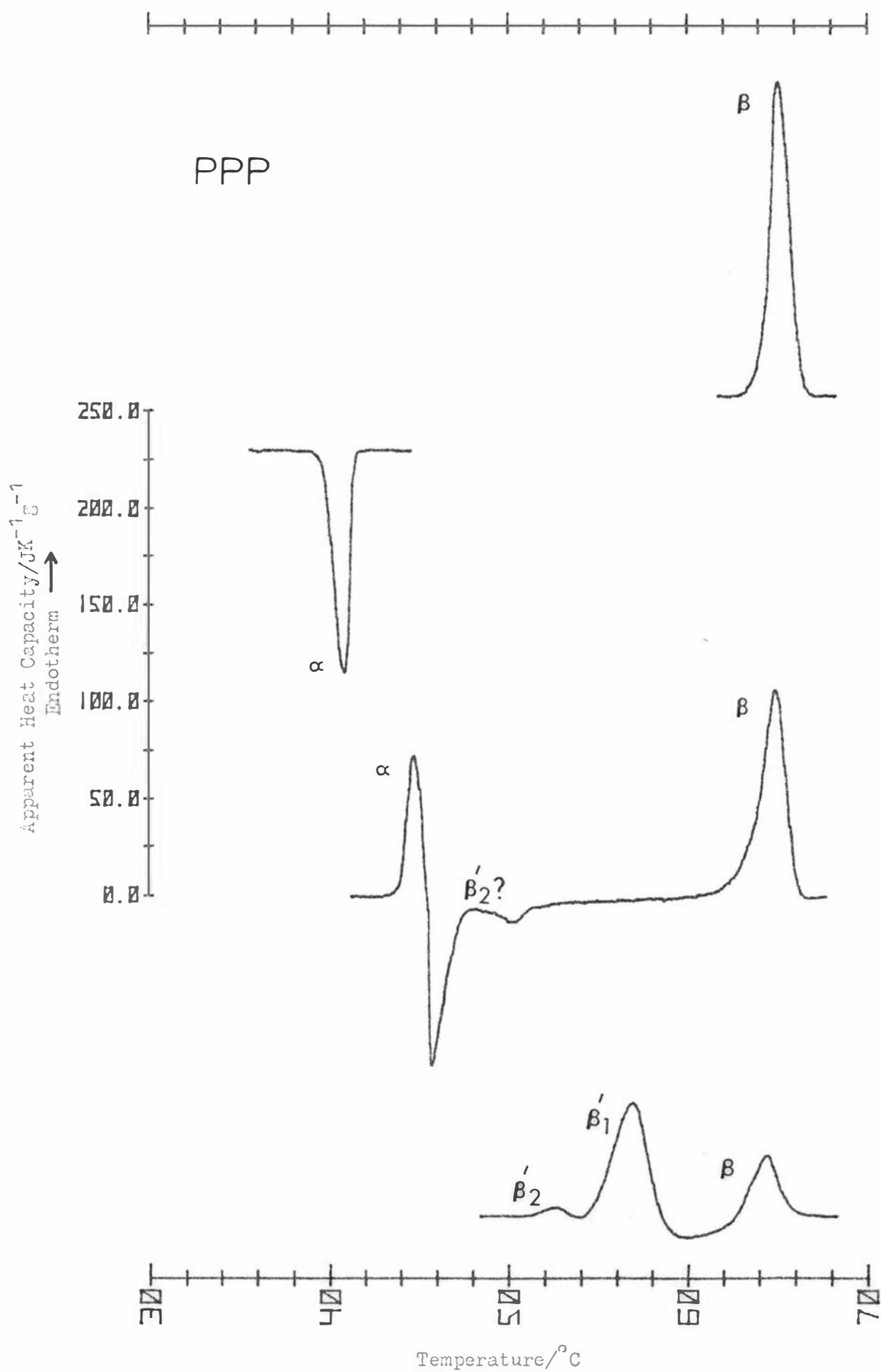


Fig. 3: Thermal behaviour of PPS.

(From top to bottom) melting of  $\beta$  from solvent (4°C/min); crystallisation of  $\alpha$  (4°C/min); melting of  $\alpha$  at 4°C/min; transformation of  $\alpha$  at 1°C/min; transformation of  $\beta'$  prepared by crystallisation of the melt at 48°C for 30 min (2°C/min).



**Fig. 4:** Thermal behaviour of PPP.  
 (From top to bottom) melting of  $\beta$  from solvent; crystallisation of  $\alpha$ ; transformation of  $\alpha$ ; transformation of  $\beta'$  prepared by crystallisation of the melt at 47°C for 7.5 min (recorded at 4, 4, 4 and 8°C/min respectively).

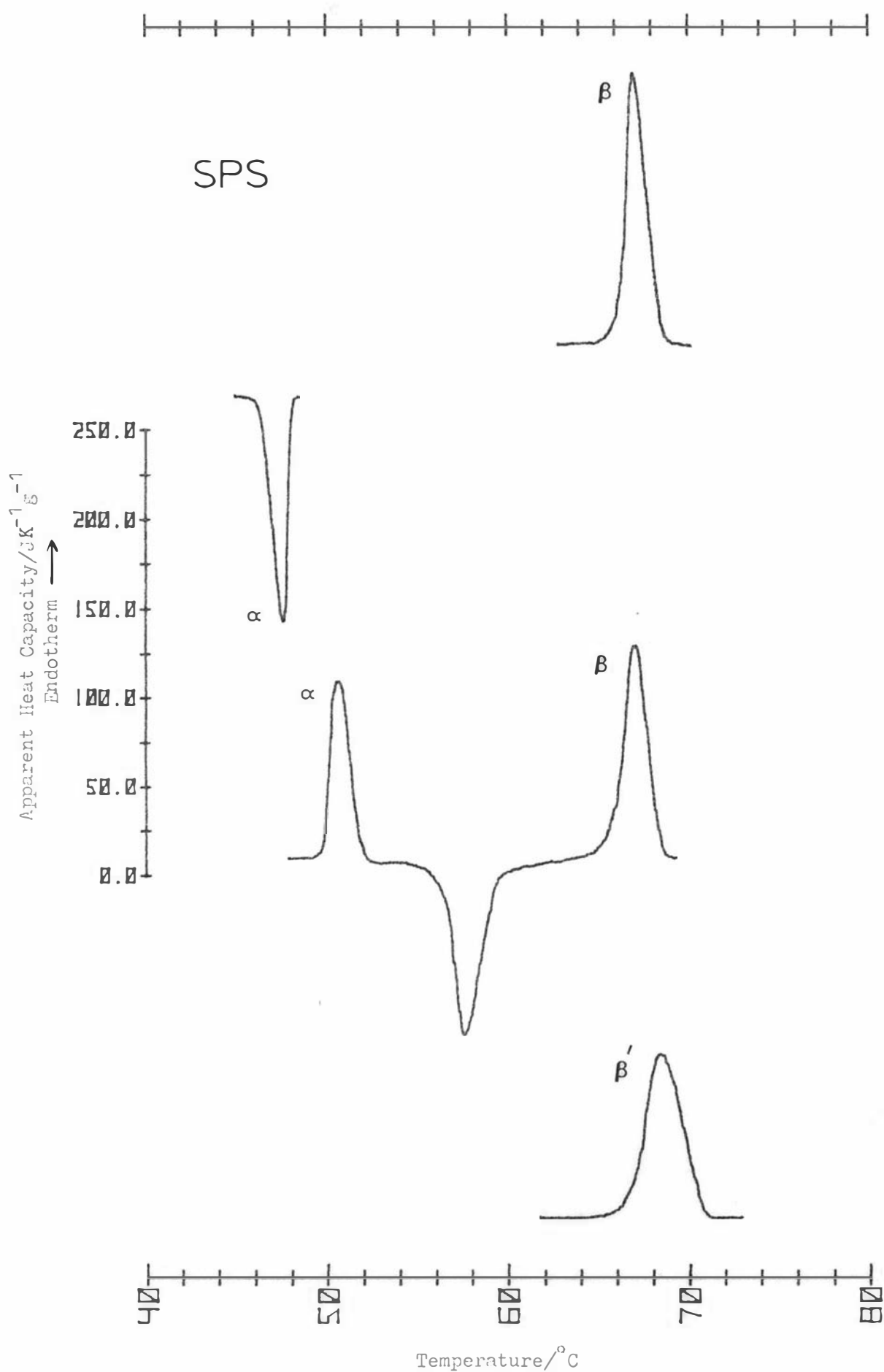
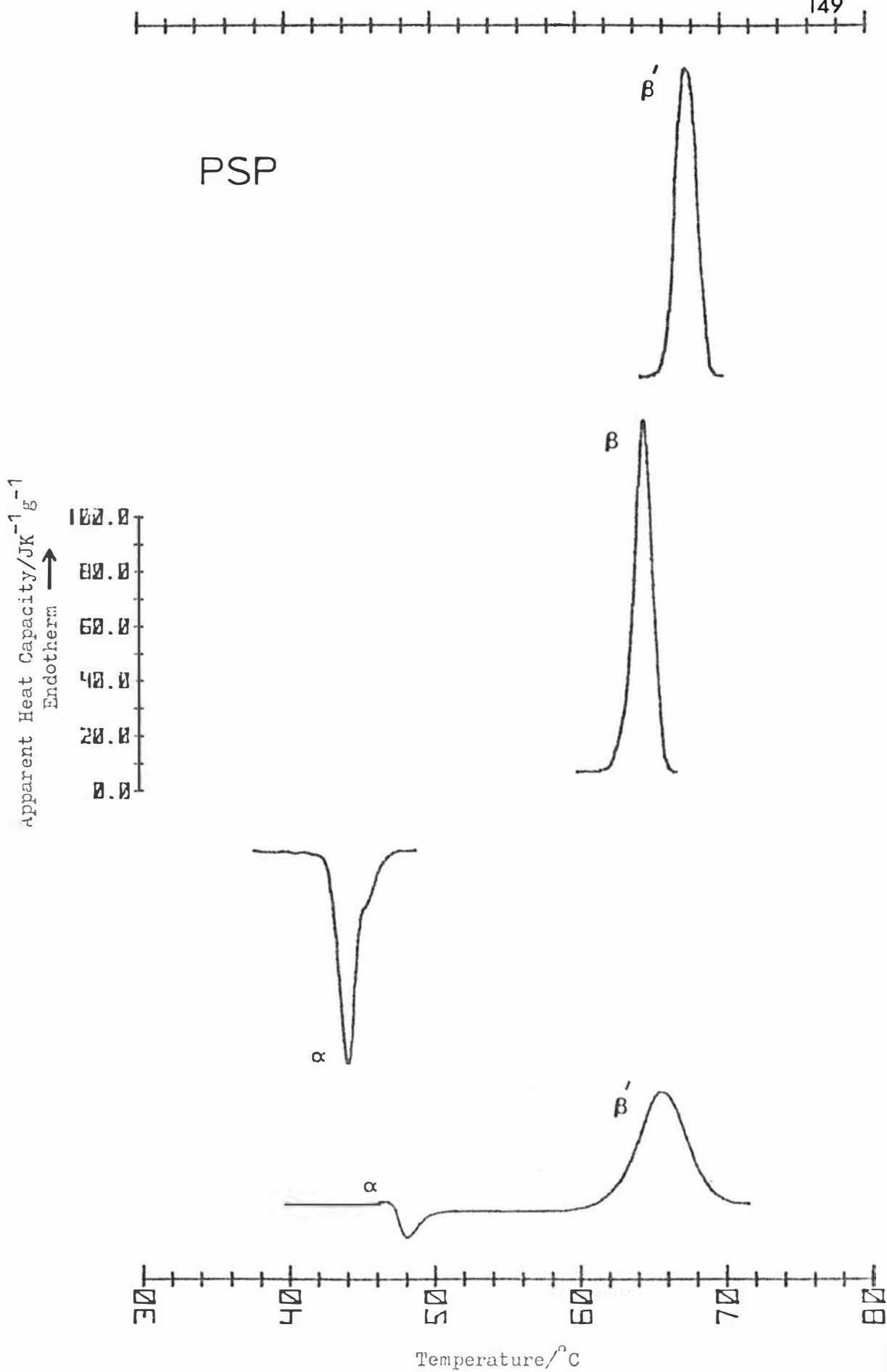


Fig. 5: Thermal behaviour of SPS.  
 (From top to bottom) melting of  $\beta$  from solvent; crystallisation of  $\alpha$ ; transformation of  $\alpha$ ; melting of  $\beta'$  from solvent (all recorded at 4 °C/min).



**Fig. 6:** Thermal behaviour of PSP.  
 (From top to bottom) melting of  $\beta'$  from solvent; melting of  $\beta$  from solvent; crystallisation of  $\alpha$  and  $\beta'$ ; transformation of  $\alpha$  from the shock-cooled melt (recorded at 4, 4, 4 and 16  $^{\circ}\text{C}/\text{min}$  respectively).

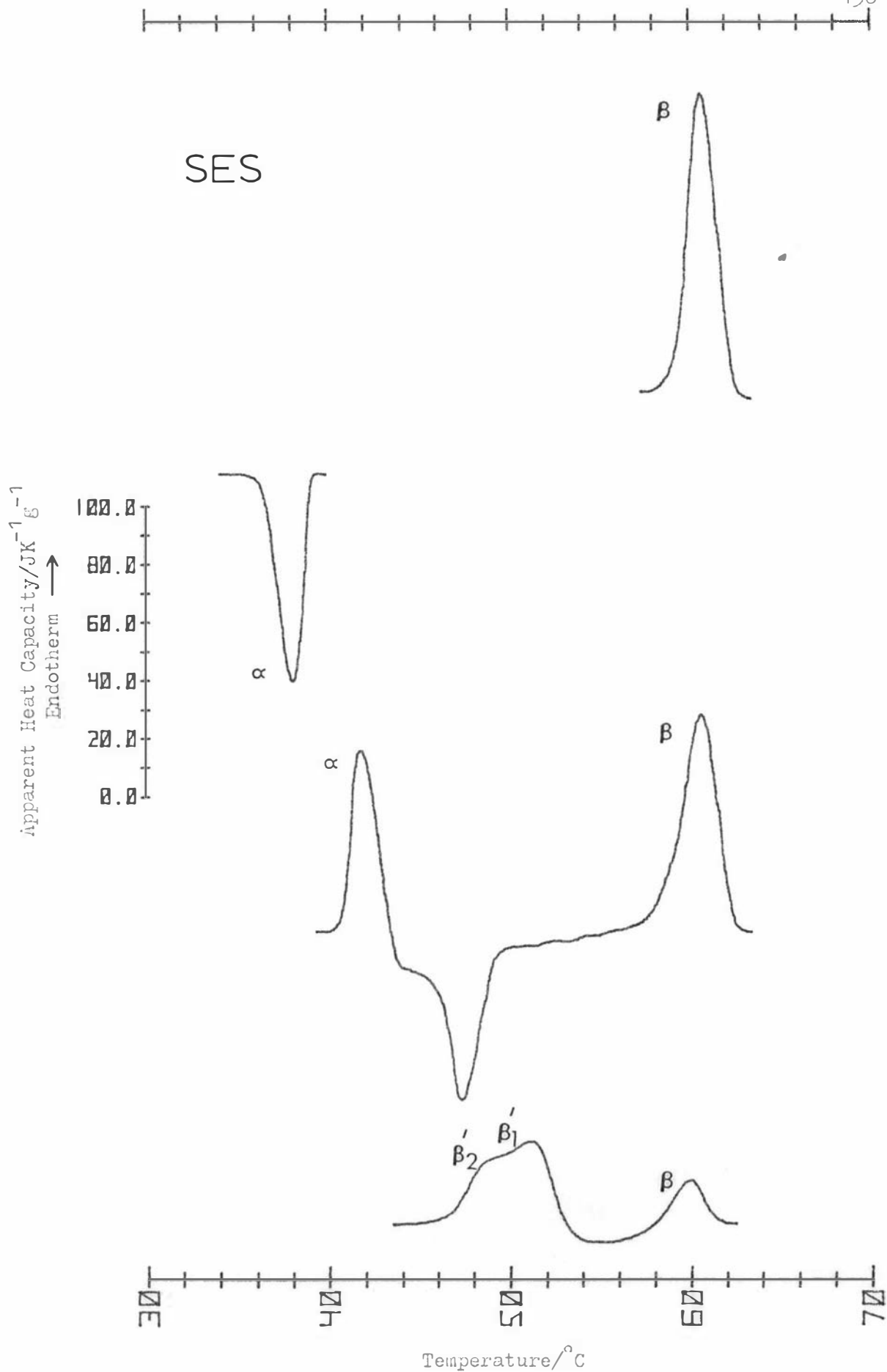
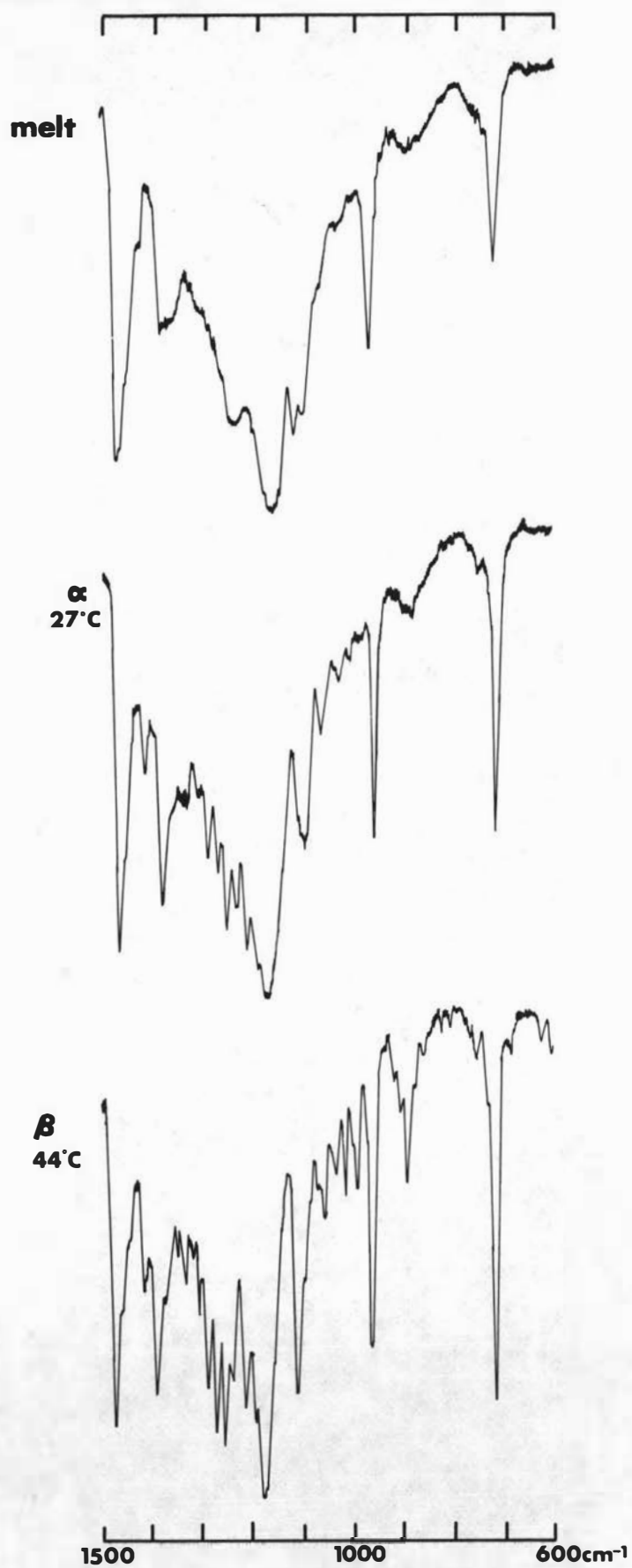
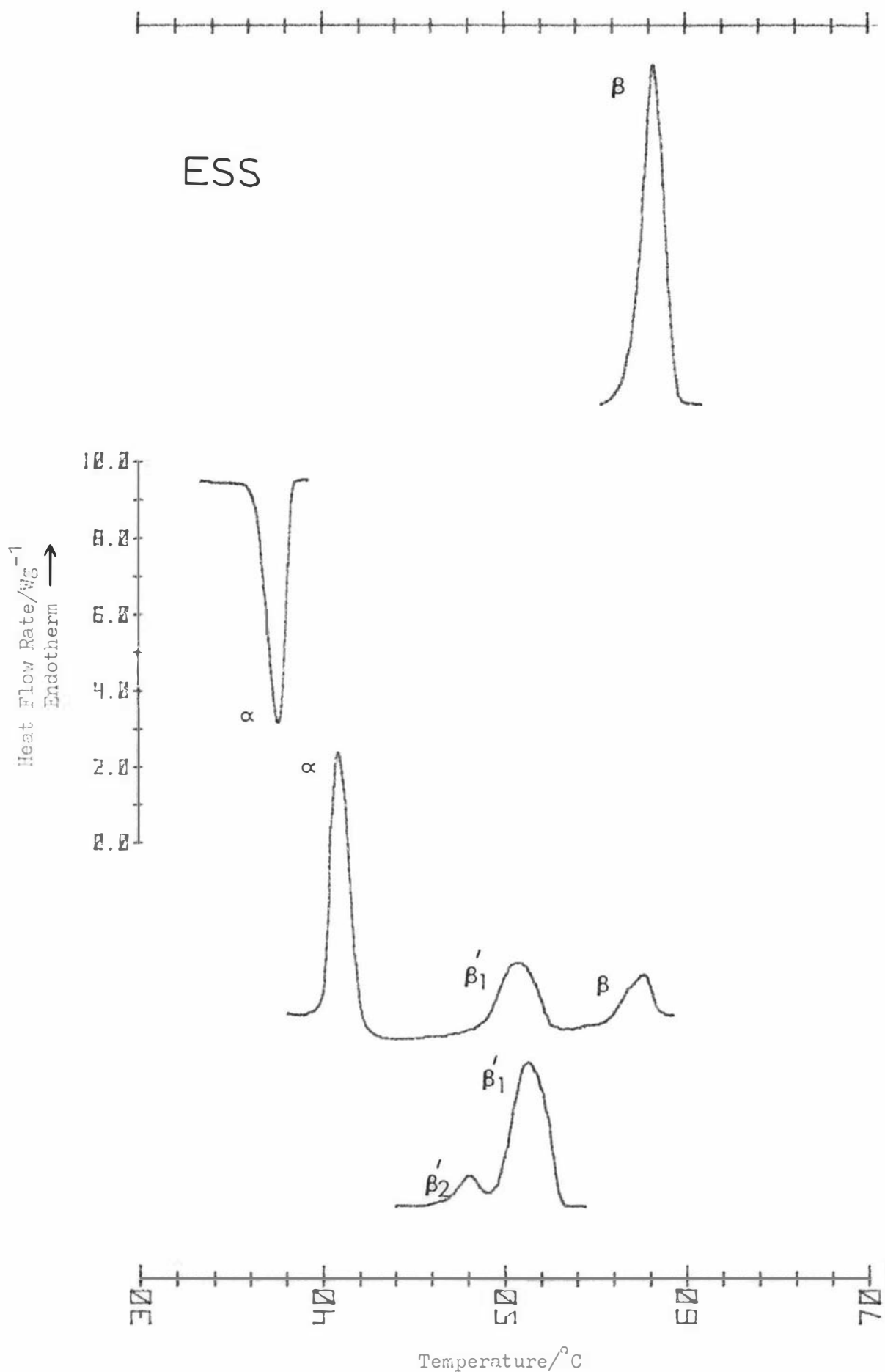


Fig. 7: Thermal behaviour of SES. (From top to bottom) melting of  $\beta$  from solvent, crystallisation of  $\alpha$ , transformation of  $\alpha$ ; transformation of  $\beta'$  prepared by crystallisation of the melt at 42°C for 20 min (recorded at 4, 4, 4 and 8 C/min respectively).



**Fig. 8 IR Spectra of SES**



**Fig. 9:** Thermal behaviour of ESS.  
 (From top to bottom) melting of  $\beta$  from solvent; crystallisation of  $\alpha$ ; transformation of  $\alpha$ ; transformation of  $\beta'$  prepared by crystallisation of the melt at 41°C for 15 min (all recorded at 4°C/min).

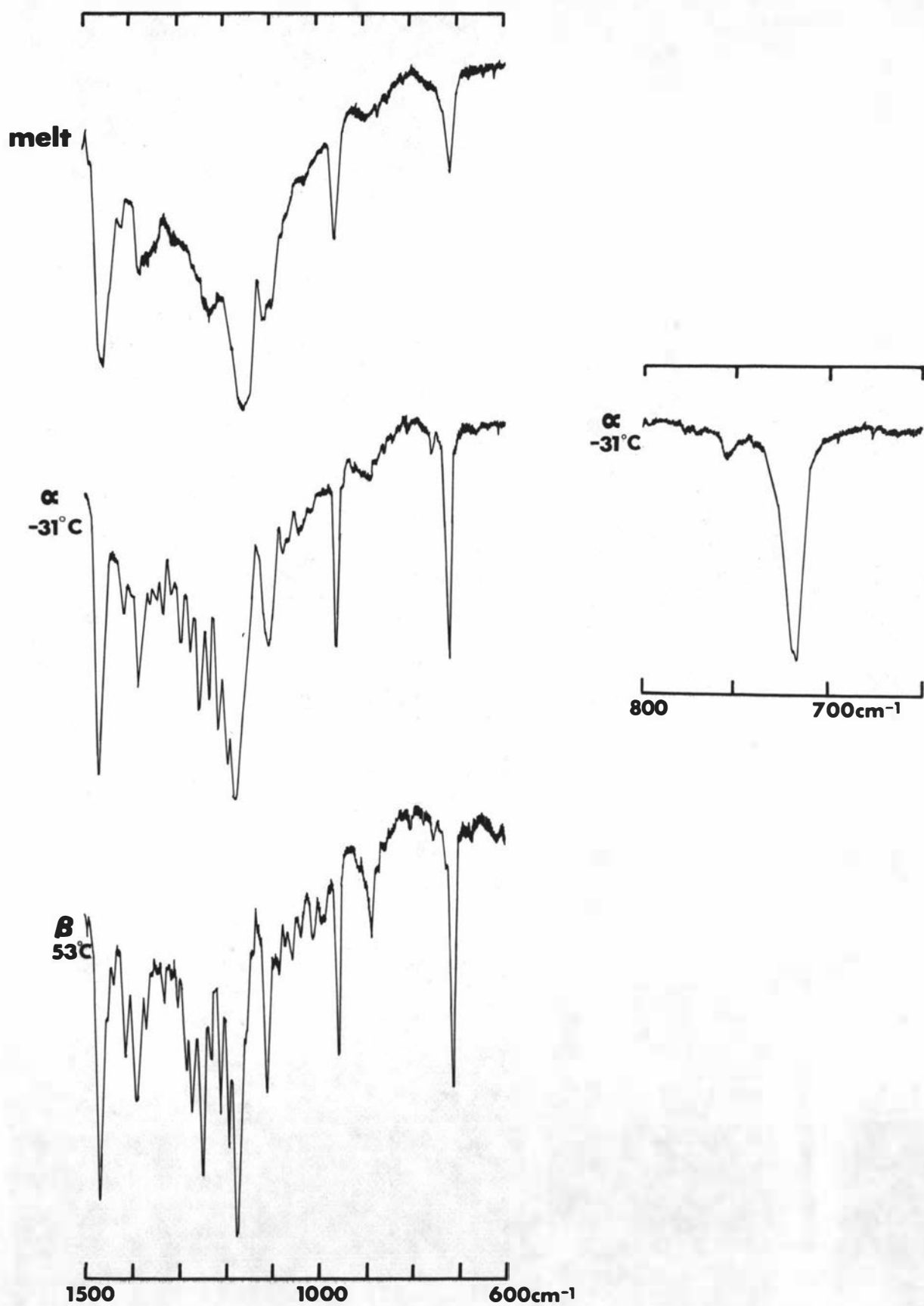


**Fig. 10 IR Spectra of ESS**

OOS

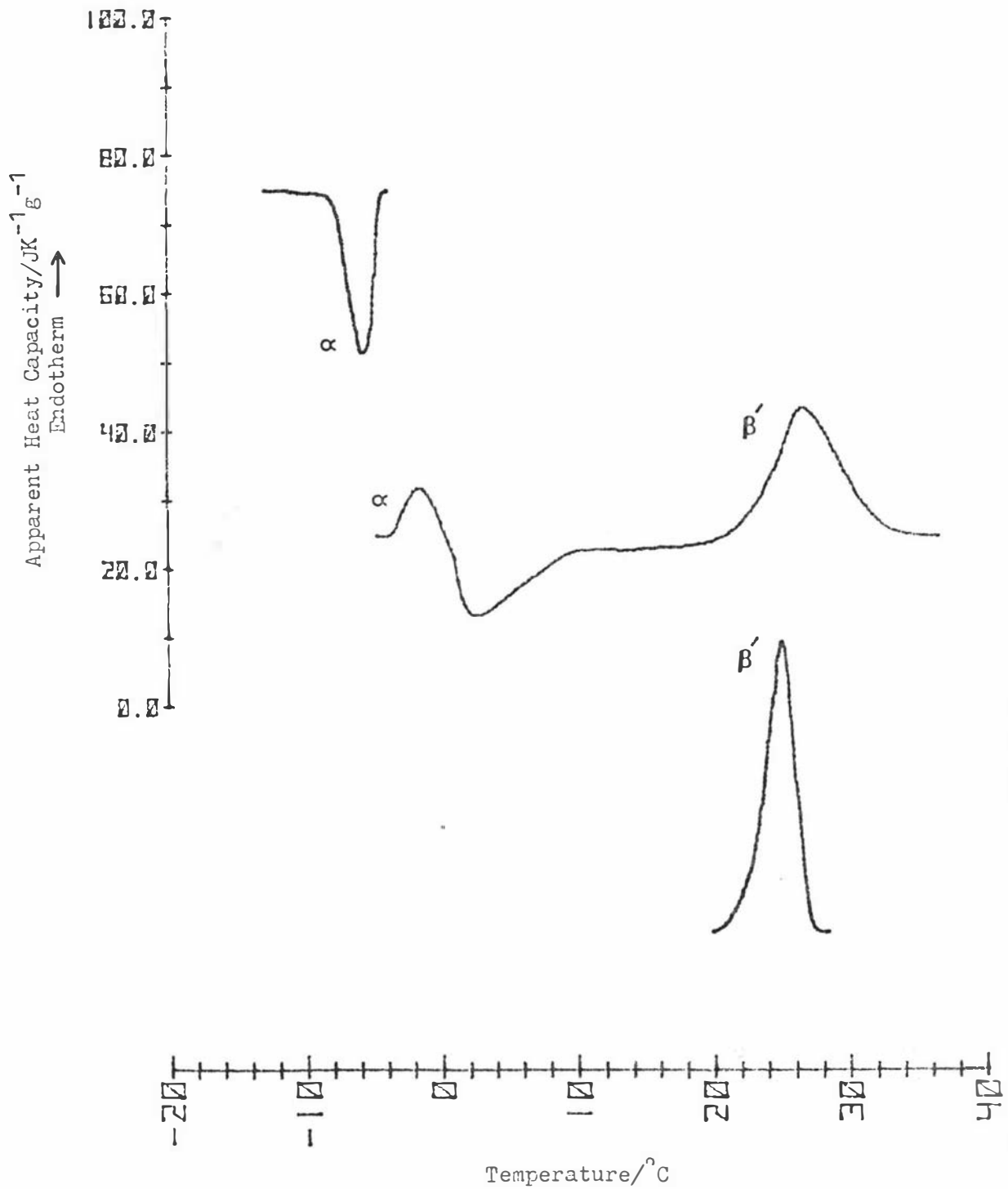
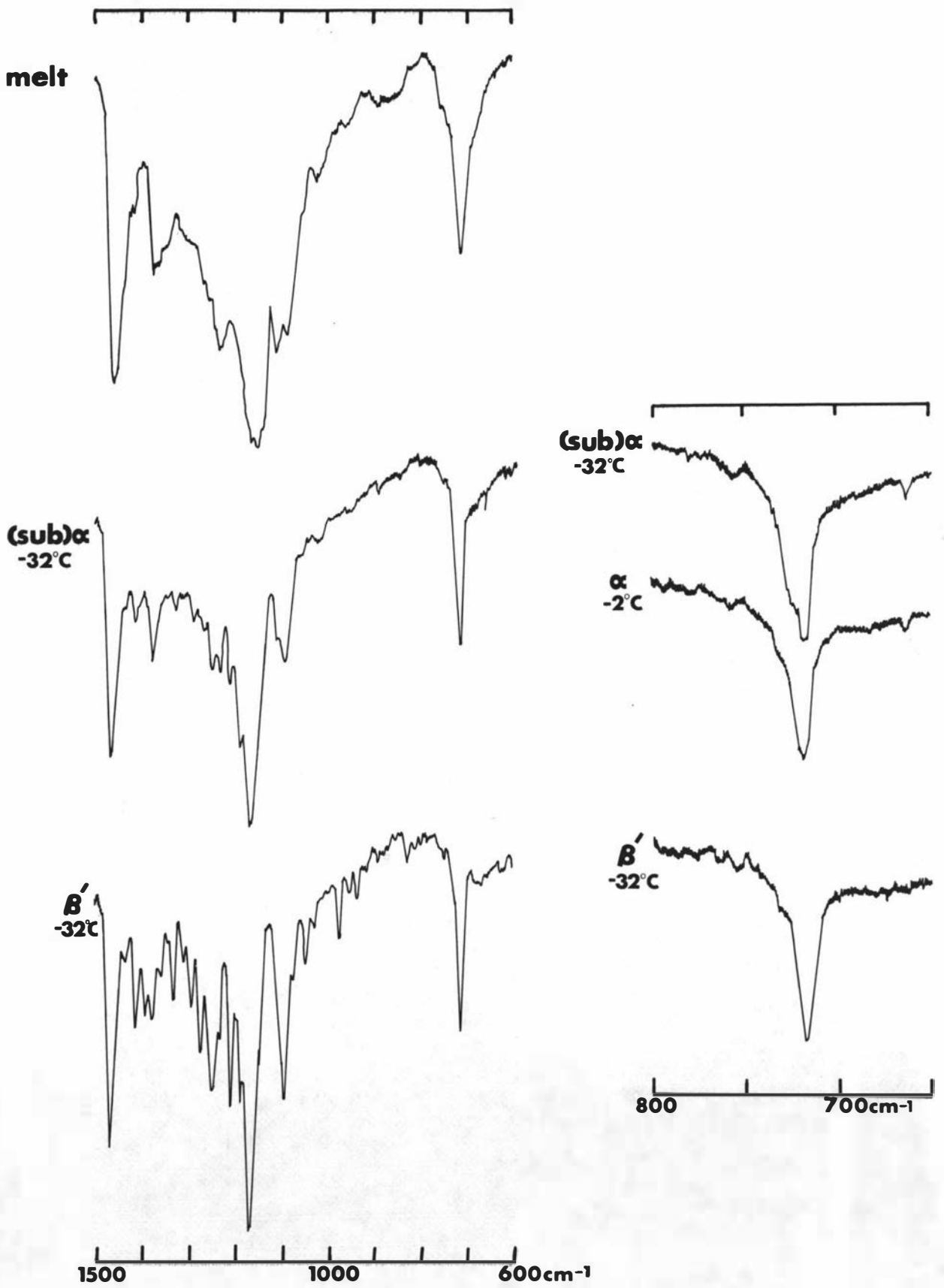


Fig. 11: Thermal behaviour of OOS.

(From top to bottom) crystallisation of  $\alpha$ ; transformation of  $\alpha$  from the shock-cooled melt; melting of the stable  $\beta'$  form prepared by transformation of  $\alpha$  (recorded at 4, 16 and 4°C/min respectively).



**Fig. 12** IR Spectra of OOS

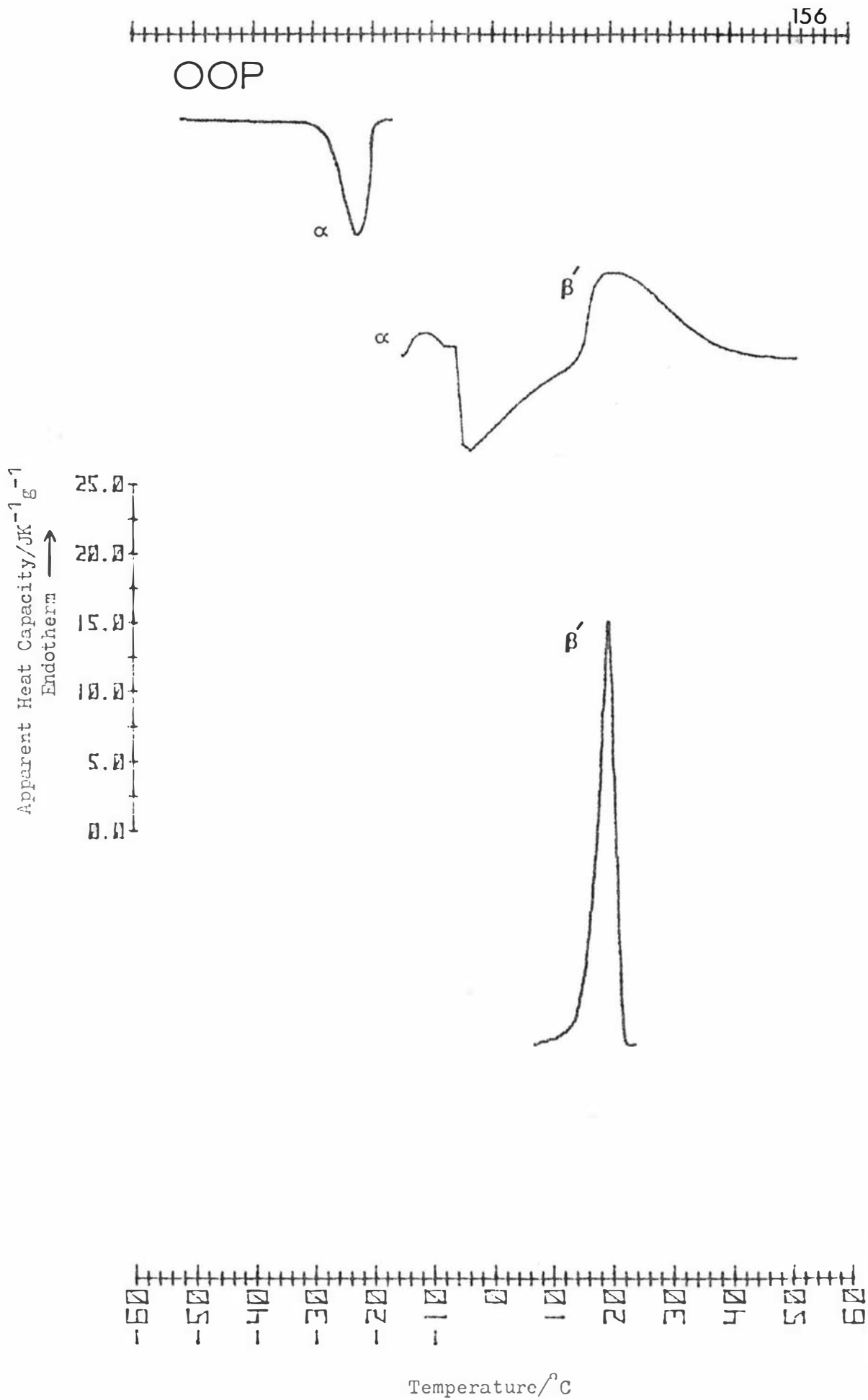
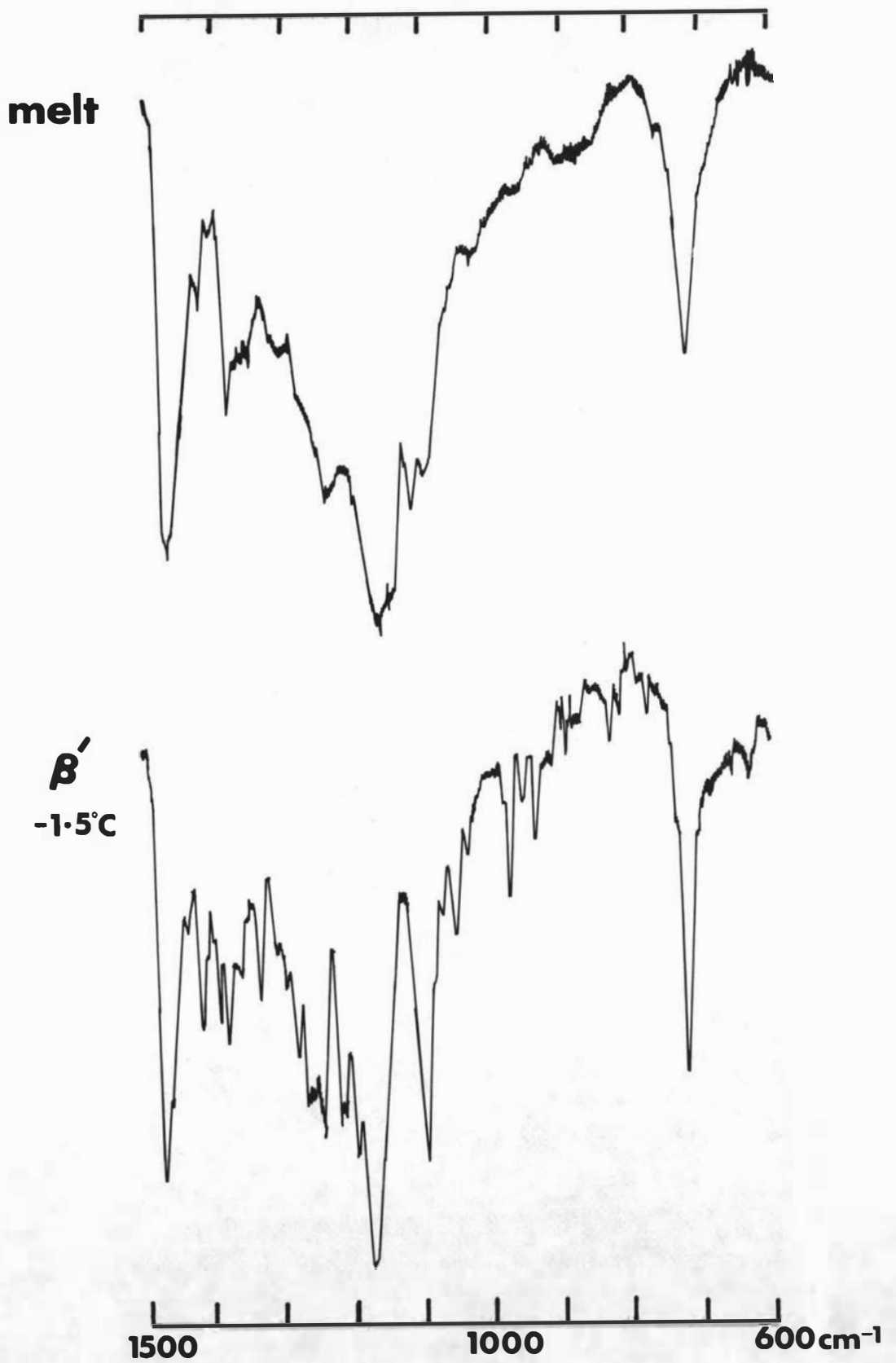


Fig. 13: Thermal behaviour of OOP. (From top to bottom) crystallisation of  $\alpha$ ; transformation of  $\alpha$ ; melting of the stable  $\beta'$  form prepared by transformation of  $\alpha$  (recorded at 16, 64 and  $4^{\circ}\text{C}/\text{min}$  respectively).



**Fig.14 IR Spectra of OOP**

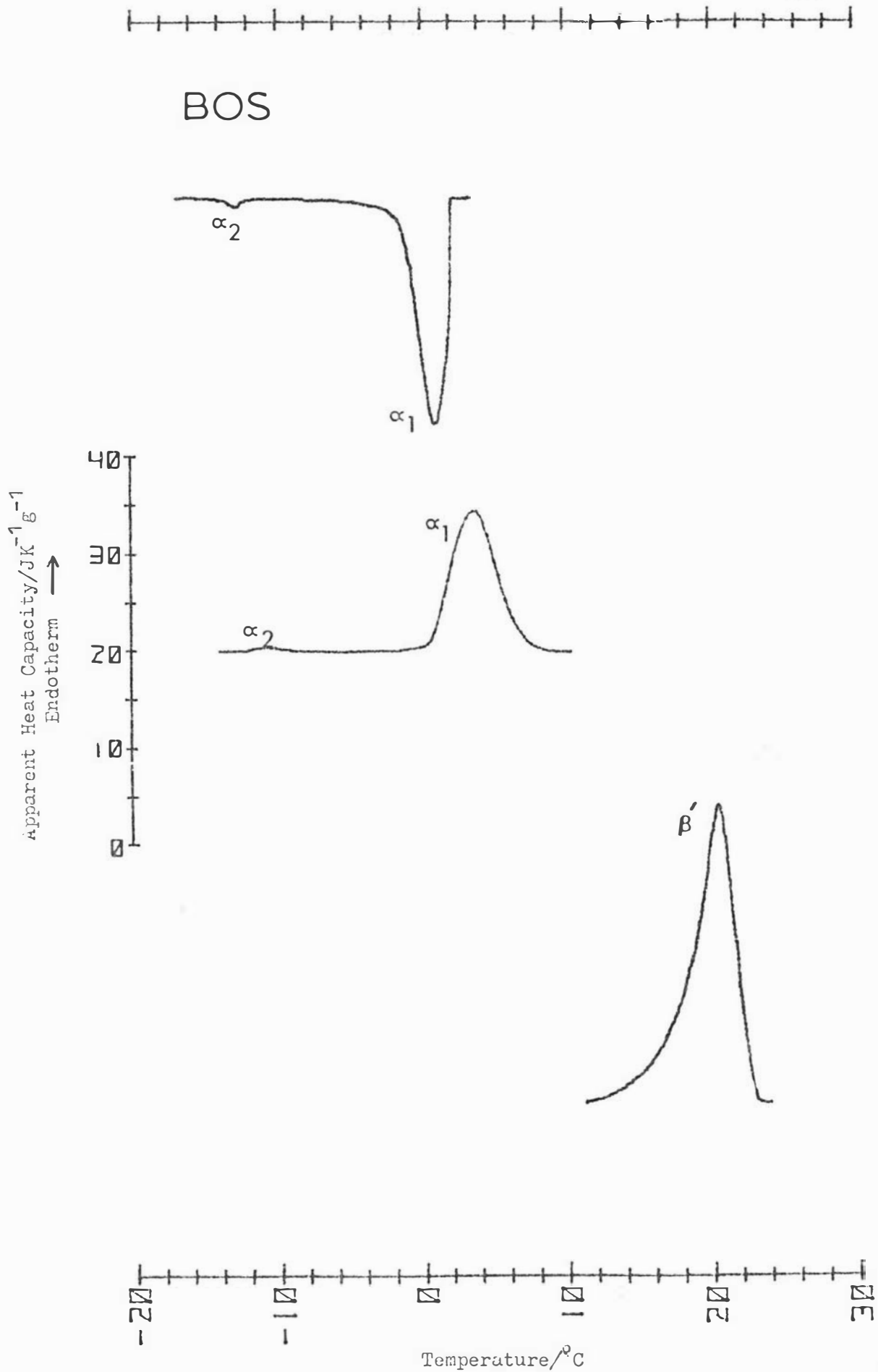
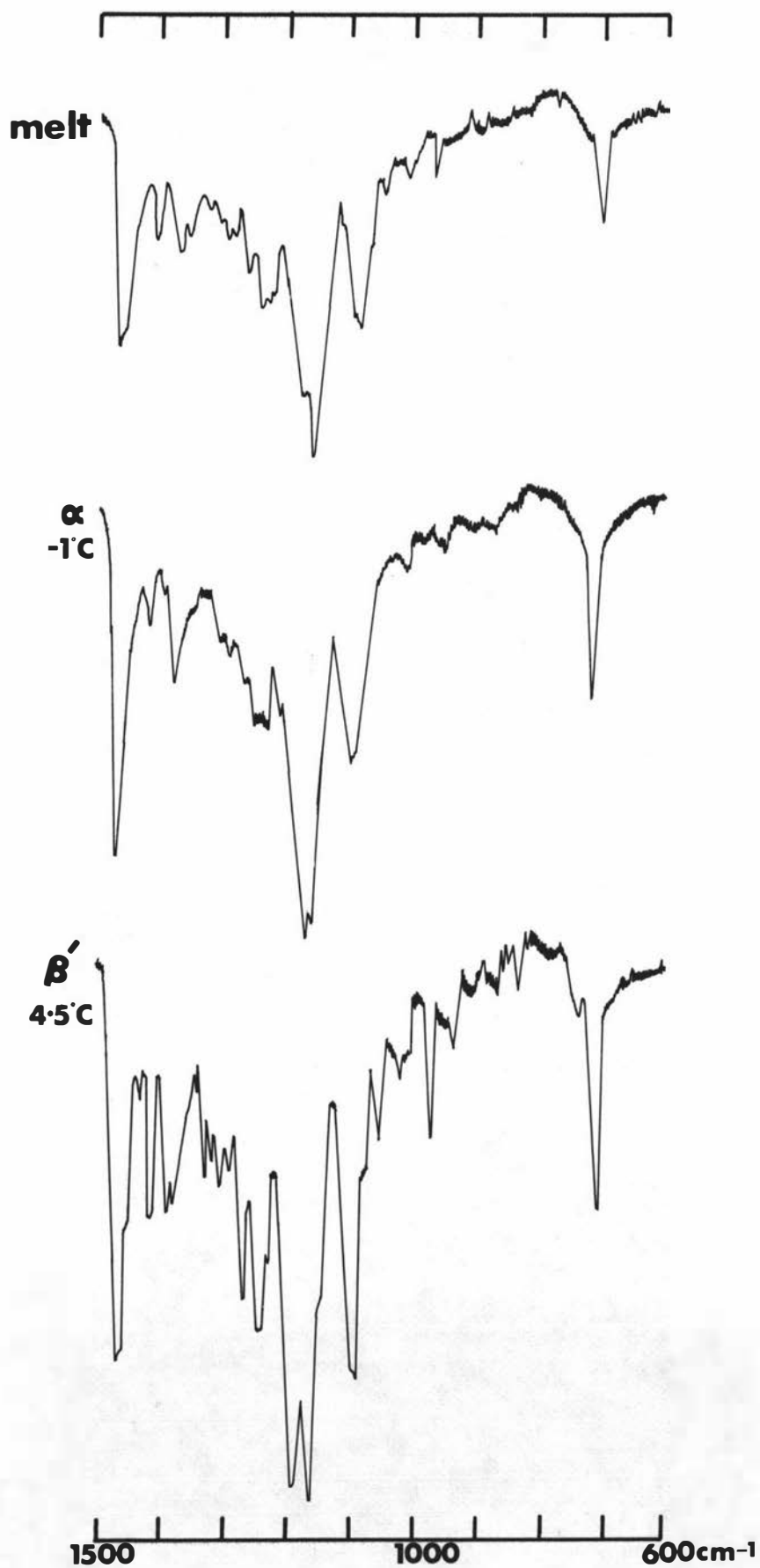


Fig. 15: Thermal behaviour of BOS.

(From top to bottom) crystallisation of  $\alpha$ ; melting of  $\alpha$ ; melting of the stable  $\beta'$  form prepared by transformation of  $\alpha$  at  $3^{\circ}\text{C}$  for 30 min (recorded at 4, 16 and  $4^{\circ}\text{C}/\text{min}$  respectively).



**Fig.16 IR Spectra of BOS**

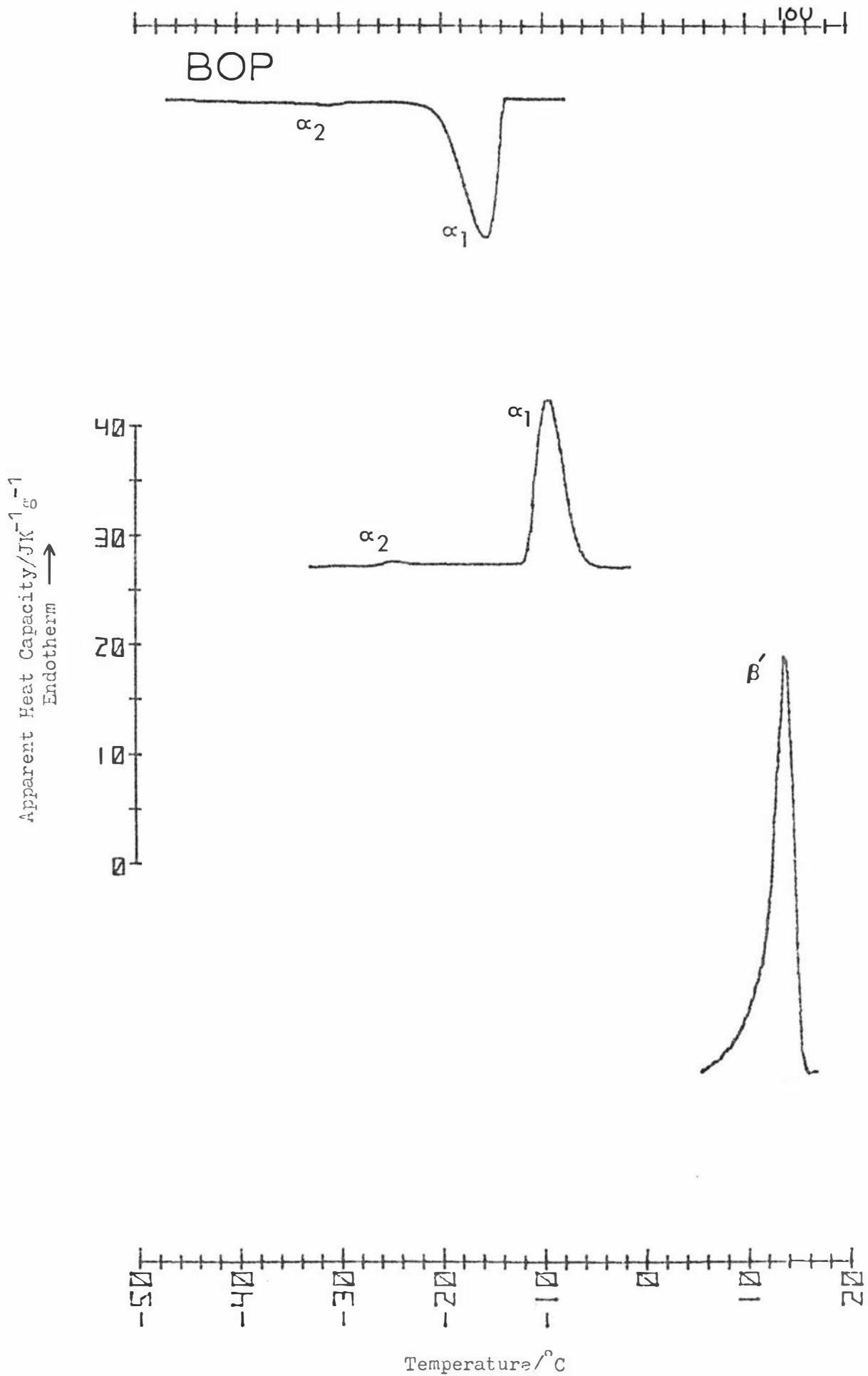
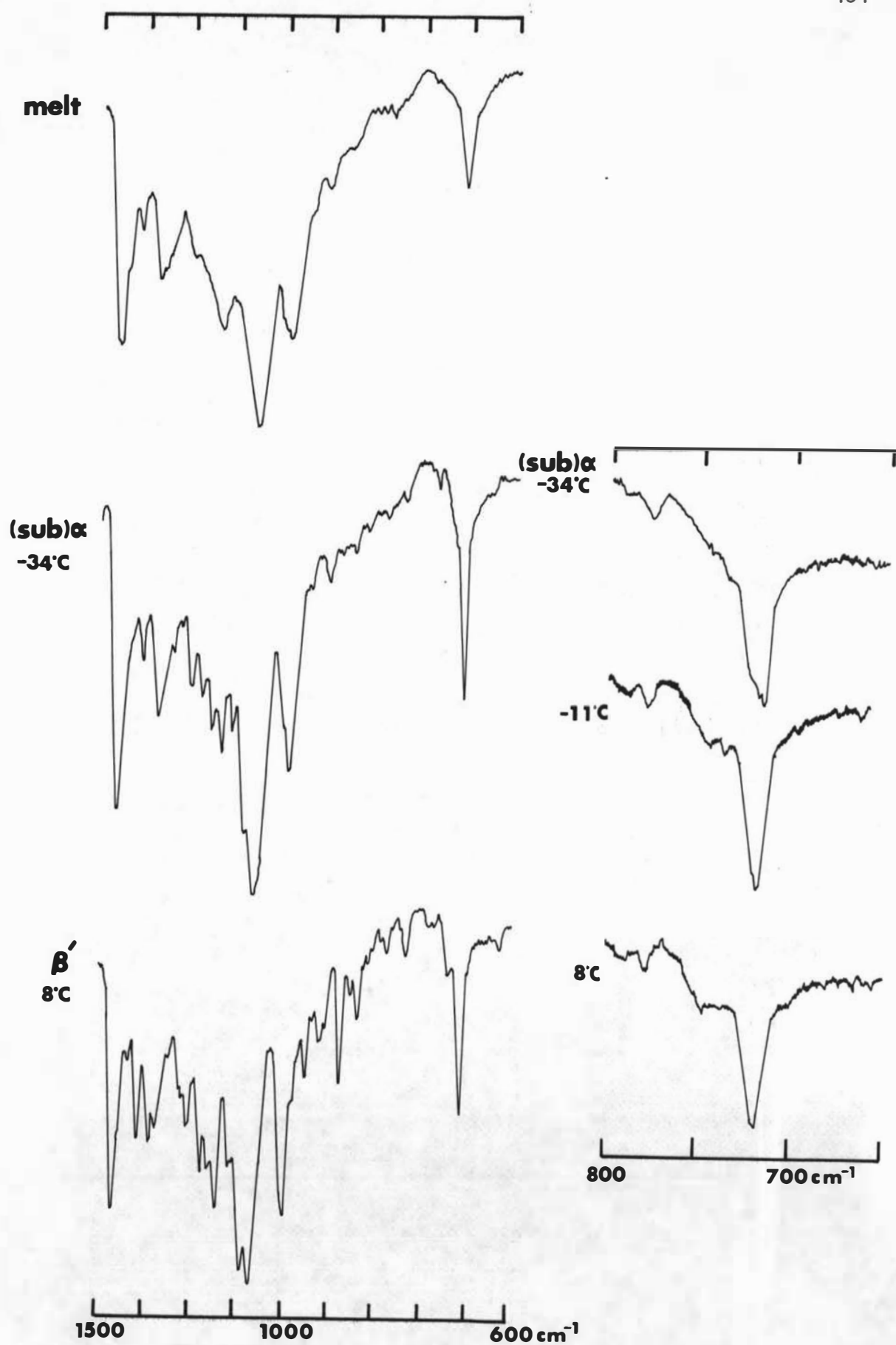


Fig. 17: Thermal behaviour of BOP.  
 (From top to bottom) crystallisation of  $\alpha$ ; melting of  $\alpha$ ; melting of the stable  $\beta'$  form prepared by transformation of  $\alpha$  (recorded at 16, 16 and 4  $^{\circ}\text{C}/\text{min}$  respectively).

**Fig.18 IR Spectra of BOP**

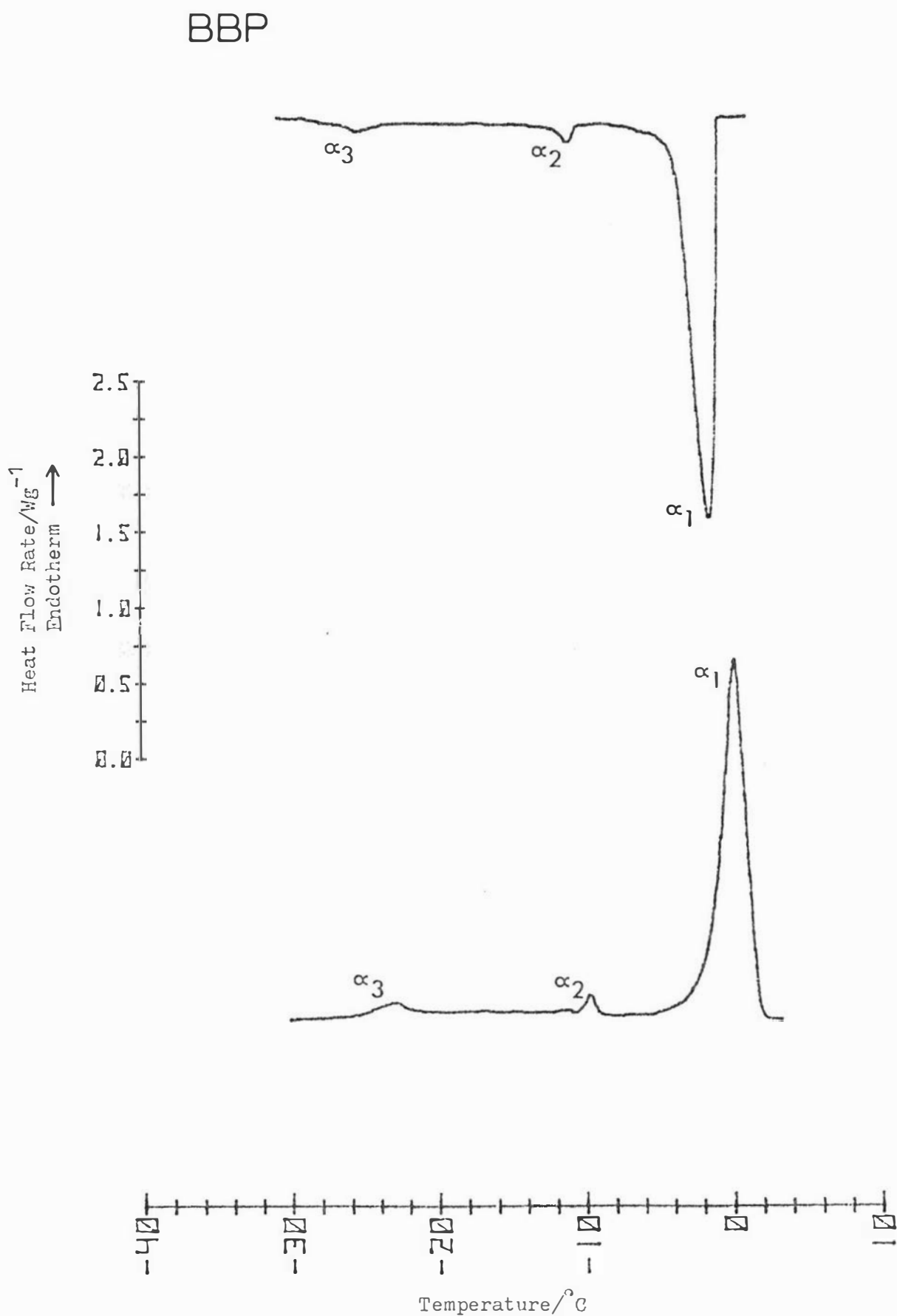
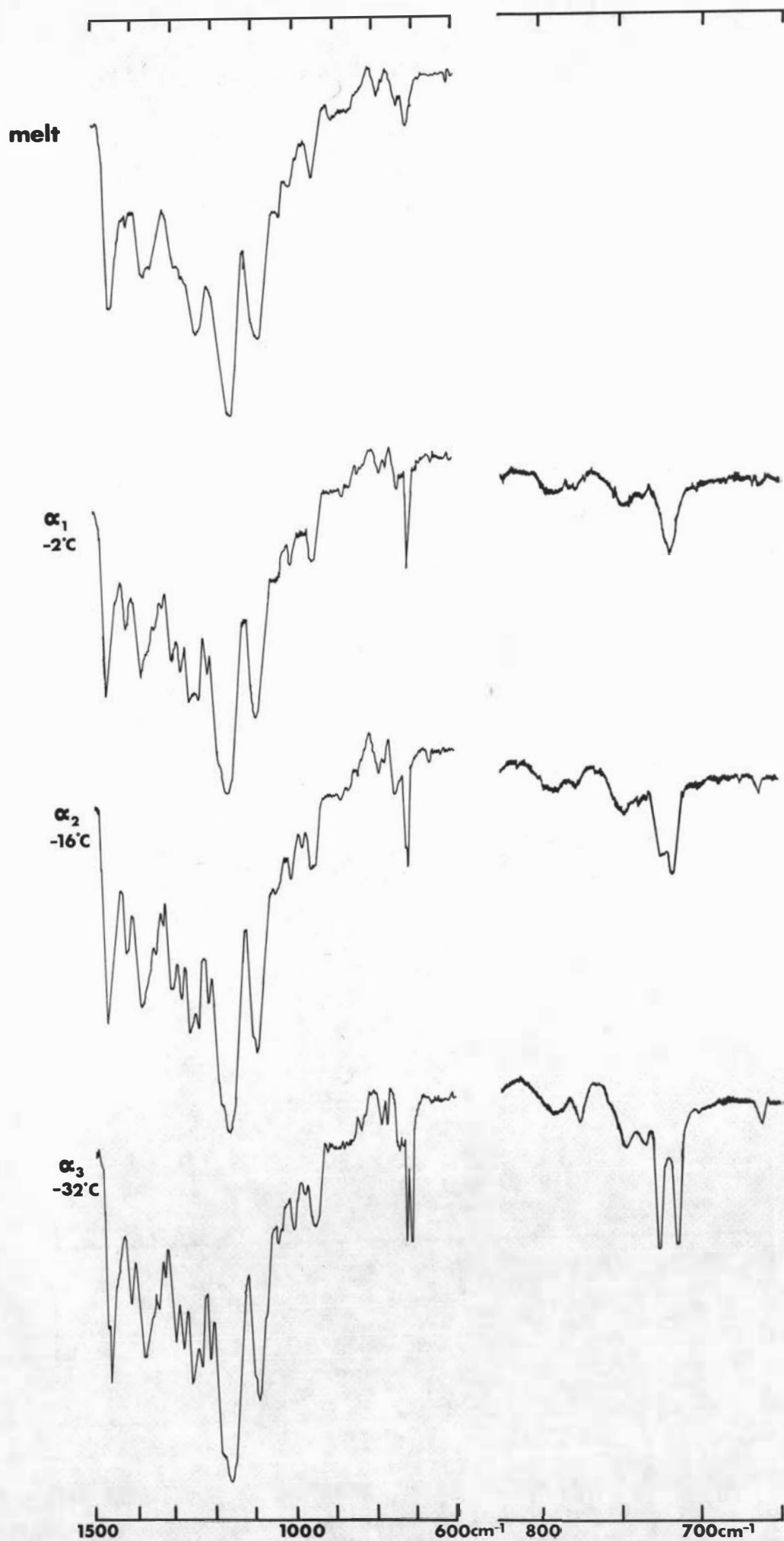


Fig. 19: Thermal behaviour of BBP.  
(From top to bottom) crystallisation of  $\alpha$ ; melting of  $\alpha$  (both recorded at 4 °C/min).

**Fig. 20 IR Spectra of BBP**

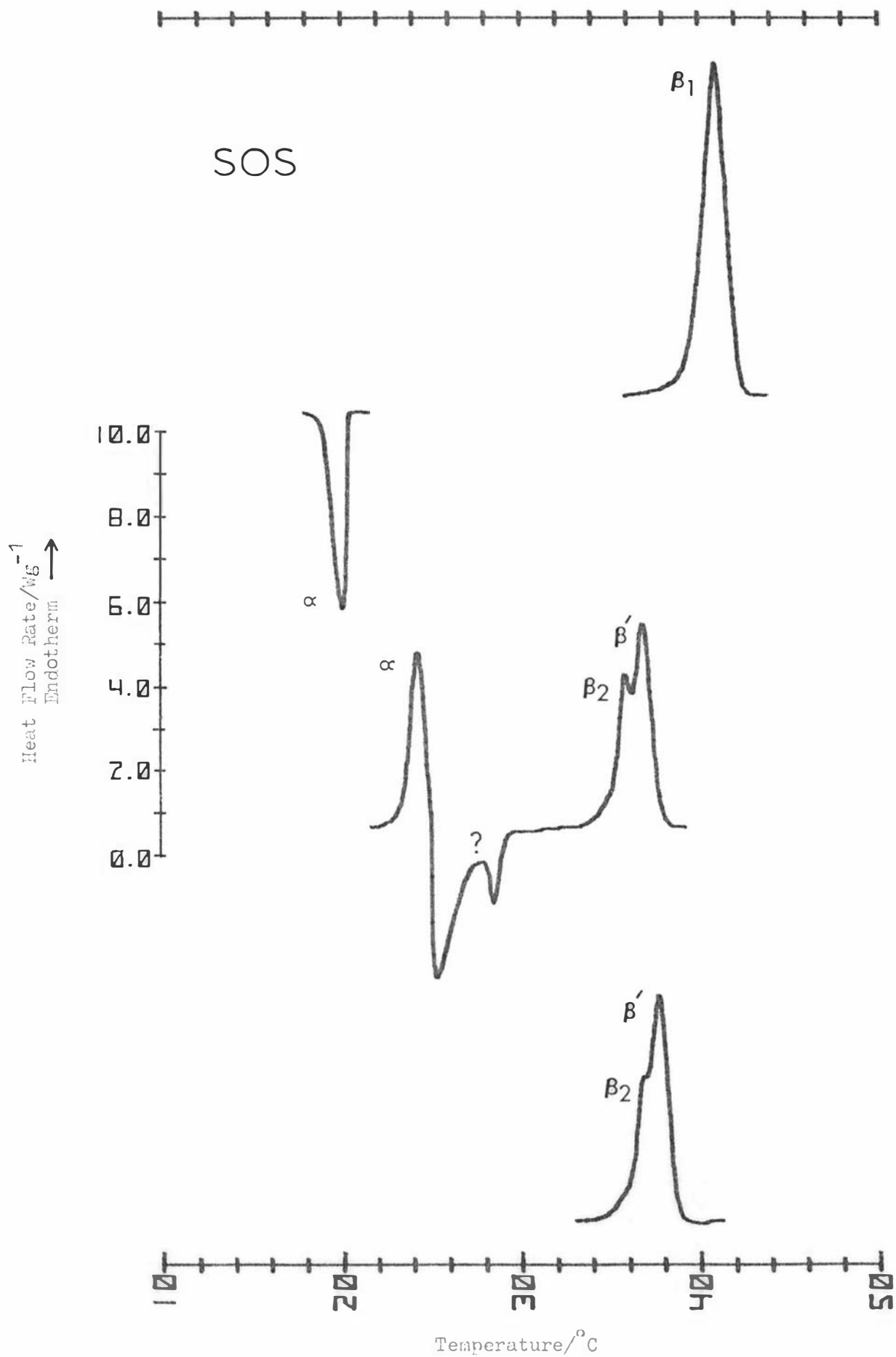


Fig. 21: Thermal behaviour of SO<sub>3</sub>.

(From top to bottom) melting of β from solvent; crystallisation of α, transformation of α; transformation of the intermediate form(s) prepared by transformation of α at 24°C for 5 min (all recorded at 4°C/min).

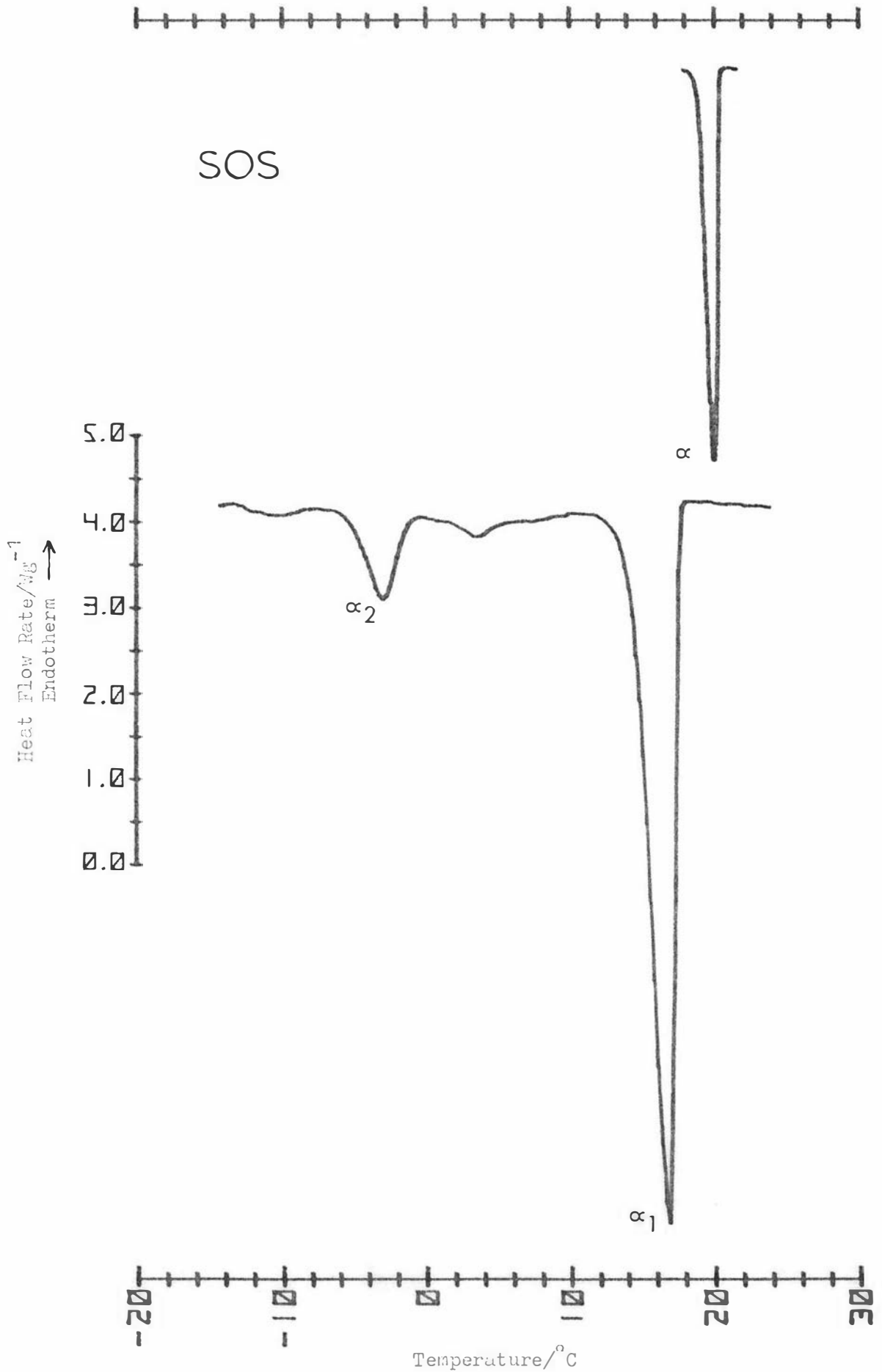


Fig. 22: Crystallisation of SOS from the melt at 4°C/min (top) and 16°C/min (bottom). The thermograms are compared on the basis of heat flow rate rather than apparent heat capacity to allow the detail in the bottom thermogram to be seen readily.

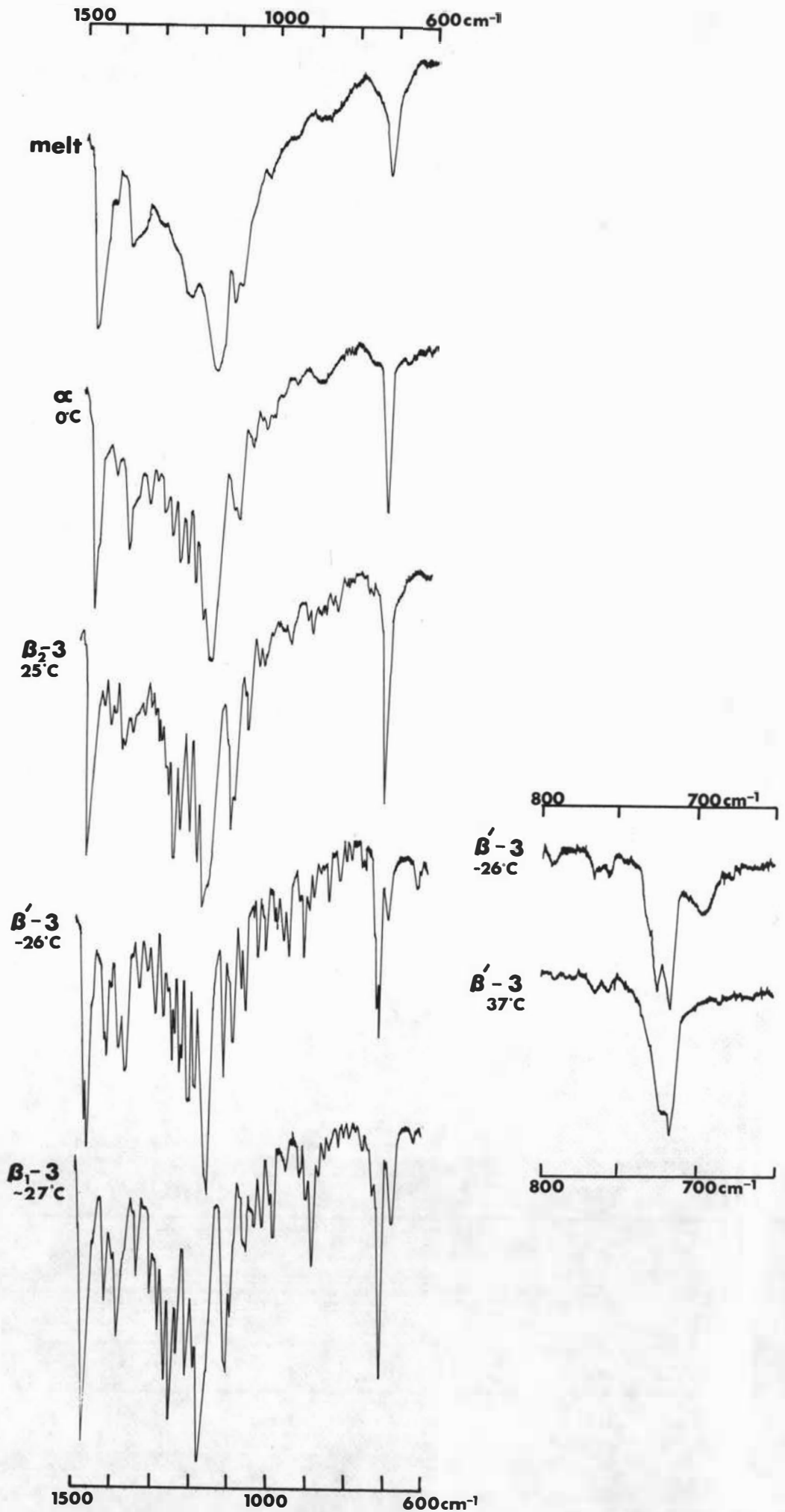
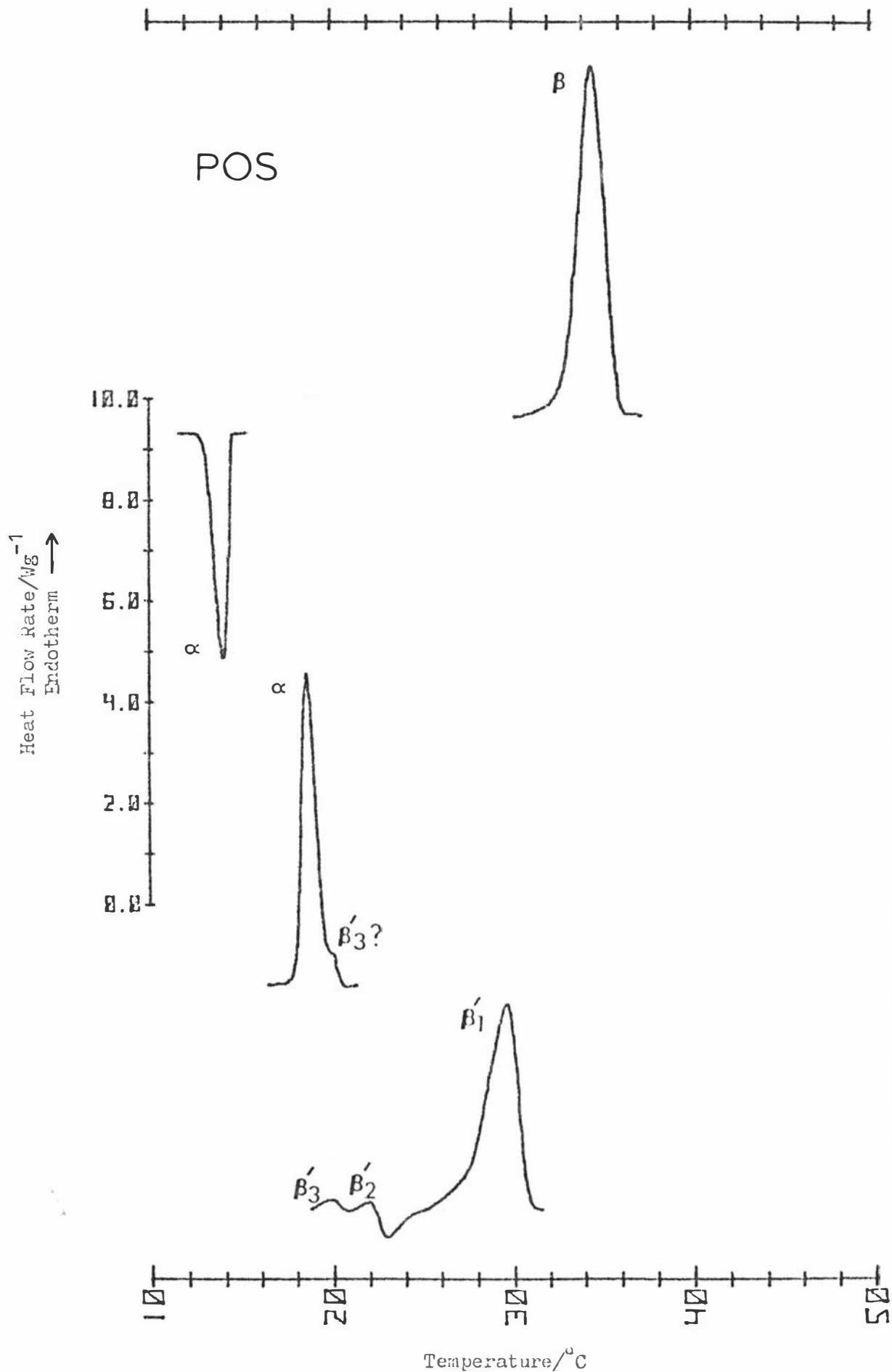
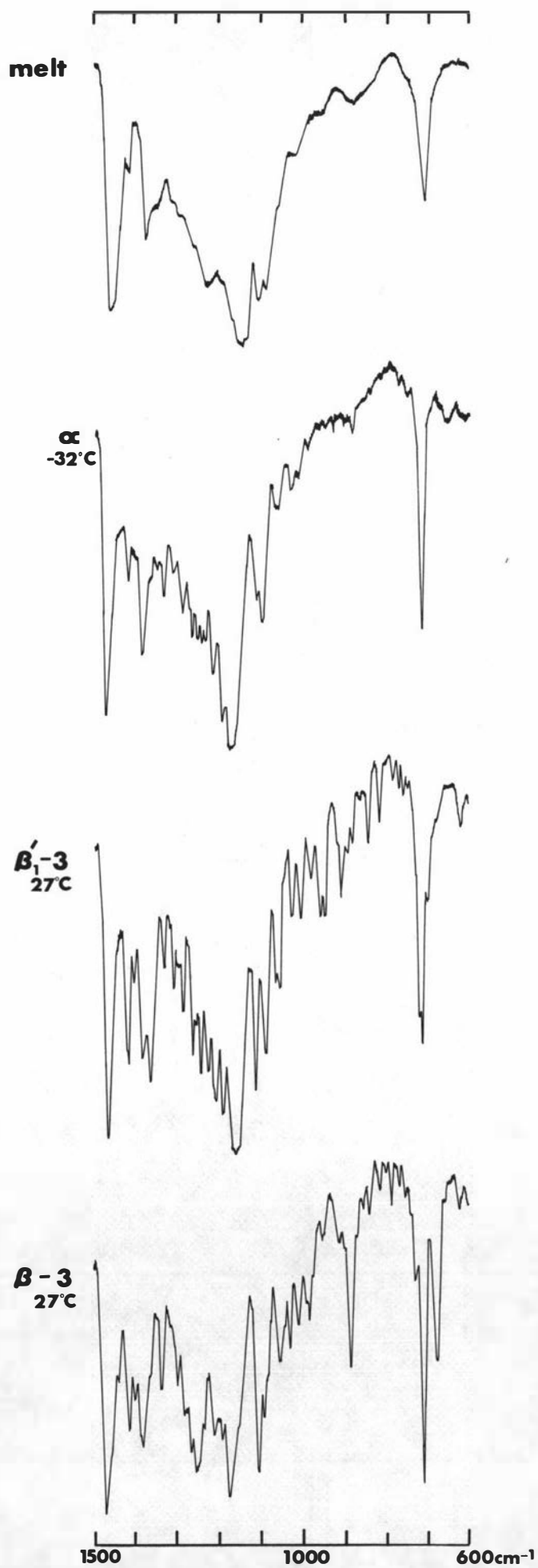


Fig.23 IR Spectra of SOS



**Fig. 24:** Thermal behaviour of POS.  
 (From top to bottom) melting of  $\beta$  from solvent; crystallisation of  $\alpha$ ; melting of  $\alpha$ ; melting of  $\beta'$  prepared by transformation of  $\alpha$  at  $19^\circ\text{C}$  for 15 min (all recorded at  $4^\circ\text{C}/\text{min}$ ).

**Fig.25 IR Spectra of POS**

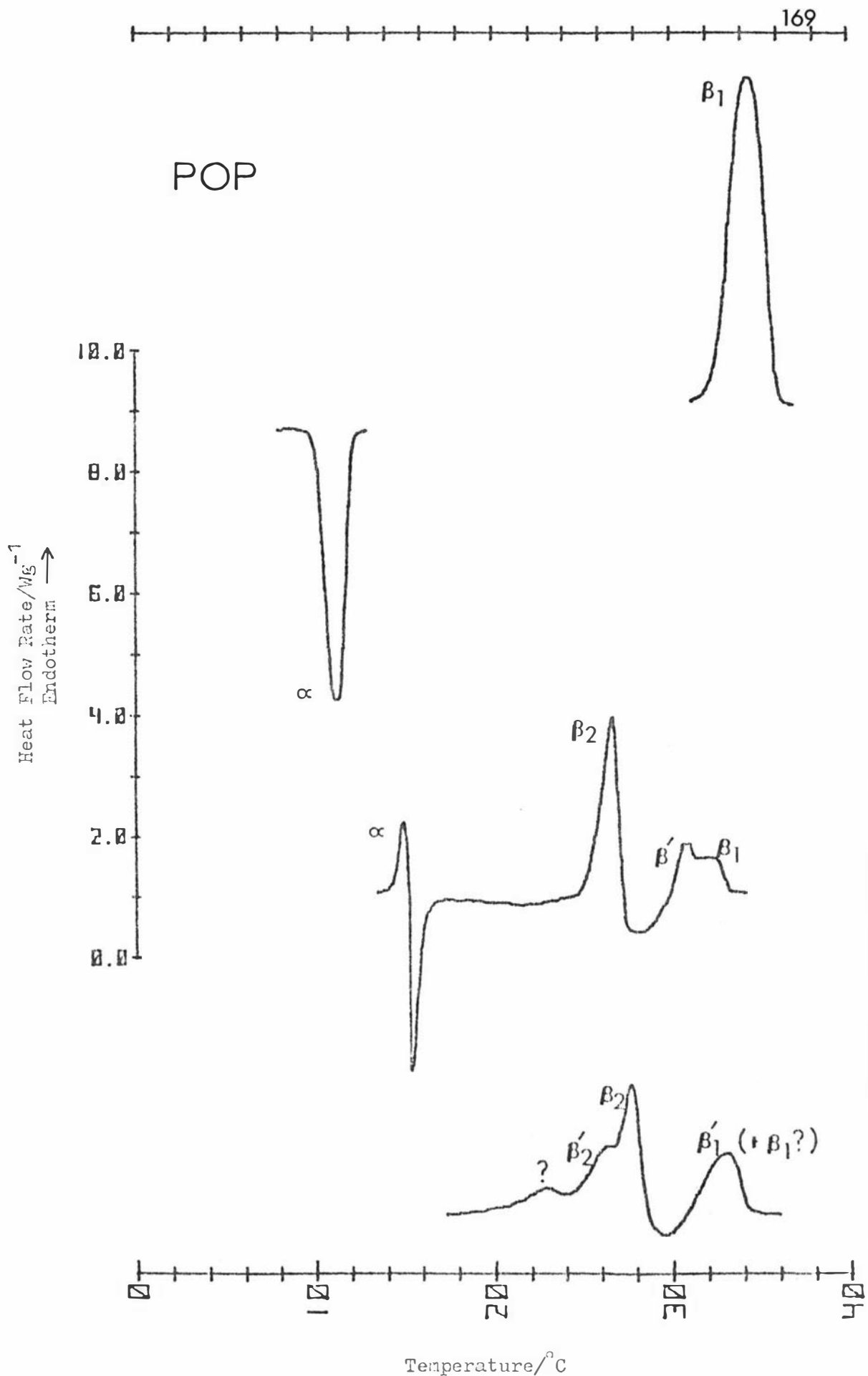


Fig. 26: Thermal behaviour of POP.

(From top to bottom) melting of  $\beta$  from solvent; crystallisation of  $\alpha$ ; transformation of the intermediate forms prepared by crystallisation of the melt at  $16^\circ\text{C}$  for 5 min (recorded at 4, 4, 2 and  $4^\circ\text{C}/\text{min}$  respectively).

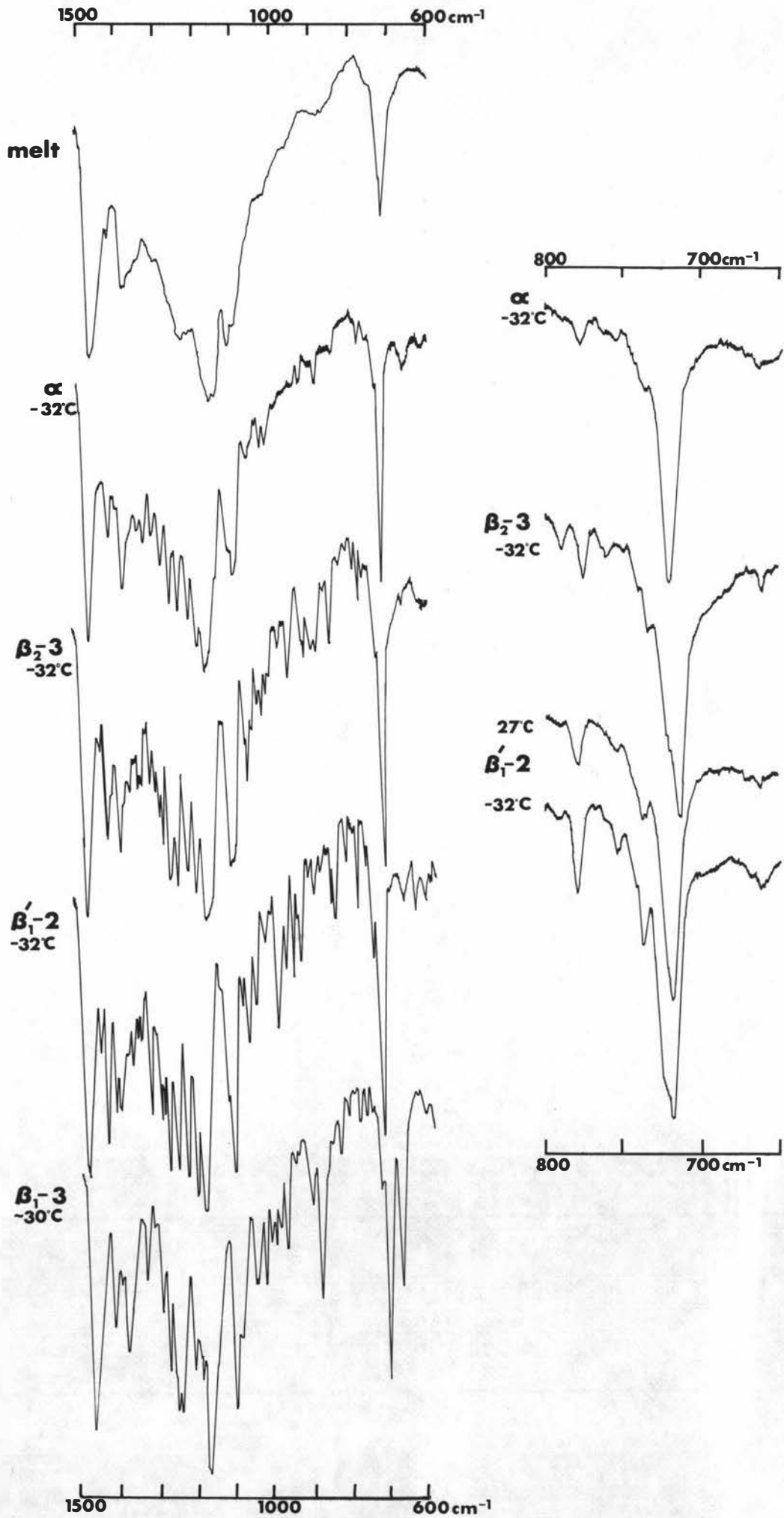


Fig. 27 IR Spectra of POP

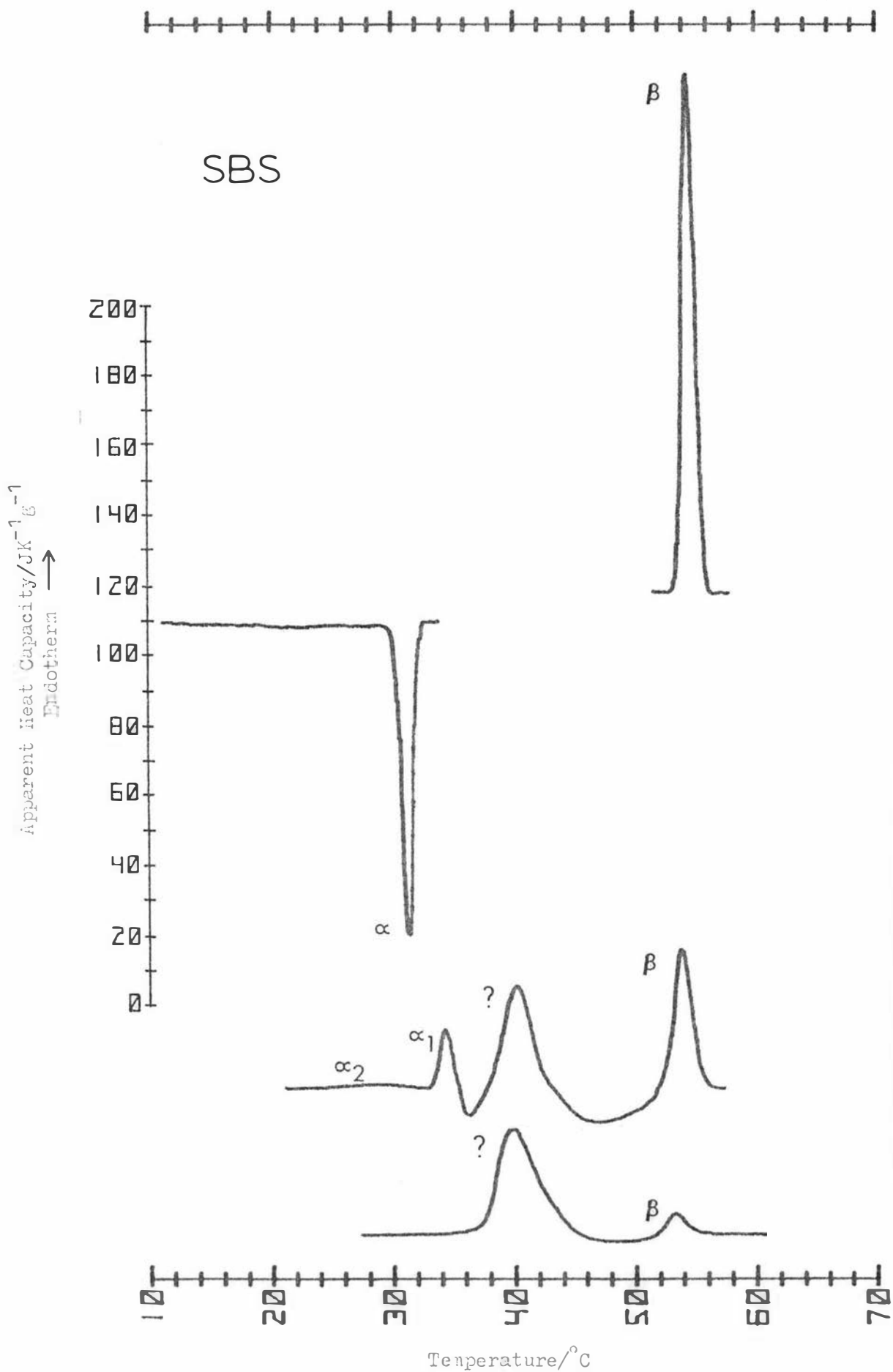
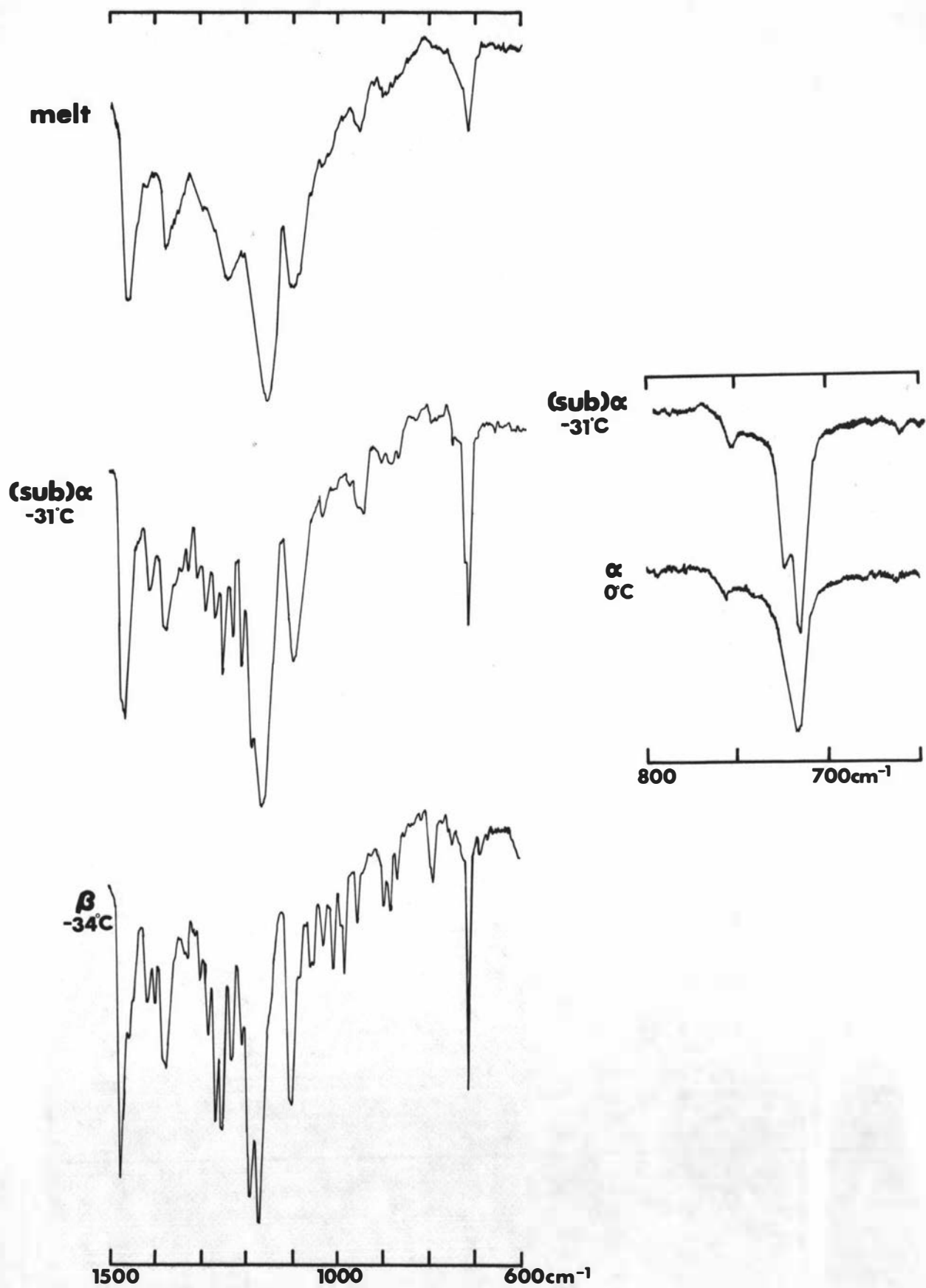
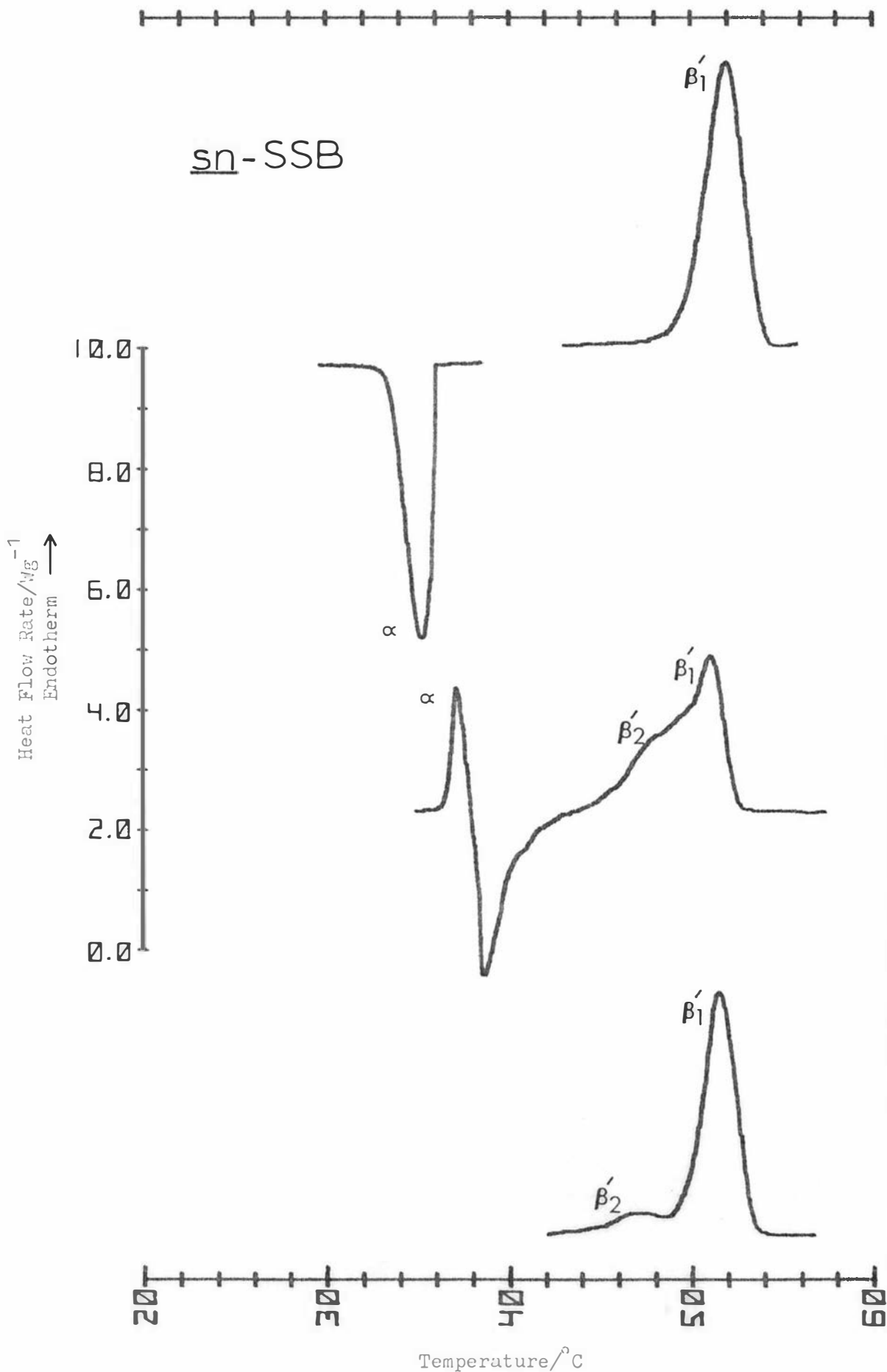


Fig. 28: Thermal behaviour of SBS.

(From top to bottom) melting of β from solvent; crystallisation of α accompanied by some transformation; transformation of α from the shock-cooled melt; melting of the intermediate form obtained by transformation of α at 34°C for 3 min (recorded at 4, 4, 6 and 16°C/min respectively).



**Fig. 29** IR Spectra of SBS



**Fig. 30:** Thermal behaviour of sn-SSB.  
 (From top to bottom) melting of  $\beta'$  from solvent; crystallisation of  $\alpha$ ;  
 transformation of  $\alpha$ ; melting of the  $\beta'$  forms obtained by crystallisation  
 of the melt at 38°C for 30-45 min (all recorded at 4°C/min).

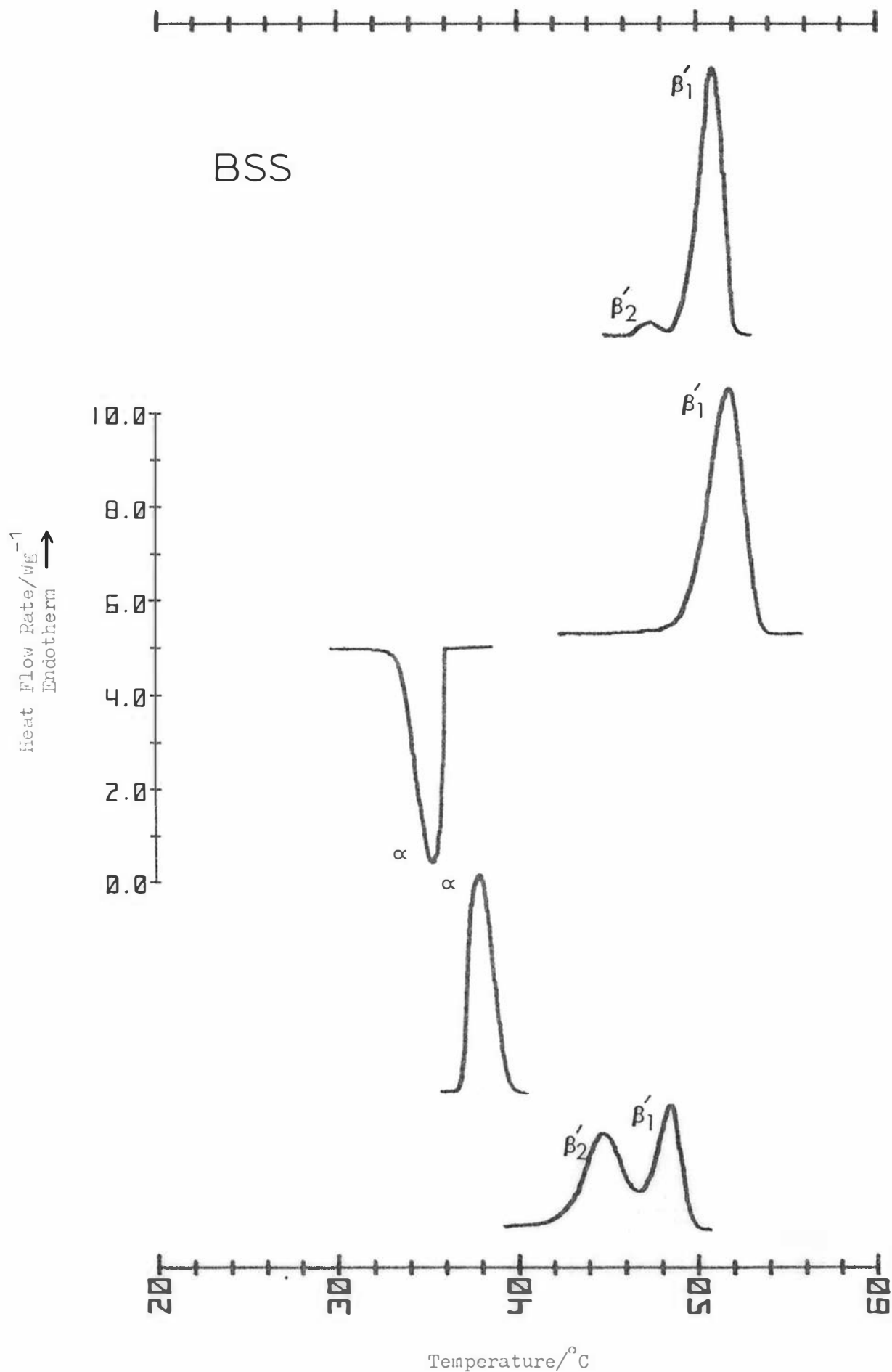


**Fig. 31:** Thermal behaviour of BSS.

(From top to bottom) melting of the  $\beta'$  forms obtained from solvent; melting of  $\beta'_1$  after momentary tempering at the  $\beta'_2$  peak temperature; crystallisation of  $\alpha$ ; melting of  $\alpha$ ; melting of the  $\beta'$  forms obtained by transformation of  $\alpha$  at  $38^\circ\text{C}$  for 45 min (all recorded at  $4^\circ\text{C}/\text{min}$ ).

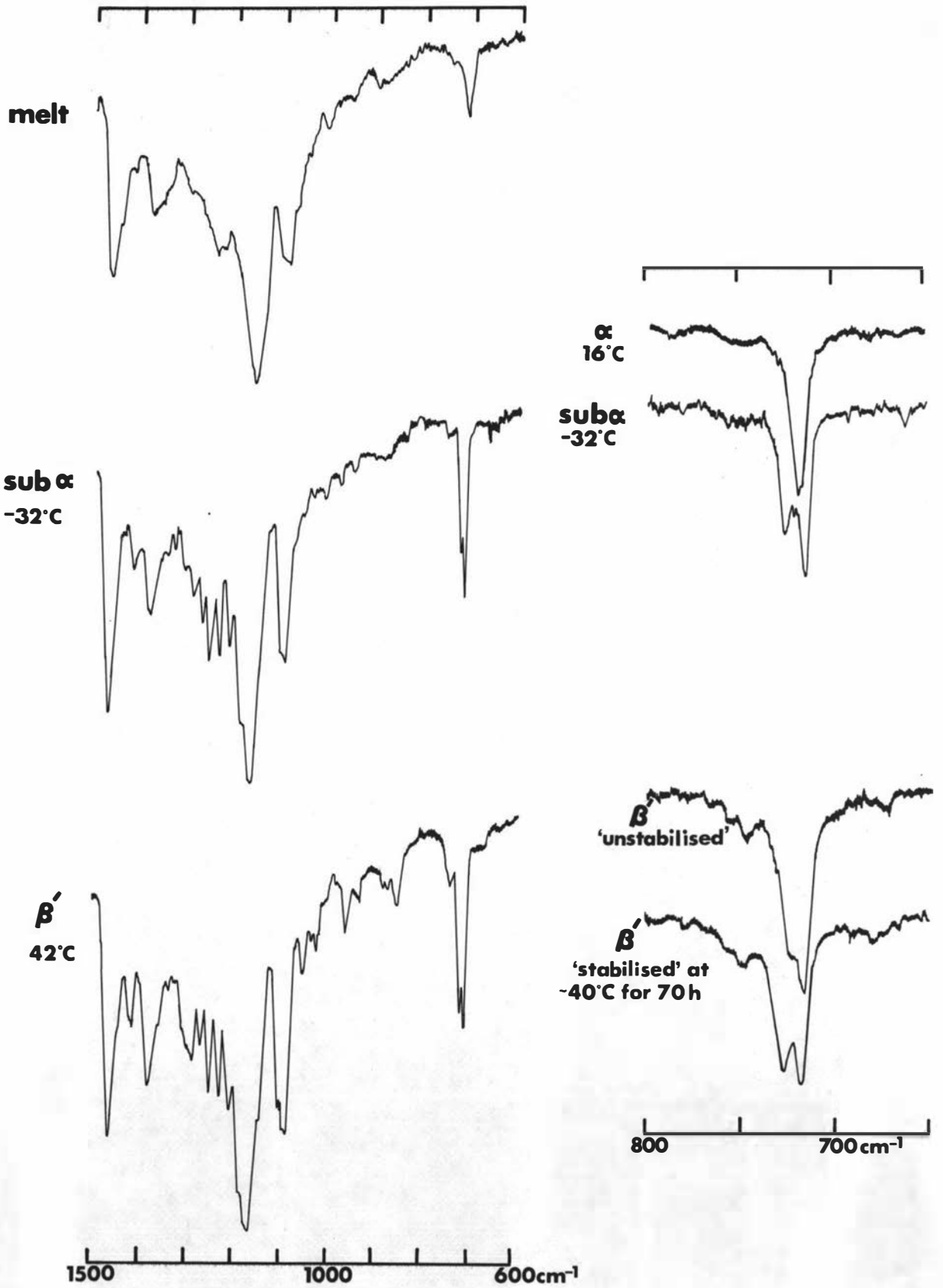


**Fig.32 IR Spectra of BSS**

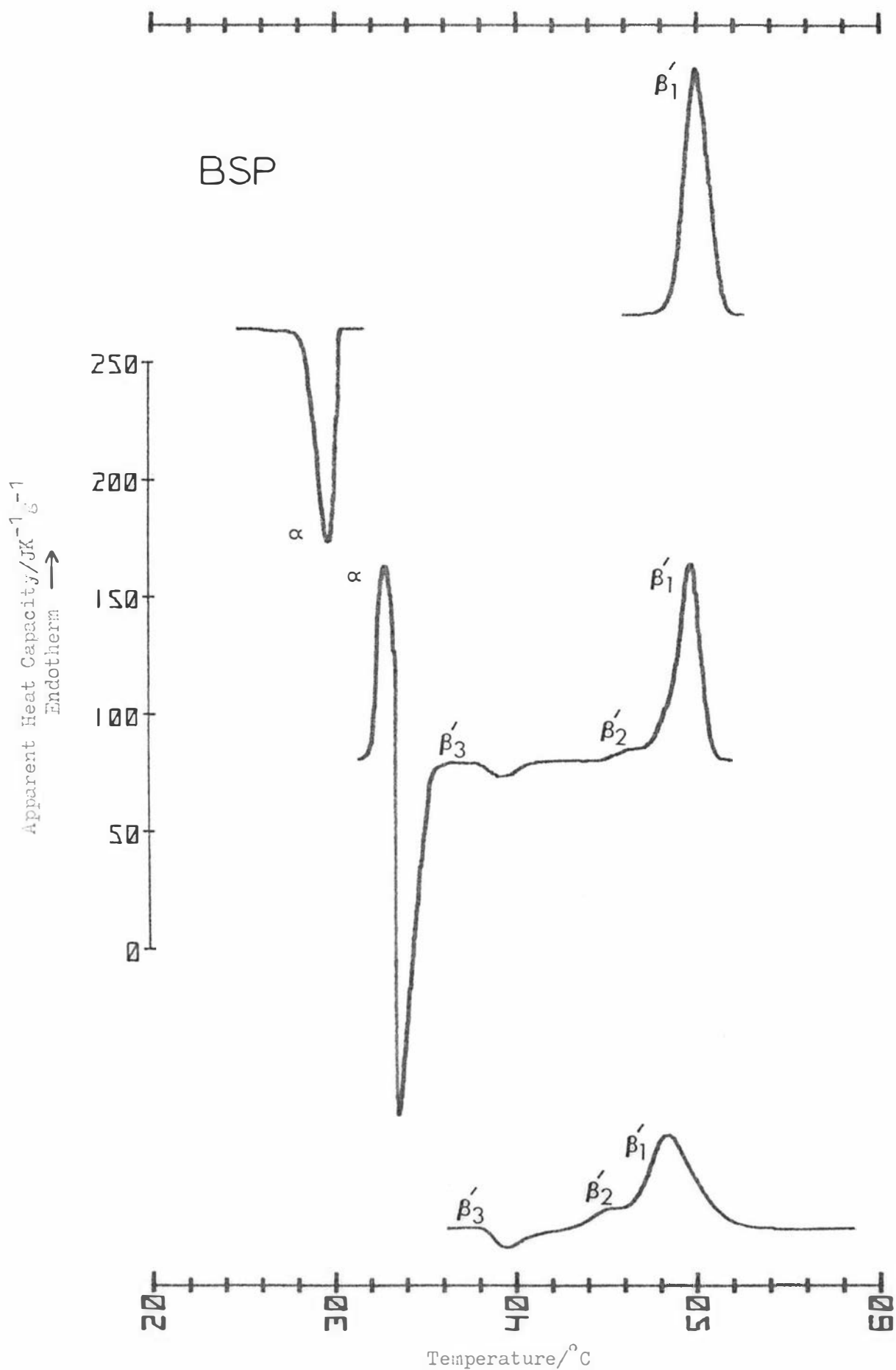


Fig. 33: Thermal behaviour of BSP.  
 (From top to bottom) melting of  $\beta'$  from solvent; crystallisation of  $\alpha$ ; transformation of  $\alpha$ ; melting of the  $\beta'$  forms obtained by transformation of  $\alpha$  at  $32^{\circ}\text{C}$  for 2 min (recorded at 4, 4, 4 and  $16^{\circ}\text{C}/\text{min}$  respectively).

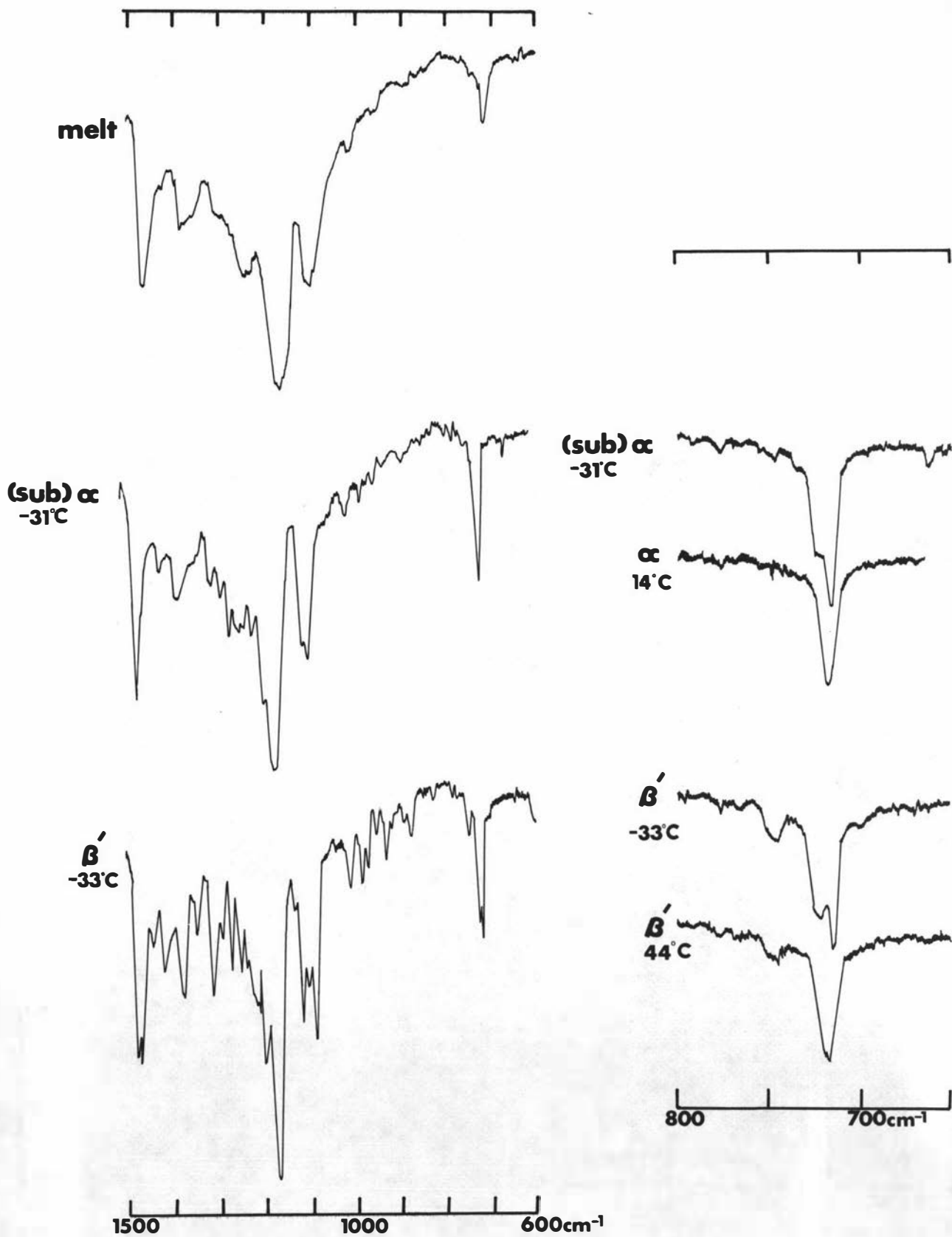


Fig. 34 IR Spectra of BSP

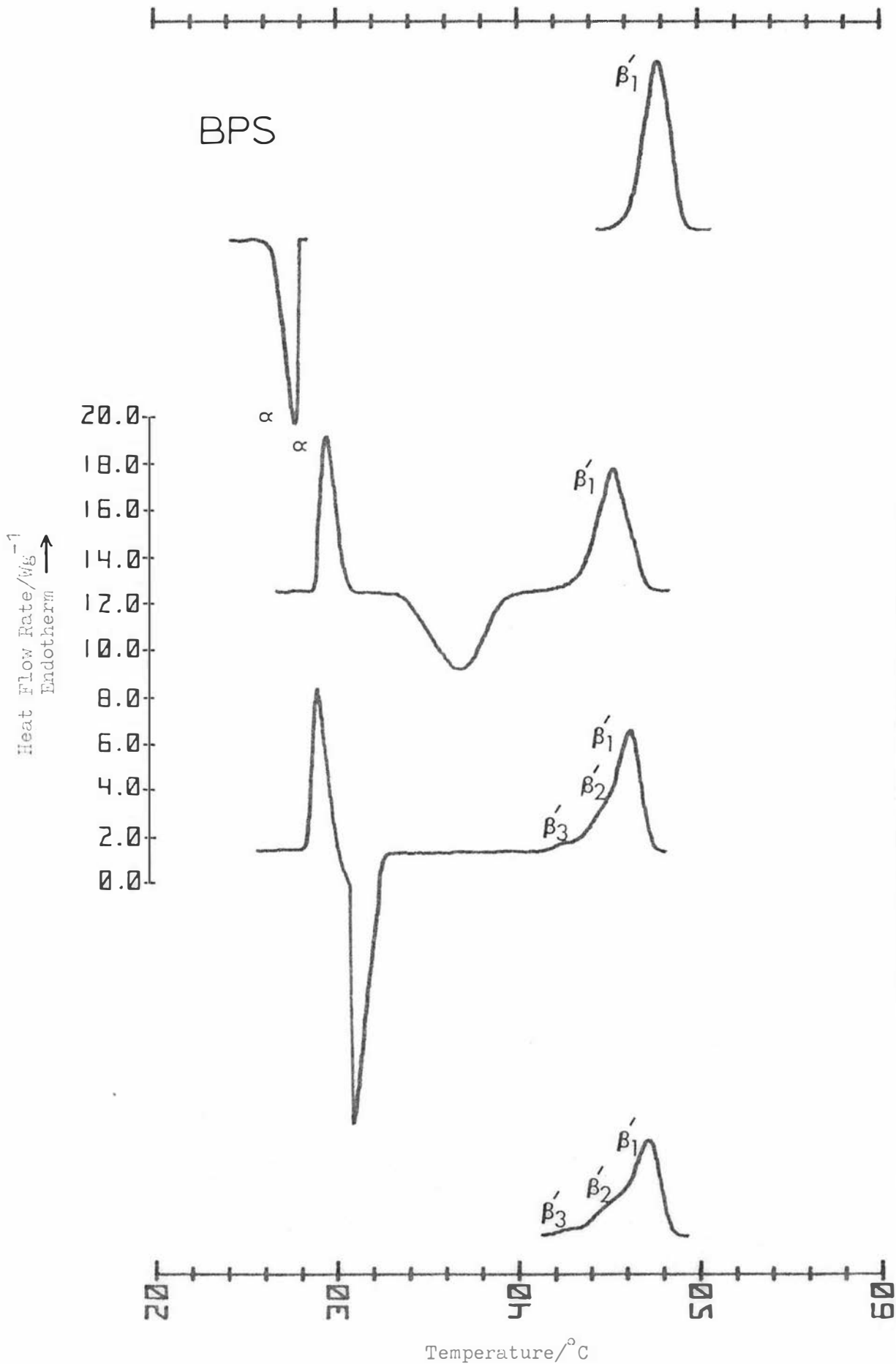
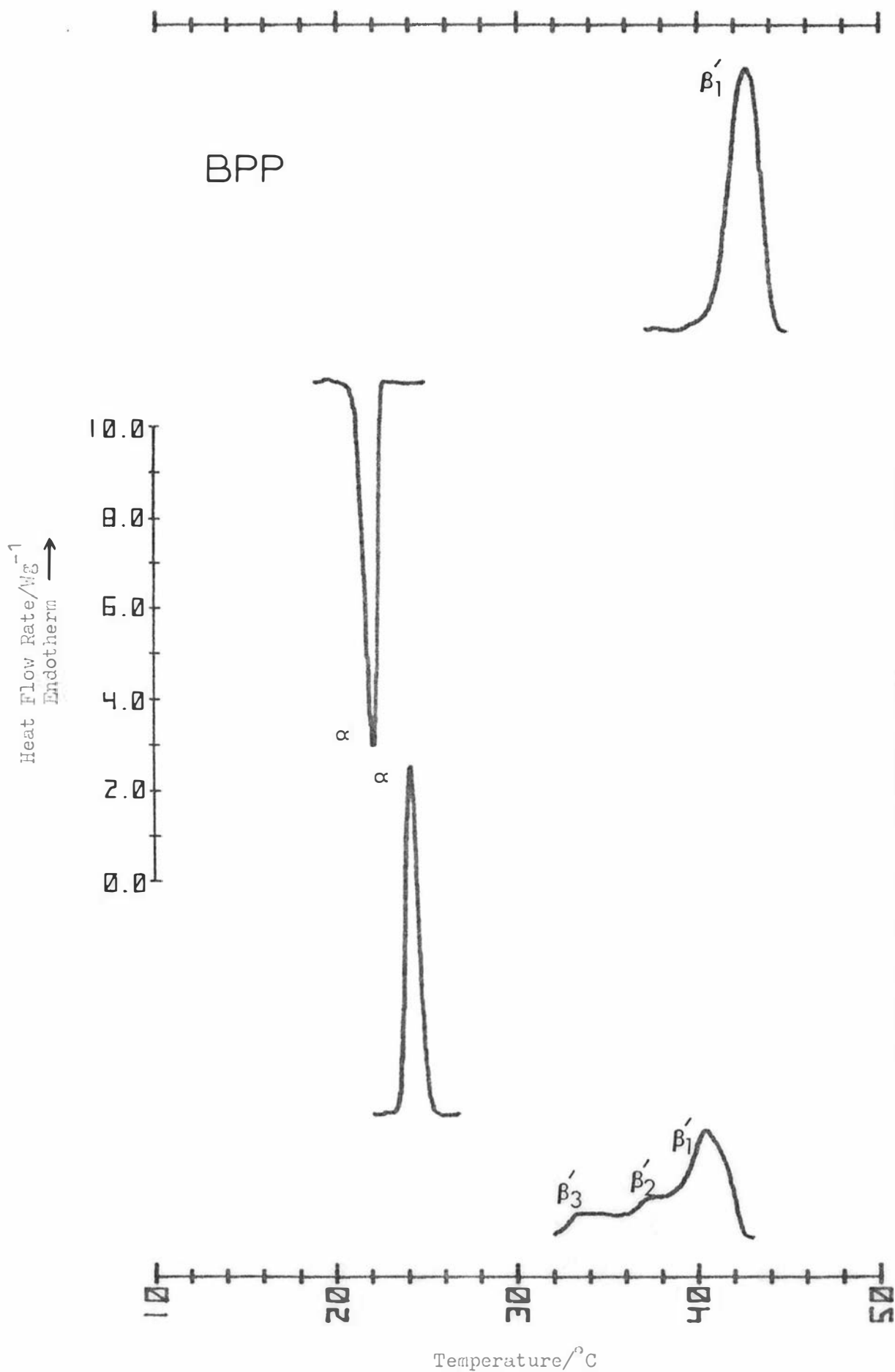
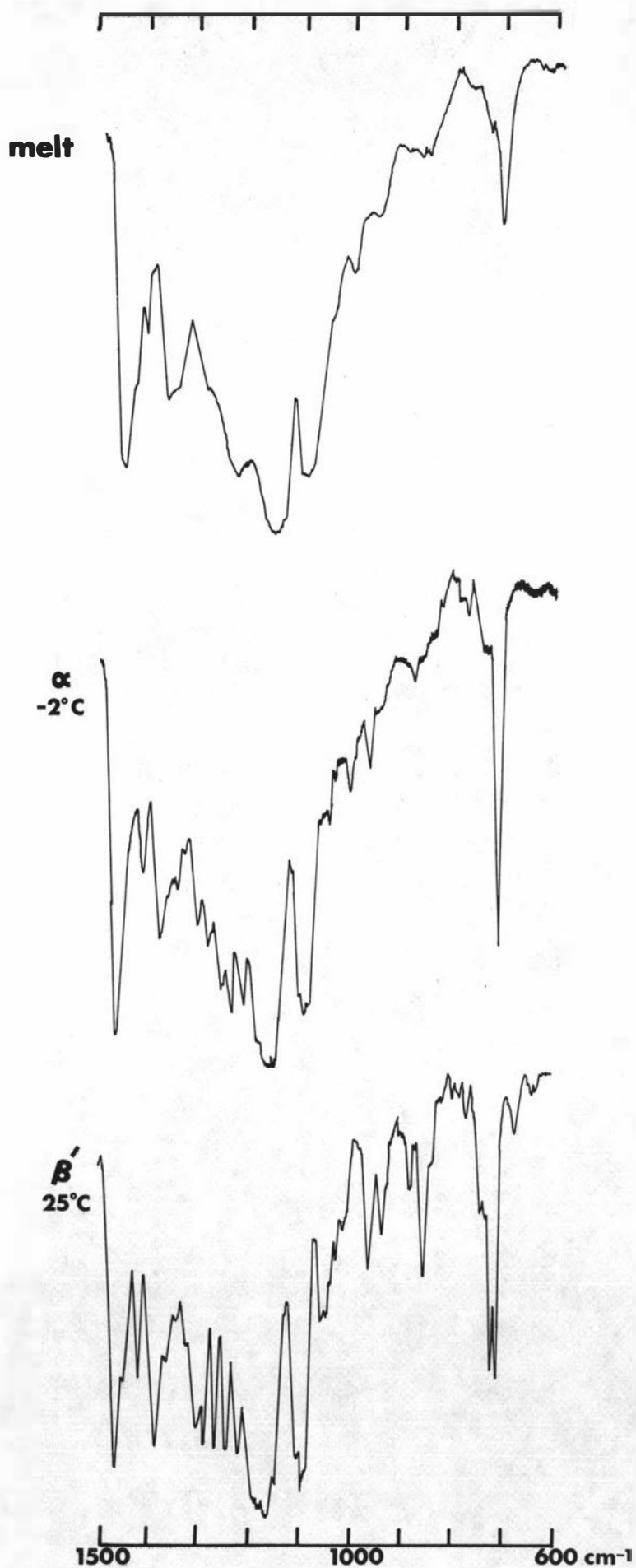


Fig. 35: Thermal behaviour of BPS.

(From top to bottom) melting of  $\beta'$  from solvent; crystallisation of  $\alpha$ , transformation of  $\alpha$  crystallised by cooling at  $4^\circ\text{C}/\text{min}$ ; transformation of  $\alpha$  crystallised by shock-cooling; melting of the  $\beta'$  forms prepared by transformation of  $\alpha$  at  $29^\circ\text{C}$  for 10 min (all recorded at  $4^\circ\text{C}/\text{min}$ ).



**Fig. 36:** Thermal behaviour of BPP.  
 (From top to bottom) melting of  $\beta'$  from solvent; crystallisation of  $\alpha$ ; melting of  $\alpha$ ; melting of the  $\beta'$  forms prepared by transformation of  $\alpha$  at 24°C for 15 min (all recorded at 4°C/min).



**Fig.37 IR Spectra of BPP**

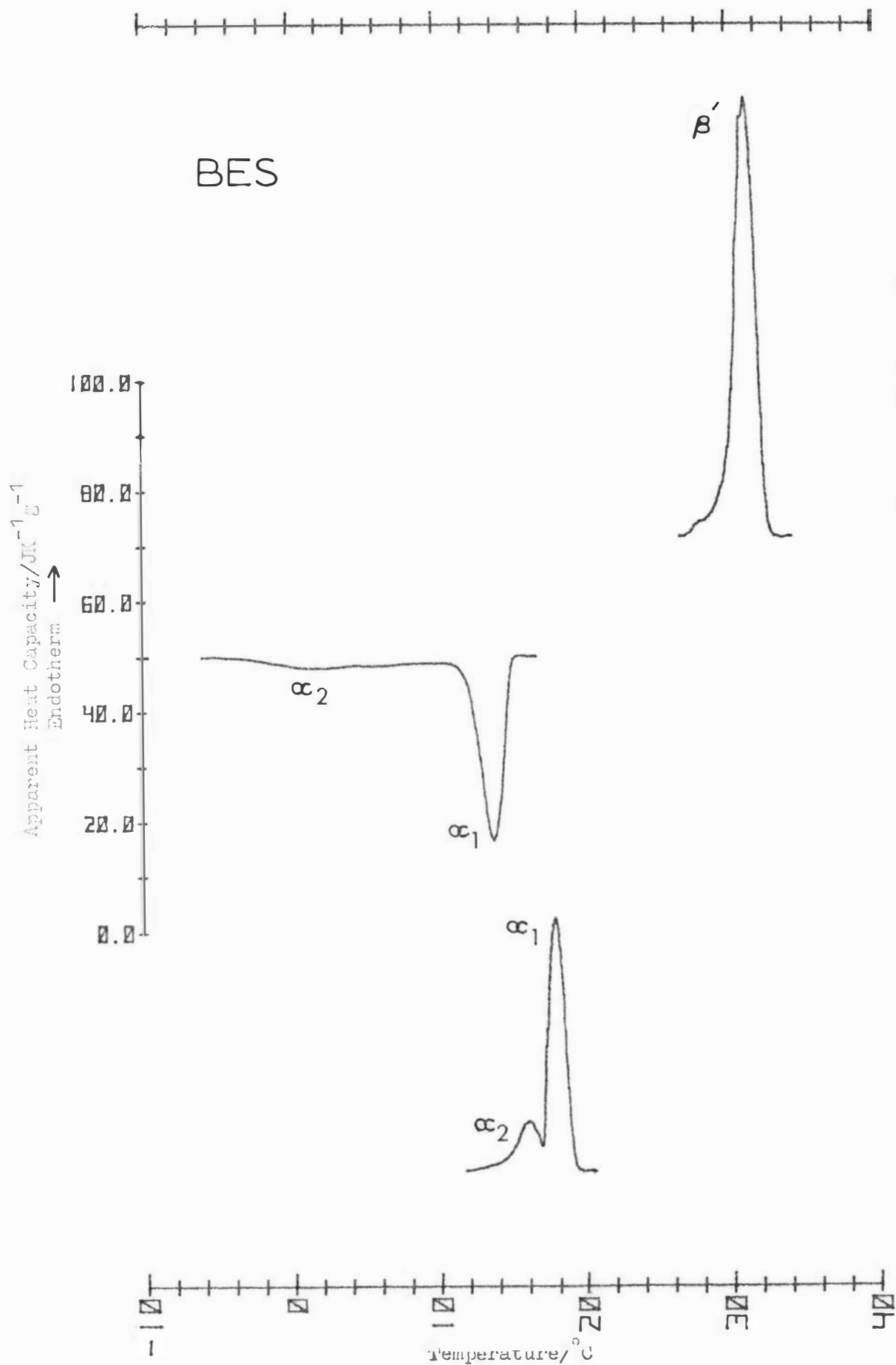


**Fig. 38:** Thermal behaviour of BES.  
 (From top to bottom) melting of  $\beta'$  from solvent; crystallisation of  $\alpha$ ;  
 melting of  $\alpha$  (recorded at 4, 8 and 4°C/min respectively).

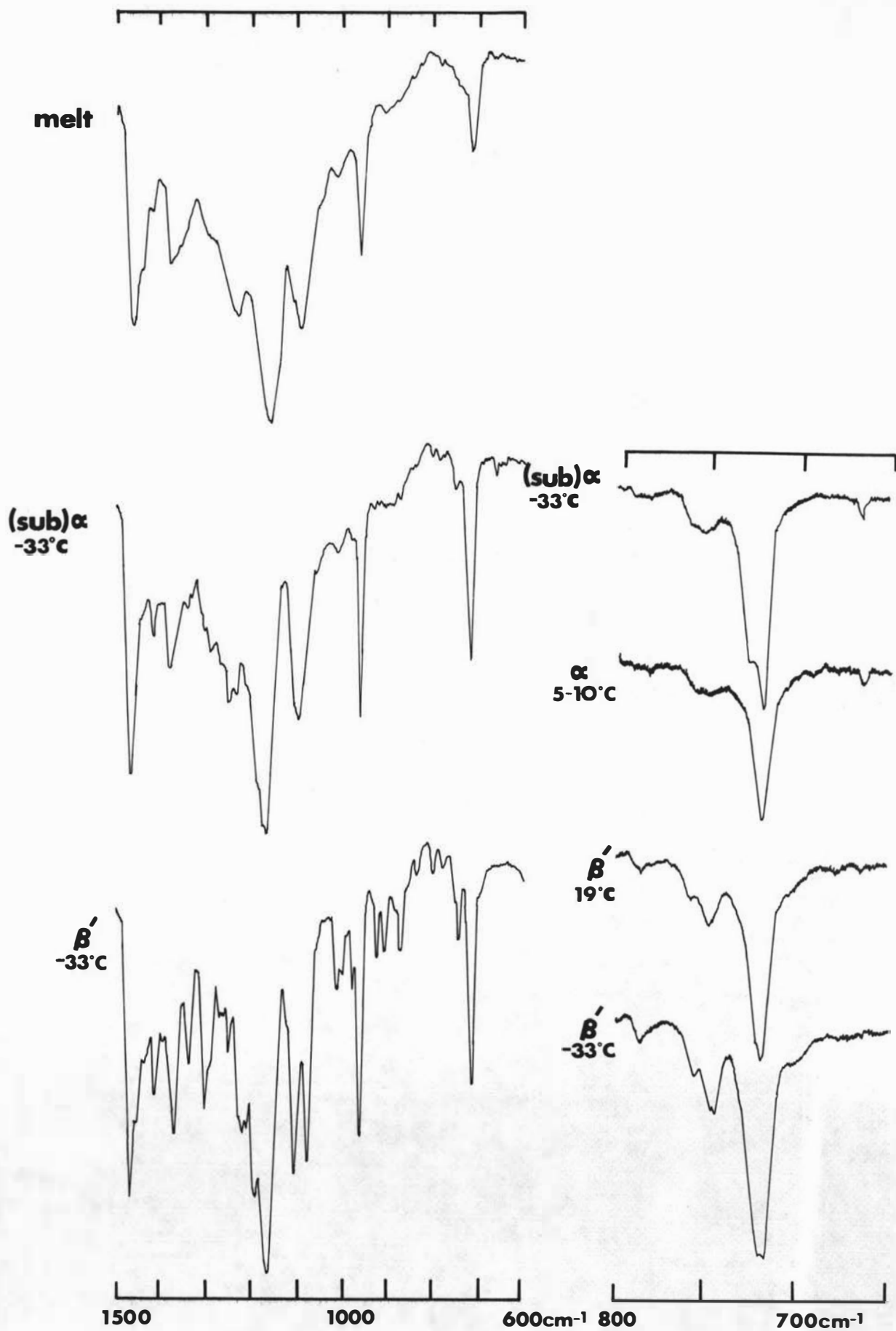
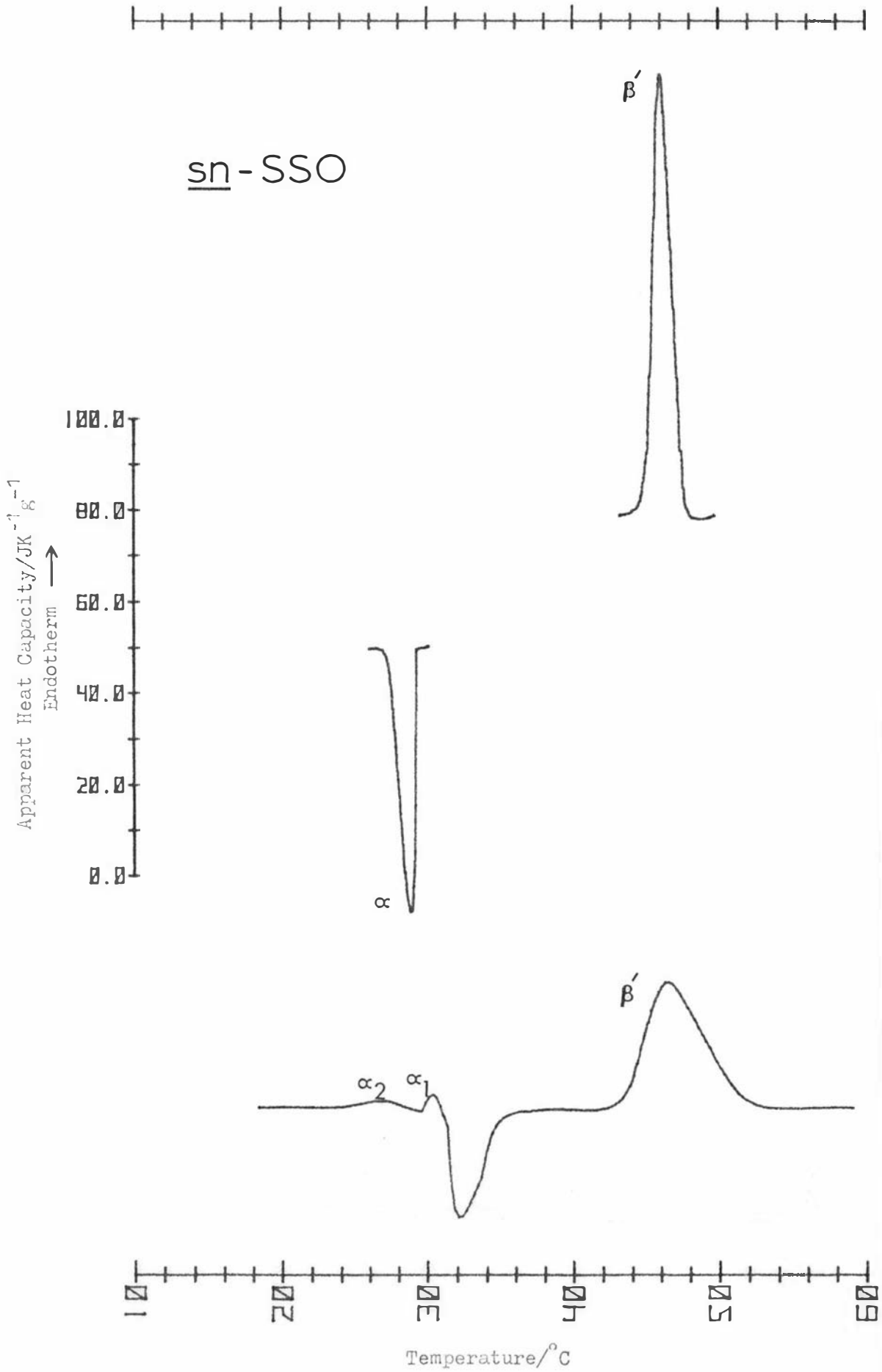
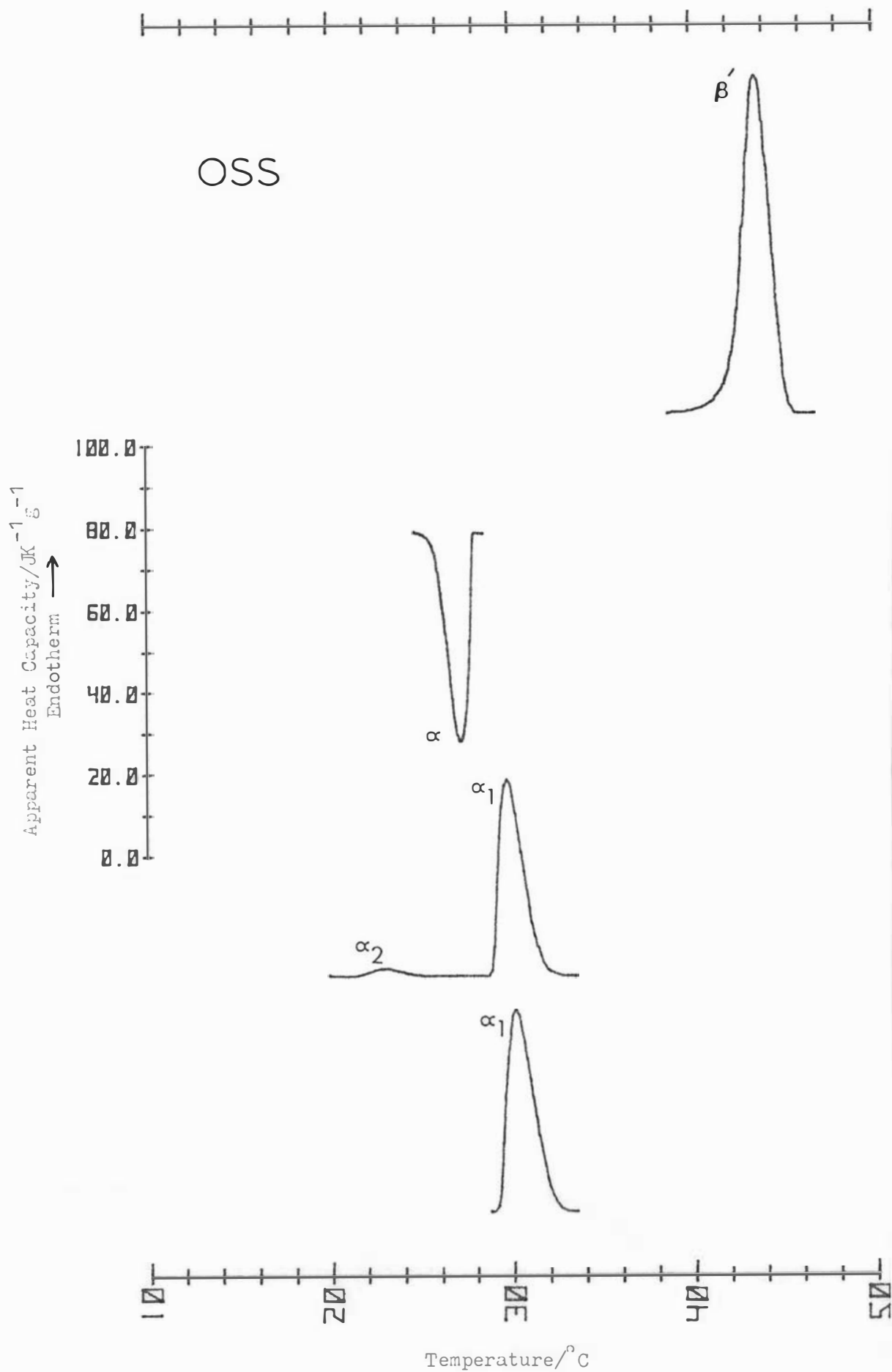


Fig. 39 IR Spectra of BES



**Fig. 40:** Thermal behaviour of sn-SSO.  
 (From top to bottom) melting of  $\beta'$  from solvent; crystallisation of  $\alpha$ ;  
 transformation of  $\alpha$  (recorded at 4, 4 and 16  $^{\circ}\text{C}/\text{min}$  respectively).



**Fig. 41:** Thermal behaviour of OSS.  
 (From top to bottom) melting of  $\beta'$  from solvent; crystallisation of  $\alpha$ ; melting of  $\alpha$ ; melting of  $\alpha$  after tempering at the  $\alpha_2$  peak temperature for 5 min (recorded at 4, 4, 8 and 8°C/min respectively).

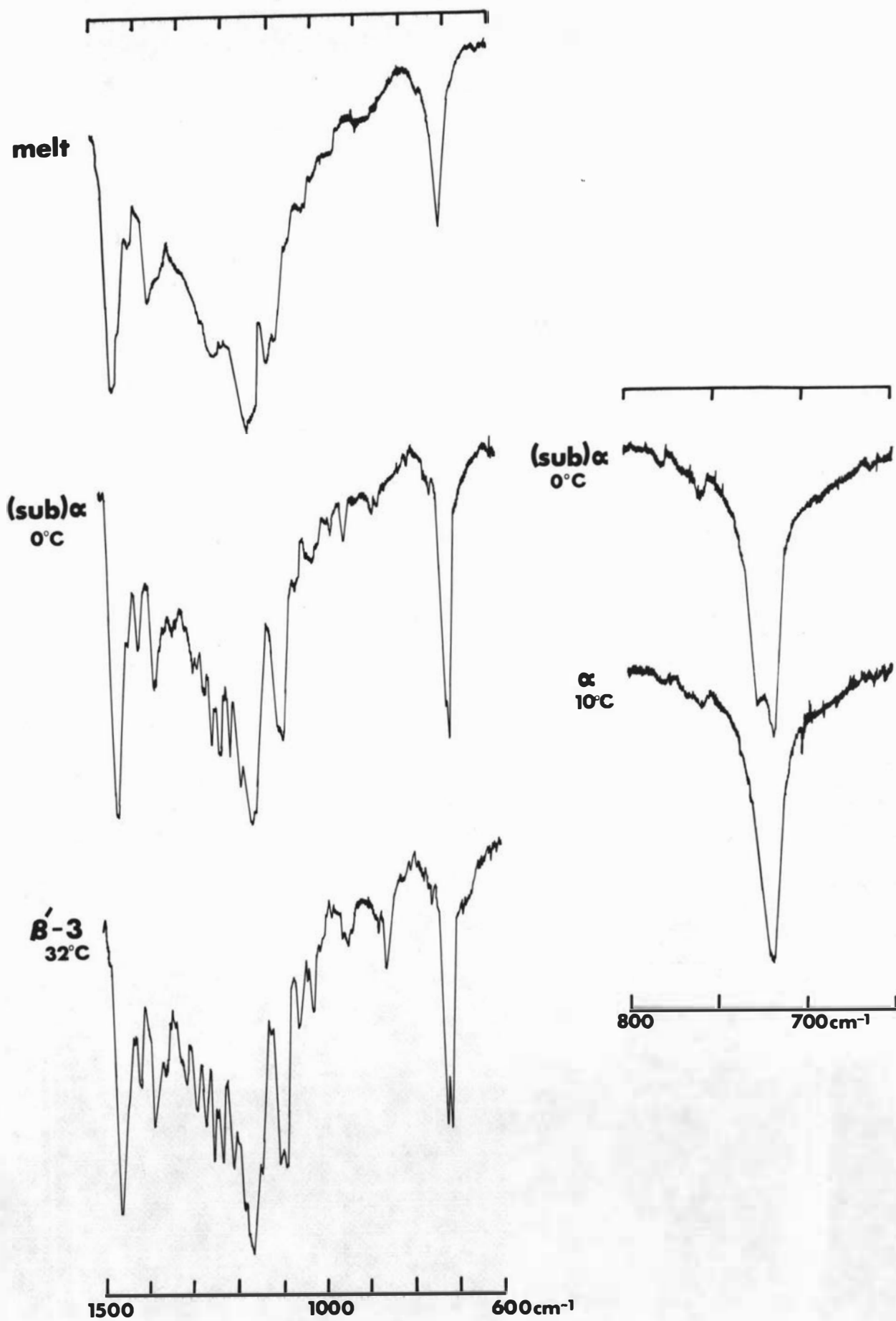
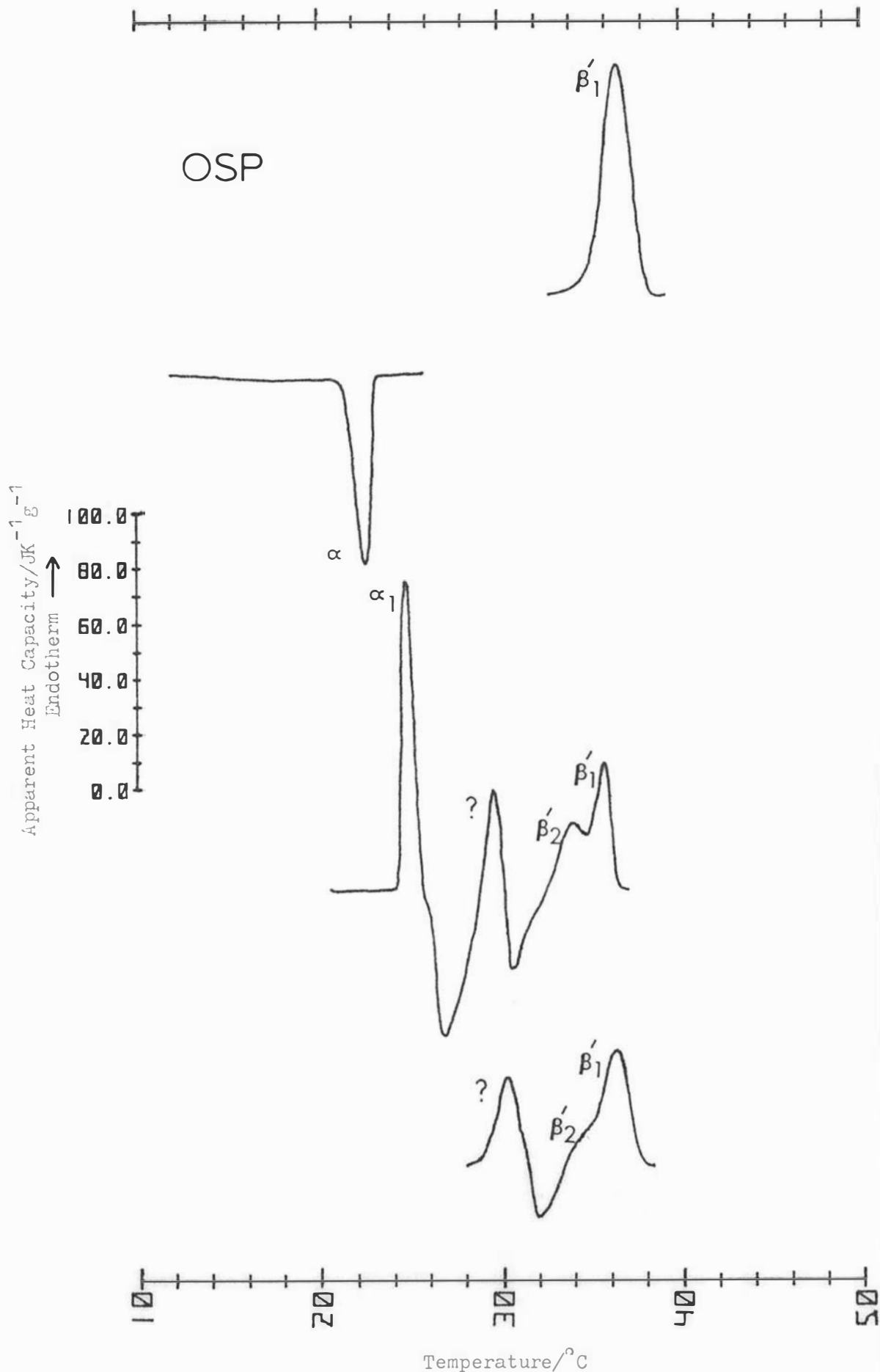


Fig. 42 IR Spectra of OSS



**Fig. 43:** Thermal behaviour of OSP.  
 (From top to bottom) melting of β' from solvent; crystallisation of α; transformation of α crystallised by cooling at 4 °C/min; transformation of intermediate form(s) prepared by transformation of α at 24 °C for 5 min (recorded at 4, 4, 2 and 4 °C/min respectively).

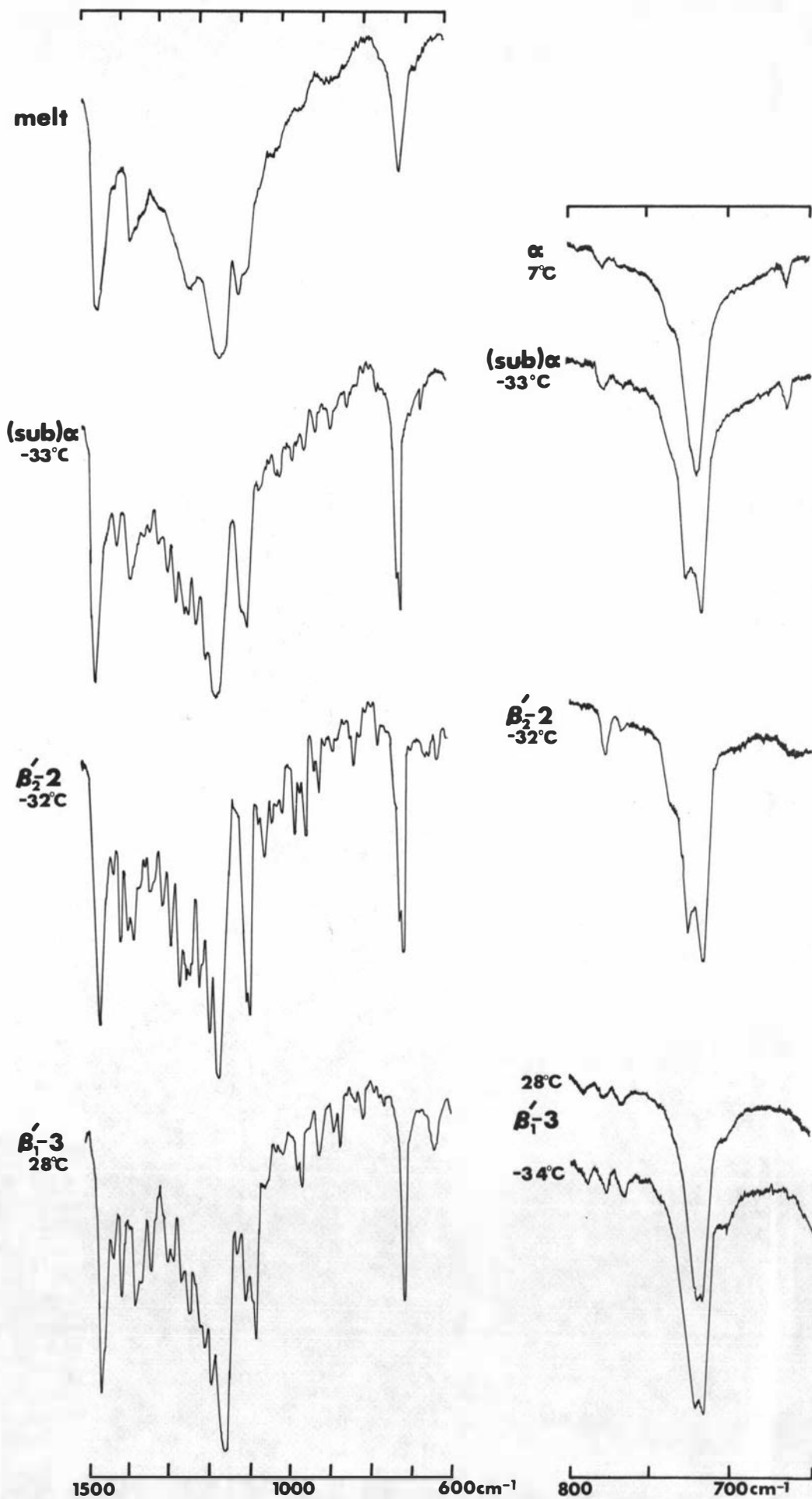


Fig. 44 IR Spectra of OSP

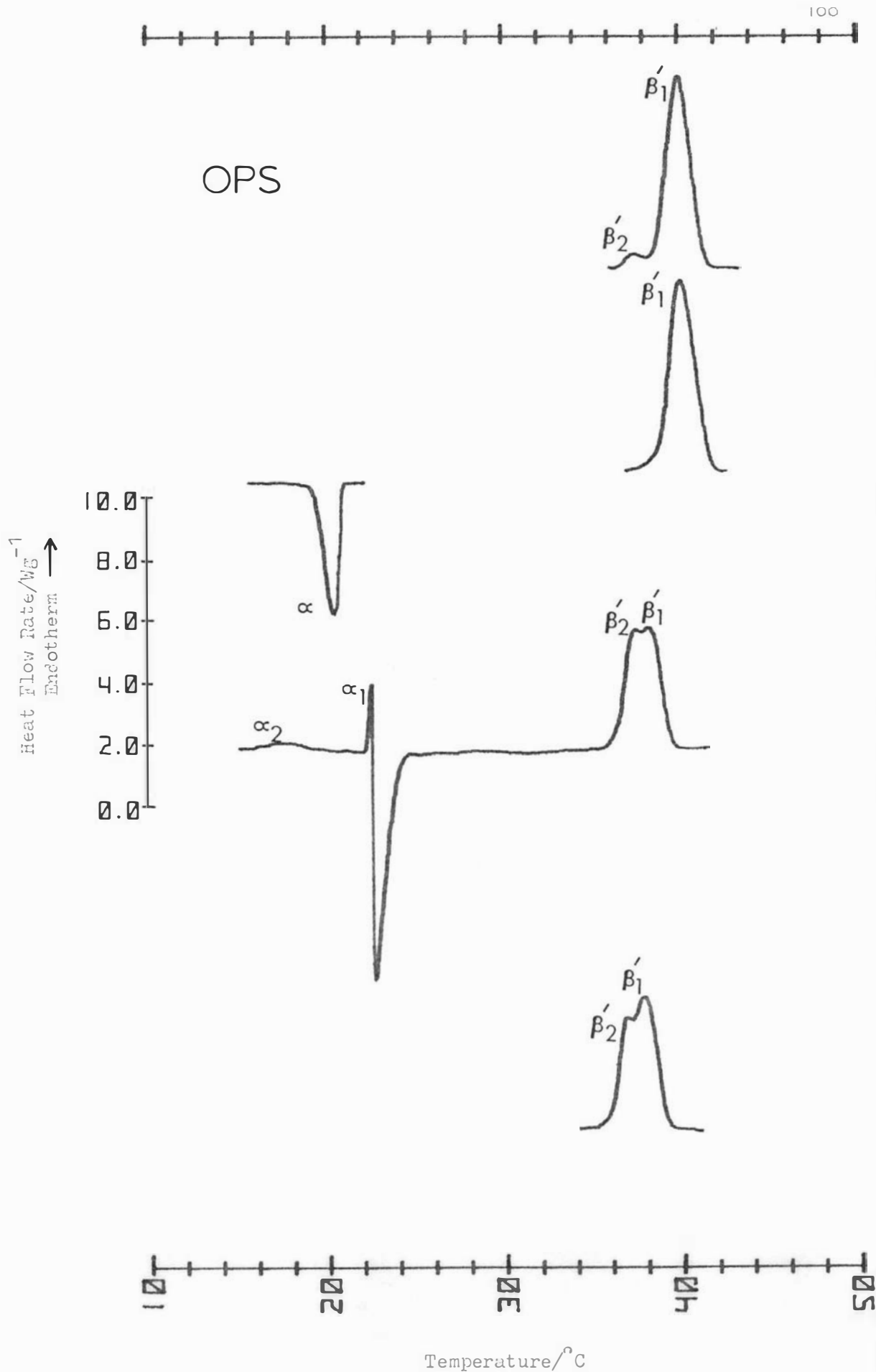


Fig. 45: Thermal behaviour of OPS.  
 (From top to bottom) melting of the  $\beta'$  forms obtained from solvent; melting of  $\beta'_1$  after tempering at the  $\beta'_2$  peak temperature for 2 min; crystallisation of  $\alpha$ ; transformation of  $\alpha$  crystallised by shock-cooling; melting of the  $\beta'$  forms obtained by crystallisation of the melt at 23°C for 3 min (all recorded at 4°C/min).

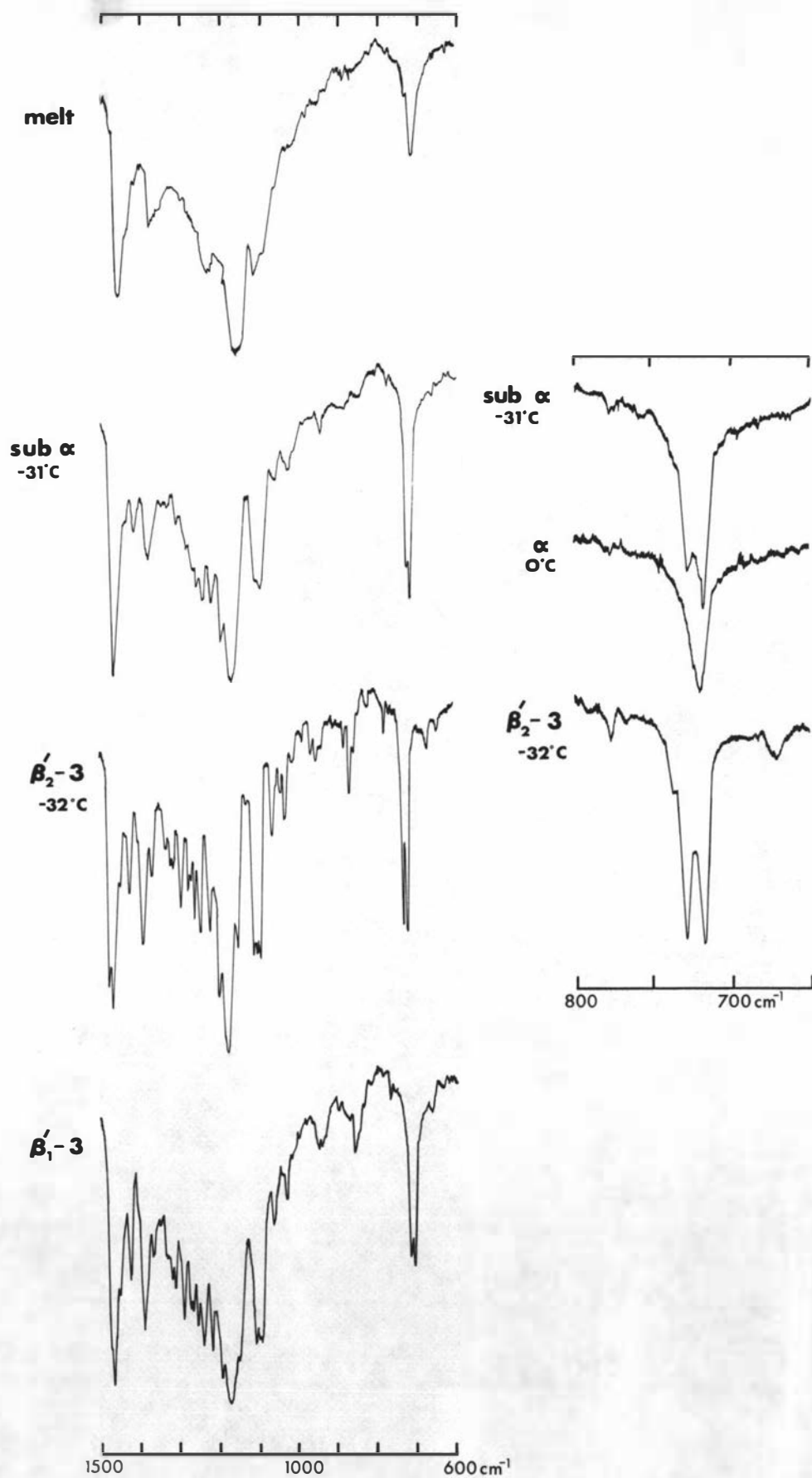


Fig. 46 IR Spectra of OPS

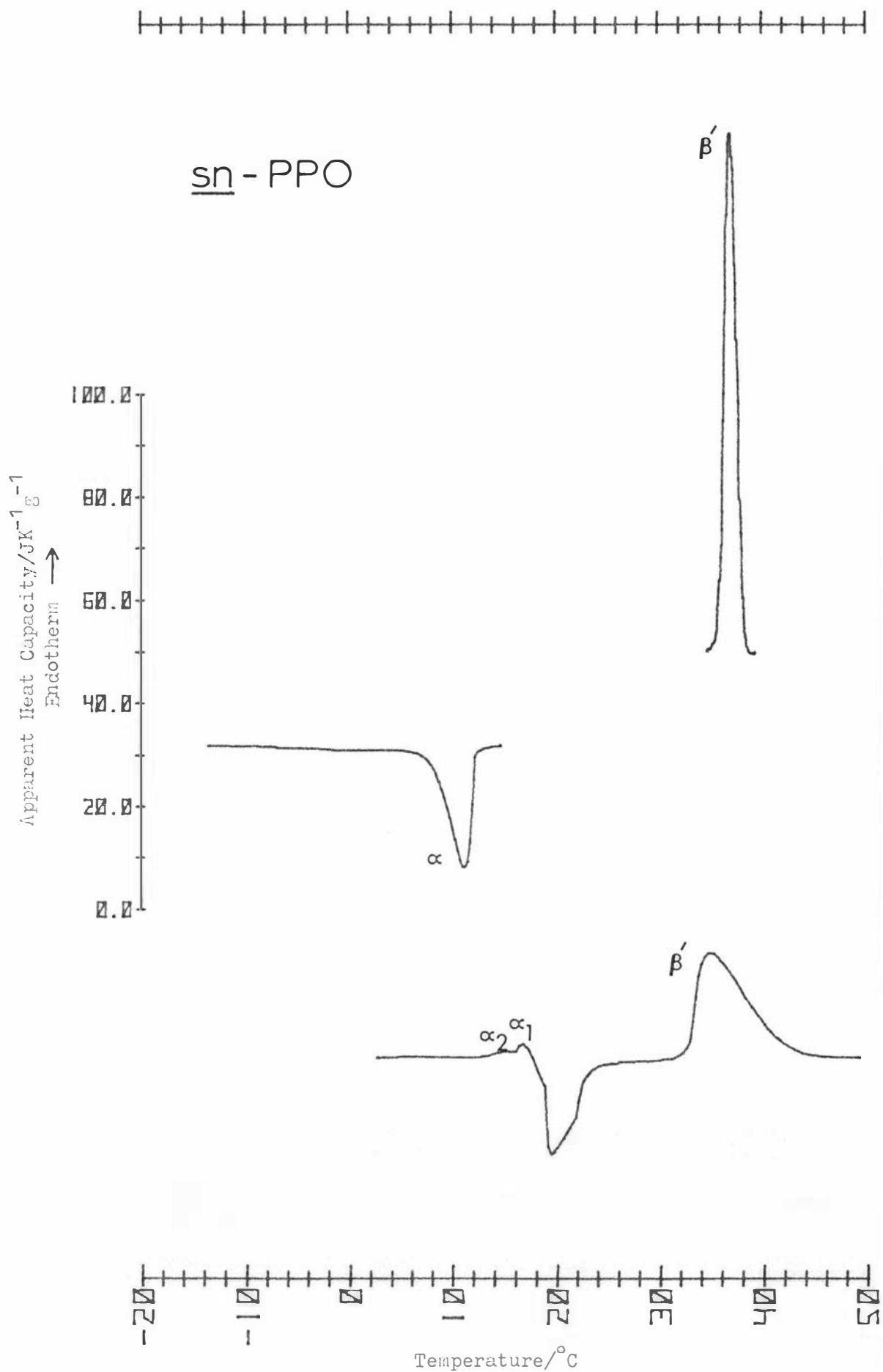


Fig. 47: Thermal behaviour of sn-PPO.  
 (From top to bottom) melting of  $\beta'$  from solvent; crystallisation of  $\alpha$ ;  
 transformation of  $\alpha$  (recorded at 4, 16 and 32  $^{\circ}\text{C}/\text{min}$ ).

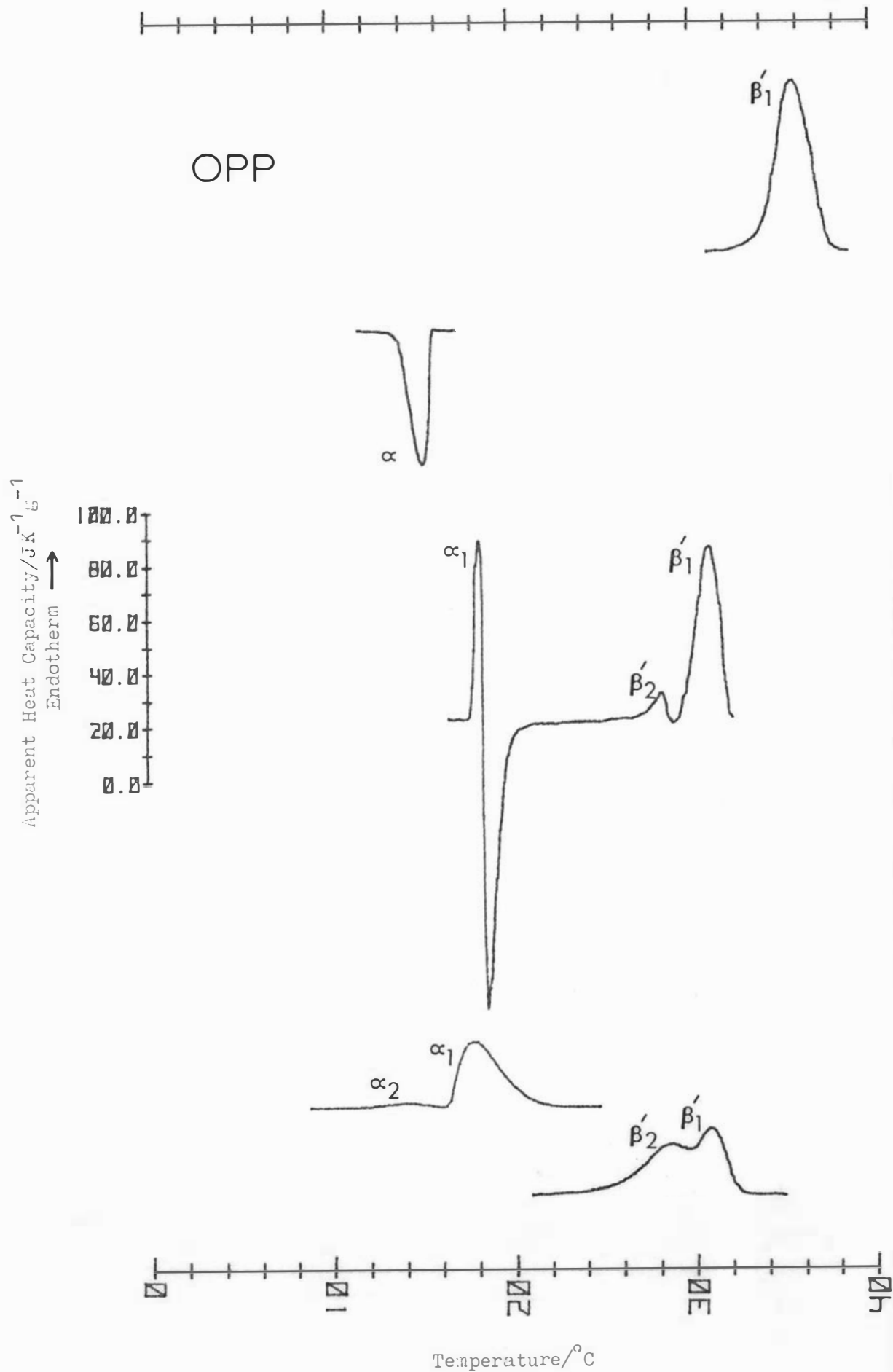


Fig. 48: Thermal behaviour of OPP.

(From top to bottom) melting of  $\beta'$  from solvent ( $4^{\circ}\text{C}/\text{min}$ ); crystallisation of  $\alpha$  ( $4^{\circ}\text{C}/\text{min}$ ); transformation of  $\alpha$  at  $2^{\circ}\text{C}/\text{min}$ ; melting of  $\alpha$  at  $16^{\circ}\text{C}/\text{min}$ ; melting of the  $\beta'$  forms obtained by crystallisation of the melt at  $19^{\circ}\text{C}$  for 25 min ( $4^{\circ}\text{C}/\text{min}$ ).

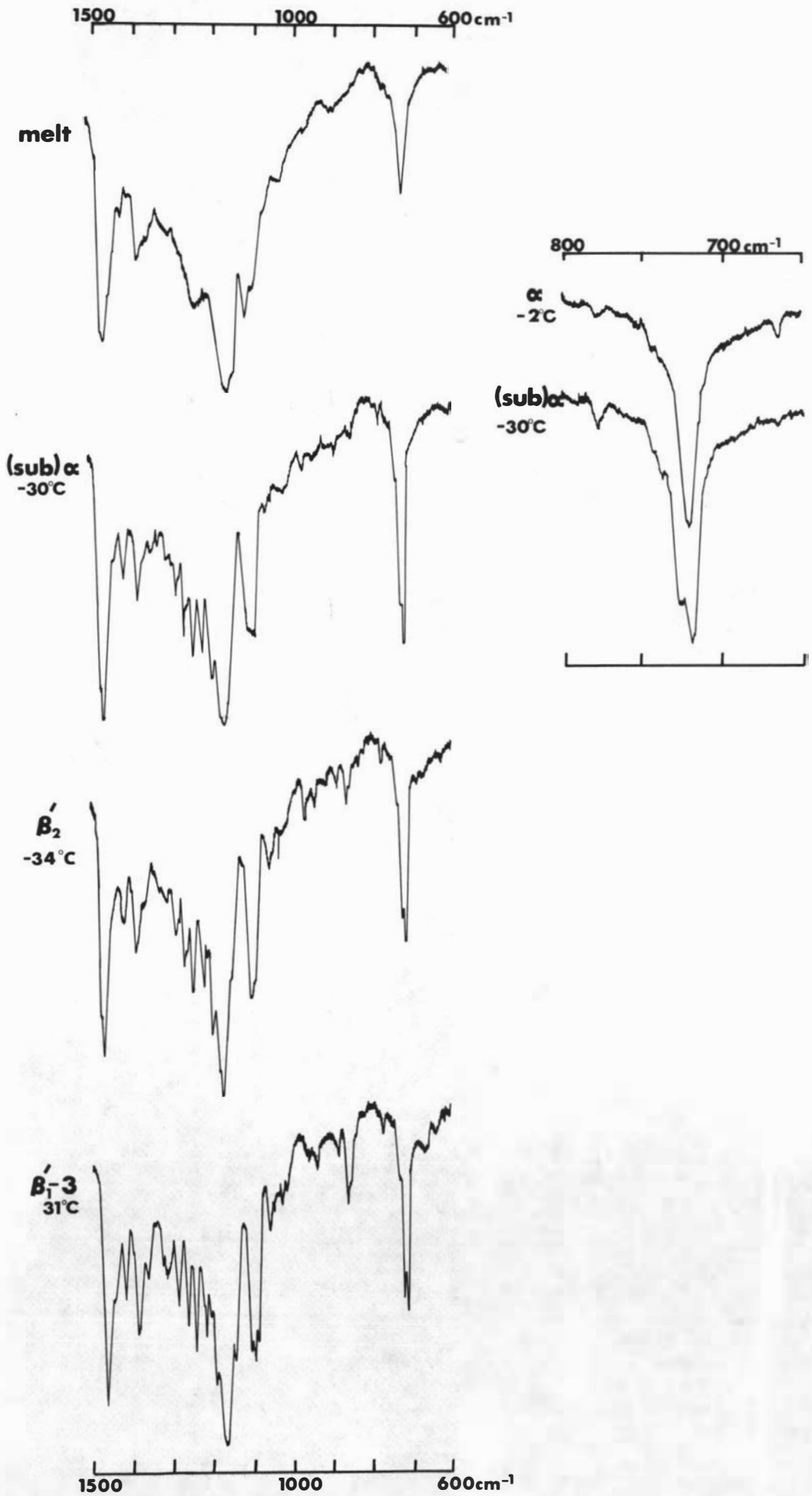


Fig. 49 IR Spectra of OPP

BIBLIOGRAPHY

- Abrahamsson, S. & Ryderstedt-Nahringbauer, I. (1962) Acta Cryst. 15, 1261.
- Abrahamsson, S., Stållberg-Stenhagen, S. & Stenhagen, E. (1963) in Progress in the Chemistry of Fats and Other Lipids (Holman, R.T., ed.), vol. 7, part 1, pp. 59-96, Pergamon Press, Oxford.
- Baer, E. (1952) Biochemical Preparations (Ball, E.G., ed.), vol. 2, p. 31, Wiley, New York.
- Baer, E. & Fischer, H.O.L. (1939a) J. Biol. Chem. 128, 463.
- Baer, E. & Fischer, H.O.L. (1939b) J. Biol. Chem. 128, 475.
- Baer, E. & Kates, M. (1950) J. Amer. Chem. Soc. 72, 942.
- Bailey, A.E. (1950) The Melting and Solidification of Fats, Interscience, New York.
- Barbano, D.M. (1973) M.Sc. thesis, Stereospecific Composition and Thermal Properties of High Melting Glyceride Fractions of Milkfat, Cornell University, U.S.A.
- Barry, P.J. & Craig, B.M. (1955) Can. J. Chem. 33, 716.
- Baur, F.J. (1954) J. Amer. Oil Chem. Soc. 31, 196.
- Bellamy, L.J. (1975) The Infra-red Spectra of Complex Molecules, 3rd edn., vol. 1, pp. 53-54, Chapman and Hall, London.
- Breckenridge, W.C. & Kuksis, A. (1968) J. Lipid Res. 9, 388.
- Breckenridge, W.C. & Kuksis, A. (1969) Lipids 4, 197.
- Bunn, C.W. (1939) Trans. Faraday Soc. 35, 482.
- Callaghan, P.T. (1977) Chem. Phys. Lipids 19, 56.
- Cason, J. & Rapoport, H. (1970) Laboratory Text in Organic Chemistry, 3rd edn., pp. 118-119, Prentice Hall, New Jersey.
- Chapman, D. (1956) Coll. Spect. Internat. VI (Amsterdam) pp. 609-617 Pergamon Press, London.
- Chapman, D. (1957) J. Chem. Soc. 1957, 2715.
- Chapman, D. (1960) J. Amer. Oil Chem. Soc. 37, 73.
- Chapman, D. (1962) Chem. Rev. 62, 433.
- Chapman, D. (1965) The Structure of Lipids by Spectroscopic and X-ray Techniques, Methuen, London.
- Chapman, D., Crossley, A. & Davies, A.C. (1957) J. Chem. Soc. 1957, 1502.
- Chapman, D., Richards, R.E. & Yorke, R.W. (1960) J. Chem. Soc. 1960, 436.
- Christie, W.W. & Moore, J.H. (1969) Biochim. Biophys. Acta 176, 445.

- Clarkson, C.E. & Malkin, T. (1934) J. Chem. Soc. 1934, 666.
- Currie, J.A. & Doyle, M. (1968) in Analytical Calorimetry (Porter, R.S. & Johnson, J.F., eds.), pp. 51-57, Plenum Press, New York.
- De Man, J.M. & Wood, F.W. (1959) J. Dairy Res. 26, 17.
- Dijkstra, G. & de Ruig, W.G. (1973) Z. analyt. Chem. 264, 204.
- Doyne, T.H. & Gordon, J.T. (1968) J. Amer. Oil Chem. Soc. 45, 333.
- Feuge, R.O. & Lovegren, N.V. (1956) J. Amer. Oil Chem. Soc. 33, 367.
- Friedman, L. & Wetter, W.P. (1967) quoted in Reagents for Organic Synthesis (Feiser, L.F. & Feiser, M.), vol. 1, p. 1158, Wiley, New York.
- Gigg, J. & Gigg, R. (1967) J. Chem. Soc. 1967, 431.
- Gronowitz, S., Hersløf, B., Ohlson, R. & Tøregard, B. (1975) Chem. Phys. Lipids 14, 174.
- Hagemann, J.W., Tallent, W.H. & Kolb, K.E. (1972) J. Amer. Oil Chem. Soc. 49, 118.
- Hagemann, J.W., Tallent, W.H., Barve, J.A., Ismail, I.A. & Gunstone, F.D. (1975) J. Amer. Oil Chem. Soc. 52, 204.
- Hampson, J.W. & Rothbart, H.L. (1969) J. Amer. Oil Chem. Soc. 46, 143.
- Hannewijk, J., Haighton, A.J. & Hendrikse, P.W. (1964) in Analysis and Characterisation of Oils, Fats and Fat Products (Boekenooogen, H.A., ed.), vol. 1, pp. 119-182, Interscience, London.
- Hartman, L. (1957) J. Chem. Soc. 1957, 3572.
- Hartman, L. (1960) Chem. Ind. 1960, 711.
- Hay, J.D. & Morrison, W.R. (1970) Biochim. Biophys. Acta 202, 237.
- Horowitz, A.F., Klein, M.P., Michaelson, D.M. & Kohler, S.J. (1973) Ann. N.Y. Acad. Sci. 222, 468.
- Howe, R.J. & Malkin, T. (1951) J. Chem. Soc. 1951 2663.
- Huang, C. (1977a) Lipids 12, 348.
- Huang, C. (1977b) Chem. Phys. Lipids 19, 150.
- Hugenberg, F.R. & Lutton, E.S. (1963) J. Chem. Eng. Data 8, 606.
- Jackson, F.L. & Lutton, E.S. (1950) J. Amer. Chem. Soc. 72, 4519.
- Jackson, F.L. & Lutton, E.S. (1952) J. Amer. Chem. Soc. 74, 4827.
- Jackson, F.L., Wille, R.L. & Lutton, E.S. (1951) J. Amer. Chem. Soc. 73, 4280.
- Jensen, L.H. & Mabis, A.J. (1963) Nature 197, 681.
- Jensen, L.H. & Mabis, A.J. (1966) Acta Cryst. 21, 770.

- Jensen, R.G. (1972) in Topics in Lipid Chemistry (Gunstone, F.D., ed.), vol. 3, pp. 1-35, Elek Science, London.
- Jensen, R.G., Marks, T.A., Sampugna, J., Quinn, J.G. & Carpenter, D.L. (1966) Lipids 1, 451.
- Kitaigorodskii, A.I. (1957) Organic Chemical Crystallography, pp. 177-240, authorised translation from the Russian, copyright 1961, Consultants Bureau, New York.
- Klein, J.M. & Wilcox, J.D. (1971) J. Appl. Cryst. 4, 88.
- Klug, H.P. & Alexander, L.E. (1954) X-Ray Diffraction Procedures, pp. 290, 384, Wiley, New York.
- Knoester, M., de Bruijne, P. & van den Tempel, M. (1972) Chem. Phys. Lipids 9, 309.
- Krabisch, L. & Borgstrom, B. (1965) J. Lipid Res. 6, 156.
- Ladbrooke, B.D. & Chapman, D. (1969) Chem. Phys. Lipids 3, 304.
- Landmann, W., Feuge, R.O. & Lovegren, N.V. (1960) J. Amer. Oil Chem. Soc. 37, 638.
- Larsson, K. (1963) Proc. Chem. Soc. 1963, 87.
- Larsson, K. (1964a) Arkiv Kemi 23, 1.
- Larsson, K. (1964b) Arkiv Kemi 23, 35.
- Larsson, K. (1966a) Acta Chem. Scand. 20, 2255.
- Larsson, K. (1966b) J. Amer. Oil Chem. Soc. 43, 559.
- Larsson, K. (1967) Nature 213, 383.
- Larsson, K. (1971) Chemica Scripta 1, 21.
- Larsson, K. (1972) Fette, Seifen, Anstrichm. 74, 136.
- Lavery, H. (1958) J. Amer. Oil Chem. Soc. 35, 418.
- Lok, C.M., Ward, J.P. & van Dorp, D.A. (1976) Chem. Phys. Lipids 16, 115.
- Lovegren, N.V., Gray, M.S. & Feuge, R.O. (1971) J. Amer. Oil Chem. Soc. 48, 116.
- Lovegren, N.V., Gray, M.S. & Feuge, R.O. (1976) J. Amer. Oil Chem. Soc. 53, 519.
- Luddy, F.E., Barford, R.A., Herb, S.F., Magidman, P. & Riemenschneider, R.W. (1964) J. Amer. Oil Chem. Soc. 41, 693.
- Lundquist, M. (1970) Arkiv Kemi 32, 27.
- Lundquist, M. (1971) Chemica Scripta 1, 5.
- Lutton, E.S. (1945) J. Amer. Chem. Soc. 67, 524.

- Lutton, E.S. (1946) J. Amer. Chem. Soc. 68, 676.
- Lutton, E.S. (1948) J. Amer. Chem. Soc. 70, 248.
- Lutton, E.S. (1950) J. Amer. Oil Chem. Soc. 27, 276.
- Lutton, E.S. (1951) J. Amer. Chem. Soc. 73, 5595.
- Lutton, E.S. (1966) J. Amer. Oil Chem. Soc. 43, 509.
- Lutton, E.S. (1967) J. Amer. Oil Chem. Soc. 44, 303.
- Lutton, E.S. (1971a) J. Amer. Oil Chem. Soc. 48, 245.
- Lutton, E.S. (1971b) J. Amer. Oil Chem. Soc. 48, 778.
- Lutton, E.S. (1972) J. Amer. Oil Chem. Soc. 49, 1.
- Lutton, E.S. & Fehl, A.J. (1970) Lipids 5, 90.
- Lutton, E.S. & Fehl, A.J. (1972) J. Amer. Oil Chem. Soc. 49, 336.
- Lutton, E.S. & Hugenberg, F.R. (1960) J. Chem. Eng. Data 5, 489.
- Lutton, E.S. & Jackson, F.L. (1950) J. Amer. Chem. Soc. 72, 3254.
- Lutton, E.S., Jackson, F.L. & Quimby, O.T. (1948) J. Amer. Chem. Soc. 70, 2441.
- Malkin, T. (1954) in Progress in the Chemistry of Fats and Other Lipids (Holman, R.T., Lundberg, W.O. & Malkin, T., eds.), vol. 2, pp. 1-50, Pergamon Press, London.
- Martin, J.B. & Lutton, E.S. (1972) J. Amer. Oil Chem. Soc. 49, 683.
- Mattson, F.H. & Volpehein, R.A. (1962) J. Lipid Res. 3, 281.
- Menz, H.-U. (1975) Fette, Seifen, Anstrichm. 77, 170.
- Minor, J.E. & Lutton, E.S. (1953) J. Amer. Chem. Soc. 75, 2685.
- Moran, D.P.J. (1963) J. Appl. Chem.(London) 13, 91.
- Mulder, H. (1953) Neth. Milk Dairy J. 7, 149.
- Muller, A. (1927) Proc. Roy. Soc. A114, 542.
- Muller, A. (1932) Proc. Roy. Soc. A138, 514.
- Norris, R. & Taylor, M.W. (1977) N.Z. J Dairy Sci. Technol. 12, 160.
- Pangborn, W.A. (1973) Ph.D. thesis, The Crystal and Molecular Structures of the Anhydride of 11-Bromoundecanoic Acid and Racemic Glycerol 1,2-(Di-11-Bromoundecanoate)-3-(p-Toluenesulphonate), University of Maryland, U.S.A.
- Parodi, P.W. (1976) J. Dairy Sci. 59, 1870.
- Patton, S. & Keeney, P.G. (1958) J. Dairy Sci. 41, 1288.

- Perron, R., Petit, J. & Mathieu, A. (1969) Chem. Phys. Lipids 3, 11.
- Pfeiffer, F.R., Miao, C.K. & Weisbach, J.A. (1970) J. Org. Chem. 35, 221.
- Quinn, J.G. (1967) Ph.D. thesis, Large Scale Preparation of Highly Purified Mixed Acid Triglycerides, University of Connecticut, U.S.A.
- Quinn, J.G., Sampugna, J. & Jensen, R.G. (1967) J. Amer. Oil Chem. Soc. 44, 439.
- Rakhit, S., Bagli, J.F. & Deghenghi, R (1969) Can. J. Chem. 47, 2906.
- Richardson, M.J. & Savill, N.G. (1975) Thermochim. Acta 12, 221.
- Rubin, L.J. & Paisley, W. (1960) J. Amer. Oil Chem. Soc. 37, 300.
- De Ruig, W.G. (1971) Infrared Spectra of Monoacid Triglycerides; with some Applications to Fat Analysis, Agricultural Research Reports (Versl. landbouwk. Onderz.) 759. Also Doctoral thesis, Utrecht, the Netherlands.
- De Ruig, W.G. and Dijkstra, G. (1975) Fette, Seifen, Anstrichm. 77, 211.
- Schlenk, Jr., W. (1965) J. Amer. Oil Chem. Soc. 42, 945.
- Schorigin, P. & Makarov-Zemlianskii, J. (1932) Ber. 65, 1293. quoted in Organic Preparations (C. Weygand), p 163, translated and revised from the German text, 1945, Interscience, New York.
- Shehata, A.Y., de Man, J.M. & Alexander, J.C. (1970) Can. Inst. Food Technol. J. 3, 85.
- Sherbon, J.W. & Coulter, S.T. (1966) J. Dairy Sci. 49, 1126.
- Sowden, J.C. & Fischer, H.O.L. (1941) J. Amer. Chem. Soc. 63, 3244.
- Stauffer, C.E. (1967) J. Amer. Oil Chem. Soc. 44, 443.
- Stein, R.A. & Nicolaidis, N. (1962) J. Lipid Res. 3, 476.
- Sundaralingham, M. (1972) Ann. N.Y. Acad. Sci. 195, 324.
- Tattrie, N.H., Bailey, R.A. & Kates, M. (1958) Arch. Biochem. Biophys. 78, 319.
- Taylor, M.W. (1973) Ph.D. thesis, A Study of the Structure of Triacylglycerols of Bovine Milk Fat, Massey University, New Zealand.
- Taylor, M.W. & Hawke, J.C. (1975a) N.Z. J Dairy Sci. Technol. 10, 40.
- Taylor, M.W. & Hawke, J.C. (1975b) N.Z. J Dairy Sci. Technol. 10, 49.
- Taylor, M.W. & Norris, R. (1977) N.Z. J Dairy Sci. Technol. 12, 166.
- Van Beresteyn, E.C.H. (1972) Neth. Milk Dairy J. 26, 117.
- Vand, V. (1951) Acta Cryst. 4, 104.

- Vand, V. (1954) Acta Cryst. 7, 697.
- Vand, V. & Bell, I.P. (1951) Acta Cryst. 4, 465.
- Van Wijngaarden, D. (1967) Anal. Chem. 39, 848.
- Vasic, J. & de Man, J.M. (1966) 17th Int. Dairy Congress, Munich C, 149.
- Verkade, P.E. (1943) Rec. Trav. Chim. 62, 393.
- Watts, Jr., P.H., Pangborn, W.A. & Hybl, A. (1972) Science, 175, 60.
- Wille, R.L. & Lutton, E.S. (1966) J. Amer. Oil Chem. Soc. 43, 491.
- Woodrow, I.L. & de Man, J.M. (1968) J. Dairy Sci. 51, 996.
- Youngs, C.G., Epp, A., Craig, B.M. & Sallans, H.R. (1957) J. Amer. Oil Chem. Soc. 34, 107.